Justus-Liebig-Universität Gießen
Fachbereich Veterinärmedizin

Institut für Parasitologie

Identifizierung und Charakterisierung von Wirkstoffen und Targets für neue Bekämpfungsansätze gegen Trematoden

HABILITATIONSSCHRIFT

Zur Erlangung der Lehrbefähigung für
das Fach *Zoologie und Molekulare Parasitologie*
im Fachbereich Veterinärmedizin
der Justus-Liebig-Universität Gießen

vorgelegt von

Dr. rer. nat. Simone Häberlein

Gießen 2021

Eine Wissenschaftlerin zu sein ist wie eine Entdeckerin zu sein. Man hat diese immense Neugier, diese Sturheit, diesen entschlossenen Willen, vorwärts zu gehen, egal was andere Leute sagen.

Sara Seager (Astrophysikerin)

Inhaltsverzeichnis

Zusammenfassung

Schistosomen und Leberegel gehören zu den medizinisch bedeutsamsten Trematoden, weshalb die Kontrolle dieser Zoonose- und NTD-Erreger und die Suche nach neuen, effizienteren Bekämpfungsansätzen hohe Priorität hat. Die Grundlagenforschung kann hierzu über die Identifizierung neuer aktiver Substanzen und die Charakterisierung von Targets, also zellbiologischer "Achillesfersen" der Erreger, einen wichtigen Beitrag leisten. Im Bereich der Target-basierten Wirkstoffforschung wurden hier erstmals Autophagie-assoziierte Proteine in *Schistosoma mansoni* und ausgewählte Proteinkinasen in *Fasciola hepatica* untersucht. Dazu gehört die Frage, welche Parasitenstadien diese Proteine exprimieren und in welchen ihrer Gewebe, und ob pharmakologische Inhibierung der Proteinaktivität zum Absterben des Parasiten führt. Im Bereich des Wirkstoffscreenings wurden ausgewählte Naturstoffe aus Insekten hinsichtlich ihres antischistosomalen Potentials untersucht.

In *F. hepatica* wurden bioinformatisch zunächst fünf vielversprechende **Proteinkinasegene** identifiziert. *In situ*-Hybridisierungen und quantitative realtime-PCR (qRT-PCR) zeigten, dass Abl-Tyrosinkinasen in allen pathologisch relevanten Parasitenstadien hoch exprimiert vorliegen, v.a. in der Gastrodermis. Aufgrund der hohen Konserviertheit vieler Protein-kinasen ist es aussichtsreich, Kinaseinhibitoren aus der Humanforschung auch gegen *Fasciola* zu testen. In der Tat zeigte der Abl-Tyrosinkinase-Inhibitor Imatinib eine deutliche, stadienübergreifende fasziolizide Wirkung *in vitro*. Um einen ersten Einblick in die Wirkungsweise von Imatinib im Leberegel zu erhalten, quantifizierten wir die Expression von Genen mit Beteiligung an der Regulation von oxidativem Stress, Zellzyklus und *drug efflux* aus Zellen. Die erhöhte Expression eines Superoxiddismutase-Gens deutete eine Induktion bzw. Abwehr oxidativen Stresses im Wurm nach Imatinib-Exposition an. Über hochauflösende bildgebende Atmosphärendruck-Matrix-unterstütze Laserdesorptions/-ionisations-Massenspektrometrie (**AP-sMALDI-MS Imaging**) wurde die Aufnahmeroute und -kinetik sowie der Gewebetropismus von Imatinib in *S. mansoni* und *F. hepatica* untersucht. Imatinib war bereits nach wenigen Minuten vorrangig im Gastrodermisgewebe detektierbar, was eine orale Aufnahme vermuten ließ. Schließlich konnten wir im Gewebe beider Spezies eine Metabolisierung von Imatinib zu N-Demethyl-Imatinib nachweisen, dem Abl-Kinase inhibierenden Metabolit, welches auch im Menschen gebildet wird. Es ist anzunehmen, dass das Metabolit zur anthelmintischen Aktivität von Imatinib beiträgt.

Neben Proteinkinasen stellen **Autophagie-assoziierte Proteine** aufgrund ihrer vielfältigen Rolle in der Zellbiologie attraktive Wirkstofftargets dar. Autophagie beinhaltet die gesteuerte Degradation zellulärer Bestandteile durch autophagolysosomalen Verdau und dürfte, wie für andere Eukaryoten, auch für Trematoden lebenswichtig sein. Beispielhaft für *S. mansoni* wurde untersucht, welche Proteine des Autophagiesystems in diesem Parasiten existieren, und welche Rolle Autophagie für dessen Zellerhalt, die Reproduktion und letztlich das Überleben des Parasiten spielt. Konservierte Autophagie-Gene konnten in *S. mansoni* sowohl bioinformatisch als auch über qRT-PCR und Western Blot erstmals nachgewiesen werden. Pharmakologische Inhibierung der Autophagie im Wurm mit Inhibitoren aus der Humanforschung hatte eine deutliche antischistosomale Wirkung *in vitro*. Bafilomycin A, ein Makrolidantibiotikum und V-ATPase-Inhibitor, und der Phospho-inositid-3-kinase (PI3K)-Inhibitor Wortmannin reduzierten nicht nur die Fitness der

Würmer, sondern schädigten spezifisch die Keimzellen in den Gonaden und beeinträchtigten die Bildung von Eiern. Wir vermuten, dass Autophagie u.a. für die Reproduktion von Schistosomen ein essentieller Prozess ist.

Neben dieser Target-basierten Forschung ist das Screening von Naturstoffbibliotheken ein wichtiger Bestandteil der Wirkstoffforschung, wobei Pflanzen die mit Abstand am häufigsten genutzte Quelle für Antiparasitika darstellen. Obwohl auch Insekten ein riesiges Arsenal bioaktiver Substanzen produzieren, wurden **Naturstoffe aus Insekten** in der Anthelmintika-Forschung bislang nahezu ignoriert. Hier wurden als Pilotstudien erstmals Substanzen aus der Hämolymphe des Asiatischen Marienkäfer *Harmonia axyridis* und dem Venom der Raubwanze *Rhynocoris iracundus in vitro* gegen *S. mansoni* getestet. Die Substanzen werden von den beiden Spezies zur Verteidigung gegen Pathogene, Konkurrenten oder Prädatoren eingesetzt, zeigten aber auch pleiotrope antischistosomale Effekte. Für beide Substanzen wurde überdies eine inhibitorische Wirkung auf die Stammzellproliferation im Parasiten festgestellt. Da Stammzellen essentiell für Wachstum und Entwicklung der Parasiten sind, stellen Substanzen, die mit der Stammzellaktivität der Parasiten interferieren, attraktive Wirkstoffkandidaten dar. Für das Alkaloid Harmonin wurde ein möglicher Wirkmechanismus in der Inhibierung der enzymatischen Aktivität der schistosomalen Acetylcholinesterase gefunden. Eine Translation der Ergebnisse auf *F. hepatica* ist vielversprechend, denn in ersten Tests tötete Harmonin juvenile Leberegel innerhalb kürzester Zeit.

Im Rahmen der Arbeiten wurden verschiedene **molekular- und zellbiologische Methoden** für die Analyse von Targets und Wirkstoffen in Trematoden optimiert bzw. etabliert. Dazu gehören die (1) Optimierung einer verlässlichen Genexpressionsanalyse in beiden Trematodenspezies durch bioinformatische und experimentelle Validierung von Referenzgenen für den Einsatz in qRT-PCRs, (2) die Quantifizierung von Stammzellen im Parasiten nach Substanzbehandlung mittels fluoreszenzbasierter 3D-Analysen, und in Kooperation (3) AP-sMALDI-MS Imaging zum bildgebenden Nachweis von Wirkstoffen im Parasitengewebe. Diese Methoden werden auch in zukünftigen Studien zu *S. mansoni* und *F. hepatica*, und bei entsprechender Translation darüber hinaus, tiefere Einblicke in den Wirkmechanismus anthelmintischer Substanzen liefern.

Die Kombination aus anwendungsorientierter Substanztestung und grundlagenwissenschaftlich orientierter, molekularer Target-Forschung stellt insgesamt eine vielversprechende Strategie zur Identifizierung neuer Bekämpfungsansätze gegen *S. mansoni* und *F. hepatica* dar. Zukünftig sollten Kombinationstherapien, etwa von Proteinkinase- und Autophagieinhibitoren, systematisch gegen Schistosomen und Leberegel getestet werden, um einen potenzierenden Effekt zu erzielen. Ziel internationaler Forschung sollte es auch sein, ein umfassenderes Wissen über das Kinom in *F. hepatica* zu erlangen und die Testung von Naturstoffen aus Insekten in den nächsten Jahren deutlich voranzutreiben, um neue Targets und Wirkstoffe zu identifizieren.

1 Einleitung

1.1 Vernachlässigte Tropenerkrankungen im Fokus der Wirkstoffforschung

Die WHO zählt aktuell 20 Krankheiten zu den sogenannten vernachlässigten Tropenerkrankungen (*neglected tropical diseases*, NTDs), unter denen vorranging Menschen in ressourcenarmen Ländern tropischer und subtropischer Regionen leiden. Weltweit sind mehr als 1,7 Milliarden Menschen betroffen (WHO 2021). Zu den NTDs gehören viele Infektionen mit parasitären Protozoen und Würmern (Helminthen). Vernachlässigt sind die endemischen Regionen auch im weiteren Sinne, denn häufig sind es ländliche Gegenden, wo Zugang zu medizinischer Behandlung fehlt oder stark eingeschränkt ist, und es an Infrastruktur und hygienischer Grundversorgung mangelt, wie Sanitäranlagen, Frischwasser- und Abwassersysteme (Boisson et al. 2016). Diese Faktoren tragen zu einer hohen Morbidität und teils Mortalität durch NTDs bei, was letztlich Armutskreisläufe in den betroffenen Regionen befördert (Bodimeade et al. 2019). Nicht zu vernachlässigen, auch unter dem globalen *One Health*-Aspekt, ist zudem die Relevanz vieler zoonotischer Erreger als Ursache für NTDs (Laing et al. 2021). Hierzu zählen auch Infektionen mit Saugwürmern (Trematoden), die ein breites tierisches Wirtsspektrum befallen können. Die Vielwirtigkeit zahlreicher NTD-Erreger, ihre komplexe Transmissionsbiologie, aber auch der Klimawandel, der eine Ausbreitung von Zwischenwirten in die nördliche Hemisphäre begünstigt, tragen zur Komplexität der Problematik entscheidend bei (Webster et al. 2016, El-Sayed and Kamel 2020). So tritt Schistosomiasis neuerdings in Europa (Korsika) auf, wo sich autochthone Infektionsherde etabliert haben (Berry et al. 2016).
Letztlich sind NTDs auch mit Blick auf unzureichende Forschungsinitiativen und Finanzierung von Bekämpfungsmaßnahmen weltweit vernachlässigte Krankheiten. Ein Grund für die geringe Aufmerksamkeit in puncto Wirkstoffentwicklung liegt in der geringen Profitspanne. Die Situation wird noch verschlimmert durch die Entwicklung von Resistenzen der Erreger gegen eine Vielzahl der bestehenden Chemotherapeutika, was sich in einem alarmierend kleinen Repertoire sicherer und wirksamer Medikamente widerspiegelt (Akinsolu et al. 2019). Diese weitreichende Problematik wurde von der WHO, politischen Entscheidungsträgern, Akademikern, und Pharmakonzernen erkannt und führte 2012 zur Verabschiedung der London-Deklaration zu NTDs. Der hier entwickelte Fahrplan zur weltweiten Bekämpfung wurde in 2021 erweitert (Balakrishnan 2021). Ausgewählte NTDs sollen bis 2030 global oder regional ausgerottet, eliminiert bzw. kontrolliert werden. Schlüssel hierzu ist neben der Impfstoffentwicklung v.a. ein ausreichend großes Portfolio neuer Therapeutika. Die Möglichkeit zur Massenbehandlung ganzer Bevölkerungsgruppen (*Mass Drug Administration*, MDA), die auch zur präventiven Chemotherapie genutzt wird, ist ein Schlüssel zum Erreichen der gesteckten Ziele (De Rycker et al. 2018).

Somit hat die Entwicklung neuer Wirkstoffe gegen Helminthen und andere NTD-Erreger höchste Priorität. Ein Fokus hierbei liegt auf der Suche nach günstigen und leicht zugänglichen Quellen für bioaktive Substanzen, wie etwa Naturstoffe oder bereits zugelassene Wirkstoffe, die für *drug repurposing* infrage kommen. Auch die Identifizierung der Zielstrukturen (Targets) von Wirkstoffen im Erreger ist wünschenswert, um Wirkmechanismen zu verstehen und damit Resistenzbildung zuvorkommen zu können.

1.2 Infektionen mit Schistosomen und dem Leberegel *Fasciola hepatica*

Trematoden sind parasitäre Vertreter im Stamm der Plattwürmer (Plathyhelminthes). Zwei der prävalentesten und medizinisch bedeutsamsten Vertreter stellen die Pärchenegel (Schistosomen) und Leberegel dar, deren Bekämpfung als Zoonose- und NTD-Erreger hohe Priorität hat. Schistosomen sind die Erreger der Bilharziose oder Schistosomiasis, einer durch Kontakt mit infestiertem Wasser übertragenen Krankheit, die u.a. die Leber betrifft. Leberegel der Gattung *Fasciola* sp. verursachen die Fasziolose, eine Nahrungsmittel- und Futter-übertragene Infektion der Leber. Die infektiösen Larvenstadien werden dabei von Wasserschnecken ausgeschieden, welche als Zwischenwirt dienen. Beide Parasiten befallen ein breites Endwirtspektrum (Mensch, Nutztiere, Wildtiere). Dabei offenbaren sie komplexe Lebenszyklen, eine interessante und nur in Teilen verstandene Entwicklungsbiologie sowie eine vielschichtige Wirt-Parasit-Interaktion, die Gegenstand vieler Forschungsansätze ist (De Bont and Vercruysse 1997, Standley et al. 2012). Trotz ihrer augenscheinlich niederen Stellung in der Phylogenie, haben Trematoden erstaunliche Anpassungsfähigkeiten entwickelt. So können Adultwürmer bis zu 30 Jahre in ihrem Wirt überdauern, wofür effiziente Adaptationsmechanismen erforderlich sind (Schmid-Hempel 2017, Maizels et al. 2018). Beide Saugwurmgruppen stellen daher faszinierende Untersuchungsobjekte dar, sowohl aus veterinär- und humanmedizinischer als auch aus biologisch-grundlagen-wissenschaftlicher Perspektive.

Aktuellen Schätzungen zufolge leben mehr als 600 Millionen Menschen in Schistosomiasis-endemischen Regionen, von denen mindestens 290 Millionen präventive Chemotherapie benötigen (WHO 2020). Zur Behandlung der Schistosomiasis existiert mit Praziquantel (PZQ) weltweit nur ein einziges Medikament, das gegen alle Schistosomenarten aktiv ist (Vale et al. 2017). Allerdings verhindert PZQ keine Reinfektion, ist subeffektiv gegen juvenile Würmer, und es mehren sich schon seit längerer Zeit Hinweise auf die Möglichkeit einer Resistenzentwicklung (Ismail et al. 1996, Vale et al. 2017). Nach Hautkontakt mit den infektiösen Larvenstadien (Gabelschwanzzerkarien) wandern diese über mehrere Wochen als Juvenilstadien (Schistosomula) über die Blutgefäße der Lunge weiter zur Pfortader, wo sie zu Adultwürmern reifen. Als Nahrungsgrundlage dienen u.a. Erythrozyten, was zu einer Anämie im Patienten beitragen kann. In der Pfortader spielt sich ein im Tierreich einzigartiges entwicklungsbiologisches Phänomen ab: der weibliche, noch unterentwickelte Wurm wird vom Körper des Männchens der Länge nach umschlossen, so dass ein Paar entsteht. Im sogenannten gynäkophoren Kanal des Männchens wirken derzeit noch unbekannte Signalfaktoren auf das Weibchen, welche dieses zur Ausreifung der Geschlechtsorgane anregt. Hier könnten neuronale Faktoren eine Rolle spielen (Hahnel et al. 2018, Lu et al. 2019). Das Schistosomenpaar wandert schließlich in die Mesenterialvenen (oder Venen der Harnblase im Fall von *S. haematobium*) als finales Ziel ein (Popiel and Basch 1984, Gryseels 2012). Nach der Paarung produziert das Weibchen mehrere hundert Eier pro Tag, die zum Großteil über den Blutstrom in den Darm einwandern und nach Freisetzung in die Umwelt den Fortlauf des Lebenszyklus sicherstellen. Die restlichen Eier landen jedoch über den Blutstrom in der Leber, wo sie pathologische Prozesse von der Granulombildung hin zur Leberfibrose induzieren (Gryseels 2012).

Leberpathologien sind ebenfalls das Hauptproblem bei der Fasziolose, die in fast der Hälfte aller Länder weltweit vorkommt und dort v.a. in der Nutztierhaltung, aber auch als Zoonose ein enormes Problem darstellt (Fürst et al. 2012). Herdenprävalenzen betragen bis zu 86% in einigen europäischen Ländern und sogar bis zu 91% in Ländern Afrikas (Mehmood et al. 2017, May et al. 2020). Es überrascht nicht, dass der globale ökonomische Verlust bei Milch- und Fleischproduktion auf mehrere Milliarden USD pro Jahr geschätzt wird (Mehmood et al. 2017). Die Fasziolose wird ebenfalls zu den NTDs gezählt, die derzeit etwa 2,4-17 Millionen Menschen betrifft (Fürst et al. 2012). Die Infektion im Menschen verläuft zumeist subklinisch, kann jedoch auch zu Anämie, Gewichtsverlust, Unterernährung und biliärer Zirrhose führen. Dadurch wird zum einen die Lebensqualität der Betroffenen eingeschränkt, zum anderen entstehen nicht zu vernachlässigende Entwicklungsdefizite v.a. in Kindern (Jonker et al. 2017) – was auch für die Folgen der Schistosomiasis gilt (Osakunor et al. 2018). Nach oraler Aufnahme der infektiösen Dauerstadien (Metazerkarien) schlüpfen sog. "newly excysted juveniles" (NEJs) im Dünndarm. Diese penetrieren die Darmwand und migrieren – mit ihrer geringen Größe von nur 200 µm – über erstaunliche Distanzen hinweg zur Leberkapsel. Fortan fressen sich die juvenilen Würmer regelrecht über mehrere Wochen durch das Leberparenchym, während sie heranreifen (akutes Infektionsstadium). Die Adultwürmer siedeln sich im Gallengang an, wo sie sich vorrangig vom Epithel ernähren (chronisches Infektionsstadium) und bis zu 30.000 Eier täglich produzieren (Dawes and Hughes 1970, Mas-Coma et al. 2009). Der bevorzugt eingesetzte Wirkstoff zur Behandlung der Fasziolose ist Triclabendazol, da dieser sowohl juvenile als auch adulte Leberegel abtötet. Vermutlich als Konsequenz des großflächigen Einsatzes in der Nutztierhaltung entstanden jedoch Triclabendazol-resistente *F. hepatica*-Stämme, die auch bereits aus Menschen isoliert wurden (Kelley et al. 2016, Kelley et al. 2020). Unter dem *One Health*-Aspekt ist die Entwicklung alternativer Wirkstoffe daher von höchster Dringlichkeit.

Zusammenfassend ist festzuhalten, dass *S. mansoni* und *F. hepatica*, trotz großer Unterschiede ihrer Biologie, bemerkenswerte Eigenschaften teilen, wie migrierende Juvenilstadien, die lange Lebensfähigkeit im Endwirt, und die Ernährung von Wirtszellen. Es scheint wahrscheinlich, dass auch Mechanismen der molekularen Zellbiologie, wie die Regulation von Zelldifferenzierung und Zelltod durch typische Signalproteine, Enzyme und Rezeptoren, in diesen eng verwandten Spezies gleichen Prinzipien folgt. Die Charakterisierung dieser Prozesse sollte es demnach ermöglichen, neue Bekämpfungsansätze für beide Erreger zu schaffen. Damit besteht durchaus die Chance, dass ein neu gefundener Wirkstoff speziesübergreifende Effekte besitzen kann. Molekularbiologische Techniken zur Erforschung und experimentellen Manipulation von *S. mansoni* und *F. hepatica* haben in den letzten Jahren eine enorme Weiterentwicklung erfahren. Erste Erfolge zur Etablierung der CRISPR/Cas9-vermittelten Genomeditierung gibt es seit Kurzem auch für Schistosomen (Du et al. 2021, You et al. 2021). Auch die Verfügbarkeit von Genomdaten und postgenomischen Methoden wie RNA-Interferenz (RNAi) ist für die Identifizierung von Wirkstofftargets und zellbiologischer "Achillesfersen" der Erreger von hoher Relevanz. Vielversprechende Angriffspunkte, mit denen sich meine eigene Forschung befasst, sind Proteinkinasen und Autophagie-assoziierte Proteine.

1.3 Proteinkinasen und Autophagie-assoziierte Proteine als Wirkstofftargets

Proteinkinasen gelten als wichtige Regulatoren fundamentaler zellulärer Prozesse, wie die Kontrolle von Zellzyklus und -differenzierung (Lane and Nigg 1996, Yuan et al. 1997). Eine Dysregulation von Proteinkinaseaktivitäten trägt zur Entstehung zahlreicher Erkrankungen des Menschen bei. Dementsprechend liegt ein starker Fokus der Pharmaindustrie auf der Entwicklung von Proteinkinaseinhibitoren zur Behandlung dieser Krankheiten, z.B. verschiedener Formen von Krebs. Proteinkinasen wurden ebenfalls als vielversprechende Targets in ganz unterschiedlichen Pathogenen identifiziert, von Bakterien über Protozoen zu Helminthen (Brumlik et al. 2011, Beckmann et al. 2012, Sukumar et al. 2020). Proteinkinasen als Targets in Parasiten wie Trematoden zu studieren ist umso attraktiver, da man aus einem riesigen Pool niedermolekularer (*small-molecule*) Wirkstoffe schöpfen kann, welche z.B. für Krebsmedikamente entwickelt wurden. Aufgrund des hohen Grades an Konserviertheit (Manning 2005) ist es durchaus möglich, dass ein humaner Inhibitor auch das entsprechende orthologe Enzym in Trematoden inhibiert.

Einige Kinaseinhibitoren wurden in den letzten Jahren im Detail durch unsere Arbeitsgruppe im Hinblick auf eine mögliche antischistosomale Aktivität untersucht, wobei der Tyrosinkinaseinhibitor Imatinib am besten studiert ist (Dissous and Grevelding 2011). Imatinib inhibiert im Menschen Proteinkinasen der Abl-Familie und wird als Medikament Glivec (Novartis, Basel, Schweiz) zur Therapie von chronisch myeloischer Leukämie und gastrointestinalen Stromatumoren eingesetzt (Manley et al. 2002, Knight and McLellan 2004, Waller 2018). *In vitro*-Tests unserer Arbeitsgruppe demonstrierten eine vielversprechende Aktivität auch gegen *S. mansoni* und *S. japonicum* (Beckmann and Grevelding 2010, Li et al. 2019). Andere Gruppen konnten dies für den Zestoden *Echinococcus multilocularis* (Hemer and Brehm 2012) und für Filarien bestätigen (O'Connell et al. 2015, O'Connell et al. 2017). In *S. mansoni* konnten wir die Expression mutmaßlicher Targets nachweisen, zweier Abl-Orthologe und einer Abl/Src-Hybridkinase, und deren Inhibierung durch Imatinib belegen (Beckmann and Grevelding 2010, Beckmann et al. 2011). Für *Fasciola* sp. dagegen herrscht bislang ein regelrechtes Vakuum im Kinaseforschungsfeld. Frühere Studien befassten sich hier vorrangig mit nicht-therapeutischen Aspekten von Kinasen als Vakzinkandidaten (Phosphoglycerat-Kinase) oder als Diagnostikmarker zur Unterscheidung von Hybriden (Phosphoenolpyruvat-Carboxy-Kinase) (Shoriki et al. 2016, Wesolowska et al. 2016). Die Phosphofructokinase stellt die einzige bislang als mögliches chemotherapeutisches Target untersuchte Kinase für *Fasciola sp.* dar und geht auf eine Studie aus 1962 zurück (Mansour and Mansour 1962, Fairweather et al. 1984). Aufgrund der Konserviertheit vieler Tyrosinkinasen kann man vermuten, dass Inhibitoren wie Imatinib auch Aktivität gegen *F. hepatica* zeigen.

Zellentwicklung und -homöostase werden, neben Proteinkinasen, auch durch einen fundamentalen, katabolischen Mechanismus reguliert: Autophagie (“Selbstverdau”). Dieser Prozess dient zum kontrollierten Abbau zellulärer Bestandteile und eliminiert zytoplasmatische Komponenten, wie beschädigte Zellorganellen und fehlgefaltete Proteine, durch autophagolysosomalen Verdau. Neben dieser zellulären “Entrümpelungsfunktion” liefert Autophagie auch neue Baubestandteile für anabolische Prozesse etwa während Nährstoffmangelsituationen (Klionsky and Emr 2000). Des Weiteren trägt zelluläre

Remodellierung durch Autophagie zur Morphogenese bei Entwicklungsprozessen bei (Song et al. 2020). Eine Dysregulation von Autophagie führt dementsprechend zu schweren Erkrankungen, auch im Menschen, weshalb die medikamentöse Modulation von Autophagieaktivität von großem pharmazeutischen Interesse ist (Kim et al. 2020). In Invertebraten wurden vorrangig Untersuchungen für *Caenorhabditis elegans* durchgeführt, bei welchem Autophagie ein wichtiger Regulator der Embryogenese ist (Song et al. 2020). Man kann davon ausgehen, dass ein funktionierendes Autophagiesystem, wie für andere Eukaryoten, auch für Trematoden lebenswichtig ist.

1.4 Naturstoffe als vielversprechende Anthelmintika

Neben einer Target-basierten Wirkstoffforschung wird noch häufiger, v.a. von Pharmakonzernen, ein *non-targeted* Screening von Substanzbibliotheken zur Identifizierung neuer Wirkstoffkandidaten durchgeführt. Naturstoffe stellen ein enormes, wenig erforschtes Reservoir für die Entdeckung neuer bioaktiver Substanzen zur Behandlung von Krankheiten dar und sind ein zentraler Teil solcher Screenings (Atanasov et al. 2021). Im Vergleich zur synthetischen Chemie besitzen Naturstoffe ein enormes Maß an struktureller Diversität, wodurch ein riesiger Pool neuer möglicher Wirkstoffkandidaten existiert. Über 33% der zwischen 1981 und 2010 neu zugelassenen Medikamente entstammten Naturstoffen, zumeist aus Pflanzen oder Pilzen (Newman and Cragg 2012). Bekannte Beispiele solcher aus Pflanzenstoffen stammender Wirkstoffe sind die Acetylsalicylsäure (in Aspirin) und Taxol (in Krebsmedikamenten) sowie im Bereich der Antiparasitika Quinin und Artemisinin zur Behandlung der Malaria (Phillipson 1994, Newman and Cragg 2012).

Auch im Bereich Anthelmintika-Forschung wurde in den vergangenen Jahren das Naturstoff-Screening zunehmend intensiviert (Neves et al. 2015). Dies betrifft fast ausschließlich medizinische Heilpflanzen und deren bioaktive Metabolite wie Alkaloide, Terpene und Peptide. *In vitro*- und *in vivo*-Aktivität gegen Schistosomen zeigten beispielsweise Piplartin (Alkaloid aus einem Pfeffergewächs), Curcumin (Polyphenol aus der Safranwurz) sowie Artemisinin und –derivate (Keiser and Utzinger 2012, Mengarda et al. 2020, Mokbel et al. 2020). Eigene Studien zeigten eine antischistosomale Wirkung von Silvestrol, einem Rocaglat eines asiatischen Mahagonigewächses (Kooperation mit Prof. Grünweller, Universität Marburg; unveröffentlichte Daten).

Im Gegensatz dazu befassten sich bislang nur sehr wenige anthelmintische Studien mit der Erforschung tierischer Naturstoffe (de Moraes et al. 2011). Insekten wurden als Wirkstoffquelle in der Anthelmintika-Forschung bislang nahezu ignoriert und das, obwohl sie die artenreichste Klasse im Tierreich darstellen und gemeinsam ein gigantisches Spektrum bioaktiver Substanzen produzieren (Mohamed et al. 2016). Diese Substanzen dienen u.a. zur chemischen Verteidigung gegen Fressfeinde, Pathogene und Kompetitoren und umfassen Stoffgruppen wie antimikrobielle Peptide sowie vielfältige sekundäre Metabolite. Erste Daten zur antischistosomalen Aktivität von Venom und Propolis von Bienen scheinen vielversprechend (Mohamed et al. 2016), zweier Produkte, die schon lange für ihre fungiziden und antimikrobiellen Eigenschaften bekannt sind (Hegazi et al. 2000). Ziel internationaler Forschung sollte sein, die Testung von Naturstoffen aus Insekten in den

nächsten Jahren deutlich voranzutreiben, um neue Wirkstoffe gegen Trematoden wie Schistosomen und *Fasciola* sp. zu entdecken. In diese Stoßrichtung bewegt sich der neu gegründete Standort „Bioressourcen“ des Fraunhofer-Instituts in Gießen (Tonk and Vilcinskas 2017).

1.5 Fragestellungen zur Findung neuer Bekämpfungsmöglichkeiten gegen Schistosomen und Leberegel

In meinen Forschungsarbeiten verfolge ich mehrere parallele Strategien zur Identifizierung neuer therapeutischer Optionen gegen *S. mansoni* und *F. hepatica*, die auf den vorangehend ausgeführten wissenschaftlichen Ansätzen basieren.

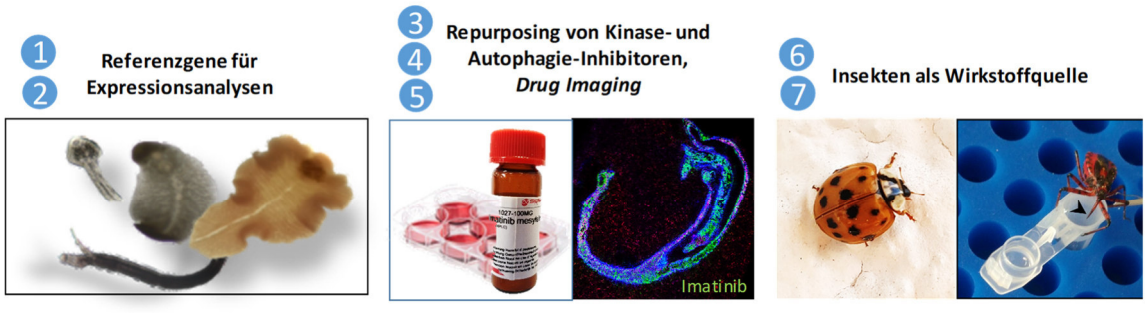

Abb. 1 Übersicht der Studieninhalte zum Themenkomplex der Wirkstoff- und Targetforschung für *Schistosoma mansoni* und *Fasciola hepatica*. Zahlen geben die Nummern der Publikationen wieder.

Zum einen untersuche ich Naturstoffe aus Insekten in Kooperation mit dem Fraunhofer-Institut für Molekularbiologie und Angewandte Ökologie (IME) hinsichtlich ihrer antischistosomalen Aktivität. Da sowohl die Naturstoffe in ihrer verfügbaren Menge, als auch Leberegel in ihrer für Experimente zur Verfügung stehenden Zahl limitiert sind, beschränken sich diese Untersuchungen zunächst auf *S. mansoni*. Ziel ist, neue anthelmintische Naturstoffe aus Insekten zu entdecken und mittelfristig auch deren Wirkmechanismen zu verstehen. In einem ersten Schritt hierzu wurde die antischistosomale Aktivität von Venom einer Raubwanze getestet sowie die eines Alkaloids aus der Hämolymphe des Asiatischen Marienkäfers (*Harmonia axyridis*), der für seine hohe ökologische Durchsetzungsfähigkeit gegen Konkurrenten dank „chemischer Waffen“ bekannt ist (Vilcinskas et al. 2013). Die Familie der Raubwanzen (Reduviidae) umfasst etwa 6800 Spezies (Hwang and Weirauch 2012) und nutzt Venom, welches zur Paralyse in Beutetiere injiziert wird oder gegen Prädatoren zum Einsatz kommt, und das aus über 200 bioaktiven Einzelsubstanzen zusammengesetzt ist (Edwards 1961, Walker et al. 2016). Ob diese Substanzen oder Harmonin anthelmintische Aktivität besitzen, war bis dato unbekannt.

Zum anderen umfasst meine Forschung eine Target-orientierte Analyse von Proteinkinasen und Autophagie-assoziierten Proteinen. Ziel ist, ausgewählte Proteine hinsichtlich ihrer *druggability* zu charakterisieren. Dazu gehören die Fragen, welche Parasitenstadien diese Proteine exprimieren, in welchen Geweben dies passiert, und ob genetische Interferenz mit der Proteinexpression oder pharmakologische Inhibierung der Proteinaktivität zum Absterben des Parasiten führt. Als Inhibitoren kommen hier vorzugsweise bereits für die

Behandlung anderer Erkrankungen des Menschen zugelassene Wirkstoffe zum Einsatz, was die Entwicklung eines Anthelmintikums im Zuge eine *drug repurposings* beschleunigen würde. Proteinkinasen wurden in der *Fasciola*-Forschung bislang vernachlässigt. Das übergeordnete Ziel ist daher, Proteinkinasen insgesamt mehr in den Fokus der Leberegel-Forschung zu rücken. Als *proof-of-concept* sollte die Wirkung des etablierten antischistosomalen Abl-Kinaseinhibitors Imatinib und das zugehörige zelluläre Target in *F. hepatica* studiert werden. Genauso wenig wie Proteinkinasen im Leberegel erforscht sind, ist Autophagie für Trematoden untersucht, obwohl es sich um einen essentiellen Zellmechanismus handelt. Beispielhaft für *S. mansoni* sollte beantwortet werden, welche Proteine des Autophagiesystems in diesem Parasiten existieren, welche Rolle Autophagie für dessen Zellerhalt, die Reproduktion und letztlich das Überleben des Parasiten spielt. Ist eine antischistosomale und fasziolizide Substanz gefunden, so ist es zusätzlich von Interesse, die Aufnahmekinetik und den Gewebetropismus dieser Substanz im Parasiten aufzuklären, um auf mögliche Wirkmechanismen schließen zu können.

Einige dieser Forschungsfragen benötigten zunächst die Etablierung grundlegender Analysemethoden. Hierzu gehört der Nachweis und die Quantifizierung der Genexpression eines möglichen therapeutischen Targets. Proteomstudien ergaben deutliche Unterschiede in der globalen Genexpression zwischen den verschiedenen im Endwirt vorkommenden Lebensstadien von *S. mansoni* und *F. hepatica* (Robinson et al. 2009, Di Maggio et al. 2016, Wangwiwatsin et al. 2020). Dies hat wichtige praktische Implikationen für die Wirkstofftarget-Forschung, denn ein neues Chemotherapeutikum soll möglichst alle Parasitenstadien eliminieren können, d.h. das Target muss in allen Lebensstadien gleichermaßen exprimiert sein. Auch *in vitro*-Kulturbedingungen können Genexpressionen in den Parasiten global verändern (Jeremias et al. 2017), jedoch sind *in vitro*-Experimente, etwa zur genetischen Manipulation der Parasiten, unerlässlich. Daher war es zunächst Ziel, eine verlässliche Methode zur Quantifizierung der Genexpression in verschiedenen Lebensstadien beider Trematodenspezies und während *in vitro*-Kultur zu finden. Als Methode zur Analyse von Aufnahme und Verteilung von anthelmintischen Substanzen in *S. mansoni* und *F. hepatica* habe ich an der Etablierung bildgebender Verfahren mit Kooperationspartnern aus der pharmazeutischen sowie analytisch-anorganischen Chemie gearbeitet.

Die Kombination aus anwendungsorientierter Substanztestung und grundlagen-wissenschaftlich orientierter, molekularer Target-Forschung stellt für mich eine vielversprechende Strategie zur Beantwortung der hier oben ausgeführten Fragestellungen und zur Identifizierung neuer Bekämpfungsansätze gegen *S. mansoni* und *F. hepatica* dar.

2 Methodische Ansätze und Ergebnisse zur Charakterisierung aktiver Substanzen und Wirkstofftargets

Die sieben vorgelegten Publikationen umfassen in internationalen Fachzeitschriften publizierte Originalartikel, wovon ich eine Erstautorenschaft und sechs Letztautorenschaften innehalte. Die Publikationen befassen sich mit dem Themenkomplex der Wirkstoff- und Targetforschung für zwei wichtige Vertreter parasitischer Saugwürmer, *S. mansoni* und *F. hepatica*, sowie dafür notwendige Methoden der molekularen Grundlagenforschung. Die methodischen Ansätze und daraus erhaltene Erkenntnisse sind im Folgenden kurz zusammengefasst.

In den **Publikationen 1 und 2** wurden die methodischen Grundlagen für aussagekräftige Genexpressionsanalysen in *S. mansoni* und *F. hepatica* gelegt, indem Referenzgene für diese Parasiten identifiziert und experimentell validiert wurden. Für die relative Quantifizierung von Transkripten (im Folgenden wird vereinfacht von „Genexpression" gesprochen) mittels quantitativer *realtime*-PCR (qRT-PCR) müssen Referenzgene im Untersuchungsorganismus bekannt sein, die unter den gegebenen Versuchsbedingungen stabil, d.h. unveränderlich exprimiert sind und somit zur Normalisierung von qRT-PCR-Daten herangezogen werden können. Zur Identifizierung solcher Referenzgene wurden vergleichende qRT-PCR-Analysen einer Vielzahl von Kandidatengenen mit zunächst quantitativer Transkriptbestimmung ausgeführt. Die Auswertung, das *Ranking* der Kandidatengene nach höchsten Stabilitätswerten, erfolgte durch mehrere bioinformatische Algorithmen. Ein besonderer Fokus lag darauf, Referenzgene für Genexpressionsanalysen *in vitro*-kultivierter Würmer zu finden, da *in vitro*-Manipulation von Würmern mit Inhibitoren oder durch RNAi eine Hauptmethode der Wirkstoffforschung darstellt. Meine eigenen Untersuchungen identifizierten das in Mitochondrien exprimierte Gen *letm-1* (*LETM1 and EF hand domain containing protein 1*) sowie das Proteasom-Gen *psmb7* (*proteasome subunit beta type 7*) als neue Referenzgene für *S. mansoni*. Wir nutzten diese beispielhaft zum Nachweis, dass bestimmte neuronale Gene im Männchen paarungsabhängig exprimiert werden. Die Studie zum Leberegel wurde unter meiner Betreuung von meinem Doktoranden Hicham Houhou angefertigt. Für *F. hepatica* wurden das Chaperon-Gen *tbcd* (*tubulin-specific chaperone D*) und ebenfalls *psmb7* als geeignete Referenzgene gefunden (Haeberlein et al. 2019, Houhou et al. 2019). Als ein Anwendungsbeispiel wurde in derselben Studie die Expression von fünf Kinasegenen (*abl1, abl2, pkc, akt1, plk1*) quantifiziert, die als mögliche Wirkstofftargets in anderen Parasiten beschrieben worden sind (Beckmann and Grevelding 2010, Long et al. 2010, Morel et al. 2014, Ressurreicao et al. 2014, Guidi et al. 2015). Die Analyse wurde dabei für drei verschiedene Lebensstadien des Leberegels erfasst, die pathologisch relevant sind. Dies offenbarte stadienabhängige Expressionsmuster dieser Kinasegene.

In den **Publikationen 3 und 4** wurde in einer interdisziplinären Kooperation mit Prof. Bernhard Spengler (Institut für Anorganische und Analytische Chemie, Justus-Liebig-Universität Gießen) eine weitere Methodik der Wirkstoffforschung in Trematoden etabliert: die hochauflösende bildgebende Atmosphärendruck-Matrix-unterstütze Laserdesorptions/-ionisations-Massenspektrometrie (AP-sMALDI-MS Imaging) (Rompp et al. 2011). Hierbei werden die Moleküle im Gewebeschnitt mit einem Laser ionisiert, was durch voriges

Besprühen des Schnitts mit einer geeigneten organischen Matrix ermöglicht wird. Das gesamte Gewebe wird mit dem Laser abgerastert, wobei eine punktförmige Ionisierung im Abstand weniger Mikrometer stattfindet, so dass eine hohe Auflösung erzielt wird. Nach massenspektrometrischer Analyse werden die gefundenen Molekülfragmente rückwirkend mit der Positionsinformation des Ionisierungsschrittes überlagert, so dass eine 2D-Information zur Verteilung der Moleküle im Gewebe erhalten wird (**Abb. 2 A,B**).

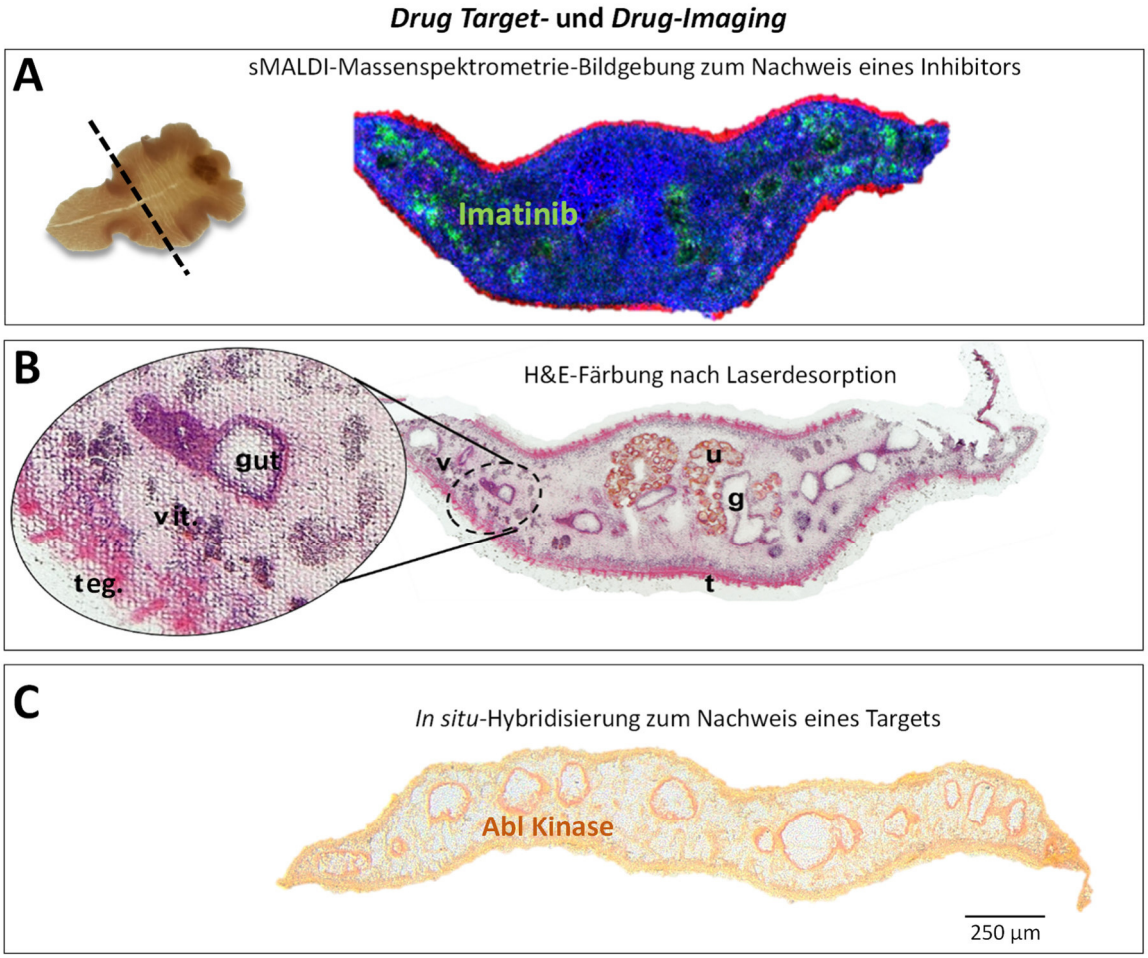

Abb. 2 Bildgebende Methoden in der Wirkstoff- und Targetanalyse am Beispiel *Fasciola hepatica*. Gezeigt sind Querschnitte eines adulten Wurms. **(A)** AP-sMALDI massenspektrometrische Bildgebung (AP-sMALDI-MSI) zeigt die Masseverteilung zweier Lipide des Wurms (blau und rot) und des Kinase-inhibitors Imatinib (grün) nach **(B)** rasterförmiger Laserdesorption von Gewebepunkten (weiße Stellen in histologischer Färbung). **(C)** *In situ*-Hybridisierung zum Nachweis von Target-Transkripten im Gewebe (hier eine Abl-Kinase, ein mutmaßliches Imatinib-Target, in hellrot).

Wir nutzten AP-sMALDI-MS Imaging zur Beantwortung der Fragen: Über welche Route wird eine Substanz vom Wurm aufgenommen - oral oder tegumental? In welchem Zeitraum findet dies statt? Lagert sich die Substanz bevorzugt in bestimmten Geweben ab, und korreliert dies mit beobachteten Gewebeschädigungen? Wird die Substanz zu bioaktiven Metaboliten im Wurm umgesetzt? Exemplarisch wurden diese Fragestellungen für *S. mansoni* und *F. hepatica* beantwortet, welche *in vitro* mit dem Abl-Kinaseinhibitor Imatinib behandelt worden sind (Mokosch et al. 2021, Morawietz et al. 2020). Für *F. hepatica* wurden in diesem Zusammenhang detaillierte Analysen des mutmaßlichen Targets von Imatinib angestellt. Neben *in situ*-Hybridisierungen wurden anhand der zuvor

validierten qRT-PCR-Referenzgene Expressionsanalysen zu Abl-Kinasegenen durchgeführt. Abl-Kinasen waren in allen pathologisch relevanten Parasitenstadien hoch exprimiert, v.a. in der Gastrodermis (**Abb. 2 C**). Die erhöhte Expression eines Superoxiddismutase-Gens deutete überdies eine Induktion bzw. Abwehr oxidativen Stresses im Wurm nach Imatinib-Exposition an (Morawietz et al. 2020). Die Ergebnisse zur Targetcharakterisierung wurden von zwei meiner Doktoranden beigesteuert, Hicham Houhou und Oliver Puckelwaldt.

Nicht nur Proteinkinasen stellen aufgrund ihrer vielfältigen Rolle in der Zellbiologie, auch von Parasiten, attraktive Wirkstofftargets dar. Die gesteuerte Degradation zellulärer Bestandteile durch Autophagie ist ein weiterer fundamentaler Zellprozess (Klionsky and Emr 2000), dessen Inhibierung wahrscheinlich fatale Folgen für das Überleben von Zellen und damit des Parasiten hat. Diese Hypothese wurde in **Publikation 5** untersucht. Mit diesem Thema habe ich ein DAAD-Stipendium für einen Doktoranden der Veterinärmedizin eingeworben, Mudassar Mughal. Zunächst identifizierten wir bioinformatisch etliche konservierte Autophagiegene in *S. mansoni*. Anschließend wurde deren Expression mittels qRT-PCR und z.T. Western Blot untersucht. Pharmakologische Inhibierung der Autophagie im Wurm mit Inhibitoren aus der Humanforschung zeigten deutliche anthelmintische Wirkungen *in vitro*. U.a. war die Zellreifung in den Gonaden des Parasiten deutlich gestört; teilweise kam es zu Degradation von Zellen und ganzer Gewebe (Mughal et al. 2021). Autophagie-assoziierte Proteine stellen demnach mögliche Targets in der Wirkstoffforschung gegen *S. mansoni* dar.

Neben der Untersuchung synthetischer Wirkstoffe aus der Humanforschung gegen Trematoden (*drug repurposing*) und der Charakterisierung assoziierter Wirkstofftargets, liegt ein zweiter Forschungsfokus auf der Identifizierung anthelmintisch aktiver Naturstoffe aus Insekten. In den **Publikationen 6 und 7** wurden Substanzen aus dem Asiatischen Marienkäfer *Harmonia axyridis* und der Raubwanze *Rhynocoris iracundus in vitro* gegen Adultwürmer von *S. mansoni* getestet. Diese Ansätze stellen die ersten Untersuchungen dieser Art für Trematoden dar. Die Substanzen werden von den beiden Insektenspezies zur Verteidigung gegen Konkurrenten oder Prädatoren eingesetzt (Vilcinskas et al. 2013, Walker et al. 2016). Darüber hinaus offenbarten sie auch vielfältige antischistosomale Effekte: Reduktion der Vitalität, der Eiproduktion, z.T. Gewebeschädigungen von Darm, Gonaden und Tegument. Für die Substanzen beider Insektenspezies wurde überdies eine inhibitorische Wirkung auf die Stammzellproliferation im Parasiten festgestellt (Kellershohn et al. 2019, Tonk et al. 2020). Zur Quantifizierung solcher Stammzelleffekte wurde eine Fluoreszenzmikroskopie-basierte 3D-Analyse von Parasitenorganen etabliert (**Abb. 3**). Ein Großteil der Ergebnisse der beiden Studien wurde von zwei Studierenden, Zainab Waad Zadiq und Josina Kellershohn, im Rahmen ihrer Bachelor- bzw. Masterarbeiten erhalten, welche durch mich betreut wurden.

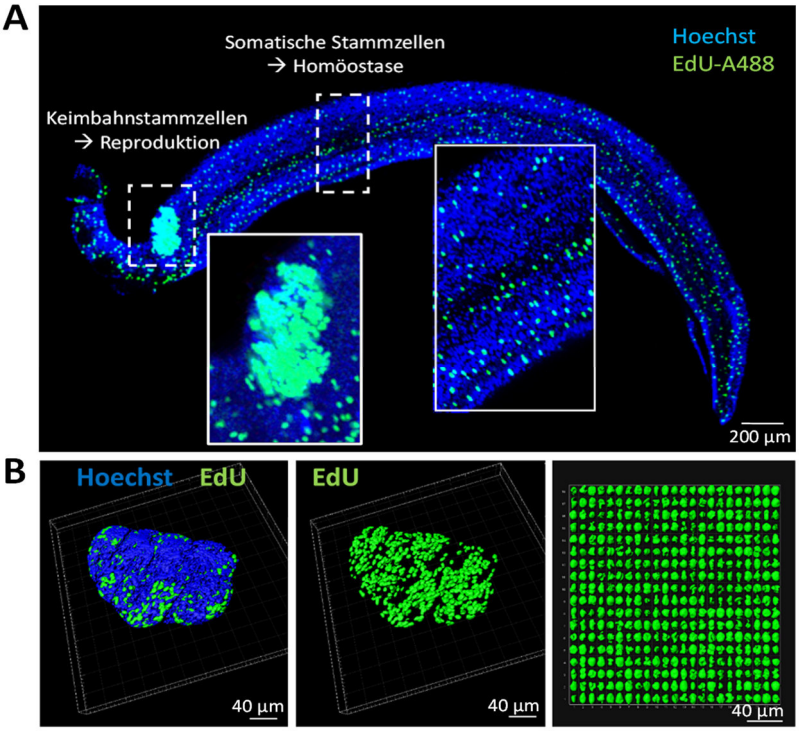

Abb. 3 Fluoreszenzmikroskopische Analyse von Stammzellproliferation in *Schistosoma mansoni*. (A) Das Basenanalogon EdU wird in neu gebildete DNA proliferierender Zellen (hier: Stammzellen, grün) des Parasiten integriert und über konfokale Laserscanning-Mikroskopie nachgewiesen. **(B)** 3D-Organrekonstruktionen erlauben die Quantifizierung der Stammzellzahl, um z.B. antiproliferative Effekte von Inhibitoren zu charakterisieren.

Zusammenfassend beinhaltet meine Forschungsarbeit verschiedenste interdisziplinäre methodische Ansätze, von *in vitro*-Kultursystemen verschiedener Parasitenstadien, genomischen und postgenomischen Methoden wie qRT-PCR und RNAi, bioinformatische Analysen, konfokale Laserscanningmikroskopie und in Kooperation AP-sMALDI-MS Imaging.

3 Übersicht der vorgelegten Publikationen

Publikation 1 **Haeberlein S**, Angrisano A, Quack T, Lu Z, Kellershohn J, Blohm A, Grevelding CG, Hahnel SR. Identification of a new panel of reference genes to study pairing-dependent gene expression in *Schistosoma mansoni*. **Int J Parasitol (2019)** 49:615-624

Publikation 2 Houhou H, Puckelwaldt O, Strube C, **Haeberlein S**. Reference gene analysis and its use for kinase expression profiling in *Fasciola hepatica*. **Sci Rep (2019)** 9:15867

Publikation 3 Mokosch A, Gerbig S, Grevelding CG, **Haeberlein S***, Spengler B*. High-resolution AP-SMALDI MSI as a new tool for drug imaging in *Schistosoma mansoni*. **Anal Bioanal Chem (2021)** 413:2755-2766

Publikation 4 Morawietz CM, Houhou H, Puckelwaldt O, Hehr L, Dreisbach D, Mokosch A, Roeb E, Roderfeld M, Spengler B*, **Haeberlein S***. Targeting kinases in *Fasciola hepatica*: anthelminthic effects and tissue distribution of selected kinase inhibitors. **Front Vet Sci (2020)** 7:611270

Publikation 5 Mughal MN, Grevelding CG, **Haeberlein S**. First characterization of autophagy-related genes in *Schistosoma mansoni.* **Int J Parasitol (2021)** S0020-7519:00092-8

Publikation 6 Kellershohn J, Thomas L, Grünweller A, Hartmann RK, Hardt M, Vilcinskas A, Grevelding CG, **Haeberlein S.** Insects in anthelminthics research: Lady beetle-derived harmonine affects survival, reproduction and stem cell proliferation of *Schistosoma mansoni*. **PLoS Negl Trop Dis (2019)** 13:e0007240

Publikation 7 Tonk M, Vilcinskas A, Grevelding, CG, **Haeberlein S.** Anthelminthic activity of assassin bug venom against the blood fluke *Schistosoma mansoni*. **Antibiotics (2020)** 9:664

4 Zusammenfassende Diskussion

4.1 *Drug Repurposing* gegen Trematoden

Unter *drug repurposing* versteht man den Einsatz bereits zugelassener Wirkstoffe für einen anderen Behandlungszweck. *Repurposing* hat zwei entscheidende Vorteile im Vergleich zur *de novo*-Wirkstoffentwicklung. Da eine Substanz essentielle präklinische und klinische Tests bereits erfolgreich absolviert hat, wird zum einen die Medikamentenzulassung erheblich beschleunigt, und zum anderen sind die Erfolgsaussichten bzgl. Aktivität und ausreichender Bioverfügbarkeit höher (Ashburn and Thor 2004). Damit einher gehen niedrigere Entwicklungskosten bis zum marktreifen Medikament, was speziell für im NTD-Bereich zum Einsatz kommende Präparate mit ihrer relativ geringen Gewinnspanne Relevanz besitzt. Die auf diese Weise erzielte Anwendungserweiterung von Wirkstoffen birgt jedoch eine Gefahr, wenn Zielproteine des Parasiten mit denen des Säugers in hohem Maße übereinstimmen. Targetprotein können evolutionär stark konserviert sein und daher in ähnlicher Form in den Erregern vorkommen. Es ist aber möglich, dass Zielmoleküle des Parasiten ausreichende Unterschiede zu den Orthologen infizierter Menschen oder Tiere aufweisen, was das Risiko möglicher Nebenwirkungen reduziert oder eine Basis für Wirkstoffmodifikation über chemische Derivatisierung darstellt. Schließlich können auch Behandlungszeiträume eine Rolle spielen, da antiparasitäre Wirkstoffapplikationen im Vergleich zu z.B. Tumor- oder Diabetestherapien deutlich kürzere Zeiträume umfassen. Daher kann *drug repurposing* auch in der Anthelmintika-Forschung eine nützliche Strategie sein (Panic et al. 2014).

Seit der Etablierung von *in vitro*-Kultursystemen für larvale und adulte Schistosomen können phänotypische Screenings *in vitro* durchgeführt werden, entweder für ausgewählte Wirkstoffe oder sogar ganze Wirkstoffbibliotheken. In einem *library screening* von 1600 Substanzen mit FDA-Zulassung wurden zwei im Tiermodel aktive Wirkstoffe gefunden (Panic et al. 2015). Insgesamt zeigten zugelassene Wirkstoffe aus der Krebs- und Malaria-forschung bislang die vielversprechendsten Ergebnisse (Panic et al. 2014). Bekannte Beispiele sind Tamoxifen, welches zur Therapie von Brustkrebs eingesetzt wird, oder die Antimalaria-Wirkstoffe Artesunat und Mefloquin (Pérez del Villar et al. 2012, Oliveira et al. 2019). Eine alternative Teststrategie ist das *in silico*-Screening von Substanzbibliotheken gegen Kristallstrukturen von im Erreger exprimierten möglichen Targetproteinen. In einer umfangreichen Studie wurden 97 von der FDA zugelassene Wirkstoffe virtuell gegen mehr als 500 schistosomale Proteine gescreent (Giuliani et al. 2018). Trotz der vielversprechenden Screeningergebnisse ist von einem Einsatz von Malariamedikamenten als Teil von Entwurmungsprogrammen insgesamt jedoch eher abzuraten, da bei vorhandenen Koinfektionen eine Ausbreitung bereits existierender Resistenzen gegen *Plasmodium* sp. zu befürchten ist (Keiser and Utzinger 2012).

In meinen eigenen Arbeiten konnte ich mittels phänotypischer Tests erstmals die antischistosomale Aktivität von Autophagieinhibitoren nachweisen (Mughal et al. 2021). Bafilomycin A, ein Makrolidantibiotikum und V-ATPase-Inhibitor, und der Phospho-inositid-3-kinase (PI3K)-Inhibitor Wortmannin reduzierten nicht nur die Fitness der Würmer, sondern schädigten spezifisch die Keimzellen in den Gonaden und beeinträchtigten

somit die Bildung von Eiern. Eine ähnliche Zellschädigung und Inhibierung der Proliferation wurde auch für gonadale Krebszellinien beschrieben (Peng et al. 2017, Wang et al. 2018). Wir vermuten, dass Autophagie u.a. für die Reproduktion von Schistosomen ein essentieller Prozess ist. Bafilomycin und Wortmannin sind zwar noch nicht als zugelassene Medikamente im Einsatz, aber präklinische Tests gegen Tumore waren vielversprechend (Ng et al. 2001, Yuan et al. 2015). Zukünftige antischistosomale Studien sollten z.B. Duvelisib testen, ein mittlerweile von der FDA zugelassener PI3K-Inhibitor (Rodrigues et al. 2019). Kombinationsbehandlung von Imatinib und Autophagieinhibitoren könnte außerdem einen potenzierenden Effekt gegen Schistosomen haben, ähnlich wie für die starke Antitumorwirkung dieser Kombination mehrfach gezeigt wurde (Aveic et al. 2018, Zheng et al. 2020).

Für *F. hepatica* fehlen bislang systematische Studien zum Potenzial des *drug repurposing*. Lediglich einige wenige, für andere Krankheiten zugelassene Wirkstoffe wurden getestet, wie Malaria-Medikamente, die sich jedoch aufgrund von Embryotoxizität im Schaf als unbrauchbar erwiesen (Keiser et al. 2006, Keiser et al. 2008). Mein Hauptfokus für *F. hepatica* liegt auf der Untersuchung von Proteinkinasen als mögliche therapeutische Targets. Durch das große Engagement der Pharmaindustrie bei der Etablierung von Kinaseinhibitoren als Chemotherapeutika gegen verschiedene Krebsformen wurden umfangreiche Substanzbibliotheken generiert, von denen die *Fasciola*-Forschung im Rahmen eines *drug repurposings* profitieren kann. Während mehrere Kinasen und Kinaseinhibitoren gegen Schistosomen bereits im Detail studiert wurden (Beckmann and Grevelding 2010, Long et al. 2010, Gelmedin et al. 2015), wurde für *F. hepatica* in der Vergangenheit nur eine einzige Kinase, eine Phosphofructokinase, als mögliches therapeutisches Target untersucht (Mansour and Mansour 1962, Fairweather et al. 1984). Die Untersuchungen mit einem Phosphofructokinaseinhibitor wurden jedoch aufgrund von geringer Effektivität im Tiermodel eingestellt (Schulman et al. 1982). Der Proteinkinasenhibitor Imatinib kam noch nie gegen *F. hepatica* zum Einsatz, trotz nachgewiesener *in vitro*-Aktivität gegen mehrere Helminthen (Beckmann and Grevelding 2010, Hemer and Brehm 2012, Li et al. 2019). Abl-Kinasen sind wichtige Regulatoren der Zelldifferenzierung und des zellulären Zytoskeletts in Eukaryoten (Yuan et al. 1997, Wang 2014). Aufgrund der hohen Konserviertheit von Abl-Kinasen und anderer Proteinkinasen ist es vielversprechend, Kinaseinhibitoren aus der Humanforschung auch gegen *Fasciola* zu testen. In der Tat konnte ich die Expression zweier Abl-Kinasen und drei weiterer Proteinkinasen in *F. hepatica* nachweisen, welche bereits als vielversprechende Targets in anderen Helminthenspezies diskutiert wurden. Die Expression der Abl1-Kinase war in *F. hepatica* stadienübergreifend ähnlich hoch (Houhou et al. 2019). Für den Abl-Kinaseinhibitor Imatinib zeigten wir nachfolgend eine deutliche, ebenfalls stadienübergreifende fasziolizide Wirkung *in vitro* (Morawietz et al. 2020). Über AP-sMALDI Imaging, *in situ*-Hybridisierung und qRT-PCR-Analysen wurden in der gleichen Studie Details zur Aufnahmeroute des Wirkstoffs, zur Gewebeexpression des vermuteten Targets sowie zu möglichen Wirkmechanismen erhalten werden (siehe Kapitel 4.3). Dies kann als Anreiz für zukünftige Studien zum systematischen Screening von Kinaseinhibitoren gegen *F. hepatica* dienen.

Im Hinblick auf eine mögliche Translation in die klinische Anwendung ist interessant, dass Imatinib adulte *F. hepatica in vitro* in einer Konzentration von 100-150 µM tötete. Dies

entspricht einer 2-3mal höheren Konzentration von Triclabendazol und weiterer fasziolizider Wirkstoffe wie Clorsulon und Closantel, für die wir letale Konzentrationen von 50 µM in unserem *in vitro*-Kultursystem erhielten, bei vergleichbarer Zytotoxizität gegen humane Zelllinien. Die Selektivität von Imatinib ist somit relativ vergleichbar zu den bereits zugelassenen Wirkstoffen, was eine *in vivo* Testung im Tier als nächsten Schritt motiviert. Ein bekanntes Problem besteht allerdings in der hohen Affinität von Imatinib für Serumproteine, was in vorangegangenen Studien die Aktivität im Schistosomen-Mausmodell stark beeinträchtigte (Beckmann et al. 2014). Bei der Planung von zukünftigen Experimenten ist daher zu beachten, dass die Plasmaproteinbindung, wie etwa des sauren α1-Glycoproteins (AGP), speziesspezifische Unterschiede aufweist (Eckersall et al. 2007, Filip et al. 2013, Smith and Waters 2018). Im Fall von Schaf-AGP wurde für mehrere Wirkstoffe gezeigt, dass diese mit geringerer Affinität banden verglichen mit AGP aus anderen Spezies (Hill et al. 1989, Son et al. 1998). Somit könnte das Schaf ein geeignetes Tiermodell für zukünftige Tests mit Imatinib sein. Da Imatinib zudem bei oraler Gabe Aktivität gegen Filarien im Menschen zeigte (O'Connell and Nutman 2017), ist auch die Behandlung der humanen Fasziolose im Bereich des Möglichen.

4.2 Insekten als innovative Quelle für neue anthelmintische Substanzen

Das Screening von Naturstoffbibliotheken ist wichtiger Bestandteil in der Wirkstoffforschung, wobei Pflanzen die mit Abstand am häufigsten genutzte Quelle für Antiparasitika darstellen (Tagboto and Townson 2001). Die Antimalaria-Wirkstoffe Artemisinin und Chloroquin sind einige der bekanntesten Beispiele solcher Naturstoffe. Auch Bakterien, wie *Streptomyces* sp., sind Quellen wichtiger Antiparasitika wie Ivermectin und Amphotericin B. Die Untersuchung von Naturstoffen aus Tieren, im Speziellen aus Insekten, steckt dagegen noch in den Anfängen (de Moraes 2015).

Nur sehr wenige Naturstoffe tierischen Ursprungs wurden bislang mit Hinblick auf eine anthelmintische Eigenschaft untersucht. Hierzu gehören Venome aus Skorpionen, Fröschen und Schlangen (El-Asmar et al. 1980, Stábeli et al. 2006, de Moraes et al. 2011, Hassan et al. 2016). Venome sind komplexe Gemische aus einer Vielzahl bioaktiver Produkte wie proteolytischer Enzyme, biogener Amine, neurotoxischer Peptide und Neurotransmitter (Walker et al. 2016). Unter den insektenstämmigen Naturstoffen sind bislang nur für Venom und Propolis der Honigbiene *Apis mellifera* antischistosomale Eigenschaften beschrieben worden. Propolis ist ein komplexes Bienenprodukt bestehend aus Steroiden, Terpenoiden, Polyphenolen und etlichen anorganischen Komponenten und wird in der Alternativmedizin aufgrund seiner antioxidativen, antibakteriellen und entzündungshemmenden Eigenschaften für verschiedene Leiden eingesetzt. Allerdings sind wissenschaftliche Studien bei Menschen rar (Daleprane and Abdalla 2013). Studienergebnisse zur Effektivität von Propolis gegen Schistosomen im Mausmodell sind widersprüchlich, was mit Unterschieden in der Komposition des Bienenprodukts je nach geographischer Lage korrelieren könnte (Mahmoud et al. 2014, Mohamed et al. 2016). Neben Propolis wurde auch für Bienenvenom eine gewisse anthelmintische Aktivität gezeigt (Mohamed et al. 2016). Bienenvenom ist ein komplexes Gemisch von Enzymen, biogenen Aminen und Peptiden und wird aufgrund

seiner antiinflammatorischen Eigenschaften in der Alternativmedizin zur Behandlung von Krebserkrankungen und inflammatorischen Erkrankungen eingesetzt (Oršolić 2012, Lee et al. 2015). Welche Einzelsubstanzen der Bienenprodukte für anthelmintische Effekte verantwortlich sind, ist bislang ungeklärt.

Wir konnten nun erstmals *in vitro*-Aktivität des Venoms einer Raubwanze, *R. iracundus*, gegen *S. mansoni* zeigen und so das Spektrum antischistosomaler Insektenvenome erweitern (Tonk et al. 2020). Raubwanzen (Reduviidae) sind eine Familie prädatorischer Insekten mit äußerst potenten Venomen, welche in Beutetiere – andere Invertebraten – injiziert werden, um diese zu paralysieren und zu verdauen (Edwards 1961, Hwang and Weirauch 2012, Walker et al. 2016). Die beobachtete Reduktion der Motilität bei Schistosomen erinnerte an diese paralytische Wirkung, während die Zellschädigung im Gewebe der Würmer durch proteolytische und zytolytische Verdauungsaktivität des Venoms erklärt werden könnte. Bei der Testung von Venomen ist auch deren mögliche unspezifische Zytotoxizität zu berücksichtigen, die ein Ausschlusskriterium für einen therapeutischen Einsatz wäre. Venom von *R. iracundus* zeigte eine vernachlässigbar geringe hämolytische Aktivität gegenüber Erythrozyten, jedoch müssen weitere Tests z.B. gegen Leberzelllinien durchgeführt werden, um auch hepatotoxische Effekte auszuschließen. Zu klären bleibt , welche der über 200 bioaktiven Einzelsubstanzen in Raubwanzenvenomen (Edwards 1961, Walker et al. 2016) für die antischistosomale Aktivität verantwortlich sind. Aktuell laufende Proteomanalysen des Venoms von *R. iracundus* (Dr. Miray Tonk, mündliche Mitteilung) und die Aufreinigung von Einzelsubstanzen werden eine Basis zur Identifizierung dieser Substanzen liefern.

Neben diesen Substanzgemischen wurden bislang nur sehr wenige definierte Einzelsubstanzen tierischen Ursprungs mit Hinblick auf antischistosomale Eigenschaften untersucht. *In vitro*-Aktivität zeigten bestimmte Glycoside (Echinoside und Holothurine) aus Seegurken und das antimikrobielle Peptid Dermaseptin 01 aus Hautsekreten von südamerikanischen Baumfröschen (de Moraes et al. 2011, Melek et al. 2012, Mona et al. 2012). Bislang war keine Einzelsubstanz aus Insekten mit antischistosomaler Wirkung bekannt. Wir konnten für das Alkaloid Harmonin aus dem Asiatischen Marienkäfer *H. axyridis* pleiotrope Effekte auf *S. mansoni in vitro* zeigen (Kellershohn et al. 2019). Eine Translation der Ergebnisse auf *F. hepatica* scheint vielversprechend, denn in ersten Tests tötete Harmonin NEJs innerhalb kürzester Zeit. Anhand unserer Daten kann man auf mehrere mögliche Wirkmechanismen des Harmonins schließen. Zum einen fanden wir eine reduzierte Zahl proliferierender Stammzellen in behandelten Würmern, was eine Inhibierung von am Zellzyklus beteiligten Targets nahelegt. Zum anderen inhibierte Harmonin die enzymatische Aktivität von Acetylcholinesterase (AChE) in Proteinextrakten der Würmer. Bestimmte Alkaloide aus Marienkäfern inhibierten nikotinische ACh-Rezeptoren bei Wirbeltieren (Leong et al. 2015) und könnten daher den Käfern zum Schutz vor Prädatoren dienen. Da Marienkäfer zudem von Nematoden befallen werden (Shapiro-Ilan and Cottrell 2005) ist anzunehmen, dass die Käfer ebenfalls ein Repertoire anthelmintischer Substanzen synthetisieren. Daher erscheint es wahrscheinlich, dass Marienkäfer der Gattung *Harmonia* sp. neben Harmonin noch weitere antischistosomale Substanzen besitzen. Alleine mehr als 500 antimikrobielle Peptide wurden in *H. axyridis* gefunden (Vogel et al. 2017).

Ein systematisches Screening von Naturstoffen aus Insekten ist momentan nur schwer möglich, denn es gibt keine frei zugänglichen Substanzbibliotheken, wie dies für andere Substanzgruppen der Fall ist (Panic et al. 2015). Auch ein *in silico*-Screening wäre nur mit großem Aufwand durchführbar, da keine für chemische Docking-Analysen aufbereitete Strukturbibliotheken existieren. In Kooperation mit dem Institut für Pharmazeutische Chemie der Universität Marburg habe ich kürzlich begonnen, über 3000 aufbereitete Molekülstrukturen aus Insekten mittels *in silico*-Docking gegen die Kristallstruktur der schistosomalen Thioredoxin-Glutathionreduktase (TGR) zu screenen, einem dokumentierten Target in Schistosomen (Kuntz et al. 2007). Hiervon erhoffen wir uns, neue TGR-Inhibitoren zu finden. Insgesamt demonstrieren die vorgestellten Pilotstudien, dass Insekten eine Fundgrube für Substanzen mit antischistosomaler Aktivität darstellen. Die Anthelmintika-Forschung sollte zukünftig ein integraler Bestandteil der Insektenbiotechnologie werden.

4.3 Neue Methoden in der Wirkstoffforschung gegen Trematoden

In meinen Arbeiten wurden verschiedene Methoden erstmalig für die Analyse von Wirkstoffen in Trematoden und deren anthelmintischer Effekte etabliert und eingesetzt. Dazu gehören AP-sMALDI MSI zum bildgebenden Nachweis von Wirkstoffen im Parasitengewebe, die Etablierung einer verlässlichen Genexpressionsanalyse durch bioinformatische und experimentelle Validierung von Referenzgenen, sowie die Quantifizierung von Stammzellen im Parasiten mittels 3D-Analysen nach Substanzbehandlung.

4.3.1 AP-sMALDI-MS Imaging zur Wirkstoffanalyse in Trematoden

Mit der Methode des AP-sMALDI-MS Imaging kann die Aufnahmeroute eines Wirkstoffs, dessen Metabolismus und Gewebetropismus in Trematoden aber auch anderen Pathogenen bildgebend untersucht werden. Diese Methodik stellt somit eine wertvolle Neuentwicklung in der Wirkstoffforschung dar. Die bislang gängigen Methoden zur Untersuchung der genannten Aspekte involvieren die radioaktive Markierung oder Fluoreszenzmarkierung einer Substanz (Ding et al. 2013). Beide Ansätze sind suboptimal, da radioaktives Arbeiten nur unter strengen Auflagen möglich ist, und das chemische Anfügen eines Fluorophors oftmals die chemische Struktur der Substanz grundlegend verändert, so dass deren Funktion und damit Aufnahme und Metabolisierung verändert werden können. Massenspektrometrie-Bildgebung hat dagegen den Vorteil, dass Moleküle in ihrem nativen Zustand ohne weitere chemische Markierung analysiert werden können (Rompp et al. 2011). Außerdem können hunderte Moleküle parallel im selben Gewebeschnitt detektiert werden. Für gewöhnlich wird MALDI-MSI für die Analyse von Phospholipiden oder kleineren Metaboliten genutzt, aber auch Peptide und exogene Moleküle wie Wirkstoffe sind detektierbar (Karlsson and Hanrieder 2017).

Unsere Arbeitsgruppe konnte in der Vergangenheit gemeinsam mit Kooperationspartnern AP-sMALDI MSI für die Visualisierung von endogenen Lipidverteilungen in *S. mansoni* etablieren (Kadesch et al. 2019). Im Rahmen meiner Arbeiten konnte die Methode

erfolgreich auf die Detektion eines Wirkstoffs (Imatinib) ausgeweitet und für einen weiteren Erreger, *F. hepatica*, etabliert werden (Morawietz et al. 2020, Mokosch et al. 2021). Unsere Ergebnisse zum *drug imaging* in *S. mansoni* und *F. hepatica* zeigten, dass Imatinib oral von den Würmern aufgenommen wird, da bereits zu einem sehr frühen Behandlungszeitpunkt deutliche Mengen der Substanz vorrangig im Gastrodermisgewebe detektiert wurden. Die intestinale Lokalisierung korrelierte zudem mit einer starken Schädigung von Darmgewebe in *S. mansoni*. Beide Befunde stimmen auch mit der gastrodermalen Lokalisierung von Abl-Kinasen als mutmaßlichen Targets überein, wie ich für *F. hepatica* bzw. frühere Studien unserer Arbeitsgruppe für *S. mansoni* zeigen konnten (Beckmann and Grevelding 2010). Gepaarte *S. mansoni*-Weibchen wiesen eine verzögerte Kinetik der Imatinibaufnahme auf. Eine Erklärung könnte die geschützte Lage des Weibchens im gynäkophoren Kanal des Männchens sein. Auch zwischen den beiden Parasitenspezies bestand eine unterschiedliche Kinetik bei derselben Imatinib-Konzentration. In männlichen Schistosomen war die Substanz bereits nach zwanzig Minuten im gesamten Gewebe der Würmer nachweisbar, während Imatinib im Leberegel erst nach einer Stunde deutlich detektierbar war. Eine Erklärung hierfür könnte die ausgedehnte Größe des Leberegels und stark verzweigte Darmstruktur im Vergleich zu Schistosomen sein, was die Wirkstoffverteilung beeinflusst. Schließlich haben wir im Gewebe beider Spezies eine Metabolisierung von Imatinib zu N-Demethyl-Imatinib nachgewiesen, dem Abl-Kinase-inhibierenden Metabolit, welches auch im Menschen gebildet wird (Mlejnek et al. 2011). Unsere bioinformatische Analysen zeigten die Expression von Cytochrom p450 2C8 im Parasiten, welches im Menschen für die Metabolisierung verantwortlich ist (Nebot et al. 2010). Es ist anzunehmen, dass das Metabolit zur anthelmintischen Aktivität von Imatinib beiträgt.

4.3.2 Genexpressionsanalysen in Trematoden mittels qRT-PCR

Genexpressionsanalysen sind in der Wirkstoffforschung gegen Trematoden in dreierlei Hinsicht von Interesse: (1) Genexpressionen, welche nach Substanzbehandlung im Parasiten verändert sind, lassen Rückschlüsse auf mögliche Wirkmechanismen zu; (2) Kenntnisse über stadienübergreifende Expression eines Wirkstofftargets sind nützlich zur Abschätzung, ob ein Wirkstoff gegen alle pathologisch relevanten Parasitenstadien (Juvenile, Adulte) aktiv sein kann; und (3) RNAi wird in Trematoden immer häufiger zur genetischen Targetvalidierung eingesetzt (Wang et al. 2020), was eine Genexpressionsanalyse zur Überprüfung des erfolgreichen *Knockdowns* des Zielgenes einschließt. Als Goldstandard für die Quantifizierung von Genexpression gilt die qRT-PCR (Endrullat et al. 2016, Costa-Silva et al. 2017). Auch globale Transkriptomanalysen Substanz-behandelter Würmer z.B. über RNAseq werden durchgeführt (Buro et al. 2014). Ausgewählte Expressionsunterschiede sollten aber im Sinne guter wissenschaftlicher Praxis anschließend ebenfalls über qRT-PCR validiert werden. Allzu häufig wird für die relative Quantifizierung in qRT-PCR Experimenten auf *housekeeping*-Gene wie *ß-actin*, *tubulin* oder *gapdh* zurückgegriffen, bei welchen davon ausgegangen wird, dass diese unveränderlich in Zellen exprimiert werden, so auch in etlichen Helminthen-Studien (Rinaldi et al. 2008, Hahnel et al. 2014, McVeigh et al. 2014, Cwiklinski et al. 2018). Diese Wahl geschieht häufig mehr aus Tradition als auf auf Basis experimentell validierter Daten. Sehr häufig sind diese Gene tatsächlich

differentiell exprimiert - in Abhängigkeit vom Entwicklungsstadium, dem Alter, dem Gewebetyp oder experimentellen Bedingungen (Chapman and Waldenström 2015). Auch unsere eigenen Analysen zeigten dies für die *housekeeper*-Gene *gapdh* und *actin* in Schistosomen und dem Leberegel (Haeberlein et al. 2019, Houhou et al. 2019). Da mit einem differentiell regulierten Referenzgen die relativen Expressionswerte sämtlicher Zielgene bei qRT-PCR-Analysen zu falschen Ergebnissen führen, ist eine vorherige Validierung von Referenzgenen elementar. Dies wird über bioinformatische Analysen von qRT-PCR-Daten mehrerer Referenzgenkandidaten erzielt (Vandesompele et al. 2002, Hayes et al. 2011). Mit diesem Vorgehen identifizierten und validierten wir jeweils zwei Referenzgene für *S. mansoni* und *F. hepatica*, die zukünftig in qRT-PCR-Analysen im Kontext von *in vitro*-Kultur der Parasiten oder eines Stadienvergleichs zum Einsatz kommen können.

Ein Anspruch heutiger Wirkstoffforschung ist es, den Wirkmechanismus einer Substanz zu verstehen. Genexpressionsanalysen von substanzbehandelten Erregern können hier aufschlussreich sein. Um einen ersten Einblick in die Wirkungsweise von Imatinib in *F. hepatica* zu erhalten, quantifizierten wir die Expression von Genen mit Beteiligung an der Regulation von oxidativem Stress, Zellzyklus und *drug efflux* aus Zellen (Morawietz et al. 2020). Ein *multi-drug-resistance* (*mdr*)-Gen, das für eine Efflux-Pumpe kodiert, sowie Superoxiddismutase-Gene waren nach Imatinib-Behandlung transkriptionell hochreguliert. Beides könnte auf eine „Verteidigungsstrategie“ des Parasiten gegen den Wirkstoff und durch ihn entstandenen oxidativen Stress hinweisen. Eine Ko-Behandlung mit Imatinib und einem Inhibitor dieser regulatorischen Prozesse könnte demnach eine verstärkende fasziolizide Aktivität haben. Reaktive Sauerstoffspezies verursachen DNA-Schäden (Slupphaug et al. 2003), was zum beobachteten anthelmintischen Effekt von Imatinib beitragen könnte.

Genexpressionsanalysen durch qRT-PCR können überdies Aufschluss über stadienspezifische versus –übergreifende Expression von Targetgenen geben. Gerade für Trematoden mit ihren verschiedenen, pathologisch relevanten Stadien von Juvenilen zu Adulten ist es relevant, zu wissen, ob ein Wirkstofftarget in all diesen Stadien exprimiert ist. Dies ist nicht selbstverständlich, denn so wie sich metabolische Bedürfnisse im Laufe der Entwicklung ändern, so verändert sich auch das Transkriptom wie u.a. für *F. hepatica* gezeigt wurde (Robinson et al. 2009, Di Maggio et al. 2016). Nur bei stadienübergreifender Expression eines Targets ist gewährleistet, dass ein entsprechender Inhibitor gegen alle untersuchten Stadien aktiv ist. Auch für derartige Expressionsanalysen ist die Kenntnis über stadienunabhängig, stabil exprimierte Referenzgene essentiell. Meine Referenzgen-basierten Expressionsanalysen für *F. hepatica* gaben hilfreiche Hinweise auf Expressionsmuster für fünf verschiedene Kinasegene, wobei eine Abl-Kinase sehr hoch in allen pathologisch relevanten Stadien exprimiert war. Hingegen dominierte die Expression einer Polo-Kinase in Adulten, was für eine Rolle bei der Reproduktion sprechen könnte.

4.3.3 Quantifizierung von Stammzellaktivität nach Substanzbehandlung

Die Wichtigkeit von Stammzellen für Wachstum und Entwicklung wurde bereits für verschiedene Helminthen gezeigt, einschließlich *S. mansoni* und *F. hepatica* (Koziol et al. 2014, McCusker et al. 2016, Wendt and Collins 2016). Substanzen, die mit der Stammzellaktivität der Parasiten interferieren, sind daher attraktive Wirkstoffkandidaten. Um Substanzeffekte auf Stammzellen in Trematoden quantitativ zu erfassen, wurden eine bildgebende und eine molekularbiologische Methode etabliert. Das Basenanalogon EdU (5-Ethynyl-2-deoxyuridin) wird während der S-Phase des Zellzyklus in neu gebildete DNA eingebaut (Buck et al. 2008) und nach Fluoreszenzmarkierung über konfokale Laserscanning-Mikroskopie im Parasiten nachgewiesen. Durch 3D-Rekonstruktion ausgewählter Gewebebereiche basierend auf über hundert fluoreszenzmikroskopischen Einzelbildern erzielten wir eine Quantifizierung teilungsaktiver Zellen. Da in Trematoden Stammzellen die einzigen proliferierenden Zellen sind (Collins et al. 2013), kann mittels der EdU-Methode eine Aussage über die absolute Zahl teilungsaktiver Stammzellen pro Gewebevolumen, pro Organ (z.B. Gonade) oder pro Gesamtzellzahl (bezogen auf die Zahl Hoechst-positiver Zellkerne) getroffen werden. Neben der bildgebenden Quantifizierung von Stammzelleffekten haben wir die Quantifizierung von Stammzellmarkergenen mittels qRT-PCR als weitere Methode eingeführt. Sind Stammzellen in ihrer Transkriptionsaktivität global betroffen, oder sinkt deren Zahl im Gewebe durch Blockade der Proliferation bzw. Zelltod, so sinkt auch die relative Menge solcher Stammzell-assoziierten Transkripte im Gewebe. Als Markergene nutzten wir *nanos-1* und *nanos-2* (Collins et al. 2013), die für RNA-Bindeproteine kodieren und für den Erhalt des Stammzellpools in Metazoen wichtig sind (Wang et al. 2007, Giri et al. 2017).

Für die Substanzen zweier Insektenspezies zeigten wir eine inhibitorische Wirkung auf die Stammzellproliferation und die –markergenexpression im Parasiten (Kellershohn et al. 2019, Tonk et al. 2020). Unklar ist, ob die reduzierte Zahl teilungsaktiver Stammzellen im Gewebe auf eine (reversible) Blockade des Zellzyklus oder alternativ auf den Tod der Stammzellen zurückzuführen ist – beides kann mit der EdU-Methode nicht unterschieden werden. In zukünftigen Studien sollte auch die Frage nach der Reversibilität von Effekten adressiert werden, indem die Testsubstanz nach einer gewissen Zeit wieder vom Parasiten entfernt und dieser weiterkultiviert wird („*wash-out*“). Liegt ein reversibler Effekt auf Stammzellen vor, würde die Zahl EdU-positiver Zellen in diesem Fall wieder steigen. Auch bleibt zu klären, ob die Substanzen als spezifische Inhibitoren von zellteilungsrelevanten Stammzellproteinen agieren, oder ob die Reduktion von Zellteilungsaktivität eine unspezifische Reaktion des Parasiten bei der Reduktion der Fitness ist. Das könnte z.B. durch die stressbedingte Bildung reaktiver Sauerstoffradikale induziert sein, welche sich negativ auf den Zellzyklus auswirken (Shenberger and Dixon 1999, Carrasco-Torres et al. 2017). Im Fall von Imatinib liegt wahrscheinlich letzteres vor, denn die Beeinträchtigung der Proliferationsaktivität in Würmern (unveröffentlichte Daten) ging mit einer erhöhten Expression von Superoxiddismutasegenen einher (Morawietz et al. 2020), die für die Bewältigung von oxidativem Stress in diesem Parasiten wichtig sind (Aragon et al. 2008).

4.4 Perspektiven in der Target- und Wirkstoffforschung gegen Schistosomen und Leberegel

4.4.1 Zukünftige Innovationen in der Wirkstoffforschung

Sowohl im Bereich der Wirkstofftestung und -charakterisierung als auch der Target-identifizierung soll in den nächsten Jahren weitere Etablierungsarbeit für *S. mansoni* und *F. hepatica* geleistet werden. Auf Seite der Wirkstoffe stellte sich heraus, dass antischistosomale Aktivität von Substanzen häufig mit einer **Inhibierung von Stammzellen** im Parasiten einherzugehen scheint, wie ich für zwei Naturstoffe aus Insekten nachweisen konnte. Noch nicht publizierte Daten zeigten ebenfalls eine Reduktion der Stammzell-proliferation in *S. mansoni* nach Behandlung mit dem Krebswirkstoff Imatinib und dem Aldehyddehydrogenase-Inhibitor Disulfiram, der seit einigen Jahren als vielversprechender Antitumor-Wirkstoff untersucht wird (Lu et al. 2021). Dass viele antitumorale Wirkstoffe gegen Schistosomen und andere Trematoden aktiv sind, ist vermutlich kein Zufall, denn Wirkstoffe, die Tumorstammzellen inhibieren (Shibata and Hoque 2019, Lernoux et al. 2020), könnten auch proliferativ hochaktive Stammzellen in Trematoden schädigen. Zukünftige phänotypische Screenings von Substanzbibliotheken gegen Schistosomen könnten daher einen besonderen Fokus auf bekanntermaßen Tumorstammzell-inhibierende Wirkstoffe legen.

Ähnlich wie in der Krebstherapie könnten außerdem **Kombinationstherapien** (Bayat Mokhtari et al. 2017) eines Erregers mit zwei Wirkstoffen bei der Behandlung von Trematodeninfektionen vielversprechend sein. Die Hauptvorteile einer Kombination zweier Wirkstoffe sind die Minimierung des Risikos von Resistenzentwicklung, da gleich mehrere Targets attackiert werden, und natürlich additive oder gar synergistische Effekte gegen den Erreger. Letzteres ermöglicht den Einsatz geringerer Dosen und minimiert dadurch Nebenwirkungen (Cheng et al. 2019). Eine erste klinische Studie zur Therapie von *S. mansoni*-Infektion ergab eine höhere Wirksamkeit bei gleichzeitiger Behandlung mit Praziquantel und einem Artemisinin-Kombinationspräparat im Vergleich zu alleiniger Gabe von Praziquantel (Mnkugwe et al. 2020). Im Schaf reduzierte eine Kombinationsbehandlung mit den beiden Standardmedikamenten Triclabendazol und Clorsulon die Zahl Triclabendazol-resistenter Leberegel um 95% und damit deutlich mehr als bei Monotherapie (Fairweather and Boray 1999). Im Bereich der Grundlagenforschung wurden kürzlich synergistische Effekte gegen *S. mansoni* bei Kombination von Praziquantel mit ausgewählten Kinaseinhibitoren gezeigt (Nawaratna et al. 2020). Die Wirkstoffe Imatinib und Disulfiram, für die ich jeweils antischistosomale und fasziolizide Aktivität gezeigt habe, sollten ebenfalls in einem nächsten Schritt *in vitro* kombiniert getestet werden. Dasselbe gilt für Imatinib plus Autophagieinhibitoren. Für beide Kombinationen wurden bereits synergistische Wirkungen gegen Tumorzellen erzielt (Aveic et al. 2018, Hassan et al. 2018, Zheng et al. 2020). Daher könnten Kombinationstherapien zukünftig systematisch gegen Schistosomen und Leberegel getestet werden.

4.4.2 Zukünftige Innovationen in der Targetforschung

Auf Seite der Targetforschung wurden sowohl für Schistosomen als auch für *F. gigantica* in den vergangenen Jahren umfangreiche **Kinomdatensätze** erstellt, welche als Basis für *in silico*-Substanzscreenings und zur Priorisierung von Kinasen für experimentelle Targetanalysen dienen (Giuliani et al. 2018, Das et al. 2020). Ich möchte in einem nächsten Schritt das Kinom von *F. hepatica* analysieren, um letztlich therapeutisch relevante Proteinkinasen zu identifizieren. Darüber hinaus ist eine Validierung von Targets im Leberegel wünschenswert, wie Abl-Kinasen und Aldehyddehydrogenasen, um deren biologische Funktion und Bedeutung für die Überlebensfähigkeit des Parasiten zu untersuchen. Zu diesem Zweck soll RNAi als Methode der Genfunktionsanalyse für adulte Leberegel etabliert werden, die momentan einzige in Trematoden praktikable Methode zur Modulation von Genexpression.

Um schließlich weitere Einblicke in zelltypspezifische Targets, wie etwa Stammzellgene, zu erhalten, wären organ- und **zelltypspezifische Transkriptomdaten** für *F. hepatica* ideal. In einem aktuellen DFG-geförderten Projekt möchte ich zu diesem Zweck Einzelzell-Transkriptom-Datensätze für *F. hepatica* mittels der 10X *single cell* RNAseq-Methodik erstellen. Ein ähnlicher Datensatz wurde kürzlich für *S. mansoni* generiert – ein Meilenstein der Trematodenforschung (Wendt et al. 2020). Die Einzelzellanalysen werden neue mögliche zellspezifische Targets sowie deren Gewebezugehörigkeit in *F. hepatica* aufzeigen. Beides kann für zukünftige Wirkstoffentwicklungen bedeutend sein.

5 Vorgelegte Publikationen

5.1 Identifizierung von Referenzgenen zur Analyse paarungsabhängiger Genexpression in *Schistosoma mansoni*

Identification of a new panel of reference genes to study pairing-dependent gene expression in *Schistosoma mansoni*

Haeberlein S, Angrisano A, Quack T, Lu Z, Kellershohn J, Blohm A, Grevelding CG, Hahnel SR

International Journal of Parasitology (2019) 49(8):615-624

Publikation online: doi: 10.1016/j.ijpara.2019.01.006

Eigener Anteil an der Entstehung der Publikation

- Leitung des Gesamtprojektes: 30%
- Durchführung/Auswertung der Experimente: 70%
- Anfertigung des Manuskripts: 10%

5.2 Referenzgen-Analyse und der Einsatz zur Expressionsanalyse von Kinasen im Leberegel *Fasciola hepatica*

Reference gene analysis and its use for kinase expression profiling in *Fasciola hepatica*

Houhou H, Puckelwaldt O, Strube C, **Haeberlein S**

Scientific Reports (2019) 9(1):15867

Eigener Anteil an der Entstehung der Publikation

- Leitung des Gesamtprojektes: 100%
- Durchführung/Auswertung der Experimente: 10%
- Anfertigung des Manuskripts: 80%

www.nature.com/scientificreports

SCIENTIFIC REPORTS
nature research

OPEN

Reference gene analysis and its use for kinase expression profiling in *Fasciola hepatica*

Hicham Houhou[1], Oliver Puckelwaldt[1], Christina Strube[2] & Simone Haeberlein[1*]

The liver fluke *Fasciola hepatica* causes fasciolosis, a foodborne zoonosis affecting humans and livestock worldwide. A reliable quantification of gene expression in all parasite life stages relevant for targeting by anthelmintics in the mammalian host is fundamental. The aim of this study was to define a set of stably expressed reference genes for qRT-PCR in *Fasciola* studies. We determined the expression stabilities of eight candidate reference genes by the algorithms NormFinder, geNorm, BestKeeper, and comparative ΔCT method. The most stably expressed reference genes for the comparison of intra-mammalian life stages were glutamyl-prolyl-tRNA synthetase (Fh*eprs*) and tubulin-specific chaperone D (Fh*tbcd*). The two best reference genes for analysis of *in vitro*-cultured juveniles were Fh*tbcd* and proteasome subunit beta type-7 (Fh*psmb7*). These genes should replace the housekeeping gene *gapdh* which is used in most *Fasciola* studies to date, but in fact was differentially expressed in our analysis. Based on the new reference genes, we quantified expression of five kinases (Abl1, Abl2, PKC, Akt1, Plk1) discussed as targets in other parasitic flatworms. Distinct expression patterns throughout development were revealed and point to interesting biological functions. We like to motivate using this set of validated reference genes for future *F. hepatica* research, such as studies on drug targets or parasite development.

The liver fluke *Fasciola hepatica* is a cosmopolitan parasitic flatworm causing zoonotic disease in humans and tremendous economic losses by infecting livestock[1]. The life cycle of *F. hepatica* is complex and includes a snail as an intermediate host and a mammal as a definitive host. The fluke develops through multiple stages: from eggs to miracidia, sporocysts, rediae, cercariae, metacercariae, newly excysted juveniles (NEJs), and immature flukes which eventually reach the adult stage. Molecular research on this and other helminths has considerably advanced in recent years, with genome data and tools such as RNA interference (RNAi) becoming available for these complex multicellular organisms. Relative quantification of gene expression by quantitative real-time PCR (qRT-PCR) is an essential component of many experimental approaches. The accuracy of such relative gene expression analyses is largely dependent on the stable expression of the reference genes used for normalisation. Housekeeping genes are typically used as reference in qRT-PCR, although in some cases their expression is known to vary in helminths depending on the experimental condition, the parasite stage, or the parasite's sex[2–4]. Classical housekeeping genes such as glyceraldehyde-3-phosphate dehydrogenase (*gapdh*) and *ß-actin* have often been used based on tradition rather than being experimentally validated as stably expressed genes for the species or parasite stage of interest. However, the validation of expression stabilities of reference genes under the desired experimental conditions is an essential step, which should precede any comparative studies on expression levels of target genes.

Comparative gene expression analysis in different life-stages is of major interest in *F. hepatica* research. This includes for instance the validation of expression of potential drug target genes. A new active compound should ideally target all life stages within the final host, including NEJs emerging from metacercariae in the host's intestine, immature flukes migrating through the body cavity to the liver capsule and through the liver parenchyma causing acute fascioliasis, and adult flukes, which trigger chronic fascioliasis while residing inside the bile ducts where egg deposition occurs[5]. Gene expression often varies between intra-mammalian life stages of *F. hepatica* as metabolic, nutritional and locomotor demands vary between stages[6,7]. Other research approaches include the *in vitro* culture of flukes, such as the recently established *in vitro* maturation of NEJs to immature flukes in order to study early development[8], or RNAi-mediated knockdown of gene expression which might involve culture for more

[1]Institute of Parasitology, BFS, Justus Liebig University, Giessen, Germany. [2]Institute for Parasitology, Centre for Infection Medicine, University of Veterinary Medicine Hanover, Hanover, Germany. *email: simone.haeberlein@vetmed.uni-giessen.de

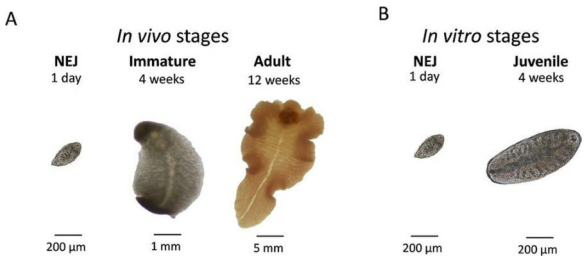

Figure 1. *In vivo* and *in vitro* stages of *F. hepatica* under investigation. Stably expressed reference genes were identified for the comparison of gene expression of (**A**) newly excysted juveniles (NEJs), immature and adult worms, i.e. stages relevant for the mammalian host; and (**B**) NEJs and *in vitro*-cultured juvenile worms, which are frequently studied as part of drug testing or knockdown of gene expression.

than 3 weeks[9]. Gene expression stability in parasites during *in vitro* culture is likely to differ from non-cultured parasites, because of the known differences from the *in vitro* conditions compared to the natural environment provided by the host. This motivated us to identify reference genes with stable expression in the intra-mammalian life stages and during *in vitro* culture of *F. hepatica*. To this end, we used four different algorithms to assess eight different candidate reference genes and their expression stability in the relevant *in vivo*-stages (NEJs, 4 week-old immature flukes, 12-week old adults), and in juvenile flukes cultured for 4 weeks *in vitro*. Out of these candidate genes, three were identified as the most stably expressed reference genes.

As a first application example, we utilised these selected reference genes to determine the expression level of potentially druggable target genes in the different life stages and during *in vitro* culture. Kinases are discussed as promising drug targets in parasitic flatworms[10,11]. For instance, promising anthelmintic effects were observed in immature and adult schistosomes by RNAi or inhibitor treatment against Abelson (Abl) tyrosine kinases and polo-like kinases (PLK)[12–15]. Surprisingly, in *Fasciola* research, kinases as drug targets have been largely neglected so far although new anthelmintics are urgently needed facing the spread of triclabendazole resistance around the globe[1,16,17]. We have identified five kinase orthologs in *F. hepatica* and characterised their expression by qRT-PCR. Based on the new reference genes, an interesting change in kinase expression patterns during fluke development was obtained. This may substantiate further research activity on kinases in *F. hepatica*.

Results

Selection of candidate reference genes. Eight different candidate reference genes were chosen among which we assumed to find stably expressed reference genes suitable for the quantification of gene expression independent from the parasite stage or *in vitro* cultivation (Fig. 1). The candidates were selected based on already available transcriptome datasets or literature on related trematode species. The candidate reference gene names, biological function and accession numbers are listed in Table 1. In detail, orthologs of two of the genes were previously shown to be stably expressed in selected life stages of the Chinese liver fluke *Clonorchis sinensis*[2]: β-actin (*actb*) and small nuclear ribonucleoprotein (*snrpa1*). Another two candidate genes were chosen because previous transcriptome analyses suggested a stable expression of their orthologs in all life stages of the blood fluke *Schistosoma mansoni*[18]: tubulin-specific chaperone D (*tbcd*) and protein phosphatase 1 catalytic subunit beta (*ppp1cb*). Two candidates were selected because we found them to be most stably expressed during *in vitro* culture of *S. mansoni*[4]: leucine zipper and EF-hand containing transmembrane protein 1 (*letm1*) and proteasome subunit beta type-7 (*psmb7*). The ortholog of a glutamyl-prolyl-tRNA synthetase (*eprs*) was included based on its stable expression in different strains of *F. hepatica*[19]. Finally, for comparison, we included the well-known housekeeping gene *gapdh*, which is currently widely used for normalisation also in *F. hepatica* studies[9,20,21]. Thus, all reference gene candidates play roles in conserved cellular processes like mRNA splicing and translation, cytoskeleton arrangement, glycolysis, mitochondrial organisation, and the regulation of cell growth (Table 1). Orthologs for all eight genes were identified by BLASTp search of known genes in *Homo sapiens* (accession numbers see Table 1) against the genome of *F. hepatica*. The presence of relevant conserved protein domains was confirmed by SMART analysis (see Supplementary Fig. S1). The identity of the orthologs was further confirmed by multiple alignment of the amino acid sequences with those of model species (see Supplementary Table S1 and Fig. S8).

RNA quality of parasite samples and performance of qRT-PCR primers. Isolation of sufficient amounts of high-quality RNA from low numbers of NEJs is often problematic because of their small size. Using the Monarch RNA Extraction Kit, we managed to isolate and analyse RNA from as little as 10 NEJs. Representative electropherograms from BioAnalyzer analysis of RNA quantity and quality are shown in Supplementary Fig. S2. From 10 and 20 NEJs, we obtained in average 4–6 ng and 9–14 ng RNA, respectively. A good RNA integrity was reflected by the distinct 18 S RNA peak. Primer specificity was confirmed by PCR yielding one specific amplification product of expected size (see Supplementary Table S2) for each candidate reference gene, without primer-dimer formation or genomic DNA contamination. The primer sequences and amplicon lengths can be found in Supplementary Table S2. Absence of unspecific products was also confirmed by melt-curve analysis, which showed a single peak. The expression level of the eight candidate reference genes was assessed by qRT-PCR by determining the Ct value for each sample. With average Ct values of 15.27 to 27.63, all candidate genes were within the range of an acceptable reference gene expression level ($15 < Ct < 30$) (Fig. 2). The highest expression was found for Fh*gapdh*, and the lowest for Fh*ppp1cb*.

Gene name	Gene ID	Homology (e-value)*	Protein function
Fh*tbcd*	maker-scaffold10x_815_pilon-snap-gene-1.87	Tubulin-specific chaperone D [*H. sapiens*, NP_005984.3] (7e-177)	Cofactor D is one of four proteins involved in the pathway leading to correctly folded beta-tubulin from folding intermediates.
Fh*eprs*	maker-scaffold10x_14_pilon-snap-gene-0.109	Glutamyl-prolyl-tRNA synthetase [*H. sapiens*, NP_004437.2] (0.0)	The protein encoded by this gene is a multifunctional aminoacyl-tRNA synthetase that catalyses the aminoacylation of glutamic acid and proline tRNA species.
Fh*letm1*	maker-scaffold10x_721_pilon-snap-gene-0.10	Leucine zipper and EF-hand containing transmembrane protein 1 [*Homo sapiens*, NP_036450.1] (2e-85)	The protein functions to maintain the mitochondrial tubular shapes and is required for normal mitochondrial morphology and cellular viability.
Fh*actb*	augustus_masked-scaffold10x_269_pilon-processed-gene-0.18	Actin, cytoplasmic 1 [*H. sapiens*, NP_001092.1] (0.0)	Actins are highly conserved proteins that are involved in cell motility, structure, integrity and intracellular signaling. The encoded protein is a major constituent of the contractile apparatus and one of the two non-muscle cytoskeletal actins that are ubiquitously expressed.
Fh*snrpa1*	maker-scaffold10x_234_pilon-snap-gene-0.20	U2 small nuclear ribonucleoprotein A' [*H. sapiens*, NP_003081.2] (5e-72)	This gene encodes a protein which is a component of the spliceosome and it is involved in pre-mRNA splicing.
Fh*ppp1cb*	maker-scaffold10x_238_pilon-snap-gene-0.95	Protein phosphatase 1 catalytic subunit beta [*H. sapiens*, NP_002700.1] (0.0)	The protein encoded by this gene is one of the three catalytic subunits of protein phosphatase 1 (PP1). PP1 is a serine/threonine specific protein phosphatase known to be involved in the regulation of a variety of cellular processes.
Fh*psmb7*	maker-scaffold10x_1452_pilon-augustus-gene-0.11	Proteasome subunit beta type-7 [*H. sapiens*, NP_002790.1] (1e-79)	Important component of the cellular protein degradation complex.
Fh*gapdh*	maker-scaffold10x_2706_pilon-snap-gene-0.15	Glyceraldehyde-3-phosphate dehydrogenase [*H. sapiens*, NP_001276674.1] (0.0)	GAPDH catalyzes the sixth step of the glycolysis by converting D-glyceraldehyde 3-phosphate to 3-phospho-D-glyceroyl phosphate.

Table 1. Overview of candidate reference genes for the study of gene expression in *F. hepatica*. *Determined by NCBI BLAST.

Identification of the most stably expressed reference genes. Expression stabilities of the eight candidate reference genes were determined by four different algorithms: NormFinder, geNorm, BestKeeper, and the comparative ΔCt method. As input data, we used expression values either of different intra-mammalian stages (NEJs, 4 week-old immature flukes, 12 week-old adults), or of NEJs prior and after 4 weeks of *in vitro*-culture (then called 4 week-old juveniles) (Fig. 1). Transcript levels for all samples were determined by absolute quantification against a standard curve. Input data for stability analysis were raw Ct values (BestKeeper), relative Ct values (geNorm, ΔCt method), and calculated concentrations of amplification products (NormFinder), respectively. The most stably expressed reference gene has a low stability value (NormFinder, geNorm, ΔCt method), or a high coefficient of correlation (BestKeeper).

Expression stability of candidate reference genes in different fluke stages. In a first step, the expression stabilities of the selected candidate genes between three different fluke stages relevant for the final host were determined. The obtained ranking of each algorithm is summarised in Fig. 3 and Supplementary Table S3.

NormFinder ranks genes according to their stability value M, which is based on the size of intra- and inter-group expression variations, i.e. the variation within an experimental group (here: biological replicates) and between different experimental groups (here: fluke stages). A good reference gene is characterised by an M value below 1 in heterogeneous cell or tissue sample sets (Vandesompele 2002). NormFinder identified the tRNA-synthetase Fh*eprs* and the proteasome subunit Fh*psmb7* as the two best candidates, whereas Fh*gapdh* turned out to be the least stably transcribed gene in a combined analysis of all fluke stages (Fig. 3A). Additionally, expression stabilities of the eight reference gene candidates were calculated using the geNorm algorithm and ranked from the most stable to least stable candidate gene (Fig. 3B). geNorm analysis ranked the tubulin chaperone Fh*tbcd* and Fh*eprs* as the two best reference genes for fluke stage comparison and, again, Fh*gapdh* as least suitable candidate. In BestKeeper analysis, the average of the pairwise variations of each gene with all other genes is used to create the stability value M: the lower M is, the more stable are the transcript levels of a gene. The calculated standard deviation [±CP] should not exceed 1. Indeed, standard deviations of all eight genes were <1. BestKeeper identified Fh*tbcd* and the actin Fh*actb* as the best reference genes, and the protein phosphatase subunit Fh*ppp1cb* as worst candidate (Fig. 3C). The fourth algorithm, the ΔCt method, revealed Fh*eprs* and Fh*tbcd* as the best candidates and Fh*gapdh* as the least stably expressed gene (Fig. 3D). These results were equivalent to those generated by geNorm. For some genes, such as Fh*actb* and Fh*gapdh*, the predicted expression stability (here: coefficient of correlation) according to BestKeeper was fairly good, whereas these genes were among the least or only average stably expressed genes in the three other analyses. This argues for using more than just one algorithm when performing studies of reference gene validation.

Because of the slightly heterogeneous rankings produced by the four algorithms, a final global ranking was obtained by assigning the numbers 1–8 to each stability coefficient (with 1 as the most stable and 8 as the least stable gene), and creating the geometric mean of these ranks for each gene. This procedure is equivalent to the global ranking done by the RefFinder tool[22]. This final ranking revealed Fh*eprs* and Fh*tbcd* as the two most stably expressed genes and, therefore, the most suitable reference genes for comparisons of intra-mammalian fluke stages. The commonly used housekeeping gene *gapdh* ranked last. The final ranking from the lowest to highest calculated average rank was as follows: Fh*eprs* < Fh*tbcd* < Fh*psmb7* < Fh*actb* < Fh*snrpa1* < Fh*letm1* < Fh*ppp1cb* < Fh*gapdh* (Fig. 5A).

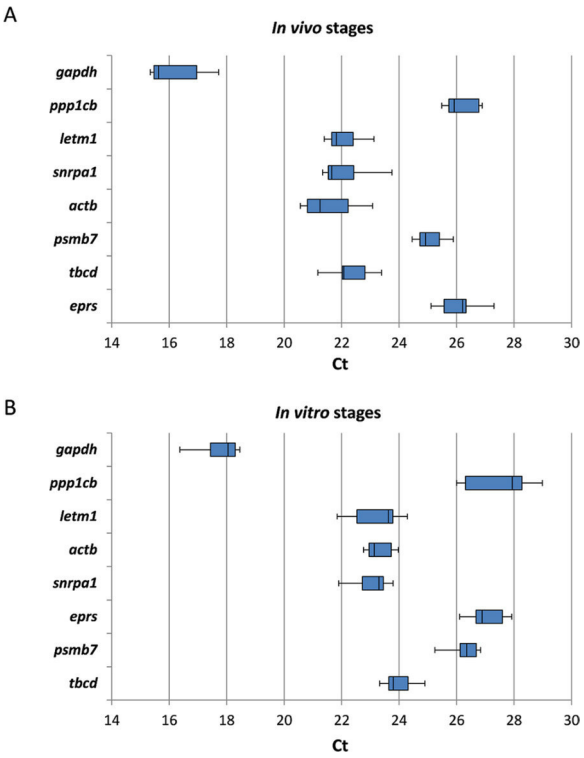

Figure 2. Distribution of threshold cycle (Ct) values of 8 candidate reference genes across all samples. The solid line represents the median, boxes indicate the 25th and 75th percentile, and the whiskers represent the minimum and maximum values of averaged qRT-PCR expression data from (**A**) 9 samples of intra-mammalian *in vivo* stages (NEJs, immature and adult flukes), and (**B**) 6 samples of *in vitro* cultured juveniles (NEJs and 4-week cultured juveniles).

Expression stability of candidate reference genes during in vitro culture of juvenile flukes. Next to quantification of gene expression in different fluke stages, gene expression analyses in *in vitro*-cultured NEJs is another standard approach for various research questions such as expression changes during maturation of juveniles or characterisation of gene function by RNAi[9,20,23]. Analogous to the stability ranking for the intra-mammalian stages, we used the four different algorithms to identify the most stably expressed reference genes for NEJs before and after 28 days of *in vitro* culture in an established long-term culture medium[8]. The individual ranking for each algorithm is summarised in Fig. 4 and Supplementary Table S4.

NormFinder, BestKeeper, and the comparative ΔCT method identified Fh*tbcd* and Fh*psmb7* as the two most stably expressed genes. geNorm identified Fh*tbcd* and Fh*eprs* as most suitable reference genes, as for the analysis of intra-mammalian stages before, followed by Fh*psmb7*. The least stably expressed gene was Fh*ppp1cb* (geNorm and ΔCT method) or Fh*gapdh* (NormFinder and BestKeeper).

Accordingly, the global ranking based on the geometric mean of individual ranks revealed Fh*tbcd* and Fh*psmb7* as the most stably expressed reference genes. The average calculated ranks were as follows: Fh*tbcd* < Fh*psmb7* < Fh*eprs* < Fh*snrpa1* < Fh*actb* < Fh*letm1* < Fh*ppp1cb* < Fh*gapdh* (Fig. 5B).

Relative expression levels of reference gene candidates during development and anthelmintic treatment. To clarify in how far the previously used reference gene Fh*gapdh*[9,20,21] is differentially regulated during *in vivo* development or *in vitro* culture, we relatively quantified its expression compared to the geometric mean of the two best reference genes. Fh*gapdh* was clearly differentially expressed with a significant upregulation during *in vitro* culture and during development from NEJs to immature and adult flukes (Fig. 6A,C). A differential expression was also found for most other reference gene candidates positioned on number 4 to 7 in the global ranking (see Supplementary Fig. S3). On the contrary, Fh*psmb7* and Fh*eprs* were not differentially expressed, being in line with their fairly good stability rank (number 3 in the global rankings) (Fig. 6B,D). Taken together, Fh*gapdh* as well as all genes from global stability rank 4 and higher appear not to be suitable as reference genes for inter-stage comparisons.

Next, we addressed whether selected reference genes are also stably expressed during anthelmintic treatment of flukes. To this end, adult *F. hepatica* were cultured with different sublethal concentrations of triclabendazole for 2 days *in vitro*. Because triclabendazole is known to affect tubulin in *F. hepatica*[24], it was of particular interest whether the tubulin-specific chaperone D Fh*tbcd* would be stably expressed. The expression of all genes investigated (Fh*tbcd*, Fh*psmb7*, Fh*gapdh*) did not change by drug exposure (Fig. 7) and thus appear suitable as reference genes for this type of experimental setting.

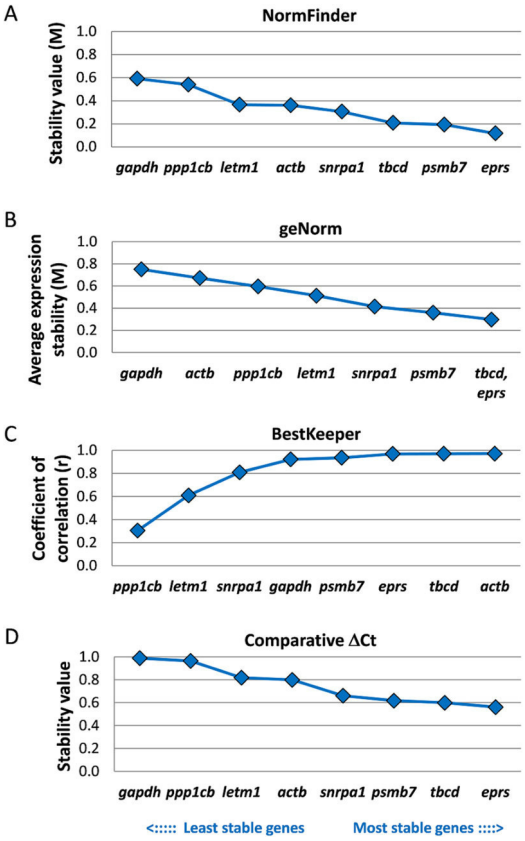

Figure 3. Stability of expression of eight candidate reference genes in three different intra-mammalian life stages of *F. hepatica*. Stability values were obtained for NEJs, 4 week-old immature, and 12 week-old adult worms using NormFinder (**A**), geNorm (**B**), BestKeeper (**C**), and the comparative ΔCT method (**D**). Genes were ranked from the least stable (on the left) to the most stable (on the right).

Validation of selected reference genes for quantification of target gene expression in different fluke stages. The performance of the selected reference genes was validated by quantification of relative expression levels of five orthologs of kinase genes in *F. hepatica*. Kinases are discussed as promising anthelmintic target of inhibitors[10,25]. In particular, Abl kinases and polo-like kinase 1 have been studied in the past as potential targets in schistosomes, tape-worms, and filariae[12,26–28]. Furthermore, the protein kinases B (also called Akt) and C have been investigated as potential targets in *S. mansoni*[13,29,30]. For all these kinases, RNAi or inhibitor treatment *in vitro* revealed anthelmintic effects on immature or adult schistosome stages.

All the more surprising is that neither of these kinases has been studied to date in *Fasciola*. Knowledge on kinase expression in all life stages relevant for drug targeting is desirable, as well as a reliable quantification of expression during *in vitro* culture, for instance as part of knockdown experiments. Therefore, we identified orthologs of above mentioned kinases by BLASTp search (Table 2): Fh*abl1* and Fh*abl2* as orthologs of the protein tyrosine kinases *abl1* and *abl2*, which play roles in a variety of cellular processes including cell differentiation and cytoskeletal rearrangements[31]; Fh*akt1* and Fh*pkc* as orthologs of the serine/threonine-protein kinases B and C, which are known to regulate many processes including cell metabolism, proliferation, and survival[32,33]; Fh*plk1* as an ortholog of polo-like kinase 1 with important roles during cell cycle progression[34]. The presence of conserved protein domains was confirmed by SMART analysis (see Supplementary Fig. S4). For instance, Fh*plk1* contained a typical kinase domain and two polo-box domains. The identity of the kinase orthologs was further confirmed by multiple alignment of the amino acid sequences against several model species (see Supplementary Fig. S9).

For both experimental groups (*in vivo* and *in vitro* stages), we quantified kinase expression using the geometric mean of the two most stably expressed reference genes for normalisation, which were Fh*eprs* and Fh*tbcd*, and Fh*psmb7* and Fh*tbcd*, respectively. The five kinase genes were found to be expressed in all intra-mammalian life stages. The highest relative expression was observed for Fh*abl1* and Fh*pkc*. Interestingly, two types of expression patterns during fluke development were revealed: while Fh*plk1* was expressed highest in adult flukes and low in NEJs and immature flukes, expression of all other kinases was highest in NEJs and significantly downregulated during development to immature and adult flukes (Fig. 8). *In vitro* maturation of NEJs to immature flukes by 4-week culture revealed very similar expression patterns (Fig. 9) as seen during *in vivo* development.

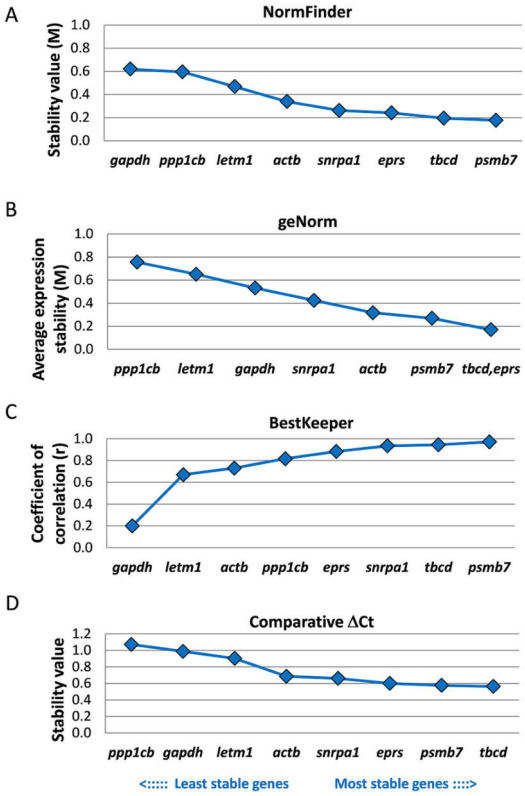

Figure 4. Stability of expression of eight candidate reference genes during *in vitro* culture of juvenile *F. hepatica*. Stability values were obtained for 1-day old NEJs and juveniles grown for 4 weeks in serum-rich medium using NormFinder (**A**), geNorm (**B**), BestKeeper (**C**), and the comparative ΔCT method (**D**). Genes were ranked from the least stable (on the left) to the most stable (on the right).

As a proof of principle, we also used Fh*gapdh* for normalisation of kinase gene expressions to assess whether using a suboptimal gene would yield different results compared to using the top ranked reference genes. While the overall kinase expression patterns were largely similar, a differing expression pattern was revealed for some kinase genes and some stages. As example, Fh*gapdh* suggested a significant downregulation of Fh*abl1* and Fh*akt1* expression from NEJs to immature flukes (Supplementary Fig. S5), while there was no expression difference based on the stable expressed reference genes (Fig. 8). On the other hand, the significantly upregulated expression of Fh*plk1* from NEJs to immature flukes was not evident when normalised against Fh*gapdh*. Even more striking, Fh*gapdh* suggested a significant downregulation of Fh*plk1* during *in vitro* culture of juveniles (Supplementary Fig. S6), while in fact a trend for increased expression was demonstrated before (Fig. 9). This clearly shows that using a suboptimal reference gene for normalisation might give differing or even opposite expression results for a gene of interest.

The developmental expression changes for kinase genes found in *F. hepatica* matched in parts with expression patterns of orthologs in the related blood fluke *S. mansoni*. Previous studies showed that the schistosome *abl* kinase genes Sm*abl1* and Sm*abl2* were downregulated during maturation from schistosomula to adults, and *plk1* was strongly upregulated, at least in adult females[3,18] (Supplementary Fig. S7). Taken together, various kinases are expressed in intra-mammalian life stages of *F. hepatica*, and expression changes during *in vivo* development are mimicked by *in vitro* culture.

Discussion

Proteomic studies revealed striking differences of gene expression among the life stages of *F. hepatica* occurring in the mammalian host[6,7]. This has important practical implication for vaccine development and drug target research. Knowledge on target gene expression in all life stages relevant for anthelmintics development is desirable as well as reliable methods for the quantification of gene expression during *in vitro* culture, for instance as part of target gene validation using knockdown experiments.

Per definition, housekeeping genes are essential for maintaining the cellular function and therefore, in theory, should be stably expressed. In practice, however, they may turn out to be regulated to some extent depending on the organisms, developmental stages, tissue types, and experimental settings[35]. This requires an accurate validation of candidate genes as reference genes for e.g. qRT-PCR studies. As classical housekeeping genes, *gapdh*

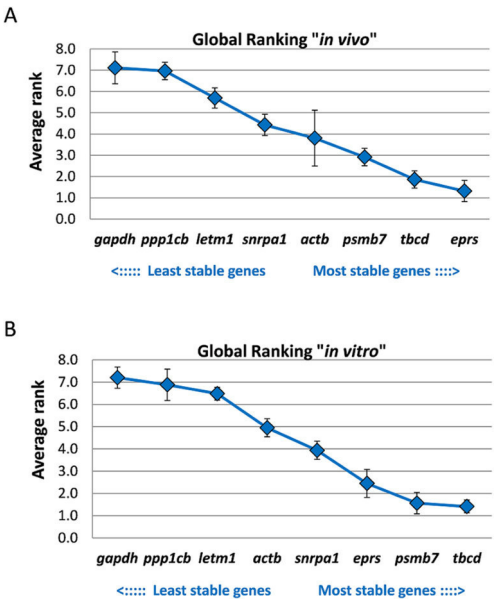

Figure 5. Mean rank of expression stability of eight candidate reference genes in *F. hepatica*. A number (from 1 to 8) was assigned to each stability coefficient obtained from four algorithms. The mean rank with SEM is shown for (**A**) the analysis of three intra-mammalian stages (NEJs, immature and adult flukes), and (**B**) the analysis of *in vitro*-cultured juveniles (NEJs before and after 28 days culture). Genes were ranked from the least stable (on the left) to the most stable (on the right).

and *ß-actin* have been used for normalisation in gene expression studies in all kind of organisms, including helminths[9,20,21,36]. At least for the oriental liver fluke, *Clonorchis sinensis*, a stable expression of *ß-actin* was demonstrated in the comparison of two life stages, metacercariae and adults. In the same study, however, *gapdh* exhibited poor expression stability[2]. Furthermore, a *gapdh* ortholog was among the least stable candidate genes for gene expression studies in adult schistosomes cultured *in vitro*[4]. In our study with *F. hepatica*, *gapdh* showed the lowest and *ß-actin* only a moderate expression stability among eight candidate genes tested. The transcript levels of *gapdh* appeared to be significantly upregulated during maturation of the fluke. This is of particular relevance as *gapdh* is currently a standard gene used for normalisation of gene expression in *F. hepatica* studies[9,20,21], but based on our results, *gapdh* may not be the most suitable reference gene for inter-stage comparison of gene expression by qRT-PCR. This implies that without additional validation, the selection of reference genes for gene expression studies in one species should not be based on results obtained in a related species because there is no guarantee for comparable expression profiles.

We aimed at identifying stably expressed genes among a selection of eight candidate reference genes for two different experimental settings often used in *Fasciola* research: the comparison of life stages relevant for the mammalian host, and the *in vitro* culture of juvenile flukes. The four algorithms resulted in a slightly divergent ranking of the genes, which was expected from previous studies on other organisms, and which can be explained by the different type of input data and data processing used by the algorithms[4,37]. Therefore, a global ranking based on the results of all algorithms was performed. In the three intra-mammalian stages, the glutamyl-prolyl-tRNA synthetase Fh*eprs* and tubulin-specific chaperone D Fh*tbcd* were most stably expressed. In cultured parasites, this applied to Fh*tbcd* and the proteasome subunit beta type-7 Fh*psmb7*.

The tubulin-specific chaperone TBCD is one of four proteins involved in the pathway leading to correctly folded beta-tubulin from folding intermediates. Being involved in the regulation of microtubule polymerisation and depolymerisation[38,39], it is required for crucial cellular processes such as proper assembly of the mitotic spindle and correct progression of mitosis. The glutamyl-prolyl-tRNA synthetase EPRS belongs to the family of aminoacyl-tRNA synthetases, which charge tRNAs with their corresponding amino acids. Accordingly, EPRS catalyses the aminoacylation of proline and glutamic acid tRNA species[40]. The proteasome subunit beta type-7 PSMB7 is part of the 20S and 26S proteasome complexes and thus involved in the proteolytic degradation of most intracellular proteins. The proteasome plays a key role in the maintenance of protein homeostasis by removing unneeded proteins, and damaged or misfolded proteins that could impair cellular functions[41]. Because microtubule function, tRNA synthesis, and proteolytic degradation are essential processes for all cells, and presumably independent of any developmental stage, it was not surprising that *tbcd*, *eprs* and *psmb7* turned out as the most stably expressed genes in our study.

The stability ranking obtained for *in vitro*-cultured liver flukes is in part similar to the ranking of a related study in *S. mansoni*. Here the ortholog for proteasome subunit beta type-7, Sm*psmb7*, ranked also second best during *in vitro* culture of adult worms, and Sm*gapdh* was among the least stably expressed genes[4]. In contrast,

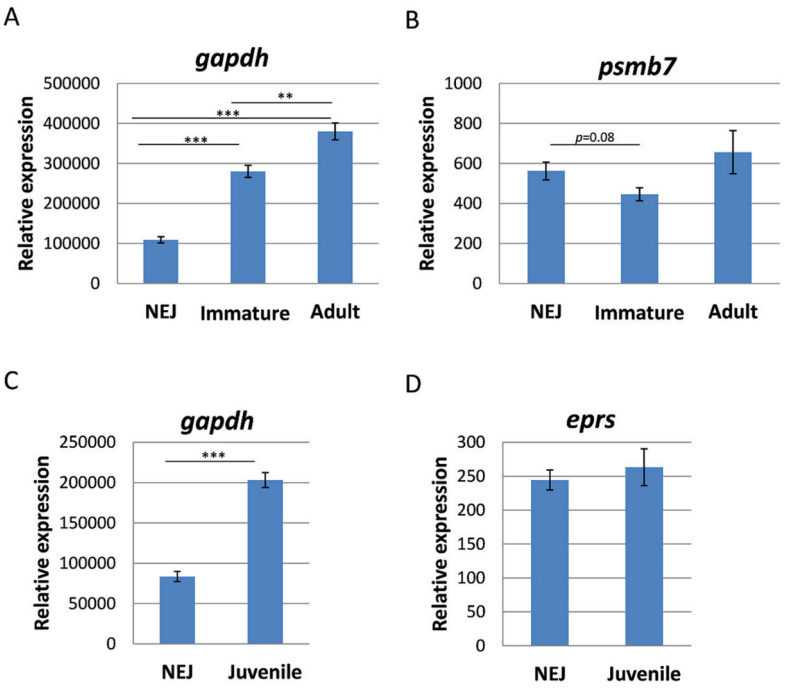

Figure 6. Relative expression levels of a stable and the least stable reference gene candidate in different stages of *F. hepatica*. Relative quantification is based on normalisation against the geometric mean of the two most stably expressed reference genes identified for (**A**,**B**) intra-mammalian stages (*tbcd* and *eprs*), or for (**C**,**D**) *in vitro* cultured juveniles (*tbcd* and *psmb7*). *gapdh* (**A**,**C**) was previously revealed as the least stable gene, *psmb7* and *eprs* (**B**,**D**) were among the three most stably expressed genes. Average values of 3–4 biological replicates with SEM are shown. Significant differences are indicated with $^{**}p < 0.01$, $^{***}p < 0.001$ (t-test).

the most stable gene in adult schistosomes, *letm1*, was among the least stable genes investigated in *Fasciola*. Heterogenous rankings were also obtained for *tbcd* and *ppp1cb*: both genes were revealed to be stably expressed in the different life stages of *S. mansoni* by a meta-analysis study[18], while in *F. hepatica*, only *tbcd* was. Taken together, the most stably expressed reference genes among the tested candidates in *F. hepatica* are housekeeping genes belonging to the family of tRNA synthetases, proteasome subunits, and the microtubule machinery.

For a first application of the newly identified reference genes in qRT-PCR experiments, we focused on kinase genes since they are discussed as potential druggable targets in various helminth species[10,26,27]. Surprisingly, kinases as drug targets have been largely neglected so far in *Fasciola* research. In the past, selected kinases have been in focus mainly as vaccine candidate (phosphoglycerate kinase) or as marker gene for discriminating hybrids of *Fasciola spp.* (phosphoenolpyruvate carboxykinase)[42,43]. Phosphofructokinase seems to be the only kinase of *F. hepatica* studied as potential chemotherapeutic target, in work by Mansour dating back as far as 1962[44,45], but was not further followed because of suboptimal *in vivo* efficacy of an phosphofructokinase inhibitor[46]. To move kinases more into the spotlight of *Fasciola* anthelmintics research, we identified five kinase genes in *F. hepatica* and quantified their expression during development at the transcriptional level, *in vivo* and *in vitro*. For orthologs of all these kinases, promising anthelmintic effects have been obtained *in vitro* by knockdown of kinase gene expression or kinase inhibitor treatment in other parasitic flatworms including *S. mansoni*[12–15,26,28–30]. Our analyses showed that these kinases were expressed in all intra-mammalian stages of *F. hepatica*. Furthermore, interesting expression patterns were detected throughout development. The potential polo-like kinase 1 ortholog Fh*plk1* was found to be highly expressed in adults but low in NEJs or immature flukes. This might suggest a role of Fh*plk1* particularly for the mature stage. A similar expression pattern was observed in *S. mansoni*, where Sm*plk1* expression was mainly found in germinal cells of adult worms[15]. Accordingly, inhibition or RNAi of Sm*plk1* affected egg production and gonad morphology[13,15]. Opposite to Fh*plk1*, orthologs of the two Abl kinases and two serine/threonine-protein kinases showed a peak of expression in NEJ. In other organisms, these kinases are amongst others involved in cytoskeleton remodeling in response to extracellular stimuli such as growth factors, and in the regulation of cell metabolism[31–34]. Thus, these kinases might play important roles during early growth and development of flukes, which still has to be substantiated in functional studies in the future.

That kinases were found to be expressed in all intra-mammalian stages appears as a prerequisite for any novel target in *F. hepatica*, because new compounds should preferably be able to hit all developmental stages in the final host, as does the current gold standard triclabendazole[17]. Whether the significantly different mRNA expression levels between parasite stages found for most kinases will lead to a difference in susceptibility to target inhibition should be part of future studies. A first target gene validation can be achieved by knockdown using RNAi.

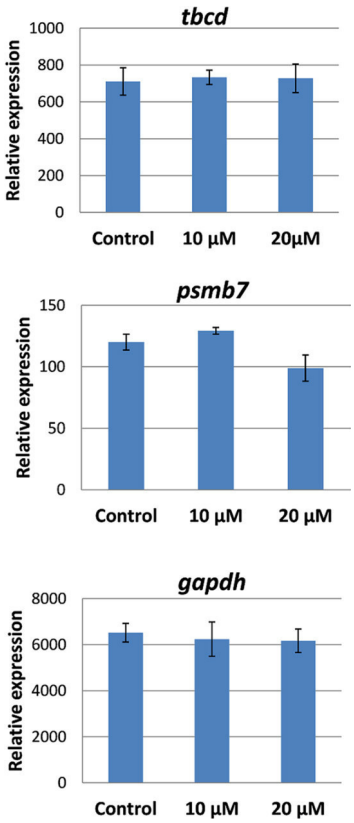

Figure 7. Relative expression of selected reference genes after culture with triclabendazole. Adult *F. hepatica* were cultured for 2 days with 10 µM and 20 µM triclabendazole, or in an equivalent concentration of DMSO as control. Expression of *tbcd* (**A**) was normalised against the geometric mean of *eprs* and *psmb7*, expression of *psmb7* (**B**) and *gapdh* (**C**) were normalised against the geometric mean of *eprs* and *tbcd*. Average values of 4 biological replicates with SEM are shown.

For such an *in vitro* culture experiment, it should be taken into account that according to our findings, kinase transcript levels significantly change during 4 weeks of culture. Furthermore, for all studied kinases, inhibitor treatment *in vitro* has revealed anthelmintic effects on other parasitic flatworms[12,14,15,26,28–30]. Thus, it is certainly worth testing several of the known kinase inhibitors, such as imatinib and BI 2536, against the different stages of *F. hepatica* in near future. To this end, first results obtained by us indicate that imatinib has also the potential of killing *Fasciola in vitro* (Haeberlein, unpublished results).

To conclude, for future expression analyses by qRT-PCR in *F. hepatica* we propose using the glutamyl-prolyl-tRNA synthetase Fh*eprs* and tubulin-specific chaperone D Fh*tbcd* as reference genes for studies dealing with the different intra-mammalian fluke stages. Beyond that, we suggest using Fh*tbcd* and the proteasome subunit beta type-7 Fh*psmb7* for studies on *in vitro*-cultured juvenile flukes, such as for RNAi experiments. Especially for inter-stage comparisons, these new reference genes have the potential to replace the traditional housekeeping gene *gapdh* which is used in many *Fasciola* studies to date[9,20,21], but turned out to be differentially expressed during fluke development in our analysis. We also like to motivate, as a good laboratory practice, to newly validate the suitability of reference genes for studies that use different experimental setups than ours, such as extended drug treatment studies. Using the newly defined reference genes from our study, we quantified expression of kinase orthologs in all relevant intra-mammalian life stages important for drug targeting, which revealed distinct expression patterns throughout development pointing to interesting biological functions. Together with the previously identified broad anthelminthic activity of some kinase inhibitors, this motivates for validation experiments on kinases as potential targets in *F. hepatica*.

Material and Methods

Ethics statement. Animal experiments were performed in accordance with the German Animal Welfare act in addition to national and international guidelines for animal welfare and were approved by the ethics commission of the Institutional Animal Care and Use Committee (IACUC) of the German Lower Saxony State Office for Consumer Protection and Food Safety (*Niedersaechsisches Landesamt für Verbraucherschutz und Lebensmittelsicherheit*) under reference number 33.8-42502-05-118A336.

Gene of interest	Gene ID	Homology (e-value)*	Protein function
Fh*abl1*	maker-scaffold10x_1995_pilon-snap-gene-0.46	ABL proto-oncogene 1, non-receptor tyrosine kinase [*H. sapiens*, NP_005148.2] (2e-119)	Protein tyrosine kinase involved in a variety of cellular processes, including cell division, adhesion, differentiation, and response to stress.
Fh*abl2*	maker-scaffold10x_873_pilon-snap-gene-0.69	ABL proto-oncogene 2, non-receptor tyrosine kinase isoform e [*H. sapiens*, NP_001129473.1] (2e-135)	Protein tyrosine kinase with a role in cytoskeletal rearrangements through its F-actin- and microtubule-binding sequences.
Fh*akt1*	maker-scaffold10x_205_pilon-augustus-gene-0.40	Rac-alpha serine/threonine-protein kinase [*H. sapiens*, NP_001014431.1] (9e-137)	The serine/threonine-protein kinase AKT1 is also known as protein kinase B. AKT kinases regulate many processes including metabolism, proliferation, cell survival, and growth.
Fh*pkc*	maker-scaffold10x_608_pilon-snap-gene-0.5	Protein kinase C iota [*H. sapiens*, NP_002731.4] (0.0)	A serine/threonine protein kinase involved in cell survival, differentiation and polarity. It plays a role in microtubule dynamics in the early secretory pathway.
Fh*plk1*	maker-scaffold10x_784_pilon-snap-gene-0.36	Polo-like kinase 1 [*H. sapiens*, NP_005021.2] (0.0)	The serine/threonine protein kinase is highly expressed during mitosis and performs several important functions throughout the M phase of the cell cycle.

Table 2. Overview of genes of interest for the study of gene expression in *F. hepatica*. *Determined by NCBI BLAST.

Parasites. Metacercariae from an Italian strain of *F. hepatica* were purchased from Ridgeway Research (UK). Excystment was done as previously described with some modifications[9]. Briefly, the outer layer of the metacercariae was physically removed using a scalpel followed by 3–5 min exposure to 10% bleach (v/v). Metacercariae were then incubated in excystment solution (0.6% w/v sodium bicarbonate, 0.45% w/v sodium chloride, 0.4% w/v sodium tauroglycocholate, 0.025 M HCl, 0.4% w/v L-cysteine) for at least 1–2 h at 37 °C and 5% CO_2 until NEJs started to hatch. NEJs were collected in complete RPMI medium (containing 1% ABAM-solution (10,000 units penicillin, 10 mg streptomycin and 25 mg amphotericin B per ml)) and snap-frozen in liquid nitrogen at 24 h after excystment. Immature and adult worms were harvested from livers of sheep experimentally infected with 250 metacercariae at week 4 and 12 post-infection, respectively. Worms were kept for 1 h in 0.9% NaCl (w/v) to allow clearance of gut contents. All parasite stages were snap-frozen in liquid nitrogen. Samples were stored at −80 °C until further usage.

***In vitro* culture.** In order to grow juvenile *F. hepatica in vitro*, NEJs were incubated on day 1 post excystment in complete RPMI1640 medium supplemented with 50% chicken serum at 37 °C and 5% CO_2[8]. Medium was changed regularly (2–3 times per week). Juveniles were incubated in density of 10 juveniles per ml. At week 4 of culture, juveniles were harvested, snap-frozen in liquid nitrogen and stored at −80 °C until further usage. To study stability of reference gene expression after anthelmintic exposure, adult *F. hepatica* were cultured for 2 days in complete RPMI1640 with 5% chicken serum and supplemented with 10 µM and 20 µM triclabendazole (dissolved in DMSO), or supplemented with DMSO as present in the highest drug concentration as a negative control. Medium and compounds were refreshed after 24 h and worms snap-frozen in liquid nitrogen and stored at −80 °C until RNA extraction.

RNA isolation and cDNA synthesis. Total RNA from all life stages was extracted using the Monarch total RNA Miniprep kit (New England BioLabs) following the manufacturer's protocol. In brief, NEJs, *in vitro*-grown juveniles, and immature worms were incubated in 300 µl of 1x RNA/DNA protection buffer. Adult worms were chopped in pieces and incubated in 600 µl of the reagent. All samples were subjected to mechanical homogenisation using pestles. Sample sizes ranged between 30–40 NEJs per replicate, 5–10 *in vitro*-grown juvenile worms, and 1 each for immature and adult worms. RNA quality and quantity were checked by electropherogram analysis using the BioAnalyzer 2100 and an Agilent RNA 6000 Pico or Nano Chip according to the manufacturer's instructions (Agilent Technologies, USA). Synthesis of cDNA was performed using the QuantiTect Reverse Transcription Kit (QIAGEN, Germany) comprising a genomic DNA wipeout step and 11 ng of total RNA per reaction. cDNAs were diluted 1:10 before being used as template in qRT-PCR.

Quantitative real-time PCR. All primers used for qRT-PCR experiments were designed for a melting temperature of 60 °C and an amplicon size of 140–200 bp (Supplementary Table S2), using the Primer3Plus software tool[47]. When possible, primer pairs were located on different exons of a gene to distinguish amplification of contaminating genomic DNA by size. Prior to qRT-PCR, all primer pairs were tested under standard PCR conditions using the FirePol taq polymerase (Solis BioDyne, Estonia). PCR products were checked for specificity and occurrence of primer dimers on a 2% agarose gel. Only primer pairs yielding in one specific product with no primer dimers were further used for qRT-PCR. Appropriate PCR products were gel extracted (GeneJET gel extraction kit; Thermo Scientific, USA) and used to prepare a standard-curve with 1:10 dilution steps to test primer efficiencies[48]. Only primers with an efficiency of 90–100% were used for subsequent analyses. Primers were commercially synthesised by Integrated DNA Technologies IDT (USA).

The 2x PerfeCTa SYBR Green SuperMix (Quantabio, USA) was used in qRT-PCRs for the detection of synthesised DNA double strands in a final volume of 10 µl and 400 nM of each primer. Analysis was performed on a Rotorgene Q cycler (QIAGEN, Germany) with the following conditions: initial denaturation step at 95 °C for 3 min, 45 cycles at 95 °C for 10 sec, 60 °C for 15 sec, and 72 °C for 20 sec. Melting point analyses were performed for each primer pair to verify primer specificity and to exclude the generation of primer dimers or unspecific side-products. All qRT-PCRs were performed in three to four biological replicates with three technical replicates for each sample. Amplified PCR products were calculated by absolute quantification against a standard curve[49]. The expression of genes of interest was determined by relative quantification against the geometric mean of two selected reference genes. Relative expression levels were calculated by expressing the data as n-fold difference by the formula: relative expression $= 2^{-\text{delta Ct}} \times f$, with $f = 1000$ as an arbitrary factor.

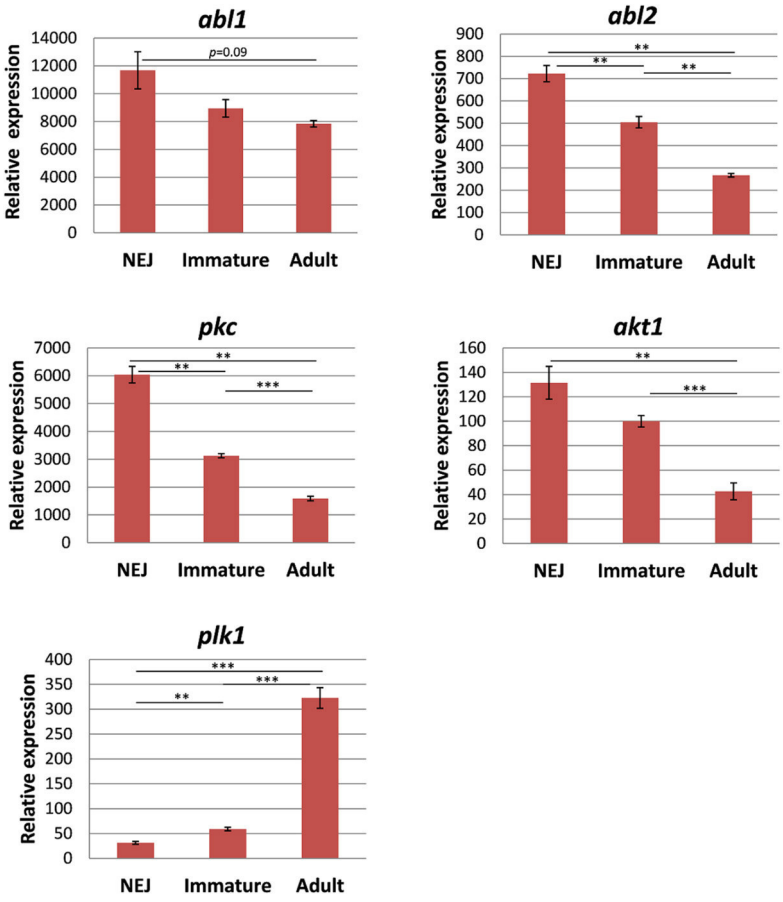

Figure 8. Relative expression levels of kinases in three different intra-mammalian life stages of *F. hepatica*. Expression data from NEJs, 4 week-old immature, and 12 week-old adult worms were normalised against the geometric mean of the two most stably expressed reference genes (*eprs* and *tbcd*). Average values of 3–4 biological replicates with SEM are shown. Significant differences are indicated with $^{**}p < 0.01$, $^{***}p < 0.001$ (t-test). *abl1*, tyrosine-protein kinase Abl1; *abl2*, tyrosine-protein kinase Abl2; *pkc*, protein kinase C; *akt1*, Rac-alpha serine/threonine-protein kinase 1; *plk1*, polo-like kinase 1

Evaluation of expression stability of reference genes. Four different software algorithms were used to determine the transcription stability of selected candidate reference genes: NormFinder, geNorm, BestKeeper, and the comparative ΔCT method[50–53]. Two separate sets of analyses were performed. On the one hand, all samples from NEJs, immature, and adult worms were analysed to obtain the most stably transcribed genes for studies dealing with different life stages of the parasite. On the other hand, all samples from NEJs and *in vitro*-grown juvenile worms were used to reveal the best reference genes for gene expression studies in *in vitro*-culture experiments.

The algorithm NormFinder determines intra- and inter-group variations across the different samples to calculate a stability value (M). Low variations give a low stability value, which indicates stable transcription of a gene. As input data, the calculated concentrations of qPCR amplification were used[50]. The geNorm algorithm calculates pairwise variations of each reference gene when compared with the other genes based on relative Ct values. The stability value (M) is based on the average of these pairwise variations. Again, a stable transcription is reflected by a low M value. BestKeeper analysis was performed on raw Ct values. This algorithm assumes that stable reference genes should display similar transcription patterns, i.e. are highly correlated to each other. This is reflected by a high coefficient of correlation (r), whereby the most stably transcribed genes exhibit values closest to 1. The comparative ΔCT method compares the difference in Ct values of reference genes in pairs. Ranking is based on the variability of averaged standard deviations[53].

***In silico* analyses.** Eight candidate reference genes and five kinase genes of *F. hepatica* were identified by BLASTp search of the known human orthologs against the genome of *F. hepatica* (Centre for Genomic Research, University of Liverpool, BioProject ID PRJEB25283) using the public domain tool WormBase ParaSite, version WBPS13 (https://parasite.wormbase.org)[54]. Gene names, biological function, and accession numbers of *H. sapiens* and *F. hepatica* are listed in Tables 1 and 2. The BLASTp cutoff for the identification of potential orthologs was

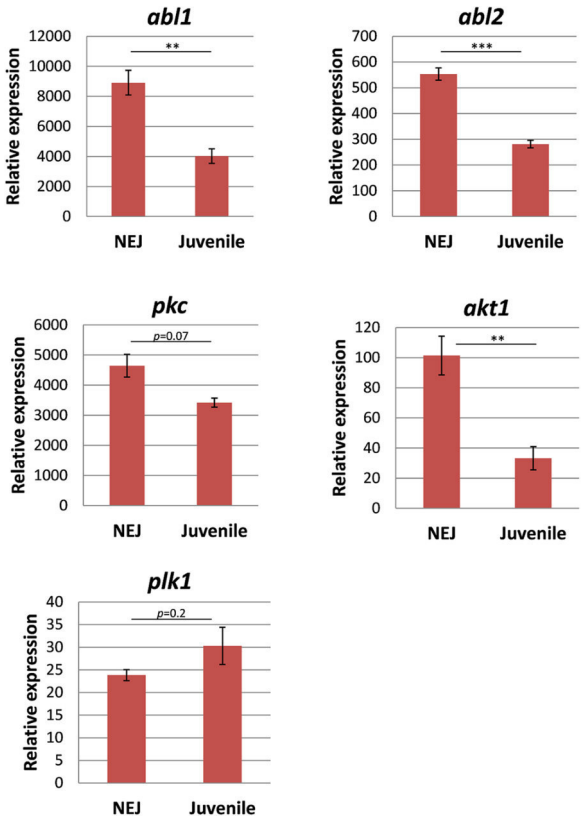

Figure 9. Relative expression levels of kinases during *in vitro* culture of juvenile *F. hepatica*. Expression data from NEJs and juvenile worms grown for 4 weeks in serum-rich medium were normalised against the geometric mean of the two most stably expressed reference genes (*tbcd* and *psmb7*). Average values of 3–4 biological replicates with SEM are shown. Significant differences are indicated with $^{**}p < 0.01$, $^{***}p < 0.001$ (t-test). *abl1*, tyrosine-protein kinase Abl1; *abl2*, tyrosine-protein kinase Abl2; *pkc*, protein kinase C; *akt1*, Rac-alpha serine/threonine-protein kinase 1; *plk1*, polo-like kinase 1.

5E-72. The identity of the potential *F. hepatica* orthologs was confirmed by analysis of conserved protein domains using SMART (http://smart.embl-heidelberg.de/)[55], and by multiple alignment of amino acid sequences against the sequences of several model species or related species (*H. sapiens*, *M. musculus*, *C. elegans*, *D. melanogaster*, *S. mansoni*) using CLUSTALW. The accession numbers for all species used for multiple alignment are listed in Supplementary Table S1.

Statistical analysis. Statistically significant differences between samples were determined by t-test. Error bars represent the standard error of the mean (SEM). p-values < 0.05 were considered significant.

Data availability

All data generated or analysed during this study are included in this published article and its Supplementary Information Files.

Received: 20 August 2019; Accepted: 17 October 2019;
Published online: 01 November 2019

References

1. Webb, C. M. & Cabada, M. M. Recent developments in the epidemiology, diagnosis, and treatment of *Fasciola* infection. *Current opinion in infectious diseases* **31**, 409–414, https://doi.org/10.1097/qco.0000000000000482 (2018).
2. Yoo, W. G. *et al*. Reference genes for quantitative analysis on *Clonorchis sinensis* gene expression by real-time PCR. *Parasitology research* **104**, 321–328, https://doi.org/10.1007/s00436-008-1195-x (2009).
3. Lu, Z. *et al*. Schistosome sex matters: a deep view into gonad-specific and pairing-dependent transcriptomes reveals a complex gender interplay. *Scientific reports* **6**, 31150, https://doi.org/10.1038/srep31150 (2016).
4. Haeberlein, S. *et al*. Identification of a new panel of reference genes to study pairing-dependent gene expression in *Schistosoma mansoni*. *International journal for parasitology* **49**, 615–624, https://doi.org/10.1016/j.ijpara.2019.01.006 (2019).
5. Dawes, B. & Hughes, D. L. Fascioliasis: the invasive stages in mammals. *Advances in parasitology* **8**, 259–274 (1970).

6. Di Maggio, L. S. *et al.* Across intra-mammalian stages of the liver fluke *Fasciola hepatica*: a proteomic study. *Scientific reports* **6**, 32796, https://doi.org/10.1038/srep32796 (2016).
7. Robinson, M. W., Menon, R., Donnelly, S. M., Dalton, J. P. & Ranganathan, S. An integrated transcriptomics and proteomics analysis of the secretome of the helminth pathogen *Fasciola hepatica*: proteins associated with invasion and infection of the mammalian host. *Molecular & cellular proteomics: MCP* **8**, 1891–1907, https://doi.org/10.1074/mcp.M900045-MCP200 (2009).
8. McCusker, P. *et al.* Stimulating neoblast-like cell proliferation in juvenile *Fasciola hepatica* supports growth and progression towards the adult phenotype *in vitro*. *PLoS neglected tropical diseases* **10**, e0004994, https://doi.org/10.1371/journal.pntd.0004994 (2016).
9. McVeigh, P. *et al.* RNAi dynamics in juvenile *Fasciola* spp. liver flukes reveals the persistence of gene silencing *in vitro*. *PLoS neglected tropical diseases* **8**, e3185, https://doi.org/10.1371/journal.pntd.0003185 (2014).
10. Gelmedin, V., Dissous, C. & Grevelding, C. G. Re-positioning protein-kinase inhibitors against schistosomiasis. *Future medicinal chemistry* **7**, 737–752, https://doi.org/10.4155/fmc.15.31 (2015).
11. Grevelding, C. G., Langner, S. & Dissous, C. Kinases: molecular stage directors for schistosome development and differentiation. *Trends in parasitology* **34**, 246–260, https://doi.org/10.1016/j.pt.2017.12.001 (2018).
12. Beckmann, S. & Grevelding, C. G. Imatinib has a fatal impact on morphology, pairing stability and survival of adult *Schistosoma mansoni in vitro*. *International journal for parasitology* **40**, 521–526, https://doi.org/10.1016/j.ijpara.2010.01.007 (2010).
13. Guidi, A. *et al.* Application of RNAi to genomic drug target validation in schistosomes. *PLoS neglected tropical diseases* **9**, e0003801, https://doi.org/10.1371/journal.pntd.0003801 (2015).
14. Long, T. *et al.* Structure-bioactivity relationship for benzimidazole thiophene inhibitors of polo-like kinase 1 (PLK1), a potential drug target in *Schistosoma mansoni*. *PLoS neglected tropical diseases* **10**, e0004356, https://doi.org/10.1371/journal.pntd.0004356 (2016).
15. Long, T. *et al. Schistosoma mansoni* polo-like kinase 1: A mitotic kinase with key functions in parasite reproduction. *International journal for parasitology* **40**, 1075–1086, https://doi.org/10.1016/j.ijpara.2010.03.002 (2010).
16. Fairweather, I. Triclabendazole progress report, 2005-2009: an advancement of learning? *Journal of helminthology* **83**, 139–150, https://doi.org/10.1017/s0022149x09321173 (2009).
17. Kelley, J. M. *et al.* Current threat of triclabendazole resistance in *Fasciola hepatica*. *Trends in parasitology* **32**, 458–469, https://doi.org/10.1016/j.pt.2016.03.002 (2016).
18. Lu, Z. *et al.* A gene expression atlas of adult *Schistosoma mansoni* and their gonads. *Scientific data* **4**, 170118, https://doi.org/10.1038/sdata.2017.118 (2017).
19. Radio, S. *et al.* Pleiotropic alterations in gene expression in Latin American *Fasciola hepatica* isolates with different susceptibility to drugs. *Parasites & vectors* **11**, 56, https://doi.org/10.1186/s13071-017-2553-2 (2018).
20. Cwiklinski, K. *et al.* Infection by the helminth parasite *Fasciola hepatica* requires rapid regulation of metabolic. *virulence, and invasive factors to adjust to its mammalian host. Molecular & cellular proteomics: MCP* **17**, 792–809, https://doi.org/10.1074/mcp.RA117.000445 (2018).
21. Rinaldi, G. *et al.* Development of functional genomic tools in trematodes: RNA interference and luciferase reporter gene activity in *Fasciola hepatica*. *PLoS neglected tropical diseases* **2**, e260, https://doi.org/10.1371/journal.pntd.0000260 (2008).
22. Xie, F., Xiao, P., Chen, D., Xu, L. & Zhang, B. miRDeepFinder: a miRNA analysis tool for deep sequencing of plant small RNAs. *Plant molecular biology*, https://doi.org/10.1007/s11103-012-9885-2 (2012).
23. McCammick, E. M. *et al.* Calmodulin disruption impacts growth and motility in juvenile liver fluke. *Parasites & vectors* **9**, 46, https://doi.org/10.1186/s13071-016-1324-9 (2016).
24. Robinson, M. W., Trudgett, A., Hoey, E. M. & Fairweather, I. Triclabendazole-resistant *Fasciola hepatica*: beta-tubulin and response to *in vitro* treatment with triclabendazole. *Parasitology* **124**, 325–338, https://doi.org/10.1017/s003118200100124x (2002).
25. Giuliani, S. *et al.* Computationally-guided drug repurposing enables the discovery of kinase targets and inhibitors as new schistosomicidal agents. *PLoS computational biology* **14**, e1006515, https://doi.org/10.1371/journal.pcbi.1006515 (2018).
26. Hemer, S. & Brehm, K. *In vitro* efficacy of the anticancer drug imatinib on *Echinococcus multilocularis* larvae. *International journal of antimicrobial agents* **40**, 458–462, https://doi.org/10.1016/j.ijantimicag.2012.07.007 (2012).
27. O'Connell, E. M., Bennuru, S., Steel, C., Dolan, M. A. & Nutman, T. B. Targeting filarial Abl-like kinases: orally available, food and drug administration-approved tyrosine kinase inhibitors are microfilaricidal and macrofilaricidal. *The Journal of infectious diseases* **212**, 684–693, https://doi.org/10.1093/infdis/jiv065 (2015).
28. Schubert, A. *et al.* Targeting *Echinococcus multilocularis* stem cells by inhibition of the Polo-like kinase EmPlk1. *PLoS neglected tropical diseases* **8**, e2870, https://doi.org/10.1371/journal.pntd.0002870 (2014).
29. Ressurreicao, M. *et al.* Protein kinase C and extracellular signal-regulated kinase regulate movement, attachment, pairing and egg release in *Schistosoma mansoni*. *PLoS neglected tropical diseases* **8**, e2924, https://doi.org/10.1371/journal.pntd.0002924 (2014).
30. Morel, M. *et al.* Compound library screening identified Akt/PKB kinase pathway inhibitors as potential key molecules for the development of new chemotherapeutics against schistosomiasis. *International journal for parasitology. Drugs and drug resistance* **4**, 256–266, https://doi.org/10.1016/j.ijpddr.2014.09.004 (2014).
31. Yuan, Z. M. *et al.* Regulation of DNA damage-induced apoptosis by the c-Abl tyrosine kinase. *Proceedings of the National Academy of Sciences of the United States of America* **94**, 1437–1440, https://doi.org/10.1073/pnas.94.4.1437 (1997).
32. Coffer, P. J. & Woodgett, J. R. Molecular cloning and characterisation of a novel putative protein-serine kinase related to the cAMP-dependent and protein kinase C families. *European journal of biochemistry* **201**, 475–481, https://doi.org/10.1111/j.1432-1033.1991.tb16305.x (1991).
33. Selbie, L. A., Schmitz-Peiffer, C., Sheng, Y. & Biden, T. J. Molecular cloning and characterization of PKC iota, an atypical isoform of protein kinase C derived from insulin-secreting cells. *The Journal of biological chemistry* **268**, 24296–24302 (1993).
34. Lane, H. A. & Nigg, E. A. Antibody microinjection reveals an essential role for human polo-like kinase 1 (Plk1) in the functional maturation of mitotic centrosomes. *The Journal of cell biology* **135**, 1701–1713, https://doi.org/10.1083/jcb.135.6.1701 (1996).
35. Bustin, S. A., Benes, V., Nolan, T. & Pfaffl, M. W. Quantitative real-time RT-PCR–a perspective. *Journal of molecular endocrinology* **34**, 597–601, https://doi.org/10.1677/jme.1.01755 (2005).
36. Hahnel, S. *et al.* Gonad RNA-specific qRT-PCR analyses identify genes with potential functions in schistosome reproduction such as SmFz1 and SmFGFRs. *Frontiers in genetics* **5**, 170, https://doi.org/10.3389/fgene.2014.00170 (2014).
37. DeLorenzo, D. M. & Moon, T. S. Selection of stable reference genes for RT-qPCR in *Rhodococcus opacus* PD630. *Scientific reports* **8**, 6019, https://doi.org/10.1038/s41598-018-24486-w (2018).
38. Martin, L., Fanarraga, M. L., Aloria, K. & Zabala, J. C. Tubulin folding cofactor D is a microtubule destabilizing protein. *FEBS letters* **470**, 93–95, https://doi.org/10.1016/s0014-5793(00)01293-x (2000).
39. Tian, G., Thomas, S. & Cowan, N. J. Effect of TBCD and its regulatory interactor Arl2 on tubulin and microtubule integrity. *Cytoskeleton (Hoboken, N.J.)* **67**, 706–714, https://doi.org/10.1002/cm.20480 (2010).
40. Cerini, C. *et al.* A component of the multisynthetase complex is a multifunctional aminoacyl-tRNA synthetase. *The EMBO journal* **10**, 4267–4277 (1991).
41. Rivett, A. J., Mason, G. G., Murray, R. Z. & Reidlinger, J. Regulation of proteasome structure and function. *Molecular biology reports* **24**, 99–102 (1997).
42. Wesolowska, A. *et al.* Immune responses in rats and sheep induced by a DNA vaccine containing the phosphoglycerate kinase gene of *Fasciola hepatica* and liver fluke infection. *Acta parasitologica* **61**, 212–220, https://doi.org/10.1515/ap-2016-0030 (2016).

43. Shoriki, T. *et al.* Novel methods for the molecular discrimination of *Fasciola* spp. on the basis of nuclear protein-coding genes. *Parasitology international* **65**, 180–183, https://doi.org/10.1016/j.parint.2015.12.002 (2016).
44. Mansour, T. E. & Mansour, J. M. Effects of serotonin (5-hydroxytryptamine) and adenosine 3',5'-phosphate on phosphofructokinase from the liver fluke *Fasciola hepatica*. *The Journal of biological chemistry* **237**, 629–634 (1962).
45. Fairweather, I., Holmes, S. D. & Threadgold, L. T. *Fasciola hepatica*: motility response to fasciolicides *in vitro*. *Experimental parasitology* **57**, 209–224 (1984).
46. Schulman, M. D., Valentino, D., Cifelli, S. & Ostlind, D. A. Dose-dependent pharmacokinetics and efficacy of MK-401 against old, and young-mature infections of *Fasciola hepatica* in the rat. *The Journal of parasitology* **68**, 603–608 (1982).
47. Untergasser, A. *et al.* Primer3–new capabilities and interfaces. *Nucleic acids research* **40**, e115, https://doi.org/10.1093/nar/gks596 (2012).
48. Dorak, M. *Real-time PCR*. 58–62 (Oxford: Taylor & Francis, 2008).
49. Leutner, S. *et al.* Combinatory microarray and SuperSAGE analyses identify pairing-dependently transcribed genes in *Schistosoma mansoni* males, including follistatin. *PLoS neglected tropical diseases* **7**, e2532, https://doi.org/10.1371/journal.pntd.0002532 (2013).
50. Vandesompele, J. *et al.* Accurate normalization of real-time quantitative RT-PCR data by geometric averaging of multiple internal control genes. *Genome biology* **3**, Research0034, https://doi.org/10.1186/gb-2002-3-7-research0034 (2002).
51. Pfaffl, M. W., Tichopad, A., Prgomet, C. & Neuvians, T. P. Determination of stable housekeeping genes, differentially regulated target genes and sample integrity: BestKeeper–Excel-based tool using pair-wise correlations. *Biotechnology letters* **26**, 509–515 (2004).
52. Andersen, C. L., Jensen, J. L. & Orntoft, T. F. Normalization of real-time quantitative reverse transcription-PCR data: a model-based variance estimation approach to identify genes suited for normalization, applied to bladder and colon cancer data sets. *Cancer research* **64**, 5245–5250, https://doi.org/10.1158/0008-5472.Can-04-0496 (2004).
53. Silver, N., Best, S., Jiang, J. & Thein, S. L. Selection of housekeeping genes for gene expression studies in human reticulocytes using real-time PCR. *BMC molecular biology* **7**, 33, https://doi.org/10.1186/1471-2199-7-33 (2006).
54. Howe, K. L., Bolt, B. J., Shafie, M., Kersey, P. & Berriman, M. WormBase ParaSite - a comprehensive resource for helminth genomics. *Molecular and biochemical parasitology* **215**, 2–10, https://doi.org/10.1016/j.molbiopara.2016.11.005 (2017).
55. Letunic, I., Doerks, T. & Bork, P. SMART: recent updates, new developments and status in 2015. *Nucleic acids research* **43**, D257–260, https://doi.org/10.1093/nar/gku949 (2015).

Acknowledgements
The authors thank Marcel Haas for excellent technical assistance as well as Aaron Maule and his team at Queen's University Belfast for introduction to the *F. hepatica* culture model. The work was funded by the excellence initiative of the Hessian Ministry of Science, Higher Education and Art (HMWK) supporting the LOEWE Centre DRUID and by a stipend of the Faculty of Veterinary Medicine of the Justus Liebig University Giessen awarded to S.H. URL: https://wissenschaft.hessen.de/wissenschaft/landesprogramm-loewe.

Author contributions
H.H. contributed to acquisition, analysis, and interpretation of data, and prepared figures and tables. O.P. contributed to acquisition of data. C.S. provided parasite material. S.H. designed the study, contributed to analysis and interpretation of data, drafted the manuscript, and provided funding. All authors have reviewed the manuscript.

Competing interests
The authors declare no competing interests.

Additional information
Supplementary information is available for this paper at https://doi.org/10.1038/s41598-019-52416-x.

Correspondence and requests for materials should be addressed to S.H.

Reprints and permissions information is available at www.nature.com/reprints.

Publisher's note Springer Nature remains neutral with regard to jurisdictional claims in published maps and institutional affiliations.

5.3 Bildgebende AP-sMALDI-Massenspektrometrie als neue Methodik zur Wirkstoffanalyse in *Schistosoma mansoni*

High-resolution AP-SMALDI MSI as a new tool for drug imaging in *Schistosoma mansoni*

Mokosch A, Gerbig S, Grevelding CG, **Haeberlein S***, Spengler B*

Analytical and Bioanalytical Chemistry (2021) 413(10):2755-2766

Eigener Anteil an der Entstehung der Publikation

- Leitung des Gesamtprojektes: 70%
- Durchführung/Auswertung der Experimente: 30%
- Anfertigung des Manuskripts: 50%

Analytical and Bioanalytical Chemistry (2021) 413:2755–2766
https://doi.org/10.1007/s00216-021-03230-w

RESEARCH PAPER

High-resolution AP-SMALDI MSI as a tool for drug imaging in *Schistosoma mansoni*

Annika S. Mokosch[1] · Stefanie Gerbig[1] · Christoph G. Grevelding[2] · Simone Haeberlein[2] · Bernhard Spengler[1]

Received: 21 October 2020 / Revised: 31 December 2020 / Accepted: 9 February 2021 / Published online: 15 March 2021

Abstract
Schistosoma mansoni is a parasitic flatworm causing schistosomiasis, an infectious disease affecting several hundred million people worldwide. Schistosomes live dioeciously, and upon pairing with the male, the female starts massive egg production, which causes pathology. Praziquantel (PZQ) is the only drug used, but it has an inherent risk of resistance development. Therefore, alternatives are needed. In the context of drug repurposing, the cancer drug imatinib was tested, showing high efficacy against *S. mansoni* in vitro. Besides the gonads, imatinib mainly affected the integrity of the intestine in males and females. In this study, we investigated the potential uptake and distribution of imatinib in adult schistosomes including its distribution kinetics. To this end, we applied for the first time atmospheric-pressure scanning microprobe matrix-assisted laser desorption/ionization mass spectrometry imaging (AP-SMALDI MSI) for drug imaging in paired *S. mansoni*. Our results indicate that imatinib was present in the esophagus and intestine of the male as early as 20 min after in vitro exposure, suggesting an oral uptake route. After one hour, the drug was also found inside the paired female. The detection of the main metabolite, N-desmethyl imatinib, indicated metabolization of the drug. Additionally, a marker signal for the female ovary was successfully applied to facilitate further conclusions regarding organ tropism of imatinib. Our results demonstrate that AP-SMALDI MSI is a useful method to study the uptake, tissue distribution, and metabolization of imatinib in *S. mansoni*. The results suggest using AP-SMALDI MSI also for investigating other antiparasitic compounds and their metabolites in schistosomes and other parasites.

Keywords *Schistosoma mansoni* · MALDI mass spectrometry imaging · Drug imaging · Drug repurposing · Neglected tropical diseases · Imatinib

Introduction

Schistosomiasis is a disease caused by trematodes of the genus *Schistosoma*, with more than 200 million people affected and around 200,000 annual deaths globally. The WHO has listed schistosomiasis as one of the neglected tropical diseases (NTDs) [1–4]. Interestingly, schistosomes have evolved two sexes, in contrast to almost all other parasitic flatworms which are hermaphrodites [5]. For pairing, the female becomes embraced by the male's body and locates in the ventral groove of the male, the gynaecophoric canal. A constant pairing contact of male and female worms is required to induce and maintain the sexual maturation of the female [5]. Following pairing, the female produces hundreds of eggs per day, which are released into the bloodstream of the final host, such as humans. Some of the eggs reach the gut lumen and are released into the environment to continue the life cycle of the parasite. The rest of the eggs, however, migrate via the bloodstream and get trapped in different organs such as the spleen and liver. Here, these eggs cause granuloma formation and inflammatory processes, finally leading to liver fibrosis [6]. For treatment of schistosomiasis, praziquantel (PZQ) is used as the only available drug effective against all schistosome species relevant to humans [7]. However, PZQ does not prevent reinfection, and indications of resistance development against this

Published in the topical collection *Mass Spectrometry Imaging 2.0* with guest editors Shane R. Ellis and Tiffany Porta Siegel.

Simone Haeberlein and Bernhard Spengler contributed equally to this work.

✉ Bernhard Spengler
Bernhard.Spengler@anorg.chemie.uni-giessen.de

[1] Institute of Inorganic and Analytical Chemistry, Justus Liebig University Giessen, 35392 Giessen, Germany

[2] Institute of Parasitology, BFS, Justus Liebig University Giessen, 35392 Giessen, Germany

drug have been recorded [8, 9]. To date, there is no vaccine available, which alarmingly limits disease control [10, 11].

Several new drugs against *S. mansoni* are currently under investigation, including newly developed substances and repurposed drugs. One of these studied drugs is imatinib, a protein tyrosine-kinase (PTK) inhibitor targeting Abl-family PTKs [12, 13]. Imatinib, also known as Gleevec or Glivec (Novartis, Basel, Switzerland; formerly referred to as STI571 or CGP57148B), is used for therapy of chronic myeloid leukemia and malignant gastrointestinal stroma tumors in humans [12, 14]. In in vitro assays, imatinib has shown additional efficacy against multicellular and unicellular parasites with high relevance to human health such as *S. mansoni* and *S. japonicum* [15, 16] but also against *Echinococcus multilocularis* [17], filaria [18, 19], *Plasmodium* [20, 21], and *Leishmania* [22]. Two Abl orthologs and an Abl/Src hybrid kinase occur in *S. mansoni* and are targets of imatinib [15, 23, 24]. Incubation of *S. mansoni* with concentrations between 10 and 100 μmol/L imatinib resulted in phenotypic changes including bulges and swellings along the entire worm body and a reduction of pairing stability and viability of *S. mansoni* couples as well as degenerations of the gonads and the gastrodermis in both genders [15]. Although the phenotypic effects following imatinib treatment of worms have been analyzed in detail, among the open questions are the following: (i) how is imatinib taken up by the parasite (orally or via a different route), (ii) whether the drug uptake kinetics differ between males and females, (iii) in which tissues does the drug occur, (iv) how does drug tropism correlate with the observed phenotypes, and (v) how is imatinib metabolized in the worm? Providing answers to these questions was central to our study.

Typically applied methods to investigate drug distribution require labeling of the compound, either by fluorescent probes or by radioactive substances [25]. Both techniques are quite expensive and laborious, and attachment of probes to a bioactive compound might influence its chemical behavior. Another possibility is to visualize drug distributions by using mass spectrometry imaging (MSI) [26]. The advantage of mass spectrometric detection is that molecules can mostly be analyzed in their native state without additional labeling. Furthermore, hundreds of other endogenous compounds or drug metabolites can be detected in parallel. Sample preparation includes the sectioning of tissue, which can be complicated for small organisms. Our lab has previously established and optimized this procedure for *S. mansoni* [27]. MSI can be carried out using several ionization techniques, the most widespread being matrix-assisted laser desorption/ionization (MALDI). After coating the sample with a thin layer of a dedicated organic matrix, the pulsed laser beam ablates sample material from the tissue surface in a rasterized fashion [28]. The resulting mass spectrum and the location of the ablated spot on the sample are recorded, allowing the generation of images that show the distributions of compounds throughout the rasterized sample area. Typically, MALDI is optimally suited for the detection of phospholipids and smaller metabolites, but it can also be used for peptides and numerous exogenous molecules [29]. Parallel detection of several hundred endogenous molecules requires highly resolved and accurate detection of m/z values by the mass spectrometric analyzer to enable the discrimination and assignment of compounds with similar mass [30]. Among the available systems, high-speed time-of-flight mass analyzers are still predominant, but Fourier-transform mass spectrometers are becoming increasingly important for MALDI imaging. Orbital trapping and ion cyclotron resonance (ICR) are techniques that provide the highest mass accuracy and resolution. While ICR is superior to Orbitraps concerning the aforementioned parameters, they require relatively costly maintenance, and measurement speed at maximum resolution is low. Therefore, Orbitrap mass analyzers are becoming more popular for high-mass-resolution analysis of biomolecules in tissue samples [31] at competitive speed [32]. Their superior resolution coupled with speed of analysis makes them very suitable for drug imaging by providing unambiguous identification through accurate mass and fragmentation.

In the present study, we have investigated imatinib distribution in cryosections of *S. mansoni* after refining the sample preparation protocol and applying high-resolution atmospheric-pressure scanning microprobe MALDI MSI (AP-SMALDI MSI). We have analyzed two concentrations of imatinib and several time points after treatment of the worms with the drug. We were able to follow the uptake and distribution of imatinib and its major metabolite in the worm and to address several characteristic anatomical features.

Materials and methods

Statement of human and animal rights

Animal experiments using Syrian hamsters (*Mesocricetus auratus*) as model hosts were performed in accordance with the European Convention for the Protection of Vertebrate Animals used for experimental and other scientific purposes (ETS No 123; revised Appendix A). Experiments have been approved by the Regional Council (Regierungspraesidium) Giessen (V54-19 c 20/15 h 02 GI 18/10 Nr. A 14/2017).

Harvesting of *Schistosoma mansoni*

A Liberian strain of *S. mansoni* was maintained in Syrian hamsters as final host and freshwater snails of the genus *Biomphalaria glabrata* as intermediate host [6, 33]. Eight-week-old hamsters were obtained from Janvier (France) and infected by the “paddling method” [34]. Adult worms were

collected at 46 days p.i. by hepatoportal perfusion and cultured in M199 medium (Sigma-Aldrich, Schnelldorf, Germany; supplemented with 10% newborn calf serum (NCS), 1% HEPES [1 M], and 1% ABAM solution [10,000 units penicillin, 10 mg streptomycin, and 25 mg amphotericin B per mL]) at 37 °C and 5% CO_2.

In vitro culture experiments

For in vitro culture with imatinib, adult *S. mansoni* were cultured in 6-well plates with 10 worm couples per well in supplemented M199 medium. Imatinib (imatinib mesylate, purity ≥ 98% (HPLC); Enzo Life Sciences, Lorrach, Germany) was dissolved in dH_2O as 50 mmol/L stock and dissolved in medium to final concentrations of 10–100 μmol/L as indicated in the text. The worms were incubated with imatinib at 37 °C and 5% CO_2 for up to 48 h, in which the medium and imatinib were refreshed every 24 h. For AP-SMALDI MSI, worms were used within the first 24 h of treatment, for morphological analysis within 48 h. Worm motility and the frequency of separation of worm couples were recorded at the indicated time points using bright-field microscopy (Labovert FS, Leitz, and SC30 camera, Olympus). Worm motility was quantified using a scoring system, following recommendations by WHO-TDR [35], with the scores 3 (normal motility), 2 (reduced motility), 1 (minimal and sporadic movements), and 0 (no movements within 30 s was considered dead).

Fixation of *Schistosoma mansoni* for AP-SMALDI MSI

After in vitro culture with imatinib for different time periods (see below), worm couples were transferred to plain culture medium using featherweight forceps and washed by a short incubation to remove excess drug and medium. Afterwards, all couples from one well were fixed in 50 μL of a 6.6% solution of glutaraldehyde (grade I, 25% in H_2O; Sigma-Aldrich) in PBS (≥ 99%, p.a.; Carl Roth, Karlsruhe, Germany) on a glass slide, frozen in liquid nitrogen, and stored at − 80 °C. Two series of measurements with 100 μmol/L (high-concentration treatment group) and 20 μmol/L (low-concentration treatment group) concentrations of imatinib were carried out. The investigated time points were 0 min (control, no imatinib added), 5 min, 20 min, 1 h, 4 h, 12 h, and 24 h for 100 μmol/L and 20 min, 1 h, 4 h, 12 h, and 24 h for 20 μmol/L.

Sectioning

Sectioning of worms was carried out on a cryostat HM525 (Thermo Fisher Scientific Inc., Waltham, USA). The sectioning protocol was adapted from Kadesch et al. [27]; the adapted protocol is pictured in Fig. 1. Aqueous gelatin solution with a mass concentration of $\beta = 80$ g/L (water: LC-MS grade, VWR International GmbH, Darmstadt, Germany; gelatin: Pharm. Eur., VWR, Radnor, USA) was prepared. Fifteen microliters of gelatin solution was placed on a sample holder (stainless steel, $d = 6$ mm) and frozen at − 25 °C in the cryotome for 30 min (step 1). Afterwards, the upper part of the droplet was sectioned to form a flat surface (step 2). The fixed and frozen worm couples were thawed in a desiccator at room temperature for 30 min before they were transferred with featherweight forceps in 200 μL water for 30 s to rinse off the residues of the fixative. Subsequently, they were placed on the gelatin plateau and again mounted in the cryotome (step 3). Fifteen microliters of gelatin solution was put on top of the worm couples, then frozen at − 25 °C in the cryotome for 30 min (step 4). After freezing, the samples were cut into sections with a thickness of 40 μm. The quality of the sections was assessed using a digital light microscope (VHX 5000, Keyence, Osaka, Japan), and optical images were recorded. Sections were stored at − 80 °C until further processing.

AP-SMALDI MSI measurements

Sections were thawed in a desiccator at room temperature for 30 min. They were sprayed with a matrix solution consisting of 2,5-dihydroxybenzoic acid (DHB, Sigma-Aldrich GmbH, St. Louis, USA) in a concentration of β (DHB) = 30 mg/mL. The solution was prepared by dissolving DHB in 1:1 (v/v) acetone:water, followed by addition of pure trifluoroacetic acid to obtain a 0.1% acidic solution (acetone, LiChrosolv, Merck, Darmstadt, Germany; TFA, spectroscopy grade, AppliChem GmbH Darmstadt, Deutschland). A SMALDIPrep sprayer (TransMIT GmbH, Giessen, Germany) was used to apply 140 μL of matrix solution to each sample with a flow rate of 10 μL/min at a nitrogen pressure of 1 bar. For the first eleven samples from the first measurement series, 80 μL matrix solution was used. The amount was then increased to 140 μL, which prevented measurement artifacts.

Imaging experiments were performed on a QExactive HF orbital trapping mass spectrometer (Thermo Fisher Scientific, Bremen, Germany) equipped with an autofocusing AP-SMALDI5 AF ion source [36, 37] (TransMIT GmbH, Giessen, Germany). Fifty UV-laser pulses per pixel at a frequency of 100 Hz were used to desorb/ionize the samples. Pixel sizes between 5 and 9 μm were set. Pixel sizes were chosen according to the available measurement time and sample size. Pixelwise autofocusing was used for all measurements. The *m/z* range was 250 to 1000 u. All measurements were performed in positive-ion mode with a mass resolution of 240,000 at *m/z* 200. A lock mass at *m/z* 716.12451, corresponding to $[5DHB - 4H_2O + NH_4]^+$ was chosen for internal calibration. The ion injection time was set to 500 ms, the s-lens level was set to 100 arbitrary units, and the capillary

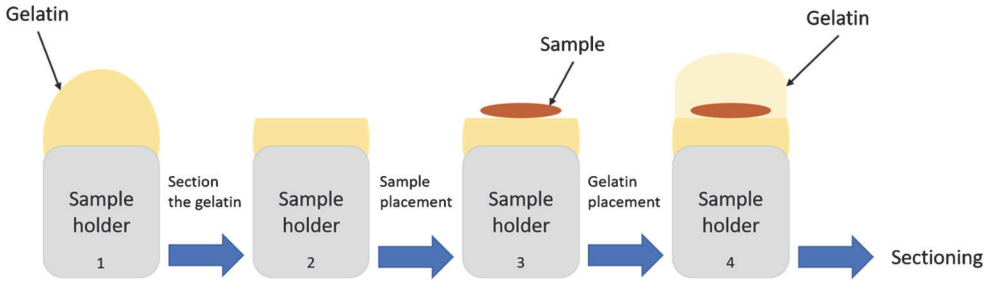

Fig. 1 Scheme of sectioning procedure

temperature was chosen to be 250 °C. An acceleration voltage of 3.0 kV was set.

Data analysis

Q Exactive Tune (version 2.4, Thermo Fisher Scientific, Bremen, Germany) was used to record spectra at the Q Exactive HF mass spectrometer. The software "SMALDI Control" (V1.1–118, TransMIT GmbH, Giessen, Germany) was used to control the stage for image acquisition and for control of the autofocus. XCalibur (Thermo Fisher Scientific, Bremen, Germany) was utilized to display mass spectra. Mirion software package was used for data visualization [38]. The absolute mass variance of spectra was set to 0.005 u, and the bin width of the histogram was set to 0.004 u. Each *m/z* signal was normalized to the total ion current (TIC) of the corresponding pixel for image generation. Lipid assignment was carried out using lipid maps [39] and metaspace (https://metaspace2020.eu) [40]. Chemical structures were drawn using ACD/ChemSketch (Advanced Chemistry Development Inc., Toronto, Canada).

Confocal laser scanning microscopy

Morphologic effects on organs such as intestine and gonads were assessed in detail after 4 h, 24 h, and 48 h of treatment with 100 µmol/L imatinib. To this end, worms were fixed with AFA (66.5% ethanol, 1.1% paraformaldehyde, 2% glacial acetic acid) and stained with carmine red (CertistainH; Merck, Germany) as described before [15, 41]. Stained worms were examined on an inverse confocal laser scanning microscope (CLSM) (Leica TSC SP5; Leica Microsystems, Wetzlar, Germany). Carmine red was excited with an argon-ion laser at 488 nm. Laser power as well as gain and offset of the photomultiplier tube (PMT) was optimized for minimizing possible bleaching effects and for full range intensity coding using the CLUT function (color look-up table) of the Leica LAS AF software. Optical section thickness and background signals were defined by setting the pinhole size to airy unit 1.

Results and discussion

Optimal in vitro culture conditions of worms with imatinib for AP-SMALDI MSI studies

Imatinib is known to induce bulges and swellings along the worm body and to destabilize tissue integrity within the gonads and the gastrodermis of *S. mansoni* after incubation times of 24–96 h at 10–100 µmol/L [15]. Using 100 µmol/L, all worm couples separated into individual males and females within 24 h. Exposure times shorter than 24 h have not yet been studied. Because single females are extremely thin, longitudinal sectioning required for AP-SMALDI MSI is difficult to achieve [27]. Therefore, we established earlier time points of treatment that allow both imaging of intact couples by AP-SMALDI MSI and analysis of drug-induced effects on tissue morphology.

Figure 2a provides an overview of the morphology of untreated paired male and female *S. mansoni*, which were of interest in our AP-SMALDI MSI study. Clearly visible are two suckers of the male, which anchor the worm couple in place within the blood vessel and allow for directed movement; the intestinal tract, consisting of the opening in the oral sucker, the connecting esophagus, and the intestine—the latter is covered by a bioactive layer, the gastrodermis, which serves for nutrient uptake; the bioactive outer surface layer, the tegument, which represents the host-parasite interface protecting the parasite from immune attack of the host, and which mediates nutrient uptake; the ventral side of the male tegument is in direct contact with the female; and finally, the gonads (female ovary and male testis), which are essential for reproduction.

To determine the onset of morphological effects on tissues, we incubated *S. mansoni* couples with 100 µmol/L imatinib to establish the optimal duration of treatment for subsequent AP-SMALDI MSI experiments. An increasing impact on worm vitality was found over time: at 1 h, worms lost fitness and detached with their suckers from the ground; at 4 h, the majority of worm couples separated into single male and female worms; from 12 h onward, worm motility started to decrease (see Supplementary Information (ESM) Fig. S1 a-c). In ESM Fig. S1 d, bright-field microscopy images of representative

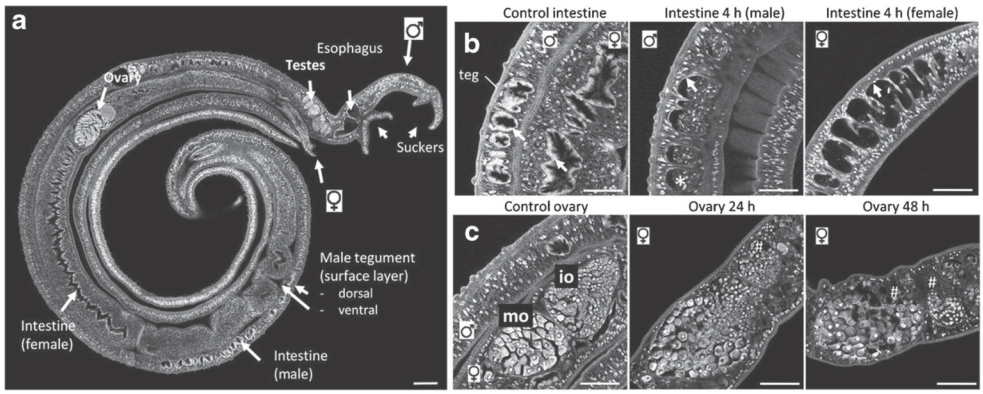

Fig. 2 Morphology of untreated and imatinib-treated *S. mansoni*. **a** Untreated control couple of adult *S. mansoni* worms with an overview of the major organs. As typical for schistosome couples, the male surrounded the female. **b** Imatinib (100 μmol/L) destroyed the gastrodermis (arrows) of male and female worms within 4 h treatment. Accumulation of cellular debris (*) was found in the intestinal lumen. **c** Imatinib (100 μmol/L) induced degradation of the female ovary as early as 24 h, and more severely after 48 h treatment (holes, #). io, immature oocytes; mo, mature oocytes; teg, tegument; scale bar, 100 μm (**a**) or 50 μm (**b**, **c**)

worm couples are depicted. The couples of the control group were paired and attached to the culture well, while after 4 h, the couples were separated, and the males curled up in comparison to the control group. After 24 h of treatment, the couples were still separated, but the males were no longer curled up. By CLSM analysis of carmine-red-stained worms, we found a degradation of the gastrodermis in both male and female worms, as early as 4 h after treatment. This included an accumulation of cellular debris especially in the male intestinal lumen (Fig. 2b) and corresponded to earlier findings at 24 h [11]. This applied also to the disintegration of the gonad tissue, which was visible after a longer exposure of 24 h, and even more prominent at 48 h (Fig. 2c). Based on these findings, we focused on time points up to 12 h for the subsequent AP-SMALDI MSI studies.

Improved cryosectioning for worm samples

The availability of adequate sections is very important for MSI applications. Since *S. mansoni* worms are very small (< 10 mm in length; 200–500 μm in diameter) and soft, sectioning is challenging. Kadesch et al. [27] developed a protocol for worm couples and individual worms, based on gelatine embedding and cryosectioning. Treatment with imatinib, however, drastically changed and destabilized the structure of treated worms (Fig. 2, ESM Fig. S1). This caused additional difficulties during sectioning and made adaptions of the sectioning protocol necessary. In the original procedure, the schistosomes were placed directly on a metal sample holder, while we used an underlying gelatin plateau in our approach (Fig. 1).

In Fig. 3a, a section obtained with the adapted method is shown. The sectioned couple was treated with a 100-μmol/L imatinib solution for 1 h. Male and female worms can still be distinguished, and it is also possible to identify the head and

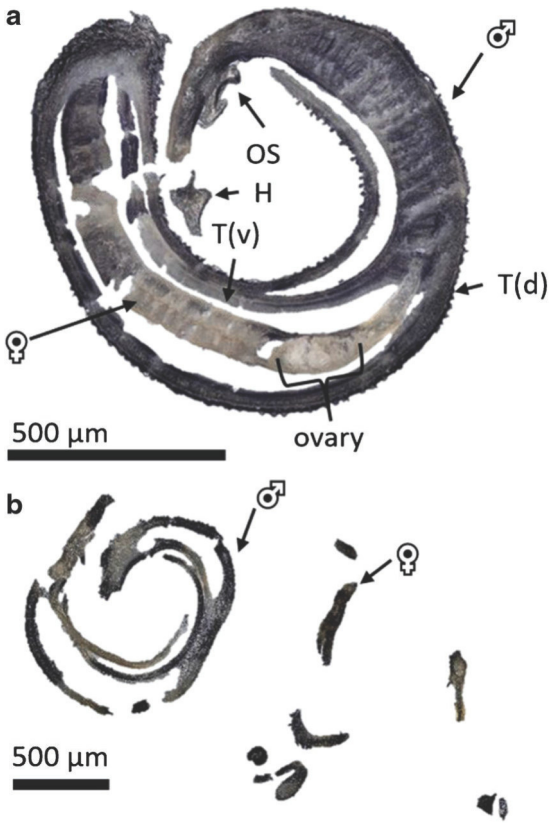

Fig. 3 **a** Optical image of a cryosection of a representative *S. mansoni* couple (100 μmol/L imatinib, 1 h incubation time). VS = ventral sucker, OS = oral sucker, T(v) = tegument ventral (in contact with the female body), and T(d) = tegument dorsal (host-parasite interface). **b** Optical image of a cryosection of a separated *S. mansoni* couple (100 μmol/L imatinib, 12 h incubation time)

the oral suckers of the male, indicating the orientation of the worms within the section. Within the female, the ovary is clearly visible as a lighter, delimited anatomic structure. There are some cracks in the cryosections due to the fragile nature of the imatinib-treated worms. This effect became more pronounced with increasing drug concentrations and incubation periods, leading to the separation of the male and female worms (Fig. 3b). Optical images of all prepared cryosections at different imatinib concentrations and time points are presented as ESM (Figs. S2, S4, and S5).

Using an imatinib concentration of 100 μmol/L, worm couples separated after an incubation time of 4 h. Since separated worms were more difficult to section, the imatinib concentration for the second measurement series was lowered to 20 μmol/L. This reduced the frequency of separation of couples within the first 24 h of treatment. In a standard dilution series, imatinib was detected up to a concentration of 0.2 μmol/L (ESM Fig. S6).

In conclusion, the adapted sectioning protocol resulted in reproducible and authentic sample morphology. Using the gelatin embedding method allowed obtaining sections of imatinib-treated worms in high quality, enabling information-rich imaging analyses.

Mass spectrometric profiling of *S. mansoni* for distinguishing worm sexes and for enabling imatinib detection

Cryosections of imatinib-treated *S. mansoni* were analyzed using high-resolution AP-SMALDI MSI. The mass spectra were obtained using pixel sizes between 5 and 9 μm. In Fig. 4, MSI images of three control measurements of worm couples without imatinib treatment are depicted. They were measured to assure that no interfering signal was detected at the *m/z* value of imatinib (no green pixels).

The displayed analytes represent two endogenous lipids in *S. mansoni*, the phosphatidylcholine (PC) PC(34:1) and the diacylglycerol (DG) DG(34:0), both assigned using the LIPID MAPS online database [39], in blue and red, respectively. No signal was detected at the *m/z* value of imatinib. The signal of PC(34:1) occurred abundantly in both animals with comparable intensities. DG(34:0) was mostly visible in the female, while the intensity in the male was low. For comparison with the optical images, please refer to the ESM (Fig. S2). The images of the individual color channels of the samples in Fig. 4 are depicted in the ESM (Fig. S3).

These first results exhibited signals representing lipid markers for *S. mansoni* females. The evaluation of signals specific for the female not only is of interest for basic research but also helps to facilitate male vs. female assignment in mass spectrometric images. One of these specific *m/z* signals was found at *m/z* 579.534639, which can be assigned to DG(34:0). The visible discrimination of male vs. female body parts became more complicated with rising imatinib concentration and incubation time, so the marker for the female worm was helpful to distinguish both worm sexes. Further marker signals were found for both male and female *S. mansoni* worms, as displayed in Table 1.

A previous study by Ferreira et al. [42] found markers for the male and female worms that differed from our study. This may be due to the fact that we investigated a Liberian strain of *S. mansoni*, while Ferreira et al. investigated two Brazilian strains. Also for the Brazilian strains, no identical sex markers were identified among the two strains, so the strains seemed to be rather different [42]. Furthermore, a 50-μm pixel size was used for image acquisition, while we used a smaller size of 5–9 μm, yielding a higher resolution and enabling discrimination of anatomical features, which might also contribute to the different outcome.

In the control samples, several endogenous lipid signals were found in the gelatin surrounding the animals. This may be due to the release of lipids from the worm to the outside of the animals in the culture medium. To prevent this leaking effect, the samples of the second measurement series were washed two times, once in plain culture medium before fixation in glutaraldehyde and once in water before the placement

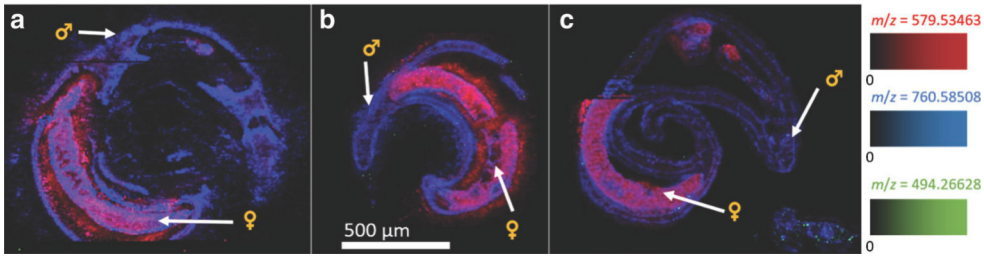

Fig. 4 MSI images of *S. mansoni* couples of the control series. Depicted signals were *m/z* 760.585083 (blue, PC(34:1)), *m/z* 579.534686 (red, DG(34:0)), and *m/z* 494.266284 (green, imatinib). No imatinib or interfering signal at the same *m/z* value was detected in these untreated controls (i.e., no green pixels were obtained).Measured m/z values and errors: **a** 760.584974 (−0.14 ppm); 579.534636 (−0.09 ppm); 494.266445 (+0.32 ppm). **b** 760.584983 (−0.13 ppm); 579.534620 (−0.11 ppm); 494.265840 (−0.9 ppm). **c** 760.584999 (−0.11 ppm); 579.534594 (−0.16 ppm); 494.266281 (−0.01 ppm)

Table 1 Lipid markers for male and female *S. mansoni*, determined via assessment of MS images using AP-SMALDI MSI (PC = phosphatidylcholine; TG = triacylglycerol; DG = diacylglycerol; SM = sphingomyelin). Exemplary signal distribution for these ions can be seen in ESM Fig. S13

Sex of the adult worms	Measured *m/z*	Theoretical *m/z*	Error [ppm]	Annotated molecule	Sum formula of the ion
Female	768.587717	768.587763	−0.06	PC(O-34:1)	$[C_{42}H_{84}NO_7P+Na]^+$
	746.605737	746.605818	−0.11	PC(O-34:1)	$[C_{42}H_{84}NO_7P+H]^+$
	883.772498	883.772511	−0.02	TG(52:1)	$[C_{55}H_{104}O_6+Na]^+$
	579.534598	579.534686	−0.15	DG(34:0)	$[C_{37}H_{72}O_5+H-H_2O]^+$
Male	785.652905	785.653102	−0.25	SM(40:2)	$[C_{45}H_{89}N_2O_6P+H]^+$
	783.637179	783.637452	−0.35	SM(40:3)	$[C_{45}H_{87}N_2O_6P+H]^+$
	703.574887	703.574852	0.05	SM(34:1)	$[C_{39}H_{79}N_2O_6P+H]^+$
	731.606070	731.606200	−0.11	SM(36:1)	$[C_{41}H_{83}N_2O_6P+H]^+$
	807.634818	807.635047	−0.28	SM(40:2)	$[C_{45}H_{89}N_2O_6P+Na]^+$
	805.619087	805.619397	−0.39	SM(40:3)	$[C_{45}H_{87}N_2O_6P+Na]^+$

on the gelatin plateau. The additional washing steps after exposition to the drug and before the sectioning process prevented any contamination of the gelatin during sectioning. An example for this is given in Fig. 4. The first sample (a) was prepared using no washing steps, while the second sample (b) was prepared applying only the second washing step, resulting in no signal spreading. In the second measurement series with the lower concentration of imatinib, both washing steps were applied.

One general challenge is the analysis of non-flat samples using MSI at high lateral resolution, which can be overcome by using the pixelwise autofocusing function of the AP-SMALDI5 AF ion source [36, 37] to counteract height variations. Artifacts of this autofocusing operation may appear for highly reflective surfaces. One example of such artifacts is shown in Fig. 4c, where the red signal has a clear edge that was caused by problems with the autofocus. Such measurement artifacts were avoided using a higher amount of matrix solution, which was increased from 80 to 140 µL after the first eleven samples.

AP-SMALDI MSI reveals imatinib distributions in different parasite tissues

The first series of MSI measurements was performed with couples treated with imatinib at a concentration of 100 µmol/L (Fig. 5). The same *m/z* values as in the control samples (Fig. 4) were selected for the images.

The lipid signals showed the same distributions as in the control samples. Males and females were easily differentiated using the female-indicative red signal of DG(34:0). The blue signal of PC(34:1) was detectable in both animals with a similar distribution characteristics. As early as 5 min after exposure to imatinib (Fig. 5a), the drug was detected at the tegumental surface but also as faint signals within the male, while there was no signal inside the female at this time point. Imatinib signals were also detected from outside the couple, which may have resulted from a smearing effect of the sample during sectioning, as it has occasionally been observed for lipids. Imatinib was mainly detected in the intestine and tegument of the male. A similar distribution was found after 20 min of treatment but with a higher signal intensity within the male. In addition, imatinib appeared at the surface of the female (Fig. 5b). This coincided with the presence of imatinib at the ventral surface of the male which faces the female body. After 1 h (Fig. 5c), imatinib was detected in the female's intestine (Fig. 5d). At this time point, the male sections showed signals inside the head area, which is indicative for the esophagus, suggesting an oral uptake route of imatinib into the digestive tract. After longer exposure times of 4 h and 12 h, imatinib was found to be distributed throughout the worms; however, the couples separated as a consequence of drug activity (Fig. 5d, e). After 12 h (Fig. 5e), the worms were very fragile, and the sections showed several cracks due to drug effects. Please refer to the ESM (Figs. S4, S8, and S9) for comparison with optical images, for individual color channel images of Fig. 5, and for complete MSI results.

AP-SMALDI MSI allowed the detection of imatinib in various parasite tissues and revealed distinct uptake kinetics for male and female worms.

Imaging *S. mansoni* couples exposed to a lower concentration of imatinib confirmed the uptake route while stabilizing the pairing status

To overcome the imatinib-induced separation of couples while imaging the uptake route of imatinib, we conducted a second measurement series for paired worms treated with a lower imatinib concentration of 20 µmol/L (Fig. 6). This was the highest possible concentration that did not affect pairing stability within 12 h, but which already induced clear effects on tissue morphology. The latter included gut dilatations which were detected by bright-field microscopy (ESM Fig. S7 d), indicating the uptake and presence of imatinib. The

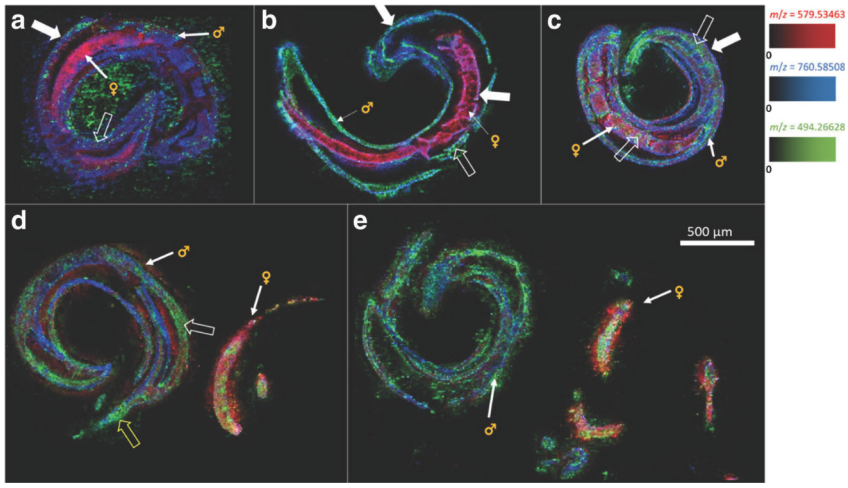

Fig. 5 MSI images of *S. mansoni* couples using imatinib at a concentration of 100 µmol/L. Depicted analytes were *m/z* 494.266284 (green, imatinib), *m/z* 760.585083 (blue, PC(34:1)), and *m/z* 579.534686 (red, DG(34:0)); incubation times were 5 min (**a**), 20 min (**b**), 1 h (**c**), 4 h (**d**), and 12 h (**e**). For each time point, three worm couples were analyzed, of which one representative is shown here (filled arrows: tegument; unfilled arrows: intestine; unfilled, yellow arrow: esophagus). Measured m/z values and errors: **a** 494.266498 (+ 0.43 ppm), 760.584981 (− 0.13 ppm), 579.534576 (− 0.19 ppm); **b** 494.266309 (+ 0.05 ppm), 760.584937 (− 0.19 ppm), 579.534705 (+ 0.03 ppm); **c** 494.265444 (− 1.70 ppm), 760.584990 (− 0.12 ppm), 579.534598 (− 0.15 ppm); **d** 494.265425 (− 1.74 ppm), 760.584976 (− 0.14 ppm), 579.534588 (− 0.17 ppm); **e** 494.266480 (+ 0.40 ppm), 760.584997 (− 0.11 ppm), 579.534606 (− 0.14 ppm)

m/z channels depicted in Fig. 6 are the same as in the control samples and the samples of the high-concentration treatment group (Figs. 4 and 5).

Imatinib, applied with 20 µmol/L concentration, was detectable almost as well as at a concentration of 100 µmol/L and showed similar kinetics. After an incubation time of 20 min

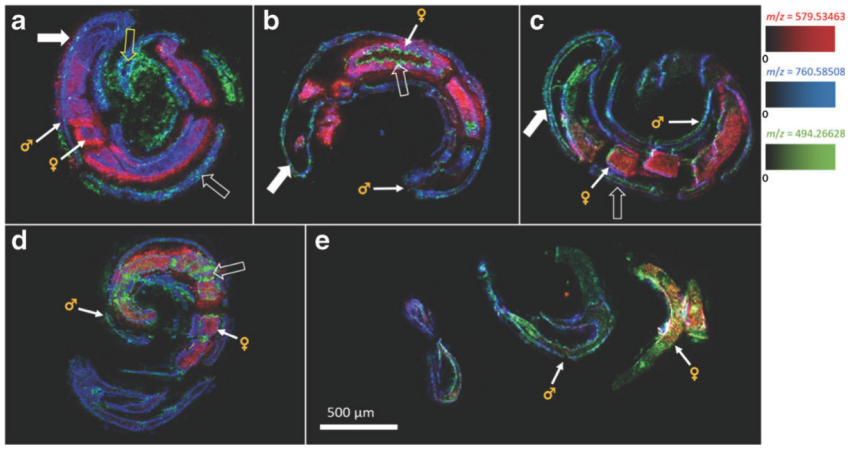

Fig. 6 MSI images of *S. mansoni* couples at an imatinib concentration of 20 µmol/L. Depicted analytes were *m/z* 494.266284 (green, imatinib), *m/z* 760.585083 (blue, PC(34:1)), and *m/z* 579.534686 (red, DG(34:0)); incubation times were 20 min (**a**), 1 h (**b**), 4 h (**c**), 12 h (**d**), and 24 h (**e**). For each time point, two worm couples were analyzed, of which one representative for each time point is shown here (filled arrows: tegument; unfilled arrows: intestine; unfilled, yellow arrow: esophagus). Measured m/z values and errors: **a** 494.266554 (+ 0.55 ppm), 760.584979 (− 0.14 ppm), 579.534635 (− 0.09 ppm); **b** 494.266600 (+ 0.64 ppm), 760.584924 (− 0.02 ppm), 579.534677 (− 0.21 ppm); **c** 494.266562 (+ 0.56 ppm), 760.584908 (− 0.23 ppm), 579.534785 (+ 0.17 ppm); **d** 494.266546 (+ 0.53 ppm), 760.584994 (− 0.12 ppm), 579.534639 (− 0.08 ppm); **e** 494.266481 (+ 0.40 ppm), 760.584981 (− 0.13 ppm), 579.534695 (+ 0.01 ppm)

(Fig. 6a), imatinib signals occurred in the esophagus, intestine, and tegument of the male, while detectable imatinib signals were absent in the female. From 1 h and onwards (Fig. 6b–e), imatinib was detected at the surface and within the internal structures of both sexes. Higher signal intensities were detected in the intestines. The example shown in Fig. 6b exhibits a strong imatinib signal covering the inner surface of the intestine, i.e., the gastrodermis, while no imatinib signal was observed in the gut lumen. The worms separated after an incubation time of 24 h (**e**), the tissue became brittle and caused more sectioning artifacts. Imatinib was evenly distributed in both animals at this time point. Please refer to the ESM (Figs. S5, S10, and S11) for comparison with optical images, for individual color channel images of Fig. 6, and for complete MSI results.

Overall, the results of this measurement series with 20 μmol/L imatinib concentration were similar to the results of the high-concentration treatment group using 100 μmol/L imatinib, with the advantage that pairing stability was maintained for 12 h despite imatinib treatment. The presence of imatinib in the female intestine found from 1 h onwards correlated with the damage of the gastrodermis, observed by bright-field microscopy.

AP-SMALDI MSI revealed possible routes of drug uptake

The various imaging series suggested that *S. mansoni* worms incorporate imatinib via an oral route. The drug was found at the oral sucker, at the esophagus, and further down in the intestine (e.g., Fig. 5d). From there, imatinib is presumably resorbed by the gastrodermis, the inner layer of the intestine, which showed high intensities of the imatinib signal (e.g., Fig. 6b). A second, additional route of uptake may occur via the tegument, the outer, physiologically active surface layer of schistosomes. With respect to the two sexes, we observed an interesting difference in the kinetics of the imatinib distribution in the tissue. For male worms, the uptake started right after imatinib exposition, within 5 min of incubation time. Imatinib signal intensities were low after 5 min (average intensity NL = $7.18 \cdot 10^2$) and two times as high after 20 min (average intensity NL = $1.64 \cdot 10^3$) at a concentration of 100 μmol/L. In contrast, imatinib signals started to occur in the tegument of females not before 20 min of incubation, and it took 60 min until imatinib was detected in inner tissues (Figs. 5c and 6b). This suggests a delay of imatinib uptake in the female compared to the male, which could be explained by the fact that the female lives in the gynaecophoric canal of the male, where it is partly protected by the male's body towards the environment.

In conclusion, AP-SMALDI MSI provided the first evidence for uptake routes of imatinib into *S. mansoni* couples.

Identification of an ovary-related lipid marker to study drug distribution

Discriminating the two sexes in a worm couple can be challenging when interpreting MSI images. This was solved by the identification of an analyte signal which occurred predominantly in paired females (Fig. 4). The discrimination of specific organs within each worm can be another challenging task. This, however, may become of interest when correlations to drug-induced tissue damages are examined. The lipid at *m/z* 778.538133, depicted as the red color channel in Fig. 7, showed highest intensities in the ovary. This lipid was identified as PC(34:3) according to the lipid maps online database [39]. The intensity of imatinib was considerably lower at this location. Thus, the uptake of imatinib into the ovary was less efficient than into the rest of the female worm.

Comparing the results from CLSM and AP-SMALDI MSI showed that the observed morphological changes correlate well with the presence of imatinib. Imatinib was found in the intestine of male and female worms after 5 min and 1 h, respectively, which caused detectable disintegration of gastrodermal tissue after 4 h. For female ovaries, however, no considerable amounts of imatinib were detectable even after 12 h, despite clear ovarian tissue destruction after an incubation time of 24 h at the same imatinib concentration [15]. Besides possible differences in tissue-specific limits of detection of ovaries and other worm organs, this might be explained by a high sensitivity of the ovaries even to low, hardly detectable concentrations of imatinib. About 30% of the schistosomal ovary is made up of proliferative stem cells [43], and stem cells are known to be particularly sensitive to certain compounds [44]. Furthermore, the presumed targets of imatinib in *S. mansoni*, the Abl kinases 1 and 2, were found to be expressed in considerably higher levels in the ovary compared to the gastrodermis [15], which might account for a higher ovarian drug sensitivity. In addition or alternatively to these direct effects, the ovary might also be affected indirectly, for instance by action of imatinib on surrounding tissues with downstream effects on the ovary.

Identification of drug metabolites within the parasite

N-Desmethyl-imatinib is the main bioactive metabolite of imatinib found in human patients. Although it is less active than imatinib, it might still contribute to drug activity [45]. We therefore investigated whether schistosomes are capable of metabolizing imatinib, and if yes, after which time the metabolite is detectable. In Fig. 8, the MS image of a *S. mansoni* couple, treated for 1 h

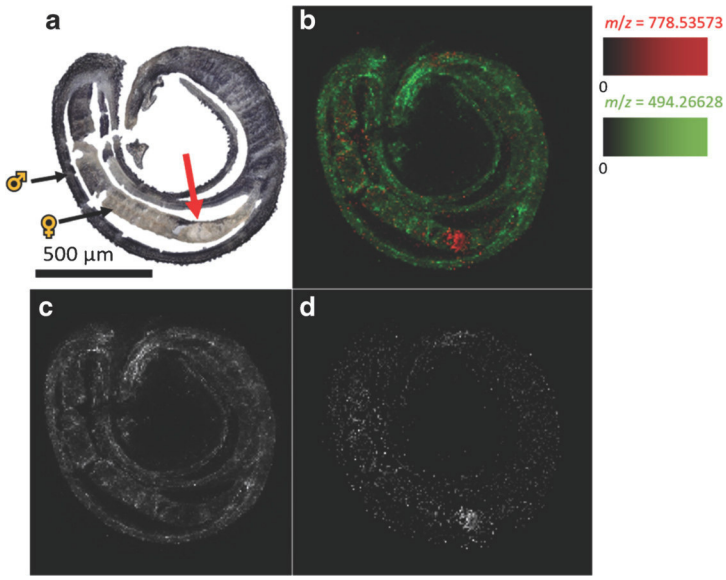

Fig. 7 Mapping of imatinib and an ovary-related lipid marker. **a** Optical image of a tissue section of an *S. mansoni* couple, 100 µmol/L imatinib, 1 h incubation time, arrow marks the ovary; **b** MSI image of the *S. mansoni* couple tissue section, *m/z* 494.266284 (green, imatinib), *m/z* 778.535728 (red, PC(34:3)); **c** MSI image of the *S. mansoni* couple, *m/z* 494.266284 (imatinib), corresponding to the green channel in **b**; **d** MSI image of the *S. mansoni* couple, *m/z* 778.535728 (PC(34:3)), corresponding to the red channel in **b**. Measured m/z values and errors: 494.265444 (− 1.70 ppm), 778.535266 (− 0.59 ppm), 579.534635 (− 0.09 ppm)

with an imatinib concentration of 100 µmol/L, is shown. The displayed signals are imatinib (*m/z* 494.266284) in red and N-desmethyl imatinib (*m/z* 480.250634) in green. Both signals showed a similar distribution throughout the bodies of male and female worms. In the measurement series of the lower-concentration treatment group (20 µmol/L), the metabolite could not be detected in all samples (ESM Fig. S12).

This result strongly suggests that imatinib is metabolized by *S. mansoni* to the same metabolite as found in humans. The signal intensities of the metabolite were much lower than of imatinib at all time points. Furthermore, the intensity ratios of N-desmethyl imatinib and imatinib increased from $1.8 \cdot 10^{-3}$ after 20 min to $3.29 \cdot 10^{-3}$ at 1 h and $3.97 \cdot 10^{-3}$ at 4 h (ESM Fig. S12). These findings suggest a low rate of metabolization and an accumulation of the metabolite over time. As the metabolite is capable of inhibiting cell proliferation and inducing apoptosis in human cells [45, 46], it might very well contribute to the tissue destruction found in imatinib-treated *S. mansoni*.

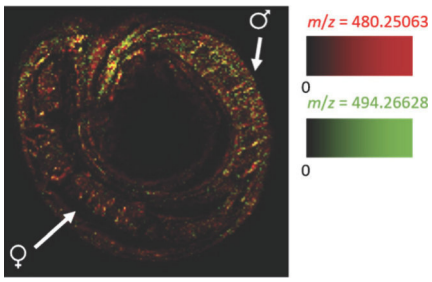

Fig. 8 MSI image of an *S. mansoni* couple tissue section, 100 µmol/L imatinib, 1 h incubation time, *m/z* 494.266284 (red, imatinib), and *m/z* 480.250634 (green, N-desmethyl imatinib). One representative of the 26 measured worm samples is shown. Measured m/z values and errors: 494.265444 (− 1.70 ppm), 480.249815 (− 1.71 ppm)

Conclusion

The distribution of imatinib in sections of *S. mansoni* can be well assessed by AP-SMALDI MSI. Two experimental series with different imatinib concentrations (100 µmol/L and 20 µmol/L) were performed using incubation times ranging from 5 min to 24 h. The data give indications that imatinib is taken up via the oral route and perhaps also via the tegumental surface of the worms. The male shields the female in the gynaecophoric canal, which might explain why imatinib was not detectable in the female after short incubation periods. Signal intensities of imatinib in the ovary of the female were lower compared to the rest of the worm. This may be due to lower uptake of substances into the ovary than into other organs. At the level of differentially occurring lipid classes, distinctions between male and female *S. mansoni* as well as the allocation of organs can be achieved.

This is the first time that the distribution of a drug was directly investigated in a parasite, the human pathogen *S. mansoni*, using AP-SMALDI MSI. Comparison to previous studies of the imatinib effects on the morphology of adult *S. mansoni* showed high congruence. Furthermore, as an untargeted approach, the applied technique opened the possibility of determining metabolites, such as N-desmethyl-imatinib.

AP-SMALDI MSI was established as a technique for studying kinetics and drug metabolism in a multicellular parasite. With respect to the urgent need of finding alternative treatments against pathogens threatening not only human but also animal health in a one-health context [47, 48], methods such as AP-SMALDI MSI can be considered as helpful tools. With this technique, it is possible to study not only the effects of repurposed drugs but also novel compounds in schistosomes as well as other pathogens of the NTD spectrum and beyond, if in vitro culture systems are available.

Supplementary Information The online version contains supplementary material available at https://doi.org/10.1007/s00216-021-03230-w.

Acknowledgements The authors thank Christina Scheld, Bianca Kulik, and Georgette Stovall for excellent technical assistance in the maintenance of the parasites.

Author contribution Conceptualization: B. Spengler and S. Haeberlein; methodology: A. Mokosch, S. Gerbig, C.G. Grevelding, S. Haeberlein, and B. Spengler; measurements and data evaluation: A. Mokosch, S. Gerbig; resources: S. Haeberlein and B. Spengler; writing—original draft preparation, A. Mokosch; writing—review and editing: S. Haeberlein, C.G. Grevelding, and B. Spengler; funding acquisition: S. Haeberlein and B. Spengler.

Funding Open Access funding enabled and organized by Projekt DEAL. The work was funded by the LOEWE Center DRUID, which is part of the excellence initiative of the Hessian Ministry of Science, Higher Education and Art (HMWK) and by Deutsche Forschungsgemeinschaft DFG (Sp314-13-1, INST 162/500-1 FUGG). Technical support by TransMIT GmbH, Giessen, Germany, is gratefully acknowledged.

Data availability MS imaging data is available through the Metaspace online data repository (https://metaspace2020.eu).

Declarations

Ethics approval Animal experiments using Syrian hamsters (*Mesocricetus auratus*) as model hosts were performed in accordance with the European Convention for the Protection of Vertebrate Animals used for experimental and other scientific purposes (ETS No 123; revised Appendix A). Experiments have been approved by the Regional Council (Regierungspraesidium) Giessen (V54-19 c 20/15 h 02 GI 18/10 Nr. A 14/2017).

Conflict of interest Financial interests: B. Spengler and C.G. Grevelding are consultants of TransMIT GmbH, Giessen. A. Mokosch, S. Gerbig, and S. Haeberlein declare that they have no financial interests. Non-financial interests: The authors declare that they have no relevant non-financial interests.

References

1. WHO. Working to overcome the global impact of neglected tropical diseases: first WHO report on Neglected Tropical Diseases. Geneva: World Health Organization; 2010.
2. Gryseels B, Polman K, Clerinx J, Kestens L. Human schistosomiasis. Lancet. 2006;368(9541):1106–18.
3. WHO. Schistosomiasis Geneva, Switzerland: World Health Organisation; https://www.who.int/en/news-room/fact-sheets/detail/schistosomiasis. Accessed 02 Oct 2020.
4. Olveda DU, Olveda RM, McManus DP, Cai PF, Chau TNP, Lam AK, et al. The chronic enteropathogenic disease schistosomiasis. Int J Infect Dis. 2014;28:193–203.
5. Despres L, Maurice S. The evolution of dimorphism and separate sexes in schistosomes. Proc R Soc Lond [Biol]. 1995;262(1364):175–80.
6. Gönnert R. Schistosomiasis Studien II. Über die Eibildung bei *Schistosoma mansoni* und das Schicksal der Eier im Wirtsorganismus. Z Tropenmed Parasit. 1955;6:33–52.
7. Vale N, Gouveia MJ, Rinaldi G, Brindley PJ, Gartner F, da Costa JMC. Praziquantel for schistosomiasis: single-drug metabolism revisited, mode of action, and resistance. Antimicrob Agents Chem. 2017;61(5).
8. Ismail M, Metwally A, Farghaly A, Bruce J, Tao LF, Bennett JL. Characterization of isolates of *Schistosoma mansoni* from Egyptian villagers that tolerate high doses of praziquantel. Am J Trop Med Hyg. 1996;55(2):214–8.
9. Wang W, Wang L, Liang YS. Susceptibility or resistance of praziquantel in human schistosomiasis: a review. Parasitol Res. 2012;111(5):1871–7.
10. Tebeje BM, Harvie M, You H, Loukas A, McManus DP. Schistosomiasis vaccines: where do we stand? Parasit Vectors. 2016;9:15.
11. Riveau G, Schacht AM, Dompnier JP, Deplanque D, Seck M, Waucquier N, et al. Safety and efficacy of the rSh28GST urinary schistosomiasis vaccine: a phase 3 randomized, controlled trial in Senegalese children. PLoS Negl Trop Dis. 2018;12(12):22.
12. Waller CF. Imatinib Mesylate. In: Martens UM, editor. Small molecules in hematology. Cham: Springer International Publishing; 2018. p. 1–27.
13. Knight GWA, McLellan D. Use and limitations of imatinib mesylate (Glivec), a selective inhibitor of the tyrosine kinase Abl transcript in the treatment of chronic myeloid leukaemia. Br J Biomed Sci. 2004;61(2):103–11.
14. Manley PW, Cowan-Jacob SW, Buchdunger E, Fabbro D, Fendrich G, Furet P, et al. Imatinib: a selective tyrosine kinase inhibitor. Eur J Cancer. 2002;38:S19–27.
15. Beckmann S, Grevelding CG. Imatinib has a fatal impact on morphology, pairing stability and survival of adult *Schistosoma mansoni in vitro*. Int J Parasitol. 2010;40(5):521–6.
16. Li XS, Haeberlein S, Zhao L, Mughal MN, Zhu T, Liu L, et al. The ABL kinase inhibitor imatinib causes phenotypic changes and lethality in adult *Schistosoma japonicum*. Parasitol Res. 2019;118(3):881–90.

17. Hemer S, Brehm K. *In vitro* efficacy of the anticancer drug imatinib on *Echinococcus multilocularis* larvae. Int J Antimicrob. 2012;40(5):458–62.
18. O'Connell EM, Bennuru S, Steel C, Dolan MA, Nutman TB. Targeting filarial Abl-like kinases: orally available, food and drug administration-approved tyrosine kinase inhibitors are microfilaricidal and macrofilaricidal. Int J Infect Dis. 2015;212(5):684–93.
19. O'Connell EM, Kamenyeva O, Lustigman S, Bell A, Nutman TB. Defining the target and the effect of imatinib on the filarial c-Abl homologue. PLoS Negl Trop Dis. 2017;11(7):17.
20. Pathak V, Colah R, Ghosh K. Tyrosine kinase inhibitors: new class of antimalarials on the horizon? Blood Cells Mol Dis. 2015;55(2): 119–26.
21. de Sousa ACC, Maepa K, Combrinck JM, Egan TJ. Lapatinib, nilotinib and lomitapide inhibit haemozoin formation in malaria parasites. Molecules. 2020;25(7):1571.
22. Moslehi M, Namdar F, Esmaeilifallah M, Hejazi S, Sokhanvari F, Siadat A, et al. Evaluation of different concentrations of imatinib on the viability of *Leishmania major*: an *in vitro* study. Adv Biomed Res. 2019;8(1):61.
23. Buro C, Beckmann S, Oliveira KC, Dissous C, Cailliau K, Marhofer RJ, et al. Imatinib treatment causes substantial transcriptional changes in adult *Schistosoma mansoni in vitro* exhibiting pleiotropic effects. PLoS Negl Trop Dis. 2014;8(6):13.
24. Beckmann S, Hahnel S, Cailliau K, Vanderstraete M, Browaeys E, Dissous C, et al. Characterization of the Src/Abl Hybrid Kinase SmTK6 of *Schistosoma mansoni*. J Biol Chem. 2011;286(49): 42325–36.
25. Ding S, Qiao X, Suryadi J, Marrs GS, Kucera GL, Bierbach U. Using fluorescent post-labeling to probe the subcellular localization of DNA-targeted platinum anticancer agents. Angew Chem Int Ed. 2013;52(12):3350–4.
26. Rompp A, Guenther S, Takats Z, Spengler B. Mass spectrometry imaging with high resolution in mass and space (HR(2) MSI) for reliable investigation of drug compound distributions on the cellular level. Anal Bioanal Chem. 2011;401(1):65–73.
27. Kadesch P, Quack T, Gerbig S, Grevelding CG, Spengler B. Lipid topography in *Schistosoma mansoni* cryosections, revealed by microembedding and high-resolution atmospheric-pressure matrix-assisted laser desorption/ionization (MALDI) mass spectrometry imaging. Anal Chem. 2019;91(7):4520–8.
28. Aichler M, Walch A. MALDI imaging mass spectrometry: current frontiers and perspectives in pathology research and practice. Lab Investig. 2015;95(4):422–31.
29. Karlsson O, Hanrieder J. Imaging mass spectrometry in drug development and toxicology. Arch Toxicol. 2017;91(6):2283–94.
30. Makarov A. Electrostatic axially harmonic orbital trapping: a high-performance technique of mass analysis. Anal Chem. 2000;72(6): 1156–62.
31. Hu QZ, Noll RJ, Li HY, Makarov A, Hardman M, Cooks RG. The Orbitrap: a new mass spectrometer. J Mass Spectrom. 2005;40(4): 430–43.
32. Müller MA, Kompauer M, Strupat K, Heiles S, Spengler B. Implementation of a high-repetition-rate laser in an AP-SMALDI MSI system for enhanced measurement performance. J Am Soc Mass Spectrom. 2020, Accepted for publication, https://doi.org/10.1021/jasms.0c00368.
33. Grevelding CG. The female-specific W1 sequence of the Puerto-Rican strain of *Schistosoma-mansoni* occurs in both genders of a Liberian strain. Mol Biochem Parasitol. 1995;71(2):269–72.
34. Dettman CD, Higginsoptiz SB, Saikoolal A. Enhanced efficacy of the paddling method for schistosome infection of rodents by a 4-step pre-soaking procedure. Parasitol Res. 1989;76(2):183–4.
35. Ramirez B, Bickle Q, Yousif F, Fakorede F, Mouries MA, Nwaka S. Schistosomes: challenges in compound screening. Expert Opin Drug Discov. 2007;2:S53–61.
36. Kompauer M, Heiles S, Spengler B. Atmospheric pressure MALDI mass spectrometry imaging of tissues and cells at 1.4-mu m lateral resolution. Nat Methods. 2017;14(1):90–6.
37. Kompauer M, Heiles S, Spengler B. Autofocusing MALDI mass spectrometry imaging of tissue sections and 3D chemical topography of nonflat surfaces. Nat Methods. 2017;14(12):1156–+.
38. Paschke C, Leisner A, Hester A, Maass K, Guenther S, Bouschen W, et al. Mirion-a software package for automatic processing of mass spectrometric images. J Am Soc Mass Spectrom. 2013;24(8):1296–306.
39. Fahy E, Sud M, Cotter D, Subramaniam S. LIPID MAPS online tools for lipid research. Nucleic Acids Res. 2007;35:W606–W12.
40. Palmer A, Phapale P, Chernyavsky I, Lavigne R, Fay D, Tarasov A, et al. FDR-controlled metabolite annotation for high-resolution imaging mass spectrometry. Nat Methods. 2017;14(1):57–60.
41. Neves R, Biolchini CD, Machado-Silva JR, Carvalho JJ, Branquinho TB, Lenzi HL, et al. A new description of the reproductive system of *Schistosoma mansoni* (Trematoda : Schistosomatidae) analyzed by confocal laser scanning microscopy. Parasitol Res. 2005;95(1):43–9.
42. Ferreira MS, de Oliveira DN, de Oliveira RN, Allegretti SM, Vercesi AE, Catharino RR. Mass spectrometry imaging: a new vision in differentiating *Schistosoma mansoni* strains. J Mass Spectrom. 2014;49(1):86–92.
43. Kellershohn J, Thomas L, Hahnel SR, Grunweller A, Hartmann RK, Hardt M, et al. Insects in anthelminthics research: lady beetle-derived harmonine affects survival, reproduction and stem cell proliferation of *Schistosoma mansoni*. PLoS Negl Trop Dis. 2019;13(3):23.
44. Karhu ST, Valimaki MJ, Jumppanen M, Kinnunen SM, Pohjolainen L, Leigh RS, et al. Stem cells are the most sensitive screening tool to identify toxicity of GATA4-targeted novel small-molecule compounds. Archi Toxicol. 2018;92(9):2897–911.
45. Mlejnek P, Dolezel P, Faber E, Kosztyu P. Interactions of N-desmethyl imatinib, an active metabolite of imatinib, with P-glycoprotein in human leukemia cells. Ann Hematol. 2011;90(7): 837–42.
46. Gschwind HP, Pfaar U, Waldmeier F, Zollinger M, Sayer C, Zbinden P, et al. Metabolism and disposition of imatinib mesylate in healthy volunteers. Drug Metab Dispos. 2005;33(10):1503–12.
47. Webster JP, Gower CM, Knowles SCL, Molyneux DH, Fenton A. One health - an ecological and evolutionary framework for tackling neglected zoonotic diseases. Evol Appl. 2016;9(2):313–33.
48. Sachs-Barrable K, Conway J, Gershkovich P, Ibrahim F, Wasan KM. The use of the United States FDA programs as a strategy to advance the development of drug products for neglected tropical diseases. Drug Dev Ind Pharm. 2014;40(11):1429–34.

5.4 Kinasen in *Fasciola hepatica*: anthelmintische Effekte und Gewebetropismus von Kinaseinhibitoren

Targeting kinases in *Fasciola hepatica*: anthelminthic effects and tissue distribution of selected kinase inhibitors

Morawietz CM, Houhou H, Puckelwaldt O, Hehr L, Dreisbach D, Mokosch A, Roeb E, Roderfeld M, Spengler B*, **Haeberlein S***

Frontiers in Veterinary Science (2020) 7:611270

Eigener Anteil an der Entstehung der Publikation

- Leitung des Gesamtprojektes: 90%
- Durchführung/Auswertung der Experimente: 20%
- Anfertigung des Manuskripts: 90%

frontiers in Veterinary Science

ORIGINAL RESEARCH
published: 21 December 2020
doi: 10.3389/fvets.2020.611270

Targeting Kinases in *Fasciola hepatica*: Anthelminthic Effects and Tissue Distribution of Selected Kinase Inhibitors

Carolin M. Morawietz[1], Hicham Houhou[2], Oliver Puckelwaldt[2], Laura Hehr[3], Domenic Dreisbach[1], Annika Mokosch[1], Elke Roeb[3], Martin Roderfeld[3], Bernhard Spengler[1†] and Simone Haeberlein[2†]*

[1] Institute of Inorganic and Analytical Chemistry, Justus Liebig University Giessen, Giessen, Germany, [2] Biomedical Research Center Seltersberg (BFS), Institute of Parasitology, Justus Liebig University Giessen, Giessen, Germany, [3] Department of Gastroenterology, Justus Liebig University Giessen, Giessen, Germany

OPEN ACCESS

Edited by:
Khalid Mehmood, Islamia University of Bahawalpur, Pakistan

Reviewed by:
Aaron Maule, Queen's University Belfast, United Kingdom
Paul McVeigh, Queen's University Belfast, United Kingdom

***Correspondence:**
Simone Haeberlein
simone.haeberlein@vetmed.uni-giessen.de

[†] These authors share senior authorship

Specialty section:
This article was submitted to Parasitology, a section of the journal Frontiers in Veterinary Science

Received: 28 September 2020
Accepted: 13 November 2020
Published: 21 December 2020

Citation:
Morawietz CM, Houhou H, Puckelwaldt O, Hehr L, Dreisbach D, Mokosch A, Roeb E, Roderfeld M, Spengler B and Haeberlein S (2020) Targeting Kinases in Fasciola hepatica: Anthelminthic Effects and Tissue Distribution of Selected Kinase Inhibitors. Front. Vet. Sci. 7:611270. doi: 10.3389/fvets.2020.611270

Protein kinases have been discussed as promising druggable targets in various parasitic helminths. New drugs are also needed for control of fascioliasis, a food-borne trematode infection and worldwide spread zoonosis, caused by the liver fluke *Fasciola hepatica* and related species. In this study, we intended to move protein kinases more into the spotlight of *Fasciola* drug research and characterized the fasciolicidal activity of two small-molecule inhibitors from human cancer research: the Abelson tyrosine kinase (ABL-TK) inhibitor imatinib and the polo-like 1 (PLK1) inhibitor BI2536. BI2536 reduced viability of 4-week-old immature flukes *in vitro*, while adult worms showed a blockade of egg production. Together with a significantly higher transcriptional expression of PLK1 in adult compared to immature worms, this argues for a role of PLK1 in fluke reproduction. Both fluke stages expressed ABL1-TK transcripts at similar high levels and were affected by imatinib. To study the uptake kinetic and tissue distribution of imatinib in *F. hepatica*, we applied matrix-assisted laser desorption/ionization (MALDI) mass spectrometry imaging (MSI) for the first time in this parasite. Drug imaging revealed the accumulation of imatinib in different fluke tissues from 20 min to 12 h of exposure. Furthermore, we show that imatinib is metabolized to N-desmethyl imatinib by *F. hepatica*, a bioactive metabolite also found in humans. Besides the vitellarium, gastrodermal tissue showed strong signal intensities. *In situ* hybridization demonstrated the gastrodermal presence of *abl1* transcripts. Finally, we assessed transcriptional changes of physiologically important genes in imatinib-treated flukes. Moderately increased transcript levels of a gene encoding a multidrug resistance protein were detected, which may reflect an attempt to defend against imatinib. Increased expression levels of the cell cycle dependently expressed histone *h2b* and of two genes encoding superoxide dismutases (SODs) were also observed. In summary, our pilot study demonstrated cross-stage activity of imatinib but not BI2536 against immature and adult *F. hepatica in vitro*; a fast incorporation of imatinib within minutes, probably via the oral route; and imatinib-induced expression

changes of physiologically relevant genes. We conclude that kinases are worth analyzing in more detail to evaluate the potential as therapeutic targets in *F. hepatica*.

Keywords: *Fasciola hepatica*, kinases, drug target, inhibitors, imatinib, BI 2536, MALDI mass spectrometry imaging, superoxide dismutase

INTRODUCTION

Parasitic zoonoses have a dual impact by afflicting humans as well as animals, the latter causing substantial economic loss in livestock farming. Fascioliasis is a widely distributed zoonotic infection reported from almost half of all countries around the world, and it is caused by liver flukes of the genus *Fasciola* spp. (1). Herd-level prevalences reach up to 86% in some European countries and up to 91% in Africa (2, 3). Not surprisingly, the global economic losses in animal milk and meat production were estimated at several billion $/year (2). Besides animals, *Fasciola* spp. infects about 2.4–17 million humans (1). The WHO classifies fascioliasis as a neglected tropical disease (NTD), because particularly resource-poor countries are afflicted and the common impetus for disease control is insufficient. While fascioliasis proceeds subclinically in most patients, it can also result in anemia, weight loss, malnutrition, and biliary cirrhosis, which decrease quality of life and cause devastating developmental deficits in children and adults (4). Under the One Health aspect, finding effective control measures for both human and livestock infections appears obligatory. Among the most important species with respect to human and animal health is *Fasciola hepatica*, which infects its final host by metacercariae. Upon oral ingestion, juvenile flukes hatch in the small intestine and penetrate the intestinal wall to reach the liver. After penetrating the liver capsule, the growing and maturing liver flukes migrate, and feed through the liver parenchyma during the acute stage of infection. As adults, they reside in the bile ducts and cause the chronic stage of disease (5). Triclabendazole is the drug of choice because of its activity against both immature and adult fluke stages. Probably as a consequence of its massive use in the livestock industry, triclabendazole-resistant *F. hepatica* strains have spread in numerous countries, which motivates the search for alternative treatment options (6).

Protein kinases (PK) have been discussed as druggable targets with high potential in various parasitic helminths, including cestodes, trematodes, and filaria (7–9). In mammalian cells, PK are known as regulators of fundamental biological processes, including cell cycle control and cell differentiation (10, 11). Employing PK as targets is even more attractive, as numerous small-molecule kinase inhibitors are at hand that have been pursued as anti-cancer drugs. This allows to piggy-back on existing drugs, which could potentially be repurposed or serve as a basis for the design of optimized anthelmintic kinase inhibitors (12). While kinase inhibitors have been intensely tested against blood flukes (*Schistosoma* spp.), the study of kinases as targets has been largely neglected in the related liver flukes. Previous studies focused on the usefulness of selected kinases as diagnostic marker for *Fasciola* spp. (phosphoenolpyruvate carboxykinase) or as vaccine candidate (phosphoglycerate kinase) (13, 14). The presumably only kinase evaluated as chemotherapeutic target is phosphofructokinase and dates back to 1962 (15, 16). However, work on a related phosphofructokinase inhibitor was not further continued because of suboptimal *in vivo* efficacy (17).

To move kinases more into the spotlight of *Fasciola* drug research, we recently demonstrated a cross-stage expression pattern of several kinases that have been described as anthelminthic targets in other species (18). Targeting several fluke stages by the same kinase inhibitor thus appears achievable. Here, we extended these studies and evaluated the fasciolicidal effects of two kinase inhibitors with well-described antischistosomal activity: the Abelson tyrosine kinase (ABL-TK) inhibitor imatinib and the polo-like kinase (PLK) inhibitor BI2536 (19–21). Biochemical studies confirmed that schistosomal ABL-TK and PLK1 are targets for imatinib and BI2536, respectively (22–24). We previously identified potential orthologs of ABL-TK and PLK1 kinases in *F. hepatica* (18), which makes imatinib and BI2536 excellent candidates for a pilot study of kinase inhibitors with fasciolicidal potential.

Next to quantifying *in vitro* effects of imatinib and BI2536 on the viability of two pathogenic stages of *F. hepatica*, we studied the tissue distribution of imatinib in adult flukes. To this end, we applied matrix-assisted laser desorption/ionization (MALDI) mass spectrometry imaging (MSI) for the first time in this parasite. Drug imaging by this technique allowed us to answer fundamental questions such as "How fast is imatinib taken up by the fluke?," "In which tissues does it accumulate?," and "Is it metabolized?" Finally, we assessed transcriptional changes of genes associated with oxidative stress, cell cycle, and drug responses in imatinib-treated flukes, which allowed us to speculate on a possible anthelmintic mode of action.

MATERIALS AND METHODS

Ethical Statement

Rats (*Rattus norvegicus*) were used as model hosts in accordance with the European Convention for the Protection of Vertebrate Animals used for Experimental and Other Scientific Purposes (ETS No 123; revised Appendix A). The experiments were approved by the Regional Council (Regierungspraesidium) Giessen (V54-19c20 15 h 02 GI 18/10 Nr. A16/2018).

Harvesting of *F. hepatica*

Male Wistar rats RjHan:WI (Janvier, France) served as final host to obtain immature and adult stages of *F. hepatica*. Rats at 5 weeks age were orally infected with 25 metacercariae from an Italian strain of *F. hepatica* (Ridgeway Research, UK). Immature flukes were collected from livers at 4 weeks p.i., and adult flukes were collected from bile ducts at 12 weeks p.i. Worms were kept for 1 h in 0.9% NaCl to allow clearance of gut contents. Parasites

were then used for *in vitro* culture experiments, or they were embedded in Tissue-Tek (Sakura Finetek, The Netherlands) for subsequent *in situ* hybridizations.

In vitro Culture and Inhibitor Treatment

The anthelminthic activity of selected kinase inhibitors against immature and adult stages of *F. hepatica* was assessed *in vitro*. The worms were individually cultured in 12-well-plates in RPMI medium supplemented with 5% chicken serum, 1% ABAM-solution (10,000 units penicillin, 10 mg streptomycin, and 25 mg amphotericin B per milliliter) (all from Gibco), and 100 µg/ml gentamycin (Sigma-Aldrich, USA). Different concentrations of a kinase inhibitor (20, 50, 100, or 150 µM) or the same volume of the inhibitor's solvent dimethyl sulfoxide (DMSO) was added as a negative control. The following kinase inhibitors were tested: the PLK1 inhibitor BI2536 (Selleckchem, Germany) and the ABL-TK inhibitor imatinib [imatinib mesylate, purity ≥ 98% (HPLC); Enzo Life Sciences, Germany]. The flukes were incubated at 37°C in a 5% CO_2 atmosphere for 72 h, and medium plus inhibitor was refreshed every 24 h. Inhibitor-induced effects on worm viability were assessed every 24 h using a stereo microscope at 10× magnification (M125 C, Leica, Germany). Worm motility was assessed using the following scores: 3 (normal motility), 2 (reduced motility), 1 (minimal and sporadic movements), and 0 (no movement even upon mechanical stimulation with forceps was considered dead). When needed, egg numbers produced in the last 24 h of the 72-h culture period were counted. After the 72-h culture, flukes were immersed in Monarch RNA Protect Buffer (New England BioLabs, USA), individually snap frozen in liquid nitrogen, and stored at −80°C until RNA extraction.

MTT Assay

The hepatocyte cell line FL83B (25) was used to study the cytotoxic effects of imatinib. The same cell line was used to quantify cytotoxicity of triclabendazole as a reference compound to allow a direct comparison of the cytotoxic potential of both compounds. FL83B cells were obtained from ATCC (#CRL-2390) and cultured as recommended by ATCC. FL83B cells were exposed to imatinib and triclabendazole (analytical standard; Sigma). Imatinib was dissolved in pure water while triclabendazole was dissolved in DMSO. Initial cell densities of 25,000–50,000 cells/well (96 well-plate, Corning, Costar, flat bottom) turned out to be in the optimum range for all of the tests and cells were allowed to settle for 24 h. Cell viability tests were performed after 24 h of exposure to the test substances. Subsequently after removal of the medium containing test substances, cells were incubated for 1 h with 0.5 mg/ml MTT (Sigma # M5655) in culture medium for all assays. After the incubation with MTT and removal of the medium, 100 µl of DMSO was added and plates were incubated for 1 h. Absorption of formazan was measured at 570 nm using a microplate reader (Tecan Infinite M Plex, Tecan, Austria). The cytotoxicity was calculated as % dead cells (26):

$$100\% - [(\text{Absorbance in test}^{*} \text{ wells}/\text{Absorbance in control}^{**} \text{ wells})/\times 100\ \text{U}]$$

*Test wells were the test-substance containing wells. **Control wells were wells without test substance, i.e., 100% survival. EC50 value was calculated in Excel by plotting log(conc.) on the ordinate against cytotoxicity (abscissa). An optimal trendline was assessed by polynomial fitting and subsequently used for calculation of the EC50 values. Non-linear least-squares data fitting was used to visualize the cytotoxicity plot (27). All tests were performed at least two times and each time in duplicate.

Identification of Orthologous Genes

Orthologs of genes were identified in the genome of *F. hepatica* (Center for Genomic Research, University of Liverpool, BioProject ID PRJEB25283, version 11.0 of August 2018) using BLASTp searches starting from known orthologs in *S. mansoni* and using the public domain tool WormBase ParaSite, version WBPS13 (https://parasite.wormbase.org) (28). Correct annotation of the hits was further confirmed by another BLASTp search in NCBI against the genome of *H. sapiens*. Gene names, accession numbers, and biological function are listed in **Supplementary Table 1**. The identity of the potential *F. hepatica* orthologs was further verified by confirming the presence of conserved protein domains using SMART (http://smart.embl-heidelberg.de/) (29). Transmembrane helices in proteins were predicted using the membrane protein topology prediction method TMHMM (Server v. 2.0), based on a hidden Markov model (http://www.cbs.dtu.dk/services/TMHMM/).

RNA Isolation and cDNA Synthesis

Total RNA from immature and adult flukes was extracted using the Monarch total RNA Miniprep kit (New England BioLabs) following the manufacturer's protocol. Individual flukes were stored and then mechanically homogenized in 300–600 µl of 1× RNA/DNA protection buffer. RNA quality and quantity were assessed using the BioAnalyzer 2100 and an Agilent RNA 6000 Nano or Pico Chip according to the manufacturer's instructions (Agilent Technologies, USA). cDNA was synthesized from 5 to 10 ng of total RNA using the QuantiTect Reverse Transcription Kit (QIAGEN, Germany) including a genomic DNA removal step. A 1:5–1:10 dilution of cDNA was used as template in quantitative real-time PCR (qRT-PCR).

Quantitative Real-Time PCR

Gene expression was determined in adult flukes after inhibitor treatment using qRT-PCR. Only living flukes were used for analyses. Primers were commercially synthesized by Integrated DNA Technologies IDT (USA) and designed for an amplicon size of 141–215 bp and a melting temperature of 60°C (**Supplementary Table 2**) using the Primer3Plus software tool (30). When possible, primer pairs were located on different exons of a gene to exclude amplification of contaminating genomic DNA. All primer pairs yielded one specific PCR product, no primer dimers, and an amplification efficiency of 85–100%. qRT-PCRs were run on a Rotorgene Q cycler (QIAGEN, Germany) using the 2× PerfeCTa SYBR Green SuperMix (Quantabio, USA) in a final volume of 10 µl and 400 nM of each primer. The following PCR conditions were applied: initial denaturation step at 95°C for 3 min, 45 cycles at 95°C for 10 s, 60°C for 15 s, and

72°C for 20 s. Melting curve analysis was performed to exclude the generation of primer dimers and to verify primer specificity. All qRT-PCRs were run with three technical replicates and mostly comprised three to five biological replicates. The expression of genes of interest was determined by relative quantification against the geometric mean of two reference genes (glutamyl-prolyl-tRNA synthetase, Fh*eprs*, and tubulin-specific chaperone D, Fh*tbcd*) (18). Relative expression levels were expressed as n-fold difference vs. the expression in control flukes based on the ΔΔCt method (relative expression $= 2^{-\Delta\Delta Ct}$). For the quantification of kinase transcript levels, relative expression values were calculated by the formula: relative expression $= 2^{-\Delta Ct} \times f$, with $f = 1{,}000$ as an arbitrary factor.

In situ Hybridization

To detect the occurrence of transcripts of Fh*abl1*, *in situ* hybridization was performed as described earlier with slight modifications (31). Twelve-week-old *F. hepatica* worms were embedded in Tissue-Tek (Sakura Finetek), frozen on dry ice, and stored at −80°C until use. Traversal cryosections of 10 µm thickness were prepared using a cryostat HM525 (Thermo Fisher Scientific, Germany). Sections were dried, post-fixed in 4% PFA, and permeabilized with PBSTx. The hybridization reaction was carried out overnight at 55°C. Following washing with saline sodium citrate buffer (SSC), the sections were incubated with anti-DIG antibodies coupled with alkaline phosphatase (Roche, Germany). After subsequent washing steps with maleic acid buffer with Tween (MAB-T), the development reaction was carried out using naphthol-AS-phosphate, and Fast Red TR (Sigma). The Riboprobes for the hybridization reaction were generated as previously described (32). The following primers were used to generate the template for probe synthesis with a length of 596 bp: 5′-GAATCTCCTTCTCCTAACGGT-3′, reverse 5′-ACCAGATTTTTTAGGAGGTCTTC-3′. The labeling reaction using digoxigenin-11-UTP (NU-803-DIGXS; Jena Bioscience, Germany) was done using T3 or SP6 RNA polymerases for sense and antisense probes. Labeled transcripts were controlled for the correct size by gel electrophoresis.

Embedding of *F. hepatica* for AP-SMALDI MSI

Imatinib-treated adult flukes were used for drug imaging by atmospheric-pressure scanning microprobe MALDI MSI (AP-SMALDI MSI). After treatment with 100 µM imatinib for different time periods (20 min, 4 h, and 12 h), the worms were quickly immersed in PBS followed by distilled water. Subsequently, they were embedded in 8 wt% aqueous gelatin solution (gelatin powder, VWR, USA) using Tissue-Tek cryomolds (15 × 15 × 5 mm^3) (Sakura Finetek), frozen on dry ice, and stored at −80°C until use. Transversal sections of embedded worms of 20 µm thickness were obtained using a cryostat HM525 (Thermo Fisher Scientific) at around −23°C. The quality of the sections was monitored by a digital light microscope (VHX-5000; Keyence, Japan) to obtain optical images in 250× magnification. Sections were stored at −80°C until AP-SMALDI MSI sample preparation. For each timepoint of imatinib treatment, two flukes were analyzed.

AP-SMALDI MSI Sample Preparation and Measurements

Before matrix application, tissue sections were defrosted and protected from humidity for 10 min in a desiccator. A matrix solution consisting of 2,5-dihydroxybenzoic acid (DHB for synthesis, Merck, Germany) in a concentration of $\beta = 30$ g/L solved in acetone/water (acetone uvasol, Merck; water HiPerSolv Chromanorm for HPLC, filtered at 0.2 µm, VWR) 1:1 *v/v* with 0.1 vol% trifluoroacetic acid (TFA, uvasol for spectroscopy, Merck) was freshly prepared before measurement. A volume of 100 µl of matrix solution was sprayed onto the sample surface using an ultrafine pneumatic sprayer system (SMALDIPrep, TransMIT GmbH, Germany) with a flow rate of 10 µl/min and N_2-pressure of 1 bar. AP-SMALDI MSI was performed on a Q Exactive orbital trapping mass spectrometer (33) (Thermo Fisher Scientific) equipped with an autofocusing AP-SMALDI5 AF ion source (34) (TransMIT GmbH). Measurements were conducted with a step size of 10 µm under activation of the pixel-wise autofocusing feature, and 50 laser pulses were applied per pixel. All imaging experiments were performed in positive-ion mode in *m/z* range of 250–1,000 with a mass resolution of 140,000 at *m/z* 200. For internal calibration, the lock masses *m/z* 273.03937 (corresponding to $[2DHB+H-2H_2O]^+$) and *m/z* 716.12462 (corresponding to $[5DHB-4H_2O+NH_4]^+$) were set. Further adjusted parameters were a maximum ion injection time of 500 ms, an s-lens level of 100.0 arbitrary units, 300°C capillary temperature, as well as an acceleration voltage of 3.00 kV.

Data Acquisition and Analysis of AP-SMALDI MSI Experiments

For data acquisition, Q Exactive Tune (version 2.9, Thermo Fisher Scientific) was used, and the ion source was operated by the SMALDIControl software (V1.1-118, TransMIT GmbH). XCalibur (version 4.0.27.13, Thermo Fisher Scientific) was applied for processing of mass spectra. Mirion software package (version 3.2.64.16) (35) (TransMIT GmbH) was utilized for visualization of imaging data; for data evaluation, the histogram bin width was adjusted to 0.005 u. No TIC normalization was used for image creation. Compounds were assigned based on accurate mass measurements with a mass tolerance of <3 ppm and LIPIDMAPS (36) database searches. For further evaluation, Root-mean-square-error (RMSE) plots were created using the Mirion software package.

H&E-Staining After AP-SMALDI MSI

After imaging, the matrix layer was washed off with 80 vol% aqueous ethanol (EtOH purissimum, Roth, Germany) and stained according to the hematoxylin and eosin (H&E) staining protocol (Mayer's Hematoxylin and Eosin-Y solution, Sigma-Aldrich; m- and p-Xylol for analysis, Merck; Eukitt quick hardening mounting medium for microscopy, Honeywell-Fluka, USA). Optical images (250 × magnification) were recorded after the mounting medium has dried, using a digital light microscope (VHX-5000, Keyence).

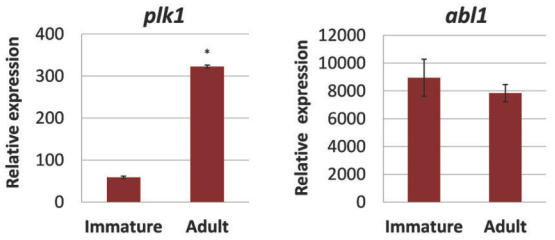

FIGURE 1 | Transcriptional expression of selected kinases in different developmental stages of *Fasciola hepatica*. Relative expression in 4-week-old immature and 12-week-old adult worms was determined by qRT-PCR and normalization against two reference genes, glutamyl-prolyl-tRNA synthetase (Fh*eprs*), and tubulin-specific chaperone D (Fh*tbcd*). Data represent the mean ± SEM of three to four biological replicates. Relative expression values were calculated by the formula $2^{-\Delta Ct} \times f$, with $f = 1{,}000$ as an arbitrary factor. Significant differences are indicated with $^*p < 0.05$ (Wilcoxon rank sum test). *abl1*, tyrosine-protein kinase ABL1; *plk1*, polo-like kinase 1. Data from (18) (modified) under the Creative Commons license (http://creativecommons.org/licenses/by/4.0/).

Statistical Analysis

Statistical significance was tested using the non-parametric Wilcoxon rank sum test (https://ccb-compute2.cs.uni-saarland.de/wtest/) (37). $p < 0.05$ was considered statistically significant. Error bars represent the standard error of the mean (SEM).

RESULTS

Transcriptional Expression of Selected Kinases in Pathogenic Stages of *F. hepatica*

Before testing kinase inhibitors, we first determined the transcript (expression) levels of potentially druggable kinases in two relevant pathologic life stages of *F. hepatica*: early immature flukes (here 4 weeks age) that typically cause acute fascioliasis while migrating through liver parenchyma and the adult flukes (here 12 weeks old) residing in the bile duct during chronic fasciolosis. We focused on two kinases that were previously discussed as promising anthelminthic targets against other types of parasitic flatworms such as schistosomes (7, 8, 19, 20, 38–41), and for which we previously described putative orthologs in *F. hepatica* (18). These were the PLK1 ortholog Fh*plk1* and the ABL-TK ortholog Fh*abl1* (for accession numbers, see **Supplementary Table 1**). Both kinases were expressed in both developmental stages as revealed by qRT-PCR, albeit with varying levels (**Figure 1**). The overall transcript levels were up to 152-fold higher for Fh*abl1* compared to Fh*plk1*. Notably, Fh*plk1* was >5-fold upregulated during development to the adult stage. Taken together, Fh*plk1* and Fh*abl1* were expressed in both stages relevant for pathogenicity of fasciolosis, and Fh*plk1* exhibited a stage-dependent regulation of expression levels.

Effect of PLK1 and ABL Kinase Inhibitors on Viability of *F. hepatica*

Next, we tested the druggability of PLK1 and ABL kinases by treating immature and adult *F. hepatica* with commercial kinase inhibitors *in vitro*. As a primary readout, fluke motility and survival were assessed every 24 h within a 72-h culture period. We tested the PLK1 inhibitor BI2536 and the ABL-TK inhibitor imatinib, at concentrations of 20–150 μM. Both inhibitors had lethal effects on immature flukes. The efficacy of imatinib (150 μM lethal after 72 h for all flukes, and 100 μM for 4 out of 6 flukes) was somewhat lower compared to BI2536 (100 μM lethal after 72 h for all flukes) (**Figure 2**). In adult *F. hepatica*, however, BI2536 failed to affect motility at any tested concentration. At 150 μM, imatinib was lethal for two of six adult flukes and reduced the motility of the others to a minimum (score of 1) within 72 h. In addition, some individuals had pronounced tegumental damage with bleb formation at their surface (**Figure 3**). Furthermore, we compared the *in vitro* efficacy of imatinib with the gold standard triclabendazole based on motility scoring of immature flukes after 72 h exposure. While imatinib clearly affected fluke vitality at 100 μM, triclabendazole reached a similar effect at 50 μM (**Supplementary Figures 1A,B**). Cytotoxicity of both drugs toward the murine liver cell line FL83B was comparable with EC50 values of 95.0–96.8 μM (**Supplementary Figures 1C,D**). Taken together, imatinib performed almost as well as triclabendazole *in vitro* and showed strong fasciolicidal effects against immature and adult flukes, while BI2536 was incapable to affect viability of adults.

The PLK1 Inhibitor BI2536 Interrupts Egg Production

Given the high transcript abundance of Fh*plk1* in adult worms, it was surprising to note the failure of the PLK1 inhibitor BI2536 to affect viability of the adults. Because PLK1 was found expressed in gonadal tissue of a related flatworm (22), we wondered whether BI2536 may affect reproduction. To answer this question, the number of eggs produced per adult liver fluke was quantified at the end of the 72-h treatment period and compared to the control group without treatment. A concentration as low as 20 μM significantly reduced the egg count to 6% of the amount produced by control worms, and 50–100 μM abolished egg production completely (**Figure 4**), while leaving motility of the worms entirely unaffected (**Figure 3**). Therefore, effects of PLK1 inhibition seem to be restricted to reproduction in adult *F. hepatica*, and a reproductive function of PLK1 mirrors the expression peak of this kinase at the adult but not immature developmental stage.

Detection of the ABL Kinase Inhibitor Imatinib in Tissues of *F. hepatica* by MALDI MSI

We studied the tissue tropism of imatinib in adult *F. hepatica* to get a first idea of the potential uptake mode, distribution, and metabolization within tissue over time. Adult flukes were treated for 20 min, 4 h, or 12 h with 100 μM of imatinib, followed by drug imaging in transverse sections using the innovative

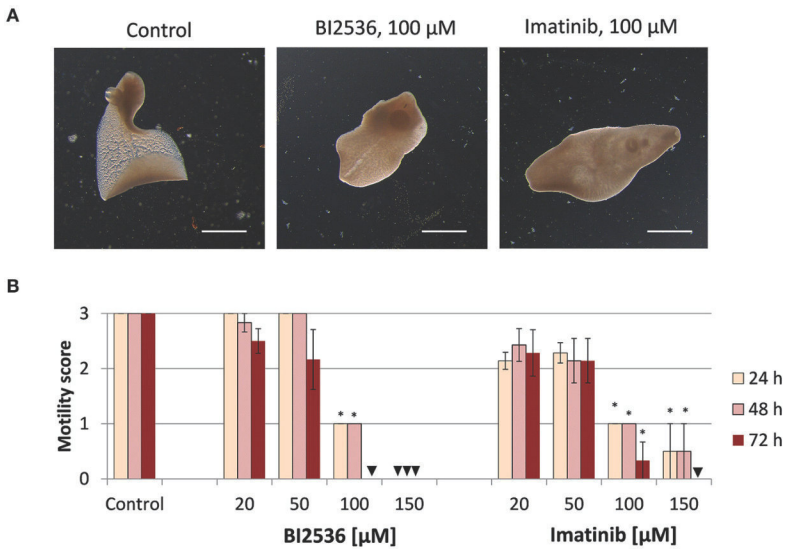

FIGURE 2 | Treatment with kinase inhibitors affects motility of *Fasciola hepatica* immature flukes *in vitro*. Four-week old flukes were treated for 72 h with different concentrations (20–150 µM) of the PLK1 inhibitor BI2536 or the ABL-TK inhibitor imatinib. Motility was assessed every 24 h. Control worms were treated with the inhibitor solvent, DMSO. **(A)** Representative images taken after 72 h treatment. **(B)** Motility scores for all timepoints and concentrations (score 3 = normal, 2 = reduced, 1 = severely reduced, 0 = no motility). Data represent the mean ± SEM of two independent experiments with two to four flukes per experiment. Significant differences are indicated with $^{*}p < 0.05$ (Wilcoxon rank sum test). Triangle indicates a score of zero. Scale bars correspond to 1 mm.

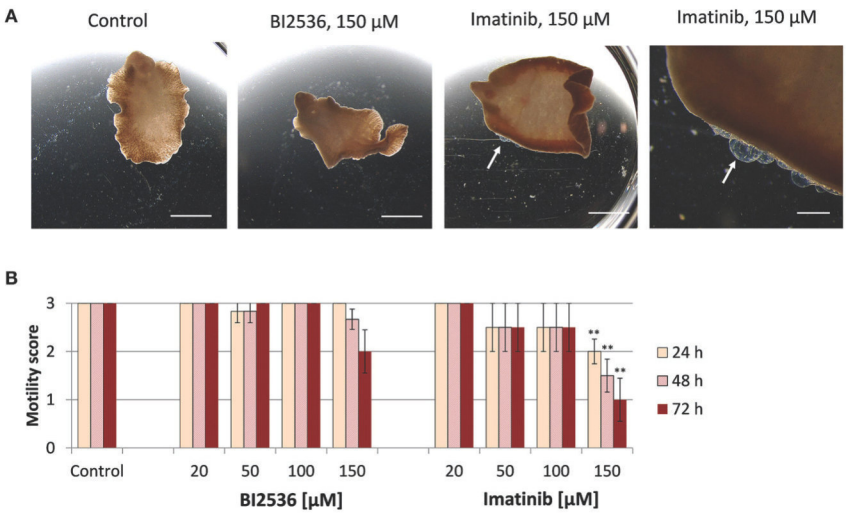

FIGURE 3 | Motility of adult *Fasciola hepatica* after treatment with kinase inhibitors *in vitro*. Twelve-week-old flukes were treated for 72 h with different concentrations (20–150 µM) of the PLK1 inhibitor BI2536 or the ABL-TK inhibitor imatinib. Motility was assessed every 24 h. Control worms were treated with the inhibitor solvent, DMSO. **(A)** Representative images taken after 72 h treatment. **(B)** Motility scores for all timepoints and concentrations (score 3 = normal, 2 = reduced, 1 = severely reduced, 0 = no motility). Data represent the mean ± SEM of two independent experiments with two to four flukes per group and experiment. Significant differences are indicated with $^{**}p < 0.01$ (Wilcoxon rank sum test). Scale bars correspond to 5 mm.

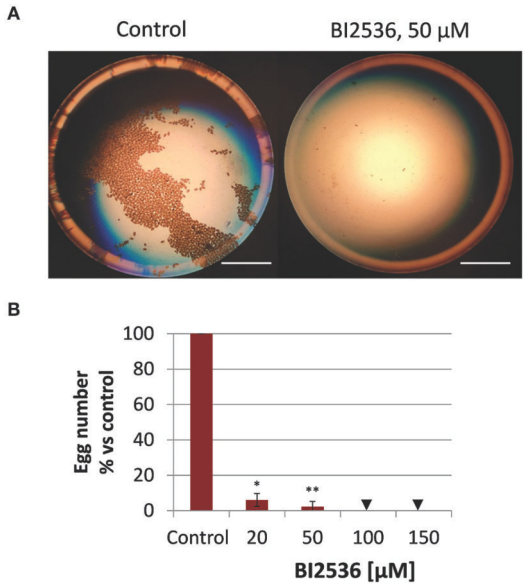

FIGURE 4 | Treatment with the PLK1 inhibitor BI2536 interrupts egg production by adult *Fasciola hepatica in vitro*. Twelve-week-old flukes were treated for 72 h with different concentrations of BI2536 (20–150 µM). Control worms were treated with the inhibitor solvent, DMSO. Eggs produced in the last 24 h of the treatment period were counted. **(A)** Representative images of eggs produced by one control fluke compared to a fluke treated with 50 µM of BI2536. **(B)** Relative egg numbers compared to control flukes. Data represent the mean ± SEM of 2 independent experiments with two to four flukes per experiment. Significant differences are indicated with $^{*}p < 0.05$, $^{**}p < 0.01$ (Wilcoxon rank sum test). Triangle indicates a score of zero. Scale bars correspond to 5 mm.

approach of AP-SMALDI MSI, which we recently established for *S. mansoni* (42). An organic matrix was sprayed onto the liver fluke section from which a highly focused, pulsed UV laser beam ablated material in a rasterized fashion. Formed ions were then subjected to AP-SMALDI MSI analysis (43). The location of the ablated spot and its mass spectrum were matched to image the spatial distribution of analytes of a certain *m/z* value, such as of protonated imatinib, within the section. Finally, H&E staining of the AP-SMALDI MSI-processed sections allowed mapping of the imatinib signal to organs of the fluke. Because of the spot-wise laser ablation with a step size of 10 µm, the H&E-stained tissue displayed a riddled-like appearance after AP-SMALDI MSI. Nevertheless, tissue structures and organs such as intestinal lumen with gastrodermis, vitellarium, uterus with eggs, tegument, and subtegumental muscle layers could still be easily discriminated (**Figure 5**). As an additional anatomical reference in AP-SMALDI MSI images, two endogenous lipids were mapped based on LIPIDMAPS (36): phosphatidylethanolamine (PE) at *m/z* 812.618589 [protonated PE(41:3)] marking the tegument and phosphatidylcholine (PC) at *m/z* 810.598235 [PC(36:1) sodium adduct] marking the parenchyma and other inner tissues. Protonated imatinib was successfully detected in sections at *m/z* 494.266464 as can be seen in lipid/imatinib overlay images and imatinib single-channel images (**Figures 5B**ii–iii). Already after 20 min of incubation time, small amounts of the drug were detectable within the flukes and, as expected, an increased accumulation of imatinib was noted over time. The imatinib signal intensity in 4 and 12-h samples was approximately one order of magnitude higher than the 20-min samples (**Supplementary Figure 2A**). With respect to the tissue tropism, imatinib was merely found in some parts of the intestine and at surface-near tissue areas after 20 min, while the drug spread throughout the parenchyma after 4 h, with the highest signal intensities in vitellarium tissue. The uterus and intestinal lumina remained negative, while intestinal walls (presumably the gastrodermis) were positive for imatinib. After 12 h, imatinib signal intensities further increased and spread throughout the body, again with the highest accumulation in intestinal walls and vitellarium (**Figure 5B**).

In humans, imatinib is metabolized and forms N-desmethyl imatinib as the main bioactive metabolite, possibly contributing to drug activity. We therefore wondered whether a similar metabolization takes place in *F. hepatica*, and how fast the metabolite signal would occur. Indeed, protonated N-desmethyl imatinib was detected in sections of the imatinib-treated flukes at *m/z* 480.251261 (**Figure 5B**iv). While imatinib was detected already after 20 min of incubation, the metabolite occurred time-delayed after 4 h, and further accumulated after 12 h. The metabolite's tissue tropism was similar to that of imatinib, with the highest signal intensities in the vitellarium. For the timepoints where the metabolite was detectable, its average signal intensity was 1.5–2 orders of magnitude lower than the average imatinib signal intensities (**Supplementary Figure 2B**). While average signal intensities of imatinib and the metabolite increased over time, signal intensities of the lipid PC (36:1), here used as control signal, largely remained stable. A representative mass spectrum of a sample from 12-h imatinib exposure depicts the signals of imatinib and the metabolite as well as corresponding intensities (**Supplementary Figure 3**). The spectrum belongs to one single pixel that is located in the vitellarium region on the right side of the worm section (**Figure 5B** at 12 h), where the drug and the metabolite accumulated. Root-mean-square error (RMSE) plots of the signals at *m/z* 494.266464 (assigned to protonated imatinib) and *m/z* 480.251261 (assigned to protonated N-desmethyl imatinib) showed one single peak with no shoulders within an *m/z* bin of 5 ppm width (**Supplementary Figure 2**), which indicates that only the analyte was detected and every green pixel in the MALDI images actually represents imatinib and its metabolite, respectively. N-demethylation of imatinib to N-desmethyl imatinib is mediated via the liver cytochrome P450 enzymes CYP2C8, CYP3A4, CYP3A5, and CYP3A7 in humans (44, 45). DeltaBLAST searches predicted a putative ortholog for CYP2C8 in *F. hepatica*. SMART protein domain analysis revealed an N-terminal transmembrane domain (**Supplementary Figure 4**) that is typical for this type of microsomal cytochromes, which form integral membrane proteins located in the endoplasmic reticulum (46).

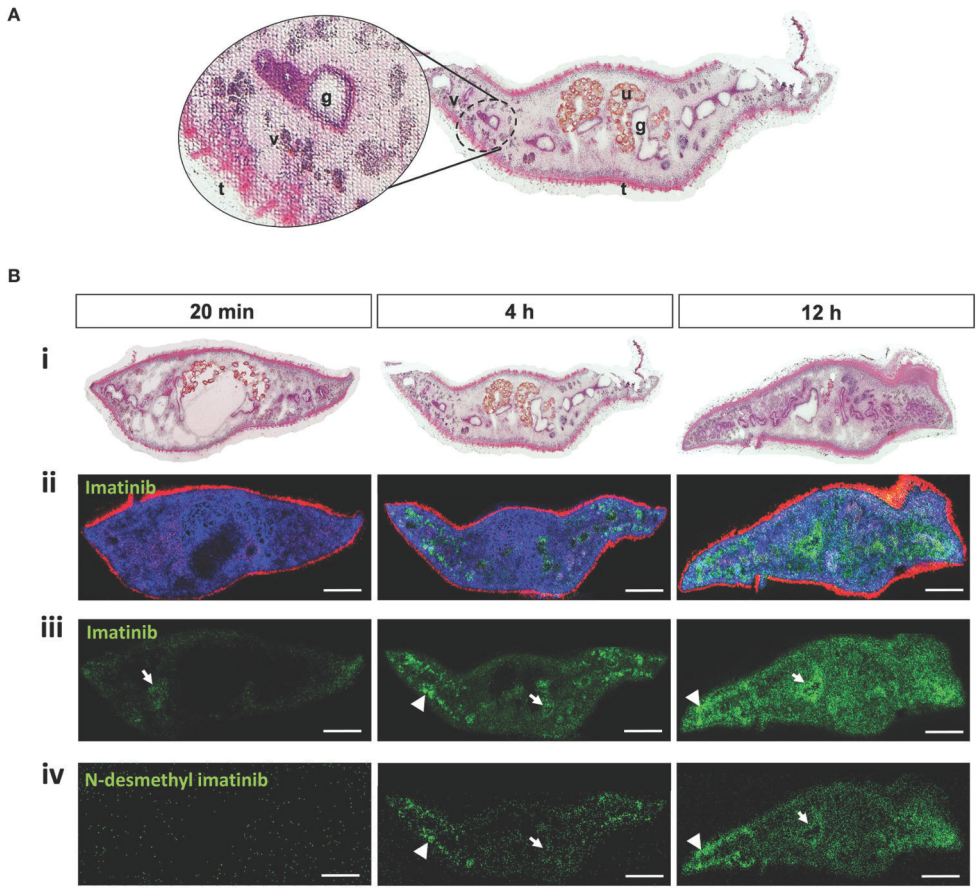

FIGURE 5 | Detection of imatinib and its main metabolite in tissues of adult *Fasciola hepatica* by MALDI mass spectrometry imaging (MSI). Twelve-week-old flukes were treated for 20 min, 4 h, or 12 h with 100 μM imatinib. Compounds and endogenous lipids were detected in transversal sections using AP-SMALDI MSI, and sections were stained with H&E afterwards. **(A)** Example of an H&E-stained section showing the typical riddled pattern with numerous white spots from which tissue was laser-ablated during MALDI. Different tissues are indicated: gut/gastrodermis (g), tegument (t), uterus (u), and vitellarium (v). **(B)** For each timepoint of imatinib treatment, two flukes were analyzed, of which one representative is depicted. (i) H&E-stained sections to visualize the fluke's tissues after AP-SMALDI MSI measurements. (ii) RGB images from AP-SMALDI MSI showing transversal sections with the following signals: *m/z* 494.266464 (green, protonated imatinib), *m/z* 812.618589 [red, protonated PE(41:3), *m/z* 810.598235; blue, PC(36:1) sodium adduct]. Lipid assignment is based on LIPIDMAPS (36) results. (iii, iv) AP-SMALDI MSI single channel images showing sections depicting the imatinib signal at *m/z* 494.266464 corresponding to $[M+H]^+$ (iii) or the metabolite N-desmethyl imatinib at *m/z* 480.251261 corresponding to $[M+H]^+$ (iv). Arrows indicate compound localized within the intestine or gastrodermis, arrowheads within the vitellarium. Scale bars correspond to 500 μm.

Taken together, AP-SMALDI MSI-assisted drug imaging of imatinib in adult *F. hepatica* revealed (a) a fast incorporation of the drug within 20 min, (b) an accumulation over time especially in intestinal and vitellarium tissue, and (c) a metabolization to the same bioactive metabolite as found in humans. To investigate whether drug distribution correlated with target distribution, we performed *in situ* hybridization to localize Fh*abl1* transcripts in tissue sections of adult *F. hepatica*. A moderate positive staining was found for the gastrodermis (**Figure 6**). Thus, the localization of both imatinib as drug and its target largely matched each other.

Gene Expression Changes in Adult Flukes After Imatinib Treatment

A previous microarray study revealed substantial transcriptional changes in adult *S. mansoni* upon imatinib treatment, which suggested a wide influence of the inhibitor on worm physiology (24). For imatinib-treated *F. hepatica*, we expected a similar impact on the expression of physiologically important genes. To test this, we quantified the expression of a collection of genes selected from the *S. mansoni* study after identifying potential orthologs in *F. hepatica* (for gene ID numbers, see

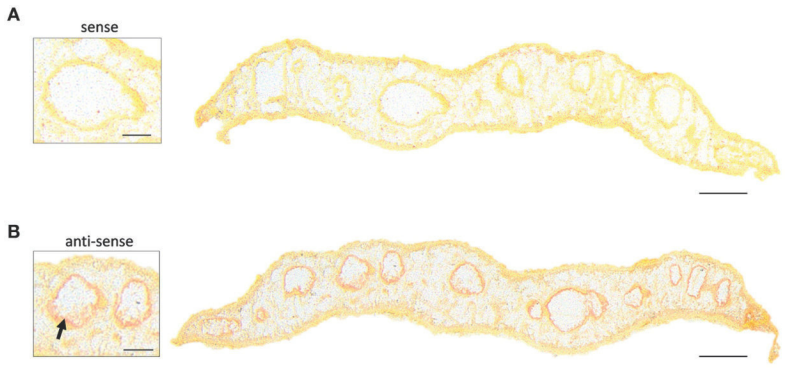

FIGURE 6 | *In situ* hybridization localizes transcripts of Fh*abl1* kinase in gastrodermal tissue of adult *Fasciola hepatica*. ISH was performed on transverse sections of 12-week-old *F. hepatica* using digoxygenin-labeled sense probes for Fh*abl1* as negative control **(A)**, or anti-sense probes to detect Fh*abl1* transcripts **(B)**. Positive, red staining localized to the gastrodermis (arrow). Scale bars correspond to 250 μm (whole sections) or 100 μm (inserts).

Supplementary Table 1): the multidrug resistance protein 1 (MDR1, also called ABCB1 or P-glycoprotein) belonging to the group of drug efflux pumps; histone 2B (H2B), which is enriched during cell cycle (47); two types of Cu/Zn superoxide dismutases (SOD), i.e., a predicted extracellular SOD (SODex) and a cytosolic SOD, both first-line defense proteins against oxidative stress (48). Orthologs were identified by BLASTp search of known genes in *S. mansoni* against the genome of *F. hepatica*, and correct annotation of the hits was further confirmed by another BLASTp search against *Homo sapiens* (accession numbers see **Supplementary Table 1**). SMART analysis confirmed the presence of conserved protein domains (**Supplementary Figure 5A**). The gene products of Fh*h2b*, Fh*sodex*, and Fh*sod* were previously identified by proteomic analyses (49–51), and their annotation was confirmed in our analysis. It was previously shown for a related flatworm species that oxidative stress upregulated the expression of SOD on a transcriptional level (52). The highest amino acid sequence identity to human MDR1 was found for the product of a gene, which we called Fh*mdr*. This is different from the protein that was named "MDR1" in a previous study of *F. hepatica* (53), but which turned out to have a lower amino acid sequence identity to human MDR1 and a lower e-value in BLASTp results compared to the here described Fh*mdr* gene product (**Supplementary Figure 6**). A hidden Markov model predicted the correct topology of the newly described membrane protein FhMDR. It contained the typical two transmembrane domains that each consist of several transmembrane helices and are interlinked by a large cytoplasmic domain with an ATP-binding site (**Supplementary Figure 5B**). qRT-PCR analyses revealed trends of upregulation for all four marker genes in adult flukes treated with imatinib when compared to control flukes (**Figure 7**). In detail, Fh*sod* and Fh*sodex* expression were significantly increased upon treatment with 150 μM imatinib, and the same trend was found for Fh*mdr* in flukes treated with 100 μM. Fh*h2b* transcript levels were 2–4-fold elevated in two out of three imatinib-treated worms (150 μM). Because the increase for Fh*h2b* and Fh*mdr* transcript levels was not significant, a drug-induced effect on these genes remains uncertain. Taken together, imatinib modified the expression of some genes with expected physiological importance not only in *S. mansoni*, but also in *F. hepatica*.

DISCUSSION

Protein kinases have been propagated as valuable drug targets against various pathogens, from bacteria to protozoan and helminth parasites (54–56). In liver flukes, however, until now only little attention was paid to kinases and kinase inhibitors. In our study, (1) we demonstrated the *in vitro* anthelminthic activity of two different kinase inhibitors against different pathogenic, intramammalian stages *F. hepatica*, (2) we demonstrated the distribution of the ABL kinase inhibitor imatinib and its presumed target within fluke tissue, and (3) we highlighted possible modes of action of imatinib by expression analysis of selected genes with suggested importance for fluke biology.

Kinases as Therapeutic Target in *F. hepatica*

An ideal drug target should be expressed and physiologically relevant in all pathogenic life stages of *F. hepatica*: in immature flukes migrating and feeding within the liver parenchyma, as well as in adult flukes that feed in the bile duct and cause chronic infections (5). This ensures that its pharmacological inhibition can have cross-stage activity. In line with this, the ABL1 and PLK1 kinases addressed in this study were transcriptionally expressed in immature as well as adult flukes. These highly conserved kinases fulfill important cellular functions as known from humans and model organisms, and we hypothesize that the same holds true for liver flukes. PLK1 proteins are key regulators of the cell cycle progression during M-phase (10). ABL-TK

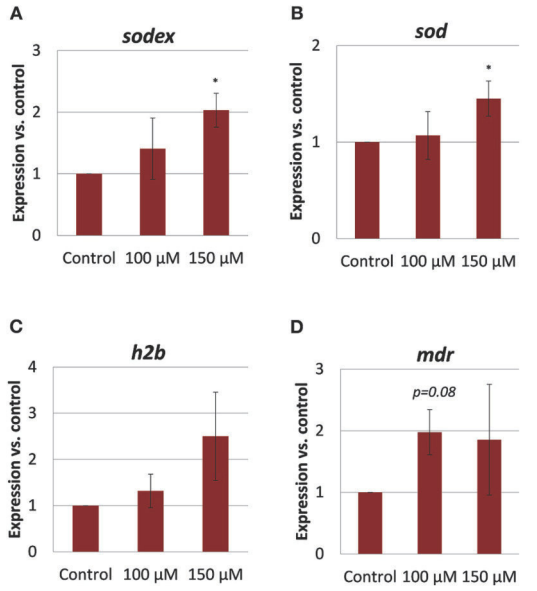

FIGURE 7 | Gene expression changes in adult *Fasciola hepatica* after imatinib treatment. Twelve-week-old flukes were treated for 72 h with 100 or 150 µM imatinib *in vitro*, and the fold change of transcripts of selected genes relative to DMSO-treated worms was quantified by qRT-PCR. Normalization was done against two reference genes, glutamyl-prolyl-tRNA synthetase (Fh*eprs*) and tubulin-specific chaperone D (Fh*tbcd*). Of interest were **(A)** extracellular superoxide dismutase (*sodex*) and **(B)** superoxide dismutase (*sod*) as genes involved in the defense toward oxidative stress, **(C)** the histone *h2b* important for DNA duplication during the cell cycle, and **(D)** a putative multidrug resistance gene (*mdr*). Data represent the mean ± SEM of two independent experiments with three to five flukes per group. Significant differences vs. control are indicated with $^*p < 0.05$ (Wilcoxon rank sum test).

regulate a variety of cellular processes such as cytoskeletal rearrangement and cell differentiation (11). The highly conserved nature of the selected kinases makes inhibitory activities in exotic species such as liver flukes likely.

To target members of these PK families, we focused on two well-described anti-cancer drugs with proven antischistosomal activity. Imatinib, also known as Gleevec or Glivec (Novartis, Basel, Switzerland; formerly referred to as STI571 or CGP57148B), inhibits protein TKs of the ABL-family and is used for therapy of chronic myeloid leukemia in humans (57). BI2536 is a small-molecule inhibitor of PLK1, which belongs to the group of serine/threonine-protein kinases. The ideal fasciolicidal compound should target all relevant life stages within the host. Currently, mainly the gold standard drug triclabendazole is cross-stage active, while other drugs in use mainly target the adult stage (6). Among the tested kinase inhibitors, imatinib fulfilled this criterion of cross-stage activity. Imatinib was lethal to immature and adult *F. hepatica* at 100–150 µM. This represents a two to three times higher active concentration compared to the current gold standard triclabendazole and two other common drugs in use, clorsulon and closantel, for which we established lethal concentrations of 50 µM in our *in vitro* culture system. Opposite to imatinib, the PLK1 inhibitor BI2536 had basically no effect on adult liver fluke viability, but killed immature liver flukes. It appears that BI2536 in general has stronger effects on the juvenile stages of flukes compared to their adult stages. Also for the blood fluke *S. mansoni*, juvenile stages died upon inhibitor treatment or interference with PLK1 expression using RNAi, while the viability of adult worms was unaffected (20, 22). We hypothesize that the described role of PLK1 in mitosis control might be of particular importance during the growth phase of juvenile flukes, when a high proliferative activity of somatic stem cells (neoblasts) might be needed. In the adult stage, however, PLK1 function may be more crucial to ensure egg production, i.e., germline stem cell proliferation, which is certainly an important function for the parasite but not essential for its survival. The critical role for reproduction of *Fasciola* was also underlined by the drop of egg release upon PLK1 inhibitor treatment. Also in *S. mansoni*, the mitotic function of PLK1 in germinal cells was important for normal egg production (22). Thus, although BI2536 is the most potent and selective PLK1 inhibitor available (58) and was shown to inhibit the catalytic activity of recombinant *S. mansoni* PLK1 even at nanomolar doses (22), targeting PLK1 might not be the most promising anthelminthic strategy. Because of its activity against early immature liver flukes, it might still be interesting as a combination therapy with other drugs for which the activity spectrum is restricted to older stages, such as clorsulon and closantel (6).

Drug Imaging as Powerful Tool for Compound Studies in *F. hepatica*

To address the kinetics of drug uptake and tissue tropism in *F. hepatica*, we applied for the first time MALDI MSI in this parasite. We managed to visualize an increasing accumulation of imatinib in different tissues from 20 min to 12 h of exposure, and could prove that imatinib is metabolized by *F. hepatica* the same way as in humans. The strong signal intensities in tissues lining the intestinal tract, probably gastrodermis, suggest an oral uptake of imatinib. A second, additional uptake route may occur via the tegument, the physiologically active outer surface layer of flukes (59). Although the tegument was not found positive for imatinib in AP-SMALDI MSI, a tegumental uptake cannot be fully excluded. Such a tegumental uptake of the drug clorsulon has been indirectly demonstrated before by ligature of the anterior body part to prevent oral ingestion (60). The pronounced tegumental damage observed in *F. hepatica* further argues for a tegumental targeting by imatinib. That the metabolite's signal intensities were about two orders of magnitude lower than the imatinib signal intensities suggests either an incomplete metabolization of imatinib or, alternatively, a slow metabolization of continuously incorporated imatinib. As in humans (44), cytochrome p450 2C8 might catalyze the metabolization of imatinib. N-desmethyl imatinib is pharmacologically active and shows a similar potency as the parent drug including potent ABL inhibition in the

nanomolar range (45). It was shown to inhibit cell proliferation and to induce apoptosis in human cells (45, 61). Thus, the metabolite likely contributes to the fasciolicidal effect seen after imatinib treatment.

Our lab has previously established and optimized AP-SMALDI MSI for the visualization of lipid distributions in *S. mansoni* (42). Recently, we also established drug imaging for this species, utilizing imatinib as proof of principle (Mokosch et al., under review). Our data suggest that *S. mansoni* and *F. hepatica* have different uptake efficiencies for imatinib when applied at the same concentration of 100 µM. The drug was distributed throughout internal tissues of adult males of *S. mansoni* already after 20 min of exposure (Mokosch et al., under review), while only traces of imatinib were detected within the same time in *F. hepatica*, and it took 1 h for a clear drug accumulation. In case of a tegumental drug uptake, the considerably thicker tegument of *F. hepatica* with around 20 µm (62) compared to *S. mansoni* with around 4 µm (63) might contribute to this delayed drug internalization. In case of an oral drug uptake, the larger body size and higher degree of intestinal branching in adult liver flukes compared to blood flukes might delay drug distribution within internal tissues. Nevertheless, within 12 h, imatinib was found distributed throughout the body of *F. hepatica*.

Taken together, AP-SMALDI MSI revealed a distinct uptake kinetic for imatinib, and it demonstrated the accumulation of imatinib in specific parasite tissues. In one of these tissues, highest expression of the putative kinase target was found. Furthermore, the obtained data support the hypothesis that *F. hepatica* incorporates imatinib orally and metabolizes it to a known bioactive metabolite.

Imatinib's Possible Mode of Action in *F. hepatica*

To shed some first light on a possible mode of action, we studied the transcriptional expression of various genes thought to be important for homeostasis. We focused on representative genes involved in the regulation of oxidative stress, cell cycle, and drug efflux. The selection of genes was inspired by a microarray study in *S. mansoni*, which revealed substantial transcriptional changes caused by imatinib treatment. Overall expression changes in gut-, muscle-, tegument- and gonad-associated genes pointed to a broad negative effect of imatinib on schistosome physiology (24). In imatinib-treated *F. hepatica*, the Fh*mdr* drug resistance gene, encoding for a drug efflux pump, was transcriptionally upregulated, which might be one mode how the fluke tries to defend against toxic compounds such as imatinib. Indeed, MDR1 has been predicted to be a drug or chemical exporter in helminths (64). While the transcriptional level of two *mdr* genes in *S. mansoni* was downregulated in response to imatinib (24), it was upregulated by praziquantel treatment (65). Eventually, *mdr* expression and its upregulation was obviously ineffective in *F. hepatica*, as imatinib was still able to affect fluke viability. It might nevertheless be interesting to treat flukes with imatinib under pharmacological inhibition of MDRs to test for an even higher drug efficacy.

Sod genes were transcriptionally upregulated by imatinib in both fluke species, which might reflect an increased oxidative stress response (52). Reactive oxygen species cause oxidative DNA damage (66), and we speculate that this might contribute to the anthelminthic effect of imatinib. TK inhibitors such as imatinib are known to cause myotoxicity as a side effect, which was associated with mitochondrial superoxide accumulation and increased SOD expression (67). Thus, imatinib might act as mitochondrial toxicant also in *F. hepatica* by inducing reactive oxygen species and an increase of SOD expression as part of the anti-oxidant defense system. In this context, it is important to note that oxidative stress and chemical inhibition of ABL-TK activity arrest cells at the S phase of the cell cycle (68–70). We found a trend of increased *h2b* expression after imatinib treatment of worms. *H2b* transcriptional expression increases to high levels when cells enter the S phase to provide histones for packing the newly synthesized DNA (71). We therefore speculate that increased *h2b* transcript levels might reflect an S-phase arrest in imatinib-treated *F. hepatica*, which may be caused by drug-induced oxidative stress. In conclusion, imatinib's anthelminthic mode of action might involve the induction of oxidative stress and/or interference with cell cycle progression. Future studies involving cell cycle analyses and quantification of ROS should prove whether this hypothesis holds true.

Outlook

Our study demonstrates that kinases are worth to be considered as therapeutic targets in *F. hepatica*. The finding that the ABL-TK inhibitor imatinib displays cross-species activity against schistosomes (19) but also *F. hepatica* as a pathogen of tremendous veterinary importance makes this drug even more attractive for further development. Importantly, imatinib displayed cross-stage activity against liver flukes, a benchmark set by the current gold standard triclabendazole. These results motivate for further validation in animal studies. In case of imatinib, serum proteins such as alpha-1-acid glycoprotein (AGP) were shown to bind the drug, which reduced its *in vivo* efficacy against schistosomes using rodents as model host (72). More motivating was a case report on orally administered imatinib in a human filariasis patient, which reduced worm burden (73). Thus, when it comes to *in vivo* studies, it needs to be considered that the degree of drug-plasma protein binding varies between species, especially between rodents and human (72). AGP concentrations vary between healthy to pathological states, and AGP exhibits species-dependent binding affinities (74–76). Various drugs were found to bind with lower affinity to AGP from sheep compared to AGP from several other species (77, 78), which makes sheep as a natural host of *F. hepatica* likely suitable for imatinib trials. Next to testing the *in vivo* efficacy of imatinib against liver flukes, another important task will be the biochemical and genetic target validation for *abl* kinases in *F. hepatica*. Finally, in-depth analyses of the kinome should be undertaken, which recently predicted the expression of 455 protein kinases in the related fluke *F. gigantica* (79). The availability of kinome data for *F. hepatica* will certainly boost the discovery of potentially druggable kinases in this parasite.

DATA AVAILABILITY STATEMENT

The original contributions presented in the study are included in the article/**Supplementary Materials**, further inquiries can be directed to the corresponding author/s.

ETHICS STATEMENT

The animal study was reviewed and approved by Regional Council (Regierungspraesidium) Giessen (approval number V54-19c20 15 h 02 GI 18/10 Nr. A16/2018).

AUTHOR CONTRIBUTIONS

SH: conceptualization. CM, HH, OP, LH, MR, ER, DD, AM, BS, and SH: methodology. CM, HH, OP, MR, LH, and SH: investigation. ER, BS, and SH: resources. CM and SH: writing—original draft preparation. CM, MR, and SH: visualization. AM, DD, ER, MR, BS, and SH: supervision. BS and SH: funding acquisition. All authors: writing—review and editing.

FUNDING

This work was funded by the LOEWE Centre for Novel Drug Targets against Poverty-Related and Neglected Tropical Infectious Diseases (DRUID), which is part of the excellence initiative of the Hessen State Ministry of Higher Education, Research and the Arts (HMWK). Part of the work was funded by grants of the Deutsche Forschungsgemeinschaft DFG to SH (HA 6963/2-1) and to BS (Sp314/13-1).

ACKNOWLEDGMENTS

The authors are grateful to Christoph G. Grevelding for his valuable comments and fruitful discussions. Technical support by TransMIT GmbH, Giessen, Germany is gratefully acknowledged.

SUPPLEMENTARY MATERIAL

The Supplementary Material for this article can be found online at: https://www.frontiersin.org/articles/10.3389/fvets.2020.611270/full#supplementary-material

REFERENCES

1. Fürst T, Keiser J, Utzinger J. Global burden of human food-borne trematodiasis: a systematic review and meta-analysis. *Lancet Infect Dis.* (2012) 12:210–21. doi: 10.1016/S1473-3099(11)70294-8
2. Mehmood K, Zhang H, Sabir AJ, Abbas RZ, Ijaz M, Durrani AZ, et al. A review on epidemiology, global prevalence and economical losses of fasciolosis in ruminants. *Microb Pathog.* (2017) 109:253–62. doi: 10.1016/j.micpath.2017.06.006
3. May K, Bohlsen E, König S, Strube C. *Fasciola hepatica* seroprevalence in Northern German dairy herds and associations with milk production parameters and milk ketone bodies. *Vet Parasitol.* (2020) 277:109016. doi: 10.1016/j.vetpar.2019.109016
4. Jonker FAM, Te Poel E, Bates I, Boele van Hensbroek M. Anaemia, iron deficiency and susceptibility to infection in children in sub-Saharan Africa, guideline dilemmas. *Br J Haematol.* (2017) 177:878–83. doi: 10.1111/bjh.14593
5. Dawes B, Hughes DL. Fascioliasis: the invasive stages in mammals. *Adv Parasitol.* (1970) 8:259–74. doi: 10.1016/S0065-308X(08)60257-2
6. Kelley JM, Elliott TP, Beddoe T, Anderson G, Skuce P, Spithill TW. Current threat of triclabendazole resistance in *Fasciola hepatica*. *Trends Parasitol.* (2016) 32:458–69. doi: 10.1016/j.pt.2016.03.002
7. Hemer S, Brehm K. *In vitro* efficacy of the anticancer drug imatinib on *Echinococcus multilocularis* larvae. *Int J Antimicrob Agents.* (2012) 40:458–62. doi: 10.1016/j.ijantimicag.2012.07.007
8. Gelmedin V, Dissous C, Grevelding CG. Re-positioning protein-kinase inhibitors against schistosomiasis. *Future Med Chem.* (2015) 7:737–52. doi: 10.4155/fmc.15.31
9. O'Connell EM, Bennuru S, Steel C, Dolan MA, Nutman TB. Targeting filarial Abl-like kinases: orally available, food and drug administration-approved tyrosine kinase inhibitors are microfilaricidal and macrofilaricidal. *J Infect Dis.* (2015) 212:684–93. doi: 10.1093/infdis/jiv065
10. Lane HA, Nigg EA. Antibody microinjection reveals an essential role for human polo-like kinase 1 (Plk1) in the functional maturation of mitotic centrosomes. *J Cell Biol.* (1996) 135:1701–13. doi: 10.1083/jcb.135.6.1701
11. Yuan ZM, Huang Y, Ishiko T, Kharbanda S, Weichselbaum R, Kufe D. Regulation of DNA damage-induced apoptosis by the c-Abl tyrosine kinase. *Proc Natl Acad Sci USA.* (1997) 94:1437–40. doi: 10.1073/pnas.94.4.1437
12. Dissous C, Grevelding CG. Piggy-backing the concept of cancer drugs for schistosomiasis treatment: a tangible perspective? *Trends Parasitol.* (2011) 27:59–66. doi: 10.1016/j.pt.2010.09.001
13. Shoriki T, Ichikawa-Seki M, Suganuma K, Naito I, Hayashi K, Nakao M, et al. Novel methods for the molecular discrimination of *Fasciola* spp. on the basis of nuclear protein-coding genes. *Parasitol Int.* (2016) 65:180–3. doi: 10.1016/j.parint.2015.12.002
14. Wesolowska A, Zawistowska-Deniziak A, Norbury LJ, Wilkowski P, Januszkiewicz K, Pyziel AM, et al. Immune responses in rats and sheep induced by a DNA vaccine containing the phosphoglycerate kinase gene of *Fasciola hepatica* and liver fluke infection. *Acta Parasitol.* (2016) 61:212–20. doi: 10.1515/ap-2016-0030
15. Mansour TE, Mansour JM. Effects of serotonin (5-hydroxytryptamine) and adenosine 3',5'-phosphate on phosphofructokinase from the liver fluke *Fasciola hepatica*. *J Biol Chem.* (1962) 237:629–34. doi: 10.1016/0006-2952(61)90182-4
16. Fairweather I, Holmes SD, Threadgold LT. *Fasciola hepatica*: motility response to fasciolicides *in vitro*. *Exp Parasitol.* (1984) 57:209–24. doi: 10.1016/0014-4894(84)90094-8
17. Schulman MD, Valentino D, Cifelli S, Ostlind DA. Dose-dependent pharmacokinetics and efficacy of MK-401 against old, and young-mature infections of *Fasciola hepatica* in the rat. *J Parasitol.* (1982) 68:603–8. doi: 10.2307/3280917
18. Houhou H, Puckelwaldt O, Strube C, Haeberlein S. Reference gene analysis and its use for kinase expression profiling in *Fasciola hepatica*. *Sci Rep.* (2019) 9:15867. doi: 10.1038/s41598-019-52416-x
19. Beckmann S, Grevelding CG. Imatinib has a fatal impact on morphology, pairing stability and survival of adult *Schistosoma mansoni in vitro*. *Int J Parasitol.* (2010) 40:521–6. doi: 10.1016/j.ijpara.2010.01.007
20. Guidi A, Mansour NR, Paveley RA, Carruthers IM, Besnard J, Hopkins AL, et al. Application of RNAi to genomic drug target validation in schistosomes. *PLoS Negl Trop Dis.* (2015) 9:e0003801. doi: 10.1371/journal.pntd.0003801
21. Li X, Haeberlein S, Zhao L, Mughal MN, Zhu T, Liu L, et al. The ABL kinase inhibitor imatinib causes phenotypic changes and lethality in adult *Schistosoma japonicum*. *Parasitol Res.* (2019) 118:881–90. doi: 10.1007/s00436-019-06224-x
22. Long T, Cailliau K, Beckmann S, Browaeys E, Trolet J, Grevelding CG, et al. *Schistosoma mansoni* polo-like kinase 1: a mitotic kinase with key functions in parasite reproduction. *Int J Parasitol.* (2010) 40:1075–86. doi: 10.1016/j.ijpara.2010.03.002
23. Beckmann S, Hahnel S, Cailliau K, Vanderstraete M, Browaeys E, Dissous C, et al. Characterization of the Src/Abl hybrid kinase SmTK6 of *Schistosoma mansoni*. *J Biol Chem.* (2011) 286:42325–36. doi: 10.1074/jbc.M110.210336

24. Buro C, Beckmann S, Oliveira KC, Dissous C, Cailliau K, Marhöfer RJ, et al. Imatinib treatment causes substantial transcriptional changes in adult *Schistosoma mansoni in vitro* exhibiting pleiotropic effects. *PLoS Negl Trop Dis.* (2014) 8:e2923. doi: 10.1371/journal.pntd.0002923
25. Breslow JL, Sloan HR, Ferrans VJ, Anderson JL, Levy RI. Characterization of the mouse liver cell line FL83B. *Exp Cell Res.* (1973) 78:441–53. doi: 10.1016/0014-4827(73)90089-X
26. Espevik T, Nissen-Meyer J. A highly sensitive cell line, WEHI 164 clone 13, for measuring cytotoxic factor/tumor necrosis factor from human monocytes. *J Immunol Methods.* (1986) 95:99–105. doi: 10.1016/0022-1759(86)90322-4
27. Kemmer G, Keller S. Nonlinear least-squares data fitting in excel spreadsheets. *Nat Protoc.* (2010) 5:267–81. doi: 10.1038/nprot.2009.182
28. Howe KL, Bolt BJ, Shafie M, Kersey P, Berriman M. WormBase parasite - a comprehensive resource for helminth genomics. *Mol Biochem Parasitol.* (2017) 215:2–10. doi: 10.1016/j.molbiopara.2016.11.005
29. Letunic I, Doerks T, Bork P. SMART: recent updates, new developments and status in 2015. *Nucleic Acids Res.* (2015) 43:D257–60. doi: 10.1093/nar/gku949
30. Untergasser A, Cutcutache I, Koressaar T, Ye J, Faircloth BC, Remm M, et al. Primer3–new capabilities and interfaces. *Nucleic Acids Res.* (2012) 40:e115. doi: 10.1093/nar/gks596
31. Castillo E, Koziol U. Analysis of gene expression in *Fasciola hepatica* juveniles and adults by *in situ* hybridization. *Methods Mol Biol.* (2020) 2137:93–105. doi: 10.1007/978-1-0716-0475-5_7
32. Collins, 3rd JJ, Hou X, Romanova EV, Lambrus BG, Miller CM, Saberi A, et al. Genome-wide analyses reveal a role for peptide hormones in planarian germline development. *PLoS Biol.* (2010) 8:e1000509. doi: 10.1371/journal.pbio.1000509
33. Michalski A, Damoc E, Hauschild JP, Lange O, Wieghaus A, Makarov A, et al. Mass spectrometry-based proteomics using Q exactive, a high-performance benchtop quadrupole orbitrap mass spectrometer. *Mol Cell Proteomics.* (2011) 10:M111.011015. doi: 10.1074/mcp.M111.011015
34. Kompauer M, Heiles S, Spengler B. Autofocusing MALDI mass spectrometry imaging of tissue sections and 3D chemical topography of nonflat surfaces. *Nat Methods.* (2017) 14:1156–8. doi: 10.1038/nmeth.4433
35. Paschke C, Leisner A, Hester A, Maass K, Guenther S, Bouschen W, et al. Mirion–a software package for automatic processing of mass spectrometric images. *J Am Soc Mass Spectr.* (2013) 24:1296–306. doi: 10.1007/s13361-013-0667-0
36. Fahy E, Sud M, Cotter D, Subramaniam S. LIPID MAPS online tools for lipid research. *Nucleic Acids Res.* (2007) 35:W606–12. doi: 10.1093/nar/gkm324
37. Marx A, Backes C, Meese E, Lenhof HP, Keller A. EDISON-WMW: exact dynamic programing solution of the wilcoxon-Mann-Whitney test. *Genom. Proteom. Bioinform.* (2016) 14:55–61. doi: 10.1016/j.gpb.2015.11.004
38. Morel M, Vanderstraete M, Cailliau K, Lescuyer A, Lancelot J, Dissous C. Compound library screening identified Akt/PKB kinase pathway inhibitors as potential key molecules for the development of new chemotherapeutics against schistosomiasis. *Int J Parasitol Drugs Drug Resist.* (2014) 4:256–66. doi: 10.1016/j.ijpddr.2014.09.004
39. Ressurreicao M, De Saram P, Kirk RS, Rollinson D, Emery AM, Page NM, et al. Protein kinase C and extracellular signal-regulated kinase regulate movement, attachment, pairing and egg release in *Schistosoma mansoni*. *PLoS Negl Trop Dis.* (2014) 8:e2924. doi: 10.1371/journal.pntd.0002924
40. Schubert A, Koziol U, Cailliau K, Vanderstraete M, Dissous C, Brehm K. Targeting *Echinococcus multilocularis* stem cells by inhibition of the polo-like kinase EmPlk1. *PLoS Negl Trop Dis.* (2014) 8:e2870. doi: 10.1371/journal.pntd.0002870
41. Grevelding CG, Langner S, Dissous C. Kinases: molecular stage directors for schistosome development and differentiation. *Trends Parasitol.* (2018) 34:246–60. doi: 10.1016/j.pt.2017.12.001
42. Kadesch P, Quack T, Gerbig S, Grevelding CG, Spengler B. Lipid topography in *Schistosoma mansoni* cryosections, revealed by microembedding and high-resolution atmospheric-pressure matrix-assisted laser desorption/ionization (MALDI) mass spectrometry imaging. *Anal Chem.* (2019) 91:4520–8. doi: 10.1021/acs.analchem.8b05440
43. Spengler B. Mass spectrometry imaging of biomolecular information. *Anal Chem.* (2015) 87:64–82. doi: 10.1021/ac504543v
44. Nebot N, Crettol S, d'Esposito F, Tattam B, Hibbs DE, Murray M. Participation of CYP2C8 and CYP3A4 in the N-demethylation of imatinib in human hepatic microsomes. *Br J Pharmacol.* (2010) 161:1059–69. doi: 10.1111/j.1476-5381.2010.00946.x
45. Mlejnek P, Dolezel P, Faber E, Kosztyu P. Interactions of N-desmethyl imatinib, an active metabolite of imatinib, with P-glycoprotein in human leukemia cells. *Ann Hematol.* (2011) 90:837–42. doi: 10.1007/s00277-010-1142-7
46. Hu G, Johnson EF, Kemper B. CYP2C8 exists as a dimer in natural membranes. *Drug Metab Dispos.* (2010) 38:1976–83. doi: 10.1124/dmd.110.034942
47. Lopez MF, Tollervey J, Krastins B, Garces A, Sarracino D, Prakash A, et al. Depletion of nuclear histone H2A variants is associated with chronic DNA damage signaling upon drug-evoked senescence of human somatic cells. *Aging.* (2012) 4:823–42. doi: 10.18632/aging.100507
48. Piacenza L, Radi R, Goñi F, Carmona C. CuZn superoxide dismutase activities from *Fasciola hepatica*. *Parasitology.* (1998) 117:555–62. doi: 10.1017/S0031182098003394
49. Jefferies JR, Campbell AM, van Rossum AJ, Barrett J, Brophy PM. Proteomic analysis of *Fasciola hepatica* excretory-secretory products. *Proteomics.* (2001) 1:1128–32. doi: 10.1002/1615-9861(200109)1:9<1128::AID-PROT1128>3.0.CO;2-0
50. Galindo M, Varela N, Espinoza I, Toro GC, Hellman U, Wernstedt C, et al. Chromatin from two classes of platyhelminthes display both protist H1 and higher eukaryote core histones. *FEBS Lett.* (2004) 567:225–9. doi: 10.1016/j.febslet.2004.04.065
51. Gourbal BE, Guillou F, Mitta G, Sibille P, Thèron A, Pointier JP, et al. Excretory-secretory products of larval *Fasciola hepatica* investigated using a two-dimensional proteomic approach. *Mol Biochem Parasitol.* (2008) 161:63–6. doi: 10.1016/j.molbiopara.2008.05.002
52. Aragon AD, Imani RA, Blackburn VR, Cunningham C. Microarray based analysis of temperature and oxidative stress induced messenger RNA in *Schistosoma mansoni*. *Mol Biochem Parasitol.* (2008) 162:134–41. doi: 10.1016/j.molbiopara.2008.08.004
53. Cameron TC, Cooke I, Faou P, Toet H, Piedrafita D, Young N, et al. A novel *ex vivo* immunoproteomic approach characterising *Fasciola hepatica* tegumental antigens identified using immune antibody from resistant sheep. *Int J Parasitol.* (2017) 47:555–67. doi: 10.1016/j.ijpara.2017.02.004
54. Brumlik MJ, Pandeswara S, Ludwig SM, Murthy K, Curiel TJ. Parasite mitogen-activated protein kinases as drug discovery targets to treat human protozoan pathogens. *J Signal Transduct.* (2011) 2011:971968. doi: 10.1155/2011/971968
55. Beckmann S, Leutner S, Gouignard N, Dissous C, Grevelding CG. Protein kinases as potential targets for novel anti-schistosomal strategies. *Curr Pharm Des.* (2012) 18:3579–94. doi: 10.2174/138161212801327310
56. Sukumar S, Krishman A, Khan MKA. Protein kinases as antituberculosis targets: the case of thymidylate kinases. *Front Biosci.* (2020) 25:1636–54. doi: 10.2741/4871
57. Manley PW, Cowan-Jacob SW, Buchdunger E, Fabbro D, Fendrich G, Furet P, et al. Imatinib: a selective tyrosine kinase inhibitor. *Eur J Cancer.* (2002) (38 Suppl) 5:S19–27. doi: 10.1016/S0959-8049(02)80599-8
58. Schöffski P. Polo-like kinase (PLK) inhibitors in preclinical and early clinical development in oncology. *Oncologist.* (2009) 14:559–70. doi: 10.1634/theoncologist.2009-0010
59. Threadgold LT. Electron-microscope studies of *Fasciola hepatica*. 3. further observations on the tegument and associated structures. *Parasitology.* (1967) 57:633–7. doi: 10.1017/S0031182000073108
60. Meaney M, Haughey S, Brennan GP, Fairweather I. Ultrastructural observations on oral ingestion and trans-tegumental uptake of clorsulon by the liver fluke, *Fasciola hepatica*. *Parasitol Res.* (2005) 95:201–12. doi: 10.1007/s00436-004-1272-8
61. Gschwind HP, Pfaar U, Waldmeier F, Zollinger M, Sayer C, Zbinden P, et al. Metabolism and disposition of imatinib mesylate in healthy volunteers. *Drug Metabol Disposit.* (2005) 33:1503–12. doi: 10.1124/dmd.105.004283
62. Abdelaal MMO, Brennan GP, Abdel-Aziz A, Fairweather I. Ultrastructural changes to the tegumental system and gastrodermal cells of adult *Fasciola hepatica* following treatment *in vivo* with a commercial preparation of myrrh (Mirazid). *J Helminthol.* (2017) 91:672–85. doi: 10.1017/S0022149X16000705
63. Hockley DJ. Ultrastructure of the tegument of *Schistosoma*. *Adv Parasitol.* (1973) 11:233–305. doi: 10.1016/S0065-308X(08)60188-8

64. James CE, Hudson AL, Davey MW. Drug resistance mechanisms in helminths: is it survival of the fittest? *Trends Parasitol.* (2009) 25:328–35. doi: 10.1016/j.pt.2009.04.004
65. Messerli SM, Kasinathan RS, Morgan W, Spranger S, Greenberg RM. *Schistosoma mansoni* P-glycoprotein levels increase in response to praziquantel exposure and correlate with reduced praziquantel susceptibility. *Mol Biochem Parasitol.* (2009) 167:54–9. doi: 10.1016/j.molbiopara.2009.04.007
66. Slupphaug G, Kavli B, Krokan HE. The interacting pathways for prevention and repair of oxidative DNA damage. *Mutat Res.* (2003) 531:231–51. doi: 10.1016/j.mrfmmm.2003.06.002
67. Bouitbir J, Panajatovic MV, Frechard T, Roos NJ, Krähenbühl S. Imatinib and dasatinib provoke mitochondrial dysfunction leading to oxidative stress in C2C12 myotubes and human RD cells. *Front Pharmacol.* (2020) 11:1106. doi: 10.3389/fphar.2020.01106
68. Shenberger JS, Dixon PS. Oxygen induces S-phase growth arrest and increases p53 and p21(WAF1/CIP1) expression in human bronchial smooth-muscle cells. *Am J Respir Cell Mol Biol.* (1999) 21:395–402. doi: 10.1165/ajrcmb.21.3.3604
69. Mazzacurati L, Pattacini L, Brusa G, Mancini M, Benvenuti M, Barbieri E, et al. Chk2 drives late G1/early S phase arrest of clonal myeloid progenitors expressing the p210 BCR-ABL tyrosine kinase in response to STI571. *Hematol J.* (2004) 5:168–77. doi: 10.1038/sj.thj.6200365
70. Carrasco-Torres G, Baltiérrez-Hoyos R, Andrade-Jorge E, Villa-Treviño S, Trujillo-Ferrara JG, Vásquez-Garzón VR. Cytotoxicity, oxidative stress, cell cycle arrest, and mitochondrial apoptosis after combined treatment of hepatocarcinoma cells with maleic anhydride derivatives and quercetin. *Oxid Med Cell Longev.* (2017) 2017:2734976. doi: 10.1155/2017/2734976
71. Heintz N. The regulation of histone gene expression during the cell cycle. *Biochim Biophys Acta.* (1991) 1088:327–39. doi: 10.1016/0167-4781(91)90122-3
72. Beckmann S, Long T, Scheld C, Geyer R, Caffrey CR, Grevelding CG. Serum albumin and α-1 acid glycoprotein impede the killing of *Schistosoma mansoni* by the tyrosine kinase inhibitor imatinib. *Int J Parasitol Drugs Drug Resist.* (2014) 4:287–95. doi: 10.1016/j.ijpddr.2014.07.005
73. O'Connell EM, Nutman TB. Reduction of Loa loa microfilaremia with imatinib - A case report. *N Engl J Med.* (2017) 377:2095–6. doi: 10.1056/NEJMc1712990
74. Eckersall PD, Lawson FP, Bence L, Waterston MM, Lang TL, Donachie W, et al. Acute phase protein response in an experimental model of ovine caseous lymphadenitis. *BMC Vet Res.* (2007) 3:35. doi: 10.1186/1746-6148-3-35
75. Filip Z, Jan K, Vendula S, Jana KZ, Kamil M, Kamil K. Albumin and α1-acid glycoprotein: old acquaintances. *Expert Opin Drug Metab Toxicol.* (2013) 9:943–54. doi: 10.1517/17425255.2013.790364
76. Smith SA, Waters NJ. Pharmacokinetic and pharmacodynamic considerations for drugs binding to alpha-1-acid glycoprotein. *Pharm Res.* (2018) 36:30. doi: 10.1007/s11095-018-2551-x
77. Hill MD, Briscoe PR, Abramson FP. Comparison of propranolol-binding plasma proteins in sheep with those in humans, dogs and rats. *Biochem Pharmacol.* (1989) 38:4199–205. doi: 10.1016/0006-2952(89)90515-7
78. Son DS, Osabe M, Shimoda M, Kokue E. Contribution of alpha 1-acid glycoprotein to species difference in lincosamides-plasma protein binding kinetics. *J Vet Pharmacol Ther.* (1998) 21:34–40. doi: 10.1046/j.1365-2885.1998.00111.x
79. Das KC, Kalita P, Tripathi T. Genome-wide identification and characterization of eukaryotic protein kinases. *Front Biosci.* (2020) 25:1787–827. doi: 10.2741/4878

Conflict of Interest: BS is a consultant of TransMIT GmbH Giessen.

The remaining authors declare that the research was conducted in the absence of any commercial or financial relationships that could be construed as a potential conflict of interest.

5.5 Erste Charakterisierung von Autophagie-assoziierten Genen in *Schistosoma mansoni*

First characterization of autophagy-related genes in *Schistosoma mansoni*

Mughal MN, Grevelding CG, **Haeberlein S**

International Journal of Parasitology (2021) S0020-7519:00092-8

Publikation online: doi: 10.1016/j.ijpara.2020.11.011

Eigener Anteil an der Entstehung der Publikation

- Leitung des Gesamtprojektes: 80%
- Durchführung/Auswertung der Experimente: 10%
- Anfertigung des Manuskripts: 50%

5.6 Insekten in der Wirkstoffforschung: Harmonin aus dem Marienkäfer reduziert Vitalität, Reproduktion und Stammzellproliferation in *Schistosoma mansoni*

Insects in anthelminthics research: Lady beetle-derived harmonine affects survival, reproduction and stem cell proliferation of *Schistosoma mansoni*

Kellershohn J, Thomas L, Grünweller A, Hartmann RK, Hardt M, Vilcinskas A, Grevelding CG, **Haeberlein S**

PLoS Neglected Tropical Diseases (2019) 13(3):e0007240

Eigener Anteil an der Entstehung der Publikation

- Leitung des Gesamtprojektes: 90%
- Durchführung/Auswertung der Experimente: 20%
- Anfertigung des Manuskripts: 90%

PLOS | NEGLECTED TROPICAL DISEASES

RESEARCH ARTICLE

Insects in anthelminthics research: Lady beetle-derived harmonine affects survival, reproduction and stem cell proliferation of *Schistosoma mansoni*

Josina Kellershohn[1], Laura Thomas[2], Steffen R. Hahnel[1], Arnold Grünweller[2], Roland K. Hartmann[2], Martin Hardt[3], Andreas Vilcinskas[4], Christoph G. Grevelding[1], Simone Haeberlein[1]*

1 Institute of Parasitology, BFS, Justus Liebig University, Giessen, Germany, **2** Institute of Pharmaceutical Chemistry, Philipps University, Marburg, Germany, **3** Biomedical Research Center Seltersberg—Imaging Unit, Justus Liebig University, Giessen, Germany, **4** Institute for Insect Biotechnology, Justus Liebig University, Giessen, Germany

* simone.haeberlein@vetmed.uni-giessen.de

OPEN ACCESS

Citation: Kellershohn J, Thomas L, Hahnel SR, Grünweller A, Hartmann RK, Hardt M, et al. (2019) Insects in anthelminthics research: Lady beetle-derived harmonine affects survival, reproduction and stem cell proliferation of *Schistosoma mansoni*. PLoS Negl Trop Dis 13(3): e0007240. https://doi.org/10.1371/journal.pntd.0007240

Editor: Klaus Brehm, University of Würzburg, GERMANY

Received: December 12, 2018

Accepted: February 13, 2019

Published: March 14, 2019

Data Availability Statement: All relevant data are within the manuscript and its Supporting Information files.

Funding: The work was funded by the excellence initiative of the Hessian Ministry of Science, Higher Education and Art (HMWK) supporting the LOEWE Centre DRUID and awarded to CGG and SH. URL: https://wissenschaft.hessen.de/wissenschaft/landesprogramm-loewe. The funder had no role in

Abstract

Natural products have moved into the spotlight as possible sources for new drugs in the treatment of helminth infections including schistosomiasis. Surprisingly, insect-derived compounds have largely been neglected so far in the search for novel anthelminthics, despite the generally recognized high potential of insect biotechnology for drug discovery. This motivated us to assess the antischistosomal capacity of harmonine, an antimicrobial alkaloid from the harlequin ladybird *Harmonia axyridis* that raised high interest in insect biotechnology in recent years. We observed remarkably pleiotropic effects of harmonine on physiological, cellular, and molecular processes in adult male and female *Schistosoma mansoni* at concentrations as low as 5 μM *in vitro*. This included tegumental damage, gut dilatation, dysplasia of gonads, a complete stop of egg production at 10 μM, and increased production of abnormally shaped eggs at 5 μM. Motility was reduced with an EC50 of 8.8 μM and lethal effects occurred at 10–20 μM within 3 days of culture. Enzyme inhibition assays revealed acetylcholinesterase (AChE) as one potential target of harmonine. To assess possible effects on stem cells, which represent attractive anthelminthic targets, we developed a novel *in silico* 3D reconstruction of gonads based on confocal laser scanning microscopy of worms after EdU incorporation to allow for quantification of proliferating stem cells per organ. Harmonine significantly reduced the number of proliferating stem cells in testes, ovaries, and also the number of proliferating parenchymal neoblasts. This was further supported by a downregulated expression of the stem cell markers *nanos-1* and *nanos-2* in harmonine-treated worms revealed by quantitative real-time PCR. Our data demonstrate a multifaceted antischistosomal activity of the lady beetle-derived compound harmonine, and suggest AChE and stem cell genes as possible targets. Harmonine is the first animal-derived alkaloid detected to have antischistosomal capacity. This study highlights the potential of exploiting insects as a source for the discovery of anthelminthics.

study design, data collection and analysis, decision to publish, or preparation of the manuscript.

Competing interests: The authors have declared that no competing interests exist.

Author summary

Natural compounds represent one of the richest sources for the discovery of new active compounds against diseases such as cancer or infections, including helminth infections that cause the highest disease burden in tropical countries. Surprisingly, insects have been almost completely neglected with respect to anthelminthics discovery although they represent the most species-rich class of animals known on earth, producing a wide spectrum of compounds with biological activities. In insect biotechnology, the harlequin ladybird *Harmonia axyridis* raised high interest being a rich source of antimicrobial compounds such as the alkaloid harmonine. Harmonine is thought to act as a chemical weapon keeping otherwise detrimental microsporidia in the beetle under control. Testing the antiparasitic potential of harmonine against adult *Schistosoma mansoni*, one of the most harmful helminths worldwide, resulted in multifaceted negative effects. The compound damaged tissues essential for survival and reproduction of schistosomes (tegument, intestine, gonads) and also affected stem-cell proliferation. Furthermore, we obtained first evidence for acetylcholinesterase as one potential molecular target, which was partially inhibited by harmonine. This is the first time to proof a direct effect of a defined insect-derived compound on a helminth parasite, a finding that will encourage further studies to explore insects as sources of novel anthelminthics.

Introduction

Natural compounds represent one of the richest sources for the discovery of new active compounds against cancer, infections, or other threats to human health. From 1981 to 2010, 33% of approved drugs represented natural compounds and derivatives, mostly from plants, algae, and fungi [1]. In recent years, the search for novel anthelmintic compounds from natural sources has been intensified with the aim to identify new hit and lead compounds for drug development [2]. So far, medicinal plants and their metabolites (like alkaloids, terpenes, and peptides) have been widely exploited as sources of novel natural compounds with anthelmintic activity. In contrast, only few studies have focused on animal-derived molecules [3]. Surprisingly, although insects are among the most successful and widespread organisms on earth, especially regarding their diversity and adaptability, they are still rather underrated as sources of compounds with medical importance. Along these lines, insects have been almost completely neglected with respect to anthelminthic discovery [4].

The chemical defense of insects against pathogens and parasites relies on effector molecules such as antimicrobial peptides and secondary metabolites. The invasive harlequin ladybird *Harmonia axyridis*, which is also known as Asian ladybird or Multicolored ladybird, represents an outstanding example in this regard [5]. Its immune system encompasses more than fifty antimicrobial peptides, the highest number ever reported for an animal [6]. In addition, its hemolymph contains extraordinarily high concentrations of the constitutively expressed antimicrobial alkaloid harmonine ((17R,9Z)-1,17-diaminooctadec-9-ene), an aliphatic, long-chain diamine which displays antimicrobial activities [7]. Its superior immune system promotes its invasive success in a multifaceted manner. The beetle's antimicrobial peptides have been demonstrated to mediate resistance against pathogenic bacteria [8], whereas harmonine has been postulated to keep its microsporidia under control. Microsporidia are highly specialized relatives of fungi that propagate as intracellular parasites in insects and other taxa [9]. *H. axyridis* carries a high load of microsporidia which can infect and kill native competitors such as the

two-spotted ladybird *Adalia bipunctata* and the seven-spotted ladybird *Coccinella septempunctata* when transmitted e.g. during intraguild predation. Therefore, these parasites have been postulated to function in invaded areas like bioweapons to successfully outcompete native competitors [6, 10, 11]. In addition, first tests against human pathogens showed that harmonine displays a broad-spectrum antimicrobial activity including *in vitro* effects against mycobacteria as well as protozoan parasites [7, 12]. Activity against helminths has so far not been investigated, even though novel active compounds are highly needed for a whole list of helminth infections, which includes neglected tropical diseases (NTDs) in humans and veterinary infectious diseases [13, 14].

Schistosomiasis is among the helminthic diseases causing highest disability and mortality in humans worldwide [15]. In endemic areas, schistosomiasis occurs as a chronic disease, which derives from the longevity of blood-resident adult schistosomes persisting many years in the host. Pathology is mainly caused by tissue deposition of eggs which are produced in hundreds per day by the female worm [16]. Approximately 700 million people are at risk of schistosomiasis [15], and there is no vaccination that might prevent infection. Treatment relies on a single drug, praziquantel (PZQ). PZQ is active against all three major schistosome species, *Schistosoma mansoni*, *S. haematobium* and *S. japonicum*, it can be produced at low cost and is well tolerated. It is therefore used in mass treatment programs and as preventive chemotherapy for people at high risk [17]. This and its continued use since the 1980s have increased the risk of resistance development. Indeed, evidence was obtained for schistosomes with lowered PZQ susceptibility in human drug administration programs and in experimental animal models [18–20]. Therefore, finding alternative treatment options has become an urgent issue [21].

Due to their outstanding species number and diversity, insects constitute a huge "drug cabinet" to be explored which might also include novel compounds with anthelmintic activity. To make a start, we focused in our study on the antimicrobial alkaloid compound harmonine derived from the harlequin ladybird. The aim of this study was to reveal whether this insect-derived compound shows anthelmintic capacity against adult *S. mansoni* worms. By physiological, cellular, and molecular analyses we observed a complex multifaceted phenotype comprising tegumental damage, gut dilatation, gonadal dysplasia, egg-production deficits as well as cellular and molecular effects on stem cells. Furthermore, we found first evidence for AChE as one potential target. With the results of our study, we want to promote insect-derived compounds and move them into spot-light as possible sources of new drugs in the treatment of schistosomiasis and further parasitic diseases.

Materials & methods

Ethics statement

Animal experiments were performed in accordance with the European Convention for the Protection of Vertebrate Animals used for experimental and other scientific purposes (ETS No 123; revised Appendix A) and have been approved by the Regional Council (Regierungspraesidium) Giessen (V54-19 c 20/15 c h 02 GI 18/10Nr. A 1/2014).

Parasites

A Liberian strain (Bayer AG, Monheim) of *S. mansoni* was used to infect freshwater snails of the genus *Biomphalaria glabrata* as intermediate host and Syrian hamsters (*Mesocricetus auratus*) as final host [22, 23]. Eight week-old hamsters were obtained from Janvier (France), infected by the "paddling method" [24], and sacrificed at 46 days p.i. to collect adult worm couples by perfusion. Unisexual worm populations were generated by monomiracidial intermediate-host infection [23]. Worms were cultured in M199 medium (Sigma-Aldrich,

Germany; supplemented with 10% Newborn Calf Serum (NCS), 1% HEPES [1 M] and 1% ABAM-solution [10,000 units penicillin, 10 mg streptomycin and 25 mg amphotericin B per ml]) at 37˚C and 5% CO_2.

In vitro culture

For *in vitro* culture of adult couples with harmonine, worms were cultured in 6-well plates in supplemented M199 medium with 10 worm couples per well. Harmonine was synthesized as described by Nagel et al. 2015 [12] and kindly provided by W. Boland (Max-Planck-Institute for Chemical Ecology, Jena, Germany). Harmonine was dissolved in DMSO and added in final concentrations of 2.5–50 μM as indicated. As negative control, M199 medium was adjusted to the same concentration of DMSO as used for the highest inhibitor concentration. The worms were incubated at 37˚C and 5% CO_2 for 72 h, medium and harmonine were exchanged every 24 h. Harmonine-induced morphological effects were assessed every 24 h using an inverted microscope (Leica, Germany). Worm motility was scored with a system following recommendations by WHO-TDR [25], with the scores 3 (normal motility), 2 (reduced motility), 1 (minimal and sporadic movements), 0 (no movements within 30 sec was considered dead). For depletion of proliferating cells, 20 mM hydroxyurea was added to the culture for 72 h, and medium plus hydroxyurea was refreshed every 24 h. For visualization of proliferating cells, EdU (5-ethynyl-2-deoxyuridine) was added to a final concentration of 10 mM for the last 24 h of *in vitro* culture. Thereafter, worms were either processed for confocal laser scanning microscopy (CLSM), or subjected to RNA extraction for quantitative real-time PCR (qPCR) analysis.

Quantitative real-time PCR

Freshly perfused or *in vitro*-cultured worm couples were separated by gender, and RNA was extracted from male and female worms using the PeqGOLD TriFast reagent (Peqlab, Germany) according to the manufacturer's protocol. RNA quality was checked using the Agilent RNA 6000 Nano kit and an Agilent Bioanalyzer 2100 instrument (Agilent Technologies, USA), followed by reverse transcription using the Quantitect RT-Kit (Qiagen, Germany). Expression levels of the *S. mansoni* orthologs of the stem cell markers *nanos-1* (Smp_055740) and *nanos-2* (Smp_051920), and the AChE ortholog (Smp_154600) were determined by qPCR using the SYBR Green method [26] with the PerfeCTa SYBR Green SuperMix (VWR, Germany), the Rotor-Gene Q instrument and Rotor-Gene Q Series Software (Qiagen). All samples were pipetted in technical triplicates. Ct values were normalized against the geometric mean of three references genes selected based on stable expression in both sexes (Haeberlein et al., submitted): orthologs of LETM1 (Smp_065110), phosphatase 2A (Smp_166290) and proteasome-beta (Smp_073410). Relative expression levels were calculated either by the delta delta Ct method [27] or by expressing the data as n-fold difference by the formula: relative expression = $2^{-\text{delta Ct}} \times f$, with f = 100 as an arbitrary factor (as indicated in the figure legends). The following primers were used, which were confirmed by test qPCRs to have efficacies between 0.9–1: LETM1_fw 5'-GAAGGTGATCAAGCTCCATTGT-3', LETM1_rev 5'-TTGTACTGCATGGATAGGTG GT-3'; phosphatase-2A_fw 5'-GTAAAACTGGTCCATTTGAAGAAC-3', phosphatase-2A_rev 5'-TACCGAATAGGAAATGTTGAACGA-3'; prot-beta_fw 5'-GGTCTGGTGGTTTCTCGT TC-3', prot-beta_rev 5'-GTACCTTCTGTTGCCCGTG-3'; nanos-1_fw 5'-ACTTGTCCATTAT GCGGTGCT-3', nanos-1_rev 5'- GGTTCCAACAAACCAGCTTCA-3'; nanos-2_fw 5'-GCCG TGTTATGACCTCTGG-3', nanos-2_rev 5'-GACGATCTGGAGACTCTGG-3'; AChE1_fw 5'-GATGATGATGATGAACGACCG-3', AChE1_rev 5'- CAGTAACTAATGATTATCGTA TACCA-3'; AChE2_fw 5'-TAAGACACGAAATGATGATTCACG-3', AChE2_rev 5'-TACTT CATATTGTGTAGTTGATTGAC-3'.

Protein isolation

Native protein lysates were prepared from 50 male or 150 female worms as described [28]. Briefly, worms were sonicated in PBS supplemented with protease inhibitors. The protein concentration was determined by the advanced protein assay reagent (APAR, Cytoskeleton Inc., USA) and measured at 590 nm in a microplate reader (VARIOSKAN FLASH; Thermo Fisher Scientific, USA).

Acetylcholinesterase assay

AChE activity was determined in native protein lysates of adult male or female *S. mansoni* using the Amplite Colorimetric Acetylcholinesterase Assay Kit (AAT Bioquest, Biomol, Germany) following the instruction of the manufacturer, which is based on Ellman's method [29]. For inhibition studies, the protocol was adapted as follows: for each harmonine concentration, 200 μg/ml of native male protein or 100 mU/ml of the AChE standard (from the electric eel *Electrophorus electricus*) were added. A negative control containing an equivalent amount of solvent of harmonine (DMSO) was included. To start the reaction, an AChE reaction mixture was added to each well. The final concentration of the substrate acetylthiocholine was 0.5 mM. Absorbance by the reaction product TNB-thiocholine, which is proportional to the AChE activity, was measured by the VARIOSKAN FLASH microplate reader at 405 nm with reads every 10 min at 37˚C.

Confocal laser scanning microscopy

For morphological analysis by CLSM, worms were fixed and stained with carmine red (CertistainH; Merck, Germany) as described before [30, 31]. For EdU labelling and detection of proliferating cells, the Click-iT Plus EdU Alexa Fluor 488 Imaging Kit (Thermo Fisher Scientific) was used. After 24 h of incubation with EdU, couples were separated, fixed and stained as described [32]. Worms were counterstained with Hoechst 33342 in a final concentration of 8 μM. Stained worms were examined on an inverse CLSM (Leica TSC SP5; Leica, Germany). Hoechst was excited with a 405 nm laser, and Alexafluor488 as well as carmine red with an argon-ion laser at 488 nm. Laser power as well as gain and offset of all photomultiplier tubes (PMTs) were optimized for minimizing possible bleaching effects and for full range intensity coding using the CLUT-function (color look-up table) of the Leica LAS AF software. Background signals and optical section thickness were defined by setting the pinhole size to airy unit 1. The software package "IMARIS for cell biologists" (Bitplane, Switzerland) was used to quantify Hoechst- and EdU-positive cells in ovaries and testes of worms. Z-stacks acquired by CLSM were used as input data. First, a so-called surface was created manually for each organ to extract it *in silico* from the surrounding tissue. Next, surfaces were created for all EdU- and Hoechst-positive cells. This allowed quantifying stained cells per organ. To minimize counting of artifacts or background noise, a threshold was set prior to surface creations that excluded objects <3 μm.

Statistical analysis

Statistical analysis was performed using an unpaired t-test. A p-value < 0.05 was considered significant.

Results

Harmonine reduces schistosome motility and viability *in vitro*

To investigate whether the insect-derived compound harmonine has anthelminthic activity, adult *S. mansoni* worms were cultured *in vitro* with different concentrations of the compound over a period of 72 h. Harmonine reduced the pairing stability of worm couples in a dose-

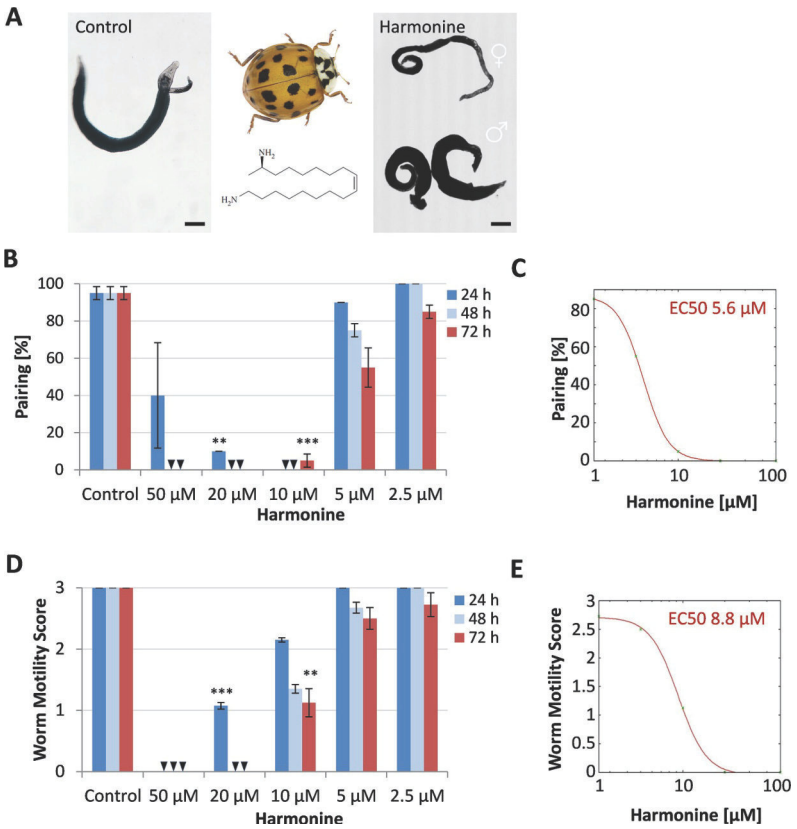

Fig 1. Effect of harmonine on motility, viability and pairing. *S. mansoni* couples were treated with different concentrations of harmonine for 72 h and microscopically screened every 24 h. As a negative control, the solvent DMSO was added in an amount as present in the highest harmonine concentration. **(A)** Representative images of a control couple and worms after treatment with 10 μM harmonine for 72 h. Scale bar: 100 μm. *H. axyridis* [33] and the structure of the alkaloid harmonine are shown in the middle. **(B)** Percentage of paired worms after harmonine treatment. **(C)** Dose-response curve for pairing stability (expressed as % pairing) after 72 h of treatment. **(D)** Worm motility reflected by motility scores 3 = normal motility, 2 = reduced motility, 1 = almost no movements, 0 = dead. **(E)** Dose-response curve for the reduction of motility by harmonine after 72 h of treatment. EC50 values were calculated by non-linear least squares curve fitting using the ic50.tk tool. A-C show a summary of two experiments with 10 worm couples per experiment and condition; error bars: SEM. Triangles indicate a value of zero. Significant differences to control worms at the respective time point are indicated with ** $p<0.01$ or *** $p<0.001$ (students t-test).

https://doi.org/10.1371/journal.pntd.0007240.g001

dependent manner (Fig 1A–1C). With ≥ 10 μM harmonine, all couples separated within 48 h and were detached from the culture-well surface. With 5 μM, around 50% of worm couples separated (calculated EC50: 5.6 μM), and 90% were detached after 72 h. A similar time- and dose-dependent pattern was found for the reduction of worm motility by harmonine (Fig 1D), with a calculated EC50 of 8.8 μM (Fig 1E). Specifically, with concentrations of 50 and 20 μM, all worms died within 2 h and 48 h, respectively. With 10 μM, worms had a significantly reduced motility with an average motility score of 1 after 48–72 h, indicating only minimal and sporadic movements; 25% of worms were dead after 72 h. Interestingly, most of the females were unaffected with 10 μM after the first day, whereas treated males showed reduced

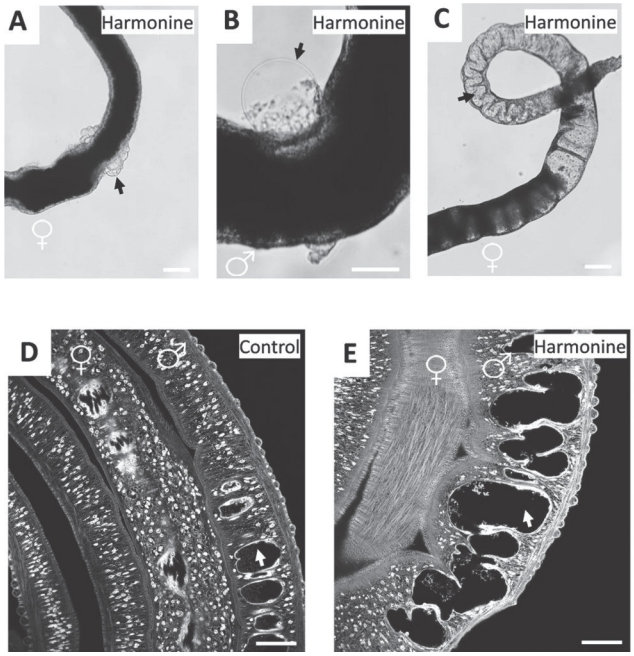

Fig 2. Tissue damage induced by harmonine. *S. mansoni* couples were cultured for 72 h with 5 μM harmonine with a change of medium and compound every 24 h. **(A, B)** Bubble formation (arrows) on the tegument surface in a representative female (A) and male (B) worm. **(C)** Gut dilatation (arrow) in a female worm, visualized by bright-field microscopy. **(D, E)** CLSM images of carmine red-stained worms showing the gut lumen of a control male (D) and the dilated lumen (arrow) of a harmonine-treated male (E). Scale bars are 100 μm (A-C) or 50 μm (D, E).

https://doi.org/10.1371/journal.pntd.0007240.g002

motility, indicating a gender bias in the effect of harmonine. Concentrations below 10 μM caused a weak, time-dependent reduction of motility. Next to its effects on motility, viability and pairing stability, harmonine affected worm tissue structure in remarkable ways. Concentrations as low as 5 μM induced bubble formation on the tegumental surface in both males and females (Fig 2A and 2B). In addition, severe gut dilatations were observed in both sexes of *S. mansoni* by bright-field microscopy, which was confirmed by CLSM (Fig 2C–2E). Taken together, harmonine showed antischistosomal activity and induced a dose-dependent spectrum of phenotypic effects in schistosomes, ranging from tissue damage and pairing-instability with 5 μM, severe impairment of worm motility up to death at 10 μM, and finally 100% lethality at 20 μM.

Harmonine reduces acetylcholinesterase activity

Reduced motility, pairing-instability and gut dilatations might point to a target of harmonine involved in (neuro)muscular activity. In addition, the observed tegumental effects suggested target localization within the tegument. Previous *in silico* docking analyses with *Leishmania* proteins suggested AChE as a possible target of harmonine [34]. AChE is a well-characterized enzyme, also in schistosomes, and it is the presumed target of metrifonate, a formerly used antischistosomal drug [35]. AChE was found to be abundantly expressed in the tegument of schistosomes [36, 37]. Therefore, we hypothesized that AChE might be one target of

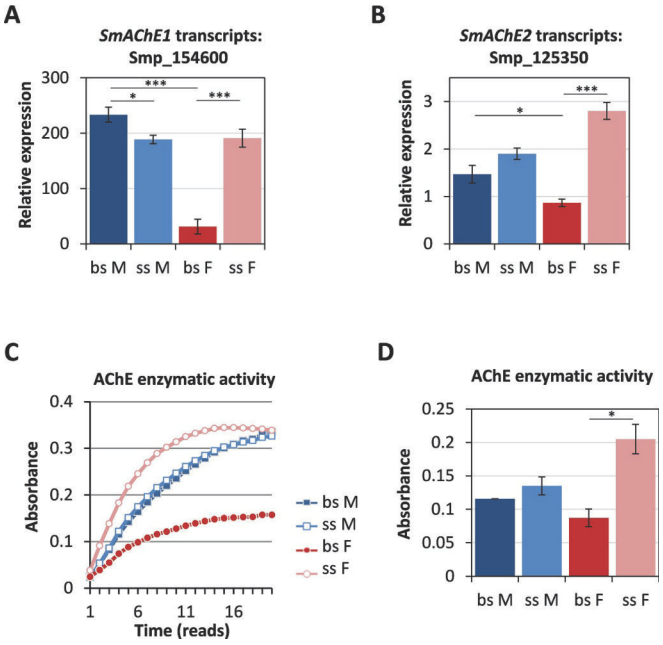

Fig 3. AChE transcript levels in *S. mansoni* and inhibition of enzymatic activity by harmonine. (A, B) Expression of *SmAChE1* (Smp_154600) and *SmAChE2* (Smp_125350) in different sexes and mating-states as determined by qPCR, expressed as relative expression vs. the geometric mean of three reference genes (x100 as an arbitrary factor). A summary of three experiments with SEM is shown. **(C, D)** Enzymatic activity present in protein lysates of male and female worms in the paired or unpaired state given as change of absorbance over time of one representative of two experiments (C) and as summary of two experiments (absorbance at 30 min) (D). Enzymatic activity was determined by Ellman's method by quantifying absorbance of 5-thio-2-nitrobenzoic acid, which is equivalent to the amount of thiocholine produced from the hydrolysis of acetylthiocholine by AChE. Significant differences as determined by the unpaired t-test are indicated with * $p<0.05$ or *** $p<0.001$. M, male; F, female; bs, bisex (paired); ss, single-sex (unpaired).

https://doi.org/10.1371/journal.pntd.0007240.g003

harmonine in *S. mansoni*. By SMART analysis of protein sequences from genes electronically annotated as AChEs in GeneDB and WormBase ParaSite, we identified two potential orthologs of AChE in *S. mansoni*: Smp_125350 and Smp_154600, which both show the typical carboxyl-esterase domain (S1 Fig). We suggest the name *SmAChE1* for Smp_154600 because of its first characterization in a previous study [38], and *SmAChE2* for Smp_125350. Based on preliminary data of a transcriptomics study [39], we first characterized the expression levels of both *SmAChE* genes in the different sexes as well as the enzymatic activity of their protein lysates. AChE transcript levels were determined by qPCR and revealed a sex- and pairing-dependent expression (Fig 3A and 3B). Notably, expression in females after pairing contact (from bisexual infection, bs F) was significantly decreased compared to females in unpaired state (from single-sex infection, ss F) or males. For females, this difference in transcript level correlated well with enzyme activity since we determined a significantly lower AChE enzymatic activity in protein lysates of paired females compared to unpaired females. A similar trend was observed for paired females vs. males (Fig 3C and 3D).

Next we investigated a possible effect of harmonine on AChE transcript levels. The expression of both genes was reduced in a dose-dependent manner in harmonine-treated compared

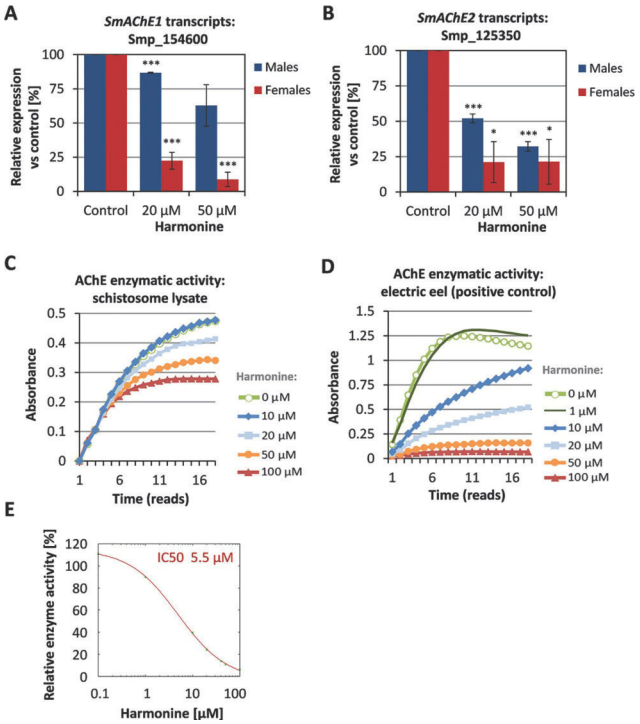

Fig 4. Inhibition of AChE enzymatic activity by harmonine. (A, B) Expression of *SmAChE1* (Smp_154600) and *SmAChE2* (Smp_125350) in male and female schistosomes after 72 h treatment with different concentrations of harmonine as determined by qPCR, expressed as relative expression vs. the geometric mean of three reference genes. The expression in control worms was set to 100%. A summary of two experiments with SEM is shown. **(C)** Enzymatic activity over time in protein lysates of paired males after adding different concentrations of harmonine (0 – 100 μM). One representative out of three similar experiments is shown. **(D)** Enzymatic activity of AChE from a model organism (electric eel) after addition of different concentrations of harmonine (0 – 100 μM). One representative out of two similar experiments is shown. **(E)** Relative AChE activity of electric eel at 30 min after adding different concentrations of harmonine, with the activity at 0 μM set as 100%. Mean values of two experiments were used. IC50 was calculated by non-linear least squares curve fitting using the ic50.tk tool. Significant differences as determined by the unpaired t-test are indicated with * $p<0.05$ or *** $p<0.001$.

https://doi.org/10.1371/journal.pntd.0007240.g004

to control male and female worms (Fig 4A and 4B). Because of the low AChE activity in protein lysates of paired females, male lysates were used to test the capacity of harmonine for inhibiting schistosomal AChE activity. Harmonine (10 – 100 μM) decreased the turnover of the substrate acetylthiocholine in a dose-dependent manner (Fig 4C). Interestingly, the inhibition of AChE from a common test organism (electric eel) [40] was even more efficient, and it occurred at lower concentrations (Fig 4D). With an IC50 of 5.5 μM against electric eel AChE (Fig 4E), harmonine can be considered a moderate inhibitor of AChE activity, whose potency might be species-dependent. Also compared to IC50 values of the known AChE inhibitor physostigmine (electric eel, 148.4 nM; schistosome lysate, 724.2 nM; S2A–S2D Fig), harmonine was clearly less potent. As increasing excess concentrations of the substrate ACh at constant harmonine concentration did not restore full AChE reaction velocity, an inhibition mechanism other than competitive inhibition is likely (S2E Fig).

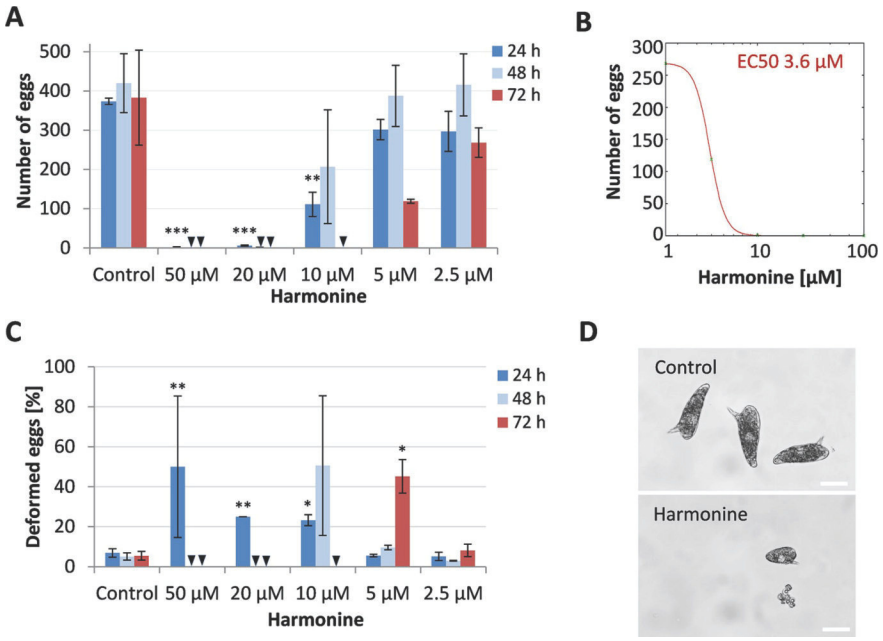

Fig 5. Effect of harmonine on egg production. *S. mansoni* couples were cultured with different concentrations of harmonine for a period of 72 h. Medium and compound were renewed every 24 h. **(A, C)** Effect of harmonine on reproduction was assessed by counting the number of total eggs being laid by 10 couples per 24 h period (A) and their percentage of deformed eggs (C). **(B)** Dose-response curve for the reduction of egg numbers being laid in the last 24 h of the 72 h culture. Summary of two experiments with 10 couples of *S. mansoni* per experiment and condition; error bars: SEM. **(D)** Representative images of eggs from control couples and after 72 h treatment with 5 μM harmonine. Deformed eggs were e.g. smaller and often lacked an oocyte, a spine, or a normal amount of vitelline cells. Scale bar is 50 μm. Significant differences to the control at the respective time point are indicated with * $p<0.05$, ** $p<0.01$ or *** $p<0.001$ (students t-test).

https://doi.org/10.1371/journal.pntd.0007240.g005

Harmonine affects reproduction and gonadal tissues

Besides motility and morphology, compound-induced effects on reproduction are also of high interest because schistosome eggs are essential for maintaining the life-cycle and causative for the pathology of schistosomiasis. We therefore determined the quantity and quality of egg production during 72 h treatment of adult worm couples with harmonine. Egg production ceased completely with 20 μM harmonine after 48 h and with 10 μM after 72 h, respectively (Fig 5A). 5 μM harmonine reduced the number of eggs to 31% compared to the control, but of note, up to 57% of these eggs were of abnormal size and shape. In addition, free vitellocytes were found in the culture medium indicating egg-production deficits (Fig 5C and 5D). Overall, the EC50 of harmonine for the reduction of egg production was 3.6 μM (Fig 5B).

To investigate whether impaired egg production was related to gonadal tissue defects, harmonine-treated worms were stained with carmine red for subsequent CLSM analysis, which allowed the detection of morphologic abnormalities at the organ level. As expected [30, 31], in control females the vitellarium was found to be tightly packed with cells, and it was arranged similar to a zipper with cell rows interlocking with the opposite side (Fig 6B). Treatment with harmonine at a concentration of 10 μM led to the formation of numerous unstained, hole-like areas, giving the whole vitellarium a *swiss cheese-like* tissue pattern (Fig 6E). In the ovary of control females, the small immature oogonia are located within the anterior part and the

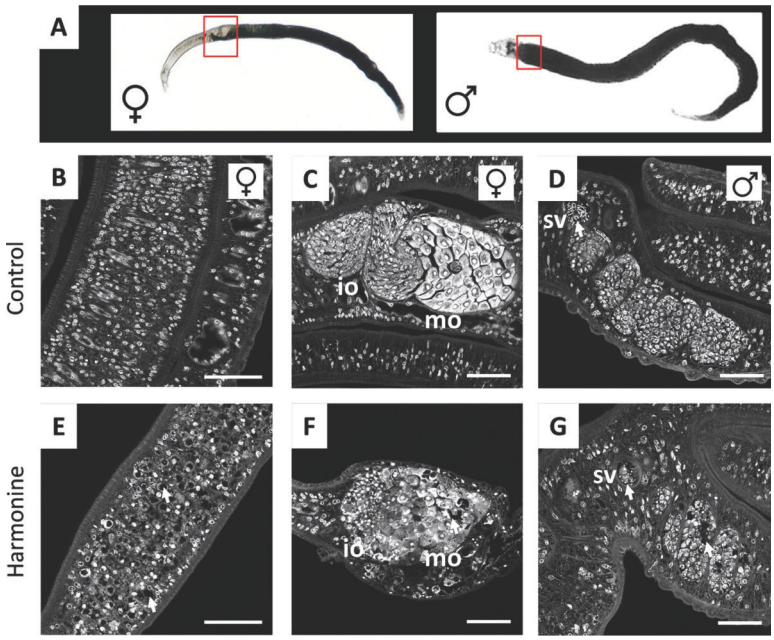

Fig 6. Effect of harmonine on gonadal tissue structure. For CLSM-analysis of gonadal tissues, *S. mansoni* couples were cultured for 72 h with 10 μM harmonine (E-G) or solvent as a control (B-D), and stained with carmine red. **(A)** Bright-field microscopic images indicating the localization of ovary and testes in worms. **(B, E)** Confocal images showing part of the intact vitellarium of a control female (still paired with a male) (B) compared to the porous appearance of the vitellarium after harmonine treatment (E). **(C, F)** Well-defined immature (iO) and mature (mO) parts of a control ovary (C), compared to the disintegrated structure of an ovary in a harmonine-treated female (F). **(D, G)** Seminal vesicle (sv) filled with spermatozoa, and testes lobes filled with spermatogonia of a control male (D), compared with the gonad of a harmonine-treated male with reduced number of spermatozoa and partially disintegrated lobes (arrows) (G). Scale bar: 50 μm.

https://doi.org/10.1371/journal.pntd.0007240.g006

bigger, mature oocytes within the larger posterior part (Fig 6A and 6C), as shown before [30, 31]. Already at 10 μM, harmonine clearly disrupted the ordered structure of the ovary (Fig 6F). The ovary appeared shrunken, oogonia of smaller size and mature oocytes poorly separated from each other. The cytoplasm stained weaker compared to control ovaries, and unstained, hole-like areas were found similar to the phenotype seen in the vitellarium.

In control males, testes consist of distinct lobes which are tightly packed with spermatogonia [30, 31]. At the anterior end, mature spermatocytes gather in the seminal vesicle (Fig 6D). After harmonine treatment, lobes also appeared shrunken and showed similar porous areas as seen in female tissues. The seminal vesicle contained less spermatocytes and an undefined cell mass instead, which probably represents undifferentiated spermatogonia (Fig 6G). All observed phenotypes were occasionally observed also after treatment with 5 μM harmonine. To sum up, treatment with harmonine led to a dramatic reduction and malformation of schistosomal eggs, which might be related to the structural disruption of ovary, vitellarium, and testes.

Defects in gonadal stem cell proliferation

Two findings led to the hypothesis that harmonine might affect stem cell proliferation. First, one of the non-neuronal functions of AChE described for humans is related to stem-cell

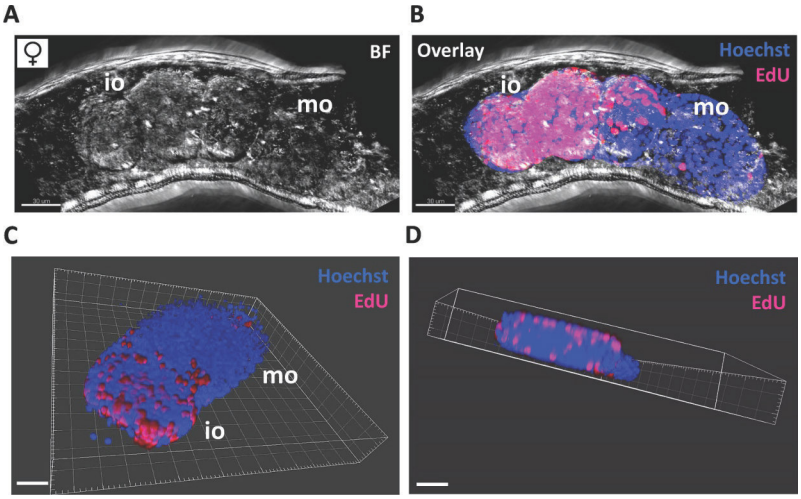

Fig 7. 3D reconstruction of *S. mansoni* ovary and stem cell localization. Couples were cultured for 24 h with EdU. Females were separated from males, stained with Hoechst, and z-stacks of the ovary and surrounding tissue were acquired by CLSM. Z-stacks were processed with the IMARIS software to release the ovary from the surrounding tissue and to quantify the number of EdU- and Hoechst-positive cells. **(A)** Representative z-stack showing the immature part (iO) and mature part (mO) of an ovary within a female worm in bright field (BF). **(B)** The same z-stack with an overlay of the BF image and the *in silico*-released ovary. Proliferating, EdU-positive stem cells are depicted in pink, Hoechst-positive cells in blue. **(C, D)** Still images of a video animation of a 3D reconstructed ovary (see supplementary video, S1 Movie). (D) shows the preferential localization of stem cells at the edges of the immature part of the ovary. Scale bar: 30 μm (A, B) or 40 μm (C, D).

https://doi.org/10.1371/journal.pntd.0007240.g007

activity [41]. Second, the observed harmonine-induced impairment of gonadal cell organization might point to a defect in a preceding step, i.e. gonadal stem-cell proliferation. Therefore, we used the thymidine analogue EdU to visualize proliferating cells in schistosomal tissues of harmonine-treated worms vs. controls by CLSM. As background staining we used Hoechst. Indeed, sublethal concentrations of 5 and 10 μM harmonine reduced the number of proliferating cells in both ovaries and testes compared to organs of control worms (S3 Fig). In order to quantify the number of proliferating stem cells per organ as an objective measure, we established a procedure to separate gonads *in silico* from the surrounding worm tissue with the help of the analysis software IMARIS. 3D visualization of ovaries revealed that proliferating stem cells are exclusively located in the anterior part (Fig 7). In addition, stem cells are not homogeneously nested between oogonia, but preferentially located at the outer edge of the organ (Fig 7C and 7D; S1 Movie). Next, we determined the percentage of EdU-positive stem cells per total Hoechst-positive cells for each ovary or testis. The percentage of proliferating stem cells per organ was significantly reduced in harmonine-treated worms compared to control worms. While control ovaries and testes showed on average 30% and 47% EdU-positive cells, respectively, the percentage dropped to 5% and 7% after exposure to harmonine (Fig 8A–8D). This resulted in a merely scattered distribution of stem cells within the gonads. To support these findings, we investigated whether harmonine might also affect the transcript level of *nanos-1* (Smp_055740), a gene described as germline-specific stem cell marker in adult *S. mansoni* [42, 43]. Indeed, the transcript level of *nanos-1* was significantly reduced in harmonine-treated male and female worms (Fig 8E and 8F).

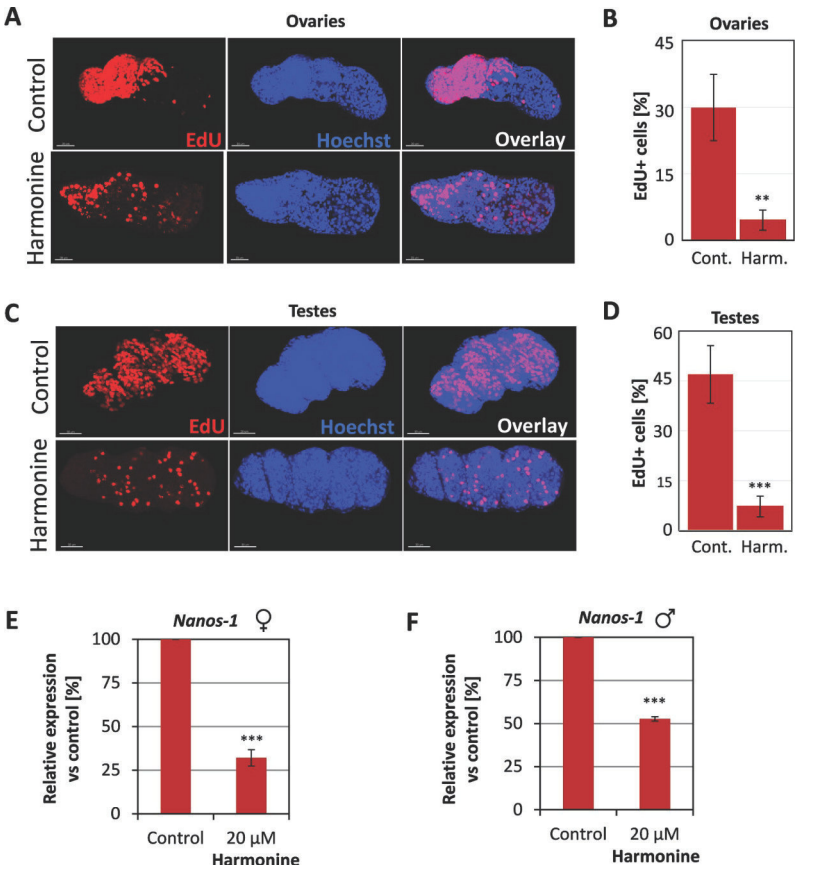

Fig 8. Reduction of gonadal stem cell proliferation upon harmonine treatment. *S. mansoni* couples were treated with 20 μM harmonine *in vitro* for 6 days. As control, an equivalent volume of the solvent DMSO was used. EdU was added for the last 24 h of culture, worm couples were separated and images were processed using the IMARIS software as described in the text and Fig 6. **(A, B)** Representative images (A) and summary of the analyses of four ovaries (B) from either control or harmonine-treated females. A significant reduction of stem cells was found after treatment, expressed as percentage of EdU-positive per Hoechst-positive cells. **(C, D)** Representative images (C) and summary of four testes (C) from control and harmonine-treated males showing a significant reduction of the percentage of stem cells following treatment. Scale bar: 30 μm. **(E, F)** Expression of the gonadal stem cell marker *nanos-1* (Smp_055740) in females (E) and males (F) after treatment with 20 μM harmonine compared to control worms as determined by qPCR. The expression in control worms was set to 100%. Summary of two experiments. An unpaired t-test was performed to reveal significant differences (** $p<0.01$, *** $p<0.001$).

https://doi.org/10.1371/journal.pntd.0007240.g008

Impairment of neoblast proliferation

In addition to the gonads, proliferating stem cell-like cells are also present in the parenchyma of *S. mansoni* [44]. These so-called neoblasts are thought to provide replenishment of tegumental and gastrodermal cells. Impairment of these cells by a compound like harmonine would therefore be a useful way to interfere with worm survival. Similar to proliferating cells in the reproductive organs, the amount of EdU-positive cells decreased after treatment with harmonine in males and females. In the representative control female depicted in Fig 9A (top,

left image), a huge number of EdU-positive cells was also detected in the vitellarium, while after treatment, only some residual cells were found (Fig 9A, bottom, left image).

Nanos-2 (Smp_051920) is a stem cell marker expressed both in germline and somatic stem cells. *Nanos-2* transcripts were found to be reduced after irradiation-mediated depletion of somatic stem cells [44]. We therefore used it as a molecular measure for compound-induced effects on neoblasts. *Nanos-2* transcript levels were determined by qPCR after treatment of worms with harmonine or hydroxyurea for comparison. Hydroxyurea is a mitotic inhibitor that was successfully used before to deplete the majority of neoblasts in helminths [45, 46]. Compared to control worms, the expression of *nanos-2* was significantly decreased by almost 50% after treatment with 20 μM harmonine (Fig 9B). Hydroxyurea reduced expression four-fold at a concentration of 20 mM (Fig 9C).

Taken together, harmonine reduced the number of proliferating stem cells, both gonadal and parenchymal ones, in *S. mansoni*, which was proven by gonad-specific quantification of EdU-positive cells and a reduced expression of the stem cell markers *nanos-1* and *nanos-2*.

Discussion

The aim of the study was to assess the antischistosomal capacity and possible targets of harmonine, an antimicrobial compound from the harlequin ladybird *Harmonia axyridis* which

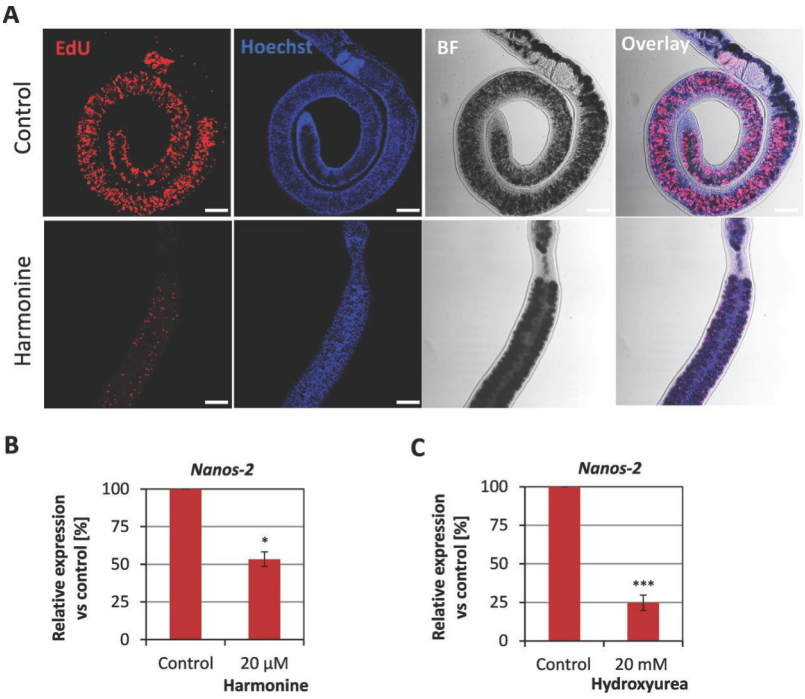

Fig 9. Reduction in the number of proliferating neoblasts upon harmonine treatment. *S. mansoni* couples were treated and processed for EdU labeling of proliferating cells as described in Fig 7. **(A)** Representative images of a control and a harmonine-treated female showing proliferating cells (neoblasts) in the parenchyma and/or vitellarium. Scale bar: 100 μm. BF, bright field. **(B, C)** Expression of the stem cell marker *nanos-2* (Smp_051920) in harmonine-treated (B) or hydroxyurea-treated (C) females related to the expression in untreated control females (set to 100%) as determined by qPCR (summary of two experiments). An unpaired t-test was performed to reveal significant differences (* $p<0.05$, *** $p<0.001$).

https://doi.org/10.1371/journal.pntd.0007240.g009

attracted increasing interest due to its antimicrobial activities [7]. Our results demonstrate a wide spectrum of effects by harmonine on *S. mansoni* adults, including (1) reduction of motility to parasite death, (2) tegumental damage in the form of blistering, (3) reduction of egg production and increased production of abnormally shaped eggs, (4) disorganization of gonadal tissue structures, and (5) a reduction of cell division activities of neoblasts and gonadal stem cells, which was paralleled by reduced transcript levels of stem-cell marker genes.

Pleiotropic effects of harmonine

Antischistosomal compounds, whether synthetic or natural, often induce alterations in vitality and motility of the adult worms, or in their reproductive fitness (disruption of mating, diminished egg production), in the integrity of the protective tegument, or in the functionality of the parasite nervous system. Remarkably, we found that harmonine affected not just one or few, but all of these parameters simultaneously.

Our *in vitro* studies showed that harmonine reduced the motility of adult worms in a dose-dependent manner, with an EC50 of 8.8 μM and lethality at 10–20 μM within 3 days of culture. These effective concentrations are desirably low, also compared to other natural compounds with described schistosomicial activity, many of which were found to be active in the range of 50–100 μM and even higher [2]. Motor activity alterations belong to the most important indicators of schistosomicidal activity. If the neuromuscular system is affected, mating may be disrupted because the female is released from the gynaecophoric canal of the male partner which eventually leads to degeneration of the female and a complete cessation of egg production [47]. In addition, intact muscle function is required for the suckers to allow the worm to attach to the host endothelial wall, and for functionality of the digestive, reproductive and excretory organs which are lined by musculature [48]. Indeed, harmonine-treated male and female worms separated from each other, were unable to attach with their suckers to the culture well, and stopped egg production at 10 μM. *In vivo*, reduced motor activities would very likely result in removal and degradation of worms by the host and, because egg production is affected, to reduced pathology and the interruption of transmission.

Harmonine also caused adverse effects on the tegument at concentrations as low as 5 μM, which plays crucial roles for nutrient uptake, secretion, osmoregulation, and immune evasion [49]. Damage of the tegument could facilitate the penetration of schistosomicide compounds but also of antibodies to deeper-lying tissues, which may culminate in greater damage to the parasite including disruption of the above-mentioned physiological processes and the ultimate elimination of worms [50, 51]. The tegument is an important target structure for drug discovery, and consequently, compounds affecting the tegument were found to make the parasites more sensitive to the host immune response *in vivo* [52]. Tegumental damage is also induced by PZQ, which may contribute to the compound's efficacy [17]. Previous work showed the induction of early necrosis in *Leishmania* parasites, which involved the loss of cell-membrane integrity [12]. Also in *S. mansoni*, induction of necrosis might contribute to the detrimental effects of harmonine.

AChE as possible target

Besides the tegument, the nervous system of helminths has been considered a promising target for drug discovery. Several components of the neuronal system are targets of currently approved anthelminthics, including monepantel, levamisole and pyrantel [35, 53, 54]. We found a reduction of schistosomal AChE activity and of AChE transcript levels by harmonine, which suggests two molecular mechanisms that contribute to the observed motility reduction and subsequent paralysis of the parasite's musculature. We conclude that the reduced

enzymatic activity in schistosome protein extracts is not exclusively a consequence of reduced gene transcription, because worms used to prepare extracts have not been treated with harmonine, instead harmonine was added directly to the enzyme assay. According to diverse studies in *S. mansoni*, *S. haematobium*, *S. japonicum*, and S. *bovis*, AChE fulfills two different functions: a classical role in the neuromuscular system for motor activity, and a non-classical role in the tegument related to glucose import from host blood [37, 55]. The tegumental damage observed in harmonine-treated worms might be correlated with the high tegumental expression of AChE [38, 56, 57], while the observed paralysis might be linked to the neuromuscular role. At cholinergic synapses, the neurotransmitter ACh binds to nicotinic ACh receptors (AChRs) and thereby mediates muscular contraction via membrane depolarization. AChE plays a central role in the termination of transmission by hydrolysis of ACh. Treatment of adult schistosomes with either ACh agonists or inhibition of AChE (resulting in higher levels of ACh) led to excessive stimulation, desensitization, and flaccid paralysis of worms [56, 58]. If harmonine inhibits AChE, this should likewise induce paralysis. Indeed, this was observed in our study. To clarify whether the antischistosomal effects of harmonine are mainly due to targeting of AChE, a gradual knock-down of AChE expression to a similar degree as found for the reduction of AChE activity by harmonine might be of interest for future work. While we found a generally high expression and enzymatic activity of AChE in males and unpaired females, both parameters were strongly decreased in paired females. This might reflect a reduced need in motor activity of the female after pairing and/or a different need for AChE-mediated glucose uptake. Up-and down-regulation of genes in females after pairing and separation, respectively, is a known phenomenon [59, 60]. We also found other genes involved in the function of the neuromuscular synapse being downregulated, such as genes annotated as nicotinic AChR (Smp_176310, Smp_139330, Smp_180570) and as choline acetyltransferase (Smp_146910), the enzyme involved in ACh synthesis [39]. Altogether, it seems likely this contributes to a reduced motor activity of females after pairing. Our findings of a sex- and pairing-dependent AChE expression and activity pattern adds novel aspects to the wealth of data on AChE function in schistosome biology, and might explain why females appeared less sensitive than males towards harmonine during the first 24 h of treatment.

The druggability of AChE was demonstrated by the use of the AChE inhibitor metrifonate against *S. haematobium* in the past [35]. However, metrifonate was withdrawn from the market because of the need for multiple doses, its toxicity to the host, and its unsatisfying efficacy against other schistosome species [61]. Nonetheless, AChE remains an interesting antischistosomal target for rational drug design. That species-specific optimization is achievable was for instance demonstrated by re-engineering inhibitors toward higher specificity for *Anopheles* AChE than human AChE [62]. Also for harmonine, rational drug design might be used to obtain even better efficacies.

Schistosome stem cells as targets

Our conclusion that there are further harmonine targets beyond AChE is based on three observations: (1) the merely weak AChE inhibitory capacity of harmonine, (2) the multifaceted phenotypes observed after treatment with harmonine, and (3) effects by the AChE inhibitor metrifonate that were different in strength involving a rapid paralysis within only 1–3 hours, which was reversible [63]. Additional targets might be related to stem-cell biology. Due to the fundamental role of stem cells in the parasite life cycle and parasite survival, it was recently proposed that many helminth infections may be considered as stem cell diseases [45, 64]. Compounds targeting stem cells are thus particularly attractive candidates for drug development. In order to not only assess but objectively quantify stem cell effects, we established a 3D

reconstruction approach of schistosome ovaries and testes to quantify proliferating stem cells. Harmonine significantly reduced the number of proliferating stem cells in gonadal tissues and the parenchyma where they are known as neoblasts [44]. Furthermore, we used for the first time quantification of *nanos* gene expression as a measure for compound-induced effects. *Nanos-1* was characterized as a germline-specific stem cell marker in adult *S. mansoni* [42, 65] and is known as a conserved regulator of germ cell development [43]. Somatic stem cells, so-called neoblasts, were only recently identified in adult schistosomes and are characterized by expression of *nanos-1* and *nanos-2* [44]. *Nanos-2* is a post-transcriptional regulator responsible for the formation, development, and maintenance of pluripotent cells in many metazoans [66]. Knock-down of *nanos-1* and *nanos-2* in *S. mansoni* resulted in loss of mature germ cells and in degenerated testes, and it was concluded that *nanos-1* and *nanos-2* are required for germ-cell differentiation [42]. Since the levels of *nanos* expression were reduced upon harmonine treatment, one could speculate about a reduction of total stem cell numbers by induction of cell death. However, it is not clear whether *nanos* expression might also be affected in alive but cell cycle-arrested stem cells. Therefore, it remains open whether harmonine induces cell-cycle arrest or cell death in gonadal and somatic stem cells. In the case of cell-cycle arrest, removal of harmonine before EdU addition to the culture would lead to a resumption of cell proliferation and may clarify this question.

AChE as the target of harmonine in schistosomal stem cells is another attractive hypothesis. Indeed, according to previous RNAseq analyses, transcripts of a variety of ACh receptors were found in ovaries and testes of *S. mansoni* [39], suggesting a non-neuronal role of the AChE-ACh-AChR axis in gonads. In addition, AChE is known to be expressed in certain stem cells where it regulates cell proliferation. For instance, embryonic stem cells of human and mouse express AChE and showed reduced proliferation upon ACh stimulation [67, 68], just like an ACh over-abundance by inhibition of AChE activity might do. Furthermore, inhibition of AChE by organophosphates in mesenchymal stem cells or by donezepil in neural stem cells led to suppression of proliferation, differentiation and self-renewal ability [41, 69]. Therefore, future studies should address the possible role of ACh signaling in schistosomal stem cells in detail, and we propose RT-qPCR analysis of sorted stem cells as a start. This might reveal new insights into AChE function in schistosomes and aid in developing novel therapies.

As a side note, it appears biologically astonishing how *H. axyridis* is able to resist the toxic potential of harmonine which accumulates in the hemolymph up to 7 μg per mg body mass [5]. This resistance is even more remarkable seeing the potential of harmonine to inhibit such crucial processes like stem cell proliferation, and will fuel the curiosity in future research.

Insects as source for antischistosomal compounds

Alkaloids are natural compounds that are widespread in plants, bacteria, fungi, and animals. *In vitro* schistosomicidal activity was demonstrated for several plant-derived alkaloids, such as piplartine from *Piper* species [2, 3]. Harmonine is the first animal-derived alkaloid found to have antischistosomal capacity. Notably, the chemical structure of the alkaloid harmonine, an aliphatic long-chain diamine, is quite different to these other active alkaloids.

To date, only very few other studies addressed animal-derived compounds and their anti-schistosomal activities. These are compounds from sea cucumbers, skin secretions of a South-American tree-frog species, and undefined compounds from snake venom [3, 70–72]. From insects, so far only two complex product mixtures, but no defined compounds, were described to have direct or indirect anthelminthic effects. Propolis ("bee glue") is a complex resinous bee hive product and was shown to have various anti-protozoal [73], fungicidal, and antimicrobial properties [74]. Furthermore, *in vivo* treatment of *S. mansoni*-infected mice with propolis

produced by *Apis mellifera* reduced the worm burden but increased granuloma diameter [4], which pointed to an immune-modulatory effect rather than a direct effect on worm vitality. Unfortunately, there are no data in the literature on *in vitro*-culture experiments that demonstrate any direct effects of propolis or propolis-derived compounds on schistosomes. The second anthelmintic insect-derived product described in literature is bee venom. Bee venom is a complex mixture of enzymes, biogenic amines and peptides with described anti-inflammatory capacity and has been studied as an alternative medicine for inflammatory diseases and cancer [75, 76]. As with propolis, a reduction of worm burden was found upon treatment of *S. mansoni*-infected mice [4], but unfortunately without analysis of direct effects, mode of action or possible schistosomal targets. Thus harmonine and its effects on AChE activity and stem cell gene expression provides the very first insight into possible mechanisms of action of an insect-derived compound.

Outlook

In view of the broad *in vitro* activity of harmonine found against microbes [7, 10], protozoans [7, 12] and helminths (this study), it is tempting to promote this insect-derived compound as a novel universal weapon, a kind of swiss-army knife against multiple pathogens. However, we found first evidence of cytotoxicity against HepG2 cells at concentrations of 50 μM and higher, indicating that harmonine in its current form is not yet an ideal lead candidate, but certainly a valuable basis for structure/activity-based compound development. The EC50 of 8.8 μM obtained for the reduction of schistosome motility by harmonine is already a promising start, as this concentration did not lead to any cytotoxic effects against HepG2 cells. In summary, this study provided clear evidence for the antischistosomal activity of the lady beetle-derived compound harmonine together with biologically highly interesting effects on AChE activity, inhibition of stem-cell proliferation and gene expression. This is the first time to proof a direct effect of a defined insect-derived compound on schistosomes, and harmonine may serve as basis for the development of new antischistosomal, or even broader antiparasitic compounds. This study highlights the potential of exploiting insects for the discovery of anthelminthics and motivates the screening of insect compound libraries for novel anthelminthic compounds in the future.

Supporting information

S1 Fig. Carboxyl-esterase domains in AChE orthologs of *S. mansoni*. PFAM domains were revealed by the online-tool SMART (http://smart.embl-heidelberg.de/).
(TIF)

S2 Fig. Characterization of AChE activity. (A-D) Inhibition of enzymatic activity by the AChE inhibitor physostigmine. Enzymatic activity over time of AChE from electric eel (A) or of protein lysates of paired *S. mansoni* males (B) after adding different concentrations of physostigmine (0 – 2500 nM). One representative out of two similar experiments is shown. Relative AChE activity of electric eel (C) and schistosome lysate (D) at 30 min after adding different concentrations of physostigmine, with the activity at 0 μM set as 100%. Mean values of two experiments were used. IC50 was calculated by non-linear least squares curve fitting using the ic50.tk tool. **(E)** Michaelis-Menten plot of the harmonine effect on AChE activity. AChE from the model organism *E. electricus* was co-incubated with 10 μM or 50 μM harmonine and increasing concentrations of the substrate (S) acetylthiocholine (up to 2.2 mM). In the control, the solvent DMSO without harmonine was added. The reaction velocity (v) describes substrate conversion in μmol/min using AChE at a constant concentration of 0.12

nM. Data points are based on technical replicates, error bars are SEM values. Assay buffer: 38 mM Tris-HCl, pH 8.0, 100 mM NaCl, 20 mM MgCl2, 330 mM 5,5′-Dithiobis(2-nitrobenzoic acid) [DTNB]. Reactions were performed in 96-well plates (206 μl/well) and absorption changes at 410 nm were recorded for 3 min; the initial slopes of absorption over time plots were used to calculate reaction velocities according to the Beer-Lambert law.
(TIF)

S3 Fig. Effect of harmonine on proliferation of gonadal stem cells (conventional CLSM without IMARIS processing). Worms were treated with 5 μM (C, D) or 10 μM (E, F) harmonine or with an equivalent amount of solvent as negative control (A, B) for 72 h, with EdU added for the last 24 h. EdU-positive proliferating stem cells in female ovaries (A, C, E) or male testes (B, D, F). Stem cells are mainly found in the immature (iO) part of the ovary, not in the mature (mO) part. One z-plane of one representative female or male per condition from two experiments is shown. Scale bar: 35 μm.
(TIF)

S1 Movie. 3D animation of a female ovary stained for EdU-positive proliferating stem cells and Hoechst-positive cells. Still images are shown in Fig 7.
(MPG)

Acknowledgments

The authors thank Christina Scheld, Bianca Kulik, and Georgette Stovall for excellent technical assistance, as well as Thomas Quack for technical help and discussions.

Author Contributions

Conceptualization: Christoph G. Grevelding, Simone Haeberlein.

Funding acquisition: Christoph G. Grevelding, Simone Haeberlein.

Investigation: Josina Kellershohn, Laura Thomas, Steffen R. Hahnel, Arnold Grünweller, Simone Haeberlein.

Methodology: Josina Kellershohn, Laura Thomas, Steffen R. Hahnel, Arnold Grünweller, Roland K. Hartmann, Martin Hardt, Simone Haeberlein.

Resources: Martin Hardt, Andreas Vilcinskas.

Software: Martin Hardt.

Supervision: Simone Haeberlein.

Visualization: Josina Kellershohn, Simone Haeberlein.

Writing – original draft: Simone Haeberlein.

Writing – review & editing: Josina Kellershohn, Laura Thomas, Arnold Grünweller, Roland K. Hartmann, Martin Hardt, Andreas Vilcinskas, Christoph G. Grevelding, Simone Haeberlein.

References

1. Newman DJ, Cragg GM. Natural products as sources of new drugs over the 30 years from 1981 to 2010. Journal of natural products. 2012; 75(3):311–35. https://doi.org/10.1021/np200906s PMID: 22316239

2. Neves BJ, Andrade CH, Cravo PV. Natural products as leads in schistosome drug discovery. Molecules (Basel, Switzerland). 2015; 20(2):1872–903.
3. de Moraes J, Nascimento C, Miura LM, Leite JR, Nakano E, Kawano T. Evaluation of the *in vitro* activity of dermaseptin 01, a cationic antimicrobial peptide, against *Schistosoma mansoni*. Chemistry & biodiversity. 2011; 8(3):548–58.
4. Mohamed AH, Hassab El-Nabi SE, Bayomi AE, Abdelaal AA. Effect of bee venom or proplis on molecular and parasitological aspects of *Schistosoma mansoni* infected mice. Journal of parasitic diseases: official organ of the Indian Society for Parasitology. 2016; 40(2):390–400.
5. Schmidtberg H, Rohrich C, Vogel H, Vilcinskas A. A switch from constitutive chemical defence to inducible innate immune responses in the invasive ladybird *Harmonia axyridis*. Biology letters. 2013; 9 (3):20130006. https://doi.org/10.1098/rsbl.2013.0006 PMID: 23466480
6. Vilcinskas A, Schmidtberg H, Estoup A, Tayeh A, Facon B, Vogel H. Evolutionary ecology of microsporidia associated with the invasive ladybird *Harmonia axyridis*. Insect science. 2015; 22(3):313–24. https://doi.org/10.1111/1744-7917.12159 PMID: 25131382
7. Röhrich CR, Ngwa CJ, Wiesner J, Schmidtberg H, Degenkolb T, Kollewe C, et al. Harmonine, a defence compound from the harlequin ladybird, inhibits mycobacterial growth and demonstrates multi-stage antimalarial activity. Biology letters. 2012; 8(2):308–11. https://doi.org/10.1098/rsbl.2011.0760 PMID: 21937493
8. Gegner T, Schmidtberg H, Vogel H, Vilcinskas A. Population-specific expression of antimicrobial peptides conferring pathogen resistance in the invasive ladybird *Harmonia axyridis*. Scientific reports. 2018; 8(1):3600. https://doi.org/10.1038/s41598-018-21781-4 PMID: 29483515
9. Keeling PJ, Fast NM. Microsporidia: biology and evolution of highly reduced intracellular parasites. Annual review of microbiology. 2002; 56:93–116. https://doi.org/10.1146/annurev.micro.56.012302.160854 PMID: 12142484
10. Vilcinskas A, Stoecker K, Schmidtberg H, Rohrich CR, Vogel H. Invasive harlequin ladybird carries biological weapons against native competitors. Science (New York, NY). 2013; 340(6134):862–3.
11. Verheggen FJ, Vogel H, Vilcinskas A. Behavioral and immunological features promoting the invasive performance of the harlequin ladybird *Harmonia axyridis*. Frontiers in Ecology and Evolution. 2017; 5 (156).
12. Nagel NC, Masic A, Schurigt U, Boland W. Efficient synthesis of (R)-harmonine—the toxic principle of the multicolored Asian lady beetle (*Harmonia axyridis*). Organic & biomolecular chemistry. 2015; 13 (18):5139–46.
13. Kenyon F, Hutchings F, Morgan-Davies C, van Dijk J, Bartley DJ. Worm control in livestock: bringing science to the field. Trends in parasitology. 2017; 33(9):669–77. https://doi.org/10.1016/j.pt.2017.05.008 PMID: 28647171
14. Weng HB, Chen HX, Wang MW. Innovation in neglected tropical disease drug discovery and development. Infectious diseases of poverty. 2018; 7(1):67. https://doi.org/10.1186/s40249-018-0444-1 PMID: 29950174
15. Hotez PJ, Alvarado M, Basanez MG, Bolliger I, Bourne R, Boussinesq M, et al. The global burden of disease study 2010: interpretation and implications for the neglected tropical diseases. PLoS neglected tropical diseases. 2014; 8(7):e2865. https://doi.org/10.1371/journal.pntd.0002865 PMID: 25058013
16. Cheever AW, Macedonia JG, Mosimann JE, Cheever EA. Kinetics of egg production and egg excretion by *Schistosoma mansoni* and *S. japonicum* in mice infected with a single pair of worms. The American journal of tropical medicine and hygiene. 1994; 50(3):281–95. PMID: 8147487
17. Doenhoff MJ, Cioli D, Utzinger J. Praziquantel: mechanisms of action, resistance and new derivatives for schistosomiasis. Current opinion in infectious diseases. 2008; 21(6):659–67. https://doi.org/10.1097/QCO.0b013e328318978f PMID: 18978535
18. Botros SS, Bennett JL. Praziquantel resistance. Expert opinion on drug discovery. 2007; 2(s1):S35–40. https://doi.org/10.1517/17460441.2.S1.S35 PMID: 23489031
19. Fallon PG, Doenhoff MJ. Drug-resistant schistosomiasis: resistance to praziquantel and oxamniquine induced in *Schistosoma mansoni* in mice is drug specific. The American journal of tropical medicine and hygiene. 1994; 51(1):83–8. PMID: 8059919
20. Mwangi IN, Sanchez MC, Mkoji GM, Agola LE, Runo SM, Cupit PM, et al. Praziquantel sensitivity of Kenyan *Schistosoma mansoni* isolates and the generation of a laboratory strain with reduced susceptibility to the drug. International journal for parasitology Drugs and drug resistance. 2014; 4(3):296–300. https://doi.org/10.1016/j.ijpddr.2014.09.006 PMID: 25516840
21. Cioli D, Pica-Mattoccia L, Basso A, Guidi A. Schistosomiasis control: praziquantel forever? Molecular and biochemical parasitology. 2014; 195(1):23–9. https://doi.org/10.1016/j.molbiopara.2014.06.002 PMID: 24955523

22. Gönnert R. Schistosomiasis-Studien. II. Über die Eibildung bei *Schistosoma mansoni* und das Schicksal der Eier im Wirtsorganismus. Zeitschrift fur Tropenmedizin und Parasitologie. 1955; 6(1):33–52. PMID: 14387065

23. Grevelding CG. The female-specific W1 sequence of the Puerto Rican strain of *Schistosoma mansoni* occurs in both genders of a Liberian strain. Molecular and biochemical parasitology. 1995; 71(2):269–72. PMID: 7477111

24. Dettman CD, Higgins-Opitz SB, Saikoolal A. Enhanced efficacy of the paddling method for schistosome infection of rodents by a four-step pre-soaking procedure. Parasitology research. 1989; 76(2):183–4. PMID: 2515540

25. Ramirez B, Bickle Q, Yousif F, Fakorede F, Mouries MA, Nwaka S. Schistosomes: challenges in compound screening. Expert opinion on drug discovery. 2007; 2(s1):S53–61. https://doi.org/10.1517/17460441.2.S1.S53 PMID: 23489033

26. Ponchel F, Toomes C, Bransfield K, Leong FT, Douglas SH, Field SL, et al. Real-time PCR based on SYBR-Green I fluorescence: an alternative to the TaqMan assay for a relative quantification of gene rearrangements, gene amplifications and micro gene deletions. BMC biotechnology. 2003; 3:18. https://doi.org/10.1186/1472-6750-3-18 PMID: 14552656

27. Livak KJ, Schmittgen TD. Analysis of relative gene expression data using real-time quantitative PCR and the 2(-Delta Delta C(T)) Method. Methods (San Diego, Calif). 2001; 25(4):402–8.

28. Hahnel S, Lu Z, Wilson RA, Grevelding CG, Quack T. Whole-organ isolation approach as a basis for tissue-specific analyses in *Schistosoma mansoni*. PLoS neglected tropical diseases. 2013; 7(7):e2336. https://doi.org/10.1371/journal.pntd.0002336 PMID: 23936567

29. Ellman GL, Courtney KD, Andres V Jr., Feather-Stone RM. A new and rapid colorimetric determination of acetylcholinesterase activity. Biochemical pharmacology. 1961; 7:88–95. PMID: 13726518

30. Neves RH, de Lamare Biolchini C, Machado-Silva JR, Carvalho JJ, Branquinho TB, Lenzi HL, et al. A new description of the reproductive system of *Schistosoma mansoni* (Trematoda: Schistosomatidae) analyzed by confocal laser scanning microscopy. Parasitology research. 2005; 95(1):43–9. https://doi.org/10.1007/s00436-004-1241-2 PMID: 15565465

31. Beckmann S, Grevelding CG. Imatinib has a fatal impact on morphology, pairing stability and survival of adult *Schistosoma mansoni in vitro*. International journal for parasitology. 2010; 40(5):521–6. https://doi.org/10.1016/j.ijpara.2010.01.007 PMID: 20149792

32. Hahnel S, Quack T, Parker-Manuel SJ, Lu Z, Vanderstraete M, Morel M, et al. Gonad RNA-specific qRT-PCR analyses identify genes with potential functions in schistosome reproduction such as SmFz1 and SmFGFRs. Frontiers in genetics. 2014; 5:170. https://doi.org/10.3389/fgene.2014.00170 PMID: 24959172

33. Schmidt U. Harmonia axyridis (Pallas, 177). 2008. p. Online Image. Retrieved from https://www.flickr.com/photos/coleoptera-us/2918252388/.

34. Nagel NC. Synthesis and bioactivity studies of harmonine–the defense alkaloid of the Asian lady beetle Harmonia axyridis (doctoral dissertation), retrieved from https://www.db-thueringen.de/servlets/MCRFileNodeServlet/dbt_derivate_00035920/NagelDis.pdf. Jena: University Jena; 2015.

35. Bueding E, Liu CL, Rogers SH. Inhibition by metrifonate and dichlorvos of cholinesterases in schistosomes. British journal of pharmacology. 1972; 46(3):480–7. PMID: 4656609

36. Arnon R, Silman I, Tarrab-Hazdai R. Acetylcholinesterase of *Schistosoma mansoni*—functional correlates. Contributed in honor of Professor Hans Neurath's 90th birthday. Protein science: a publication of the Protein Society. 1999; 8(12):2553–61.

37. You H, Liu C, Du X, McManus DP. Acetylcholinesterase and nicotinic acetylcholine receptors in schistosomes and other parasitic helminths. Molecules (Basel, Switzerland). 2017; 22(9).

38. Bentley GN, Jones AK, Agnew A. Expression and comparative functional characterisation of recombinant acetylcholinesterase from three species of *Schistosoma*. Molecular and biochemical parasitology. 2005; 141(1):119–23. https://doi.org/10.1016/j.molbiopara.2005.01.019 PMID: 15811534

39. Lu Z, Sessler F, Holroyd N, Hahnel S, Quack T, Berriman M, et al. Schistosome sex matters: a deep view into gonad-specific and pairing-dependent transcriptomes reveals a complex gender interplay. Scientific reports. 2016; 6:31150. https://doi.org/10.1038/srep31150 PMID: 27499125

40. Sopkova-de Oliveira Santos J, Lesnard A, Agondanou JH, Dupont N, Godard AM, Stiebing S, et al. Virtual screening discovery of new acetylcholinesterase inhibitors issued from CERMN chemical library. Journal of chemical information and modeling. 2010; 50(3):422–8. https://doi.org/10.1021/ci900491t PMID: 20196555

41. Prugh AM, Cole SD, Glaros T, Angelini DJ. Effects of organophosphates on the regulation of mesenchymal stem cell proliferation and differentiation. Chemico-biological interactions. 2017; 266:38–46. https://doi.org/10.1016/j.cbi.2017.01.020 PMID: 28174098

42. Wang B, Lee J, Li P, Saberi A, Yang H, Liu C, et al. Stem cell heterogeneity drives the parasitic life cycle of *Schistosoma mansoni*. eLife. 2018; 7.

43. Wang Y, Zayas RM, Guo T, Newmark PA. Nanos function is essential for development and regeneration of planarian germ cells. Proceedings of the National Academy of Sciences of the United States of America. 2007; 104(14):5901–6. https://doi.org/10.1073/pnas.0609708104 PMID: 17376870

44. Collins JJ 3rd, Wang B, Lambrus BG, Tharp ME, Iyer H, Newmark PA. Adult somatic stem cells in the human parasite *Schistosoma mansoni*. Nature. 2013; 494(7438):476–9. https://doi.org/10.1038/nature11924 PMID: 23426263

45. Koziol U, Rauschendorfer T, Zanon Rodriguez L, Krohne G, Brehm K. The unique stem cell system of the immortal larva of the human parasite *Echinococcus multilocularis*. EvoDevo. 2014; 5(1):10. https://doi.org/10.1186/2041-9139-5-10 PMID: 24602211

46. McCusker P, McVeigh P, Rathinasamy V, Toet H, McCammick E, O'Connor A, et al. Stimulating neoblast-like cell proliferation in juvenile *Fasciola hepatica* supports growth and progression towards the adult phenotype *in vitro*. PLoS neglected tropical diseases. 2016; 10(9):e0004994. https://doi.org/10.1371/journal.pntd.0004994 PMID: 27622752

47. Erasmus DA. A comparative study of the reproductive system of mature, immature and "unisexual" female *Schistosoma mansoni*. Parasitology. 1973; 67(2):165–83. PMID: 4795964

48. Mair GR, Maule AG, Day TA, Halton DW. A confocal microscopical study of the musculature of adult *Schistosoma mansoni*. Parasitology. 2000; 121 (Pt 2):163–70.

49. Van Hellemond JJ, Retra K, Brouwers JF, van Balkom BW, Yazdanbakhsh M, Shoemaker CB, et al. Functions of the tegument of schistosomes: clues from the proteome and lipidome. International journal for parasitology. 2006; 36(6):691–9. https://doi.org/10.1016/j.ijpara.2006.01.007 PMID: 16545817

50. Popiel I, Erasmus DA. *Schistosoma mansoni*: ultrastructure of adults from mice treated with oxamniquine. Experimental parasitology. 1984; 58(3):254–62. PMID: 6499999

51. Glauert AM, Butterworth AE, Sturrock RF, Houba V. The mechansim of antibody-dependent, eosinophil-mediated damage to schistosomula of *Schistosoma mansoni in vitro*: a study by phase-contrast and electron microscopy. Journal of cell science. 1978; 34:173–92. PMID: 748337

52. Xiao S, Shen B, Chollet J, Utzinger J, Tanner M. Tegumental changes in adult *Schistosoma mansoni* harbored in mice treated with artemether. The Journal of parasitology. 2000; 86(5):1125–32. https://doi.org/10.1645/0022-3395(2000)086[1125:TCIASM]2.0.CO;2 PMID: 11128492

53. Kaminsky R, Gauvry N, Schorderet Weber S, Skripsky T, Bouvier J, Wenger A, et al. Identification of the amino-acetonitrile derivative monepantel (AAD 1566) as a new anthelmintic drug development candidate. Parasitology research. 2008; 103(4):931–9. https://doi.org/10.1007/s00436-008-1080-7 PMID: 18594861

54. Robertson AP, Martin RJ. Ion-channels on parasite muscle: pharmacology and physiology. Invertebrate neuroscience: IN. 2007; 7(4):209–17. https://doi.org/10.1007/s10158-007-0059-x PMID: 17999098

55. Camacho M, Agnew A. *Schistosoma*: rate of glucose import is altered by acetylcholine interaction with tegumental acetylcholine receptors and acetylcholinesterase. Experimental parasitology. 1995; 81(4):584–91. https://doi.org/10.1006/expr.1995.1152 PMID: 8543000

56. Jones AK, Bentley GN, Oliveros Parra WG, Agnew A. Molecular characterization of an acetylcholinesterase implicated in the regulation of glucose scavenging by the parasite *Schistosoma*. FASEB journal: official publication of the Federation of American Societies for Experimental Biology. 2002; 16(3):441–3.

57. You H, Gobert GN, Du X, Pali G, Cai P, Jones MK, et al. Functional characterisation of *Schistosoma japonicum* acetylcholinesterase. Parasites & vectors. 2016; 9(1):328.

58. Barker LR BE, Timms AR. The possible role of acetylcholine in *Schistosoma mansoni*. Br J Pharmacol Chemother. 1966; 26(3):656–65. PMID: 4381202

59. Fitzpatrick JM, Hoffmann KF. Dioecious *Schistosoma mansoni* express divergent gene repertoires regulated by pairing. International journal for parasitology. 2006; 36(10–11):1081–9. https://doi.org/10.1016/j.ijpara.2006.06.007 PMID: 16875694

60. Waisberg M, Lobo FP, Cerqueira GC, Passos LK, Carvalho OS, Franco GR, et al. Microarray analysis of gene expression induced by sexual contact in *Schistosoma mansoni*. BMC genomics. 2007; 8:181. https://doi.org/10.1186/1471-2164-8-181 PMID: 17578584

61. Kramer CV, Zhang F, Sinclair D, Olliaro PL. Drugs for treating urinary schistosomiasis. The Cochrane database of systematic reviews. 2014(8):Cd000053. https://doi.org/10.1002/14651858.CD000053.pub3 PMID: 25099517

62. Hartsel JA, Wong DM, Mutunga JM, Ma M, Anderson TD, Wysinski A, et al. Re-engineering aryl methylcarbamates to confer high selectivity for inhibition of *Anopheles gambiae* versus human acetylcholinesterase. Bioorganic & medicinal chemistry letters. 2012; 22(14):4593–8.

63. Denham DA, Holdsworth RJ. The effect of metrifonate *in vitro* on *Schistosoma haematobium* and *S. mansoni* adults. Transactions of the Royal Society of Tropical Medicine and Hygiene. 1971; 65(5):696. PMID: 5159156

64. Wendt GR, Collins JJ, 3rd. Schistosomiasis as a disease of stem cells. Current opinion in genetics & development. 2016; 40:95–102.

65. Wang J, Collins JJ 3rd. Identification of new markers for the *Schistosoma mansoni* vitelline lineage. International journal for parasitology. 2016; 46(7):405–10. https://doi.org/10.1016/j.ijpara.2016.03.004 PMID: 27056273

66. Giri BR, Du X, Xia T, Chen Y, Li H, Cheng G. Molecular characterization and expression profile of nanos in *Schistosoma japonicum* and its influence on the expression several mammalian stem cell factors. Parasitology research. 2017; 116(7):1947–54. https://doi.org/10.1007/s00436-017-5476-0 PMID: 28555405

67. Landgraf D, Barth M, Layer PG, Sperling LE. Acetylcholine as a possible signaling molecule in embryonic stem cells: studies on survival, proliferation and death. Chemico-biological interactions. 2010; 187 (1–3):115–9. https://doi.org/10.1016/j.cbi.2010.03.007 PMID: 20223227

68. Paraoanu LE, Steinert G, Koehler A, Wessler I, Layer PG. Expression and possible functions of the cholinergic system in a murine embryonic stem cell line. Life sciences. 2007; 80(24–25):2375–9. https://doi.org/10.1016/j.lfs.2007.03.008 PMID: 17459421

69. Imamura O, Arai M, Dateki M, Takishima K. Donepezil promotes differentiation of neural stem cells into mature oligodendrocytes at the expense of astrogenesis. Journal of neurochemistry. 2017; 140(2):231–44. https://doi.org/10.1111/jnc.13856 PMID: 27664791

70. Melek FR, Tadros MM, Yousif F, Selim MA, Hassan MH. Screening of marine extracts for schistosomicidal activity *in vitro*. Isolation of the triterpene glycosides echinosides A and B with potential activity from the sea cucumbers *Actinopyga echinites* and *Holothuria polii*. Pharmaceutical biology. 2012; 50 (4):490–6. https://doi.org/10.3109/13880209.2011.615842 PMID: 22136393

71. Mona MH, Omran NE, Mansoor MA, El-Fakharany ZM. Antischistosomal effect of holothurin extracted from some Egyptian sea cucumbers. Pharmaceutical biology. 2012; 50(9):1144–50. https://doi.org/10.3109/13880209.2012.661741 PMID: 22486556

72. Hassan EA, Abdel-Rahman MA, Ibrahim MM, Soliman MF. *In vitro* antischistosomal activity of venom from the Egyptian snake *Cerastes cerastes*. Revista da Sociedade Brasileira de Medicina Tropical. 2016; 49(6):752–7. https://doi.org/10.1590/0037-8682-0241-2016 PMID: 28001223

73. Regueira-Neto MDS, Tintino SR, Rolon M, Coronal C, Vega MC, de Queiroz Balbino V, et al. Antitrypanosomal, antileishmanial and cytotoxic activities of Brazilian red propolis and plant resin of *Dalbergia ecastaphyllum* (L) Taub. Food and chemical toxicology: an international journal published for the British Industrial Biological Research Association. 2018; 119:215–21.

74. Hegazi AG, Abd El Hady FK, Abd Allah FA. Chemical composition and antimicrobial activity of European propolis. Zeitschrift fur Naturforschung C, Journal of biosciences. 2000; 55(1–2):70–5. PMID: 10739103

75. Lee WR, Pak SC, Park KK. The protective effect of bee venom on fibrosis causing inflammatory diseases. Toxins. 2015; 7(11):4758–72. https://doi.org/10.3390/toxins7114758 PMID: 26580653

76. Orsolic N. Bee venom in cancer therapy. Cancer metastasis reviews. 2012; 31(1–2):173–94. https://doi.org/10.1007/s10555-011-9339-3 PMID: 22109081

5.7 Anthelmintische Effekte des Venoms einer Raubwanze gegen *Schistosoma mansoni*

Anthelminthic activity of assassin bug venom against the blood fluke *Schistosoma mansoni*

Tonk M, Vilcinskas A, Grevelding, CG, **Haeberlein S**

Antibiotics (2020) 9(10):664

Eigener Anteil an der Entstehung der Publikation

- Leitung des Gesamtprojektes: 90%
- Durchführung/Auswertung der Experimente: 80%
- Anfertigung des Manuskripts: 90%

antibiotics

MDPI

Article

Anthelminthic Activity of Assassin Bug Venom against the Blood Fluke *Schistosoma mansoni*

Miray Tonk[1,2], Andreas Vilcinskas[1,2,3], Christoph G. Grevelding[4] and Simone Haeberlein[4,*]

[1] Institute for Insect Biotechnology, Justus Liebig University of Giessen, Heinrich-Buff-Ring 26-32, 35392 Giessen, Germany; miray.tonk@agrar.uni-giessen.de (M.T.); andreas.vilcinskas@agrar.uni-giessen.de (A.V.)
[2] LOEWE Centre for Translational Biodiversity Genomics (LOEWE-TBG), Senckenberganlage 25, 60325 Frankfurt, Germany; miray.tonk@agrar.uni-giessen.de (M.T.); andreas.vilcinskas@agrar.uni-giessen.de (A.V.)
[3] Fraunhofer Institute for Molecular Biology and Applied Ecology, Department of Bioresources, Winchester Strasse 2, 35394 Giessen, Germany; andreas.vilcinskas@agrar.uni-giessen.de
[4] Institute of Parasitology, BFS, Justus Liebig University of Giessen, Schubertstr. 81, 35392 Giessen, Germany; christoph.grevelding@vetmed.uni-giessen.de
* Correspondence: simone.haeberlein@vetmed.uni-giessen.de

Received: 31 July 2020; Accepted: 28 September 2020; Published: date

Abstract: Helminths such as the blood fluke *Schistosoma mansoni* represent a major global health challenge due to limited availability of drugs. Most anthelminthic drug candidates are derived from plants, whereas insect-derived compounds have received little attention. This includes venom from assassin bugs, which contains numerous bioactive compounds. Here, we investigated whether venom from the European predatory assassin bug *Rhynocoris iracundus* has antischistosomal activity. Venom concentrations of 10–50 µg/mL inhibited the motility and pairing of *S. mansoni* adult worms in vitro and their capacity to produce eggs. We used EdU-proliferation assays to measure the effect of venom against parasite stem cells, which are essential for survival and reproduction. We found that venom depleted proliferating stem cells in different tissues of the male parasite, including neoblasts in the parenchyma and gonadal stem cells. Certain insect venoms are known to lyse eukaryotic cells, thus limiting their therapeutic potential. We therefore carried out hemolytic activity assays using porcine red blood cells, revealing that the venom had no significant effect at a concentration of 43 µg/mL. The observed anthelminthic activity and absence of hemolytic side effects suggest that the components of *R. iracundus* venom should be investigated in more detail as potential antischistosomal leads.

Keywords: assassin bug; *Rhynocoris iracundus*; *Schistosoma mansoni*; venom; in vitro culture; natural compound; stem cells; cell proliferation

1. Introduction

Helminths (parasitic worms) infect more than 3.5 billion people worldwide, causing significant morbidity and economic losses [1, 2]. Novel anthelminthic compounds are urgently needed to achieve better control of this important group of parasites given the limited availability of effective vaccines and drugs [3-5]. Among helminths, blood flukes (schistosomes) such as *Schistosoma mansoni* cause schistosomiasis, a neglected tropical disease that globally affects more than 200 million people and causes 200,000 deaths each year [6, 7]. Male and female schistosomes mate in the blood vessels of their host and produce hundreds of eggs per day, which, if trapped in the liver, can trigger chronic diseases including liver fibrosis [6, 8]. The treatment of schistosomiasis currently relies on a limited drug repertoire, with praziquantel as the current gold standard [9]. The continual use of this drug

since its approval in the 1980s likely promotes emergence of resistant helminth populations, as evidenced by animal studies and human drug administration programs [10-12]. The discovery of alternative antischistosomal drugs is therefore a high priority in neglected tropical disease research [13].

Natural products represent a treasure trove for the discovery of new drugs, particularly novel anti-infectives. Plant-derived natural products have been extensively studied for their antischistosomal activity, whereas animal-derived compounds have received comparatively little attention [14], despite being the focus of drug discovery for various other therapeutic applications [15, 16]. Only a few studies have reported on the antischistosomal activity of bee, scorpion, frog and snake venoms [17-21]. Venoms are injected by animals into the body of their victims using stings, spines or bites [22-24]. These complex fluids include proteolytic enzymes, biogenic amines, neurotoxic peptides, neurotransmitters, and compounds that bind to and disrupt the function of multiple molecular targets in the victim [25]. Assassin bugs (Reduviidae) are a family of predaceous hemipteran insects comprising ~6800 species [26]. They are known for their potent venom, which is injected via a straw-like proboscis to paralyze and liquefy other invertebrates as prey. Assassin bugs can also use their venom defensively against (mainly vertebrate) predators [25, 27]. The composition and function of assassin bug venom is poorly understood, but more than 200 compounds have recently been identified in two reduviid species: *Platymeris biguttatus* L. and *Psytalla horrida* (both Hemiptera, Reduviidae) [28]. This is an important step toward the repurposing of venom toxins for biomedical applications. Here, we investigated the potential anthelminthic properties of venom from the European predatory assassin bug *Rhynocoris iracundus* against adult *S. mansoni*. We assessed the effects of the venom on parasite motility, reproduction, and cell proliferation in vitro for a cultivation period of 3 days.

2. Results

2.1. Assassin Bug Venom Reduces Motility, Pairing, Attachment and Egg Production in S. Mansoni

Venom was collected from *R. iracundus* by physical stimulation (Figure 1). The venom was tested for its anthelminthic activity against pairs of adult *S. mansoni* using an in vitro culture system over a period of 72 h. To assess the vitality of the worms, we determined their motility and the percentage of worms fit enough to (a) maintain the pairing state and (b) attach via their suckers to the base of the culture plate. As a positive control, worm couples were treated with different concentrations of praziquantel which caused death to all worms at 5 μM (Supplementary Figure S1). While pairs of worms in the control group remained motile and attached, those treated with 25 or 50 μg/mL of venom showed an overall loss of vitality (Figure 2, Videos S1–S4). Both males and females treated with the high dose of venom also became stunted (Figure 2C). At a venom concentration of 25 μg/mL, the motility of worms was significantly inhibited after 72 h, with male worms often being more affected (motility score 1) than females (scores 1 or 2). At the higher venom concentration (50 μg/mL), a significant loss of motility was observed already after 24 h (Figure 3A). Some (25 μg/mL) or all (50 μg/mL) worms were unable to attach to the base of the culture plate or maintain their pairing status (Figure 3B,C). Finally, a dose-dependent reduction in egg production was observed, while the shape of eggs appeared normal (Figure 3D–F). The lowest tested concentration of venom (10 μg/mL) had a slight impact on motility in some worms, but significantly reduced pairing stability and egg production (Figure 3 C,D). Taken together, these results confirmed that *R. iracundus* venom affects *S. mansoni* motility, pairing stability, attachment and fecundity, starting at concentrations as low as 10 μg/mL.

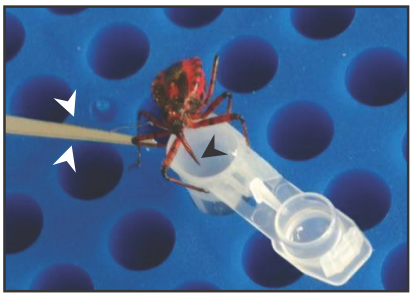

Figure 1. The European predatory assassin bug *Rhynocoris iracundus*. Stimulation of *R. iracundus* on the hind legs using entomological forceps (white arrow heads) encourages the insect to use its proboscis (black arrow head) to inject venom through laboratory film (Parafilm) stretched over a collection tube containing phosphate-buffered saline (PBS).

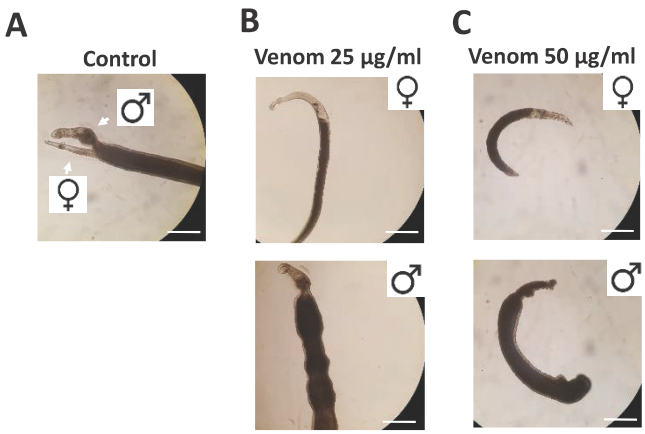

Figure 2. *Rhynocoris iracundus* venom affects the vitality of *Schistosoma mansoni*. Worm pairs were treated with different concentrations of venom (25 or 50 µg/mL). Representative images show worms after 72 h. **(A)** Untreated control worms remained paired and attached via their suckers to the base of the culture plate. The addition of venom at **(B)** 25 µg/mL or **(C)** 50 µg/mL induced the separation of pairs and detachment from the plate. Scale bars = 250 µm.

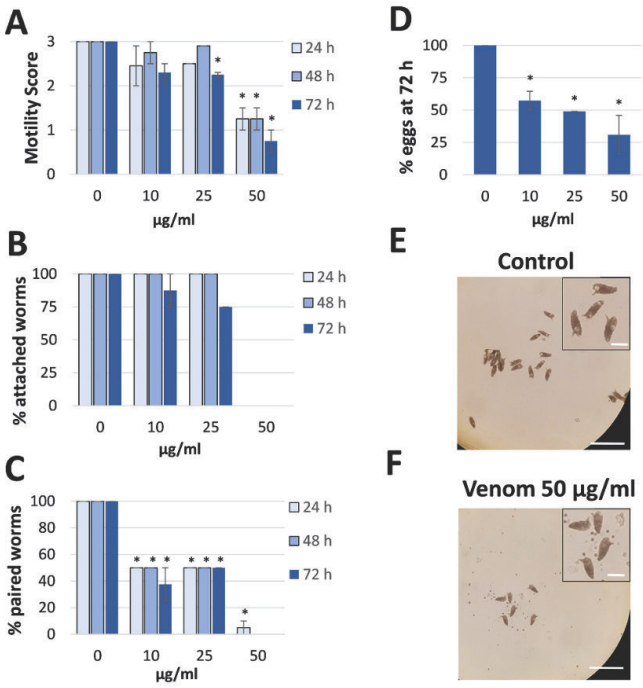

Figure 3. Effect of *Rhynocoris iracundus* venom on *Schistosoma mansoni* motility, pairing and egg production. Worm pairs were treated with different concentrations of venom (10–50 µg/mL) for a period of 72 h. We measured **(A)** motility, **(B)** the percentage of worms attached to the base of the plate, and **(C)** pairing stability every 24 h. **(D)** The number of eggs produced within 72 h relative to the untreated control. The shape of the eggs appeared normal after venom treatment (inserts). Graphs show a summary of two experiments with 5–8 worm pairs (mean ± SEM). Significant differences *vs* the control are indicated (*$p < 0.05$, Wilcoxon rank sum test). **(E, F)** Representative images showing the number of eggs produced by untreated control worms and venom-treated worms (50 µg/mL). Scale bars = 250 µm, for inserts = 60 µm.

2.2. Proliferating Stem Cells Are Depleted By Assassin Bug Venom

Antischistosomal effects may be associated with a decrease in the number of proliferating stem cells [29], which are considered essential for parasite development and survival [30]. We therefore investigated whether *R. iracundus* venom had a similar effect. Because stem cells are the only proliferating cells in adult schistosomes [31], we made use of the thymidine analog EdU (5-ethynyl-2-deoxyuridine) in order to visualize proliferating stem cells in whole-mount worms. EdU-positive stem cells were observed throughout the parenchyma of male and female worms (Figure 4A). These are known as neoblasts and have been shown to provide a constant stream of new cells for the development of the tegument, gastrodermis and potentially other tissues [31]. EdU-positive stem cells were also abundant in the gonads: spermatogonia in testes and oogonia in the ovary (Figure 4A), which give rise to germ cells. The analysis of venom-treated female worms by confocal laser scanning microscopy (CLSM) revealed no obvious change in the number of EdU-positive stem cells compared to untreated controls. However, the number of proliferating stem cells in males treated with 50 µg/mL venom fell to near zero in both the parenchyma and gonads (Figure 4B). To quantify this effect, we performed 3D image analysis to determine the numbers of EdU-positive stem cells and of Hoechst-positive total cells in the testes (Figure 5A-D) and the parenchyma (Figure 5E-H). This revealed a significant reduction in the frequency of stem cells and of the density of stem cells per defined tissue volume with 50 µg/mL venom. This was observed for both, spermatogonial stem cells (Figure 5C,D) and parenchymatic neoblasts (Figure 5G,H).

We used carmine red staining to gain a deeper insight into the cellular composition of the testicular lobes and to assess effects on cell differentiation. Control males typically featured pronounced testicular lobes filled with a large number of large spermatogonia, various stages of maturing cells, and mature spermatozoa (Figure 6A). In contrast, the testicular lobes were shrunken after venom treatment, included atypical cell-free areas, and lacked most of the large spermatogonial stem cells. The few remaining spermatogonia showed evidence of intracellular degradation (Figure 6B). Given the abundance of spermatozoa in the lobes and seminal vesicle (Figure 6B) and the reduction of stem cell frequency and density, these results argue for the selective depletion of proliferating stem cells by assassin bug venom.

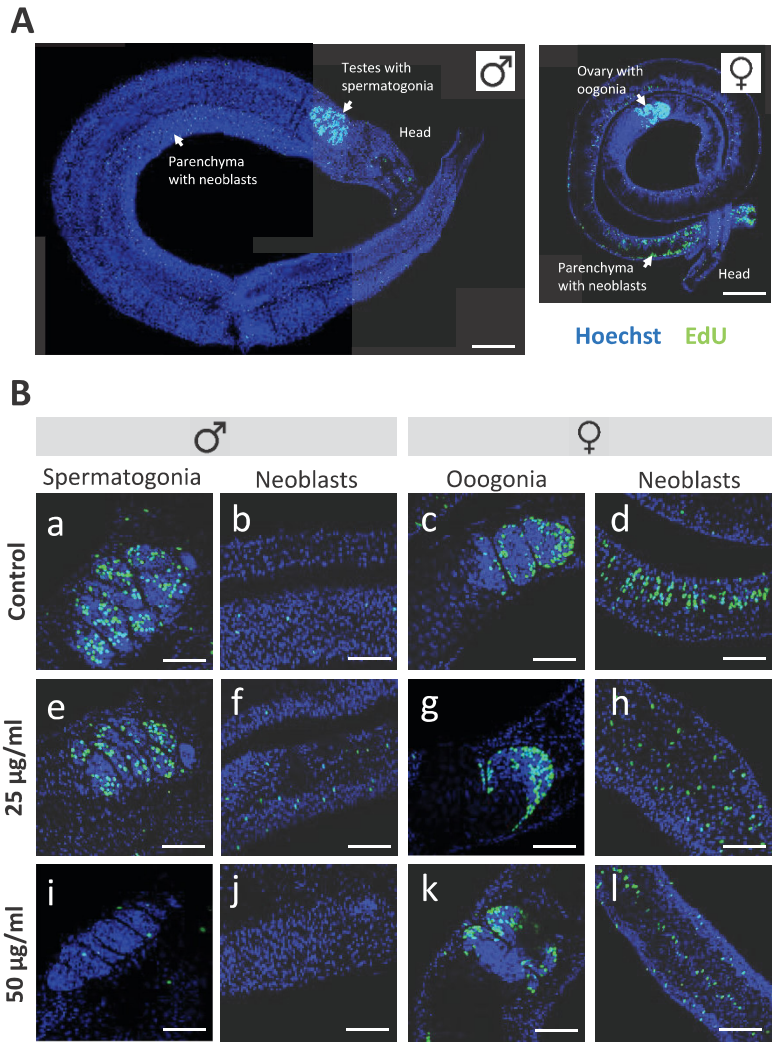

Figure 4. Effect of *Rhynocoris iracundus* venom on the proliferation of *Schistosoma mansoni* stem cells. **(A)** Overview of the location of parenchymal stem cells (neoblasts) and gonadal stem cells (spermatogonia and oogonia) in male and female worms. Stem cells are labeled with EdU (green), and nuclei are counterstained with Hoechst 33342 (blue). Scale bars = 100 µm. **(B)** Worm pairs were treated for 72 h with 25 or 50 µg/mL of venom or cultured without venom as a control. EdU was added during the final 24-h period. The abundance of EdU-positive proliferating stem cells was comparable in worms of the control group (a-d) and those treated with 25 µg/mL of venom (e-h) whereas 50 µg/mL of venom reduced the number of proliferating stem cells in males (i, j) but not in females (k, l). Scale bars = 50 µm. Representative images of four worms per treatment group are shown.

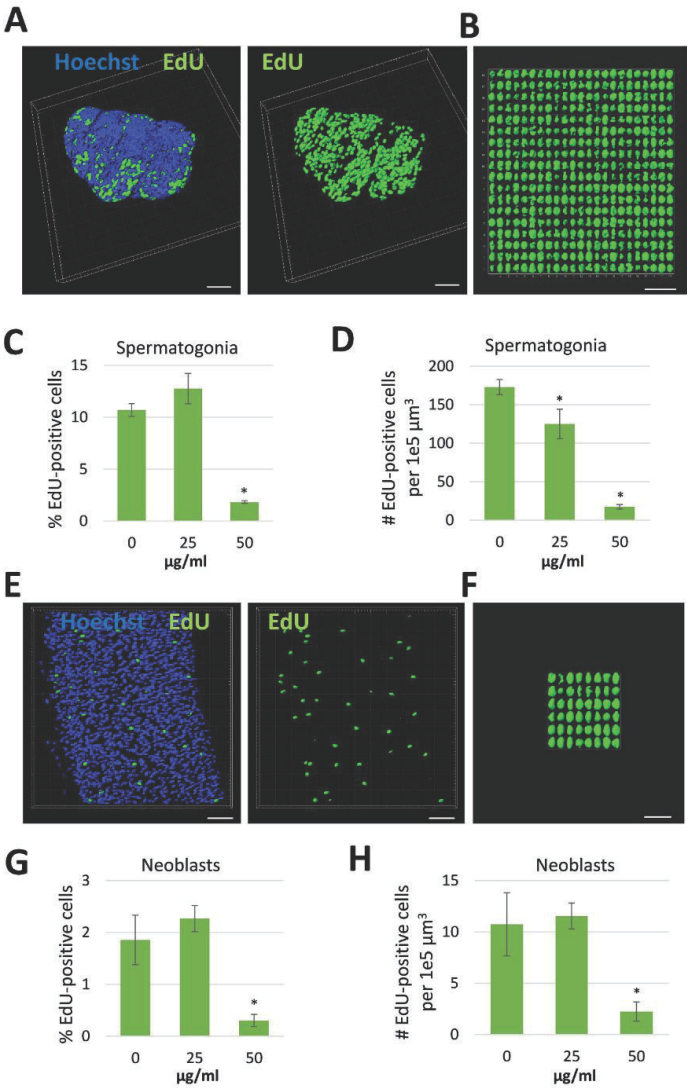

Figure 5. Reduction in stem cell frequency and density in male *Schistosoma mansoni* treated with *Rhynocoris iracundus* venom. Worm pairs were treated for 72 h with 25 or 50 µg/mL of venom or cultured without venom as a control. Proliferating stem cells were labeled with EdU and nuclei of all cells with Hoechst 33342. Cell numbers were quantified in z-stacks using the software package "IMARIS for cell biologists" (Bitplane). The percentage of EdU-positive cells related to the total cell number (C, G) and the number of EdU-positive cells per 1e5 µm³ tissue were calculated (D, H). **(A)** Representative images of testes from one worm which was digitally separated from the surrounding tissue using IMARIS**.** Nuclei are depicted in blue, stem cells in green. Scale bar = 40 µm. **(B)** All EdU-positive stem cells (spermatogonia) from the testes shown in (A) were aligned and quantified. Scale bar = 25 µm. The frequency **(C)** and density **(D)** of spermatogonial stem cells in testes were calculated. **(E)** Representative images of parenchyma from one worm after processing with IMARIS**.** Nuclei are depicted in blue, stem cells in green. Scale bar = 30 µm. **(F)** All EdU-positive stem cells (neoblasts) from the parenchymatic area shown in (E) were aligned and quantified. Scale bar = 15 µm. The frequency **(G)** and density **(H)** of neoblasts were calculated. Four worms per treatment group were analyzed. Statistical differences compared to the untreated group are indicated with * $p < 0.05$ (Wilcoxon rank sum test).

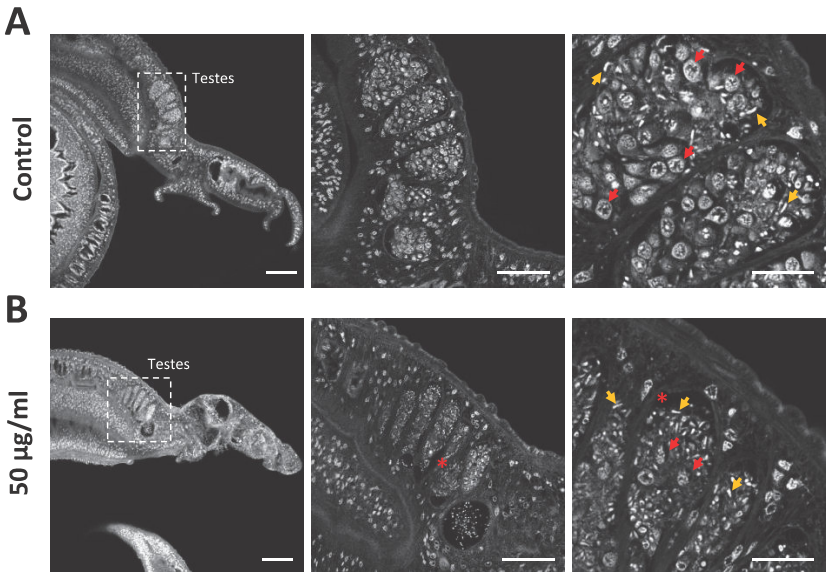

Figure 6. *Rhynocoris iracundus* venom reduces the number of spermatogonia in the testes of *Schistosoma mansoni*. Pairs of worms were treated with 50 µg/mL of venom for 72 h and males were stained with carmine red to reveal morphological details. **(A)** Control males feature typically pronounced testicular lobes filled with large spermatogonia (red arrows show examples) and different stages of maturing cells. Mature spermatozoa appear as small white comma-shaped cells (yellow arrows). **(B)** Testicular lobes in venom-treated males appear shrunken, include atypical cell-free areas (marked with *), and lack most of the spermatogonia, whereas mature spermatozoa are still present. The remaining spermatogonia show evidence of intracellular degradation. Scale bars = 100 µm (left), 50 µm (center), 20 µm (right).

2.3. Hemolytic analysis of assassin bug venom

Certain insect venoms are known for their ability to lyse eukaryotic cells, which limits their suitability as therapeutic leads [32, 33]. To assess the hemolytic activity of the crude venom, we carried out hemolytic assays using porcine red blood cells, with 10% Triton X-100 as a positive control (100% lysis). The crude venom at a concentration of 43 µg/mL caused only 6.3% hemolysis, which can be regarded as non-significant (Figure 7).

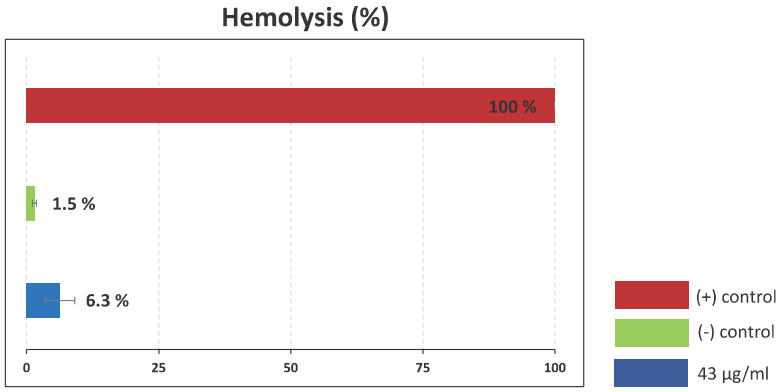

Figure 7. Hemolytic activity of *Rhynocoris iracundus* venom against porcine red blood cells. Relative proportion of cells lysed by *R. iracundus* venom (43 µg/mL) compared to 10% Triton X- 100 as a positive (+) control (100% lysis) and PBS as a negative (–) control.

3. Discussion

The aim of the study was to test whether venom from *R. iracundus* has anthelminthic activity and might therefore be of interest in drug discovery research. Our data reveal that venom reduced the vitality and egg production of *S. mansoni* adult worms, which was paralleled by the depletion of proliferating stem cells in male worms.

3.1. Antischistosomal Effects of Assassin Bug Venom

Reduced motor activity and detachment are important antischistosomal phenotypes. In vivo, both phenotypes would very likely result in the detachment of worms from the endothelial walls of mesenteric veins and thereby the displacement and degradation of the parasite by its host. Venom clearly reduced motility and caused detachment of worms during in vitro culture. Furthermore, diminished egg production was observed, which would reduce the pathological effect of helminths in vivo because fewer eggs accumulate in the liver [6]. It is unclear whether the impairment of egg production is a direct or indirect effect of the venom. A direct effect would require venom components to interfere with pathways involved in oogenesis, as an example. However, we would argue for a rather indirect effect: when separated from their male partners, female worms arrest egg production within a few days [34]. This seems more likely because exposure to 10 μg/mL of the venom triggered the separation of mating pairs and fewer eggs were laid, but the overall fitness of most females (in terms of motility and substrate attachment) was unaffected.

The antischistosomal effects of *R. iracundus* venom are difficult to compare with other insect-derived compounds due to the sparse literature published in this field. Bee venom and bee propolis (a complex beehive product) have previously been tested in vivo in mouse models of schistosomiasis. Both products reduced the pathogen burden [21], possibly reflecting their known immunomodulatory capacity within the host [35]. However, the potential direct effects of these compounds on worm vitality were not assessed in vitro, which leaves the question unanswered whether bee-derived compounds have a direct influence on the parasite. Recently, we demonstrated a direct schistosomicidal effect for the alkaloid harmonine [29], which is produced by the harlequin ladybird *Harmonia axyridis* (Coleoptera, Coccinellidae) as a bioweapon [36]. In *S. mansoni*, harmonine not only affected motility, pairing, substrate attachment and egg laying, but also caused damage to the tegument [29], which is the physiologically active surface layer of schistosomes [37]. *R. iracundus* venom triggered mild antischistosomal effects at 10 μg/mL and severe effects at 50 μg/mL, whereas harmonine was more active, triggering mild effects at 5 μg/mL and severe effects at 10 μg/mL. It has to be taken into account that harmonine is a defined compound, whereas assassin bug venom is a complex mixture of ~220 different enzymes, toxins and other compounds [38]. In future studies, it will be important to identify the active antischistosomal components of the crude venom, and such components are likely to be active against *S. mansoni* at a much lower concentration than the crude venom.

3.2. Antiproliferative Effect of Assassin Bug Venom

The importance of stem cells for growth and development has been demonstrated in various helminths, including *S. mansoni* [30, 39]. Compounds affecting stem cell proliferation and hence the viability of schistosomes are therefore attractive drug candidates. The venom of *R. iracundus* caused a strong depletion of proliferating stem cells in male but not in female worms. Together with the more severe reduction of motility, males appeared more sensitive to assassin bug venom compared to females. This may reflect the fact that paired females are mostly shielded from the environment, here the culture medium containing venom, by the male's body. However, we find this unlikely because one early effect of the venom is to cause pair separation, which would expose females to the venom after ~24 h. A more plausible explanation for these phenotypes is based on sex-dependent differences in the efficiency of uptake and/or mode of action of the venom. Interestingly, lady-beetle-derived harmonine also impaired stem cell proliferation, but it affected both sexes. Enzyme activity assays suggested this may involve the inhibition of a schistosome acetylcholine esterase [29]. It is

unclear whether the depletion of EdU-positive cells by harmonine reflects cell cycle arrest or cell death among the stem cell population. Our experiments with *R. iracundus* venom suggest that EdU-positive cell depletion is not based on an arrest in cell differentiation because differentiated spermatozoa were still present. Schistosome stem cells appear more sensitive towards venom than other cells, indicating that the mechanism of action targets proliferating rather than quiescent cells.

The available literature indicates a double-edged effect of animal-derived venom components on the proliferation of various cell types. Either cell proliferation was promoted, as reported for cobra, scorpion and lizard venom components tested against embryonic stem cells and mesenchymal stem cells [40, 41], or venom components inhibited proliferation, as demonstrated for bufalin (a steroid hormone) and bombesin (a peptide hormone) isolated from toad venom and tested against stem cells [42, 43]. Hormones may also be responsible for the anti-proliferative effect of *R. iracundus* venom. In addition, venom necrotoxins and cytotoxins might be involved, both of which typically kill cells [44]. Redulysins have been found in the venoms of other assassin bugs and were defined as putative pore-forming proteins with a cytolytic motif [45, 46]. Therefore, we assume that *R. iracundus* redulysins may play a role for the observed cytotoxic effects against schistosome stem cells, with support from other compounds.

3.3. Venom as Source for Antischistosomal Compounds

Results of the hemolytic assay indicated that the crude venom is not hemolytic, and from this perspective appears suitable for biotechnological applications and for the development of therapeutic leads. The absence of hemolytic activity is particularly important in the context of antischistosomal drugs, which must be bioavailable and efficacious in the blood where schistosomes live. Once active components in *R. iracundus* venom have been identified in future studies, cytotoxicity testing against different cell lines would be crucial. Together with the characterization of EC50 values against *S. mansoni*, this will allow for judging whether the selectivity is suitable to pursue venom components, e.g., to preclinical animal studies.

4. Materials and Methods

4.1. Ethical Statement

Syrian hamsters (*Mesocricetus auratus*) were used as model hosts in accordance with the European Convention for the Protection of Vertebrate Animals used for Experimental and Other Scientific Purposes (ETS No 123; revised Appendix A). The experiments were approved by the Regional Council (Regierungspraesidium) Giessen (V54-19 c 20/15 h 02 GI 18/10 Nr. A 14/2017).

4.2. Production of Adult Worms

Freshwater snails of the genus *Biomphalaria glabrata* were used as the intermediate host for a Liberian strain (Bayer AG, Monheim) of *S. mansoni* [47, 48]. Syrian hamsters from Janvier (France) were infected at 8 weeks of age by the paddling method [48]. In brief, hamsters were exposed to shallow water containing 1700-2000 cercariae for 45 min during which cercariae penetrated the host's skin. Adult worm couples were collected by hepatoportal perfusion of hamsters 46 days post-infection [49]. Worms were cultured in M199 medium (Sigma-Aldrich, Germany) supplemented with 10% newborn calf serum (Sigma), 1% 1 M HEPES and 1% ABAM solution (10,000 units/mL penicillin, 10 mg/mL streptomycin and 25 mg/mL amphotericin B) at 37 °C in a 5% CO_2 atmosphere.

4.3. Assassin Bug Collection and Rearing

The adult *R. iracundus* specimens were collected from North Rhine-Westphalia, Germany, with permission granted (Permission No. 425-104.1713) from the nature conservation authority (Obere Naturschutzbehörde) as part of the County Government of Rhineland-Palatinate. The insects used in

this study were reared on a diet of mealworm larvae (*Tenebrio molitor* L.) in a ventilated box under constant conditions (24 ± 1 °C, 55–75% relative humidity).

4.4. Venom Collection

In order to stimulate the production of venom used by *R. iracundus* for defense purposes, hind legs were gently pressed with entomological forceps to mimic a predatory attack (Figure 1). This induced the insects to display a defense posture and to penetrate laboratory film (Parafilm) stretched across the opening of a pre-cooled 200-µl Eppendorf tube containing 100 µl phosphate-buffered saline (PBS). Following this procedure, the tubes were centrifuged briefly. Four specimens of *R. iracundus* were used and venom was collected every 2–3 days. The protein content was determined using the Pierce bicinchoninic acid (BCA) assay kit (Thermo Fisher Scientific, Germany). Venom then was stored at –20 °C.

4.5. Evaluation of the Physiological Effects of Venom

The anthelminthic activity of *R. iracundus* venom against adult pairs of *S. mansoni* was assessed in vitro. The worms were cultured in 96-well plates in supplemented M199 medium (one worm pair per well) mixed with different concentrations of the venom (10, 25 or 50 µg/mL) or the same volume of PBS as a negative control. The worms were incubated at 37 °C in a 5% CO_2 atmosphere for 72 h, and the medium plus venom was refreshed every 24 h. Venom-induced effects on worm motility, pairing stability and attachment to the culture plate were assessed every 24 h using an inverted microscope (Labovert, Germany). Worm motility was scored as recommended by WHO-TDR [50], with the scores 3 (normal motility), 2 (reduced motility), 1 (minimal and sporadic movements) and 0 (no movement within 30 s was considered dead). Egg numbers per well were counted after the 72-h culture period.

4.6. Proliferation Assay and CLSM

To assess the potential effect of venom on cell proliferation, EdU was added to a final concentration of 10 µM for the last 24 h of the in vitro culture period. The worms were then fixed with 4% paraformaldehyde, stained with the Click-iT Plus EdU Alexa Fluor 488 imaging kit (Thermo Fisher Scientific) and counterstained with Hoechst 33342 as previously described [29, 51]. Morphological effects on testicular cells were assessed by fixing worms in AFA (66.5% ethanol, 1.1% paraformaldehyde, 2% glacial acetic acid) and staining with CertistainH carmine red (Merck, Germany) as previously described [52, 53]. A TSC SP5 inverse confocal laser scanning microscope (Leica, Germany) was used for imaging. AlexaFluor488 and carmine red were excited using an argon-ion laser at 488 nm, and Hoechst at 405 nm. Optical section thickness and background signals were defined by setting the pinhole size to 1 Airy unit in the Leica LAS AF software. Z-stacks were acquired by CLSM with a step-size of 0.3 µm for quantification of EdU-positive stem cells and Hoechst-positive total cell numbers. For each worm, testes and two selected parenchymatic tissue areas were manually selected using the software package "IMARIS for cell biologists" (Bitplane, Switzerland). Cells were quantified applying the automatic surface creation of the software. To minimize background noise or counting of artifacts, a threshold was set prior to cell quantification that excluded objects <3 µm.

4.7. Hemolytic Activity Assay

Porcine blood was obtained from a local butcher and was mechanically treated to remove coagulants. Red blood cells were harvested by centrifugation (1500 × g, 3 min, room temperature) and washed three times with PBS. A cell suspension was prepared with a dilution factor of 1:10 in PBS. Crude venom (final concentration 43 µg/mL) was mixed with the red blood cells (4.8×10^7 cells/mL) in a 96-well plate and incubated for 1 h at 37 °C. Venom-induced hemolysis was then measured in relation to 10% Triton X-100 as a positive control (set at 100%) and PBS as a negative control [54].

4.8. Statistical Analysis

Homogeneity of variance was checked with Levene's test (https://www.statskingdom.com/230var_levenes.htmL). Statistical significance was tested using the nonparametric Wilcoxon rank sum test (https://ccb-compute2.cs.uni-saarland.de/wtest/) [55]. $p < 0.05$ was considered statistically significant.

5. Conclusions

We have demonstrated antischistosomal effects of venom from the European predatory assassin bug *R. iracundus*. The effects included impairment of motility, pairing stability, attachment and egg production. Thus, assassin bug venom not only affects prey invertebrates but also helminths. Furthermore, the venom also caused the ablation of proliferating stem cells in male schistosomes. These phenotypes are reminiscent of the effects induced by paralytic and cytolytic assassin bug venoms used to subdue invertebrate prey [25, 27]. The observed anthelminthic effects, together with the absence of hemolytic activity, warrant further studies to identify the antischistosomal components of *R. iracundus* venom and assess their suitability for therapeutic applications in the field of parasitology. The transcriptomic and proteomic data recently obtained for this venom will greatly facilitate future research in this direction [38] and provide insight into a new and underexploited resource for the development of anthelminthic drugs.

Supplementary Materials: The following are available online at www.mdpi.com/xxx/s1
Figure S1: Effect of praziquantel on *Schistosoma mansoni* motility as a positive control for the in vitro culture assay. Worm pairs were treated with different concentrations of praziquantel (0.1–5 μM) for a period of 72 h. Motility was measured every 24 h and compared to DMSO-treated control worms. The graph shows a summary of two experiments with 10 worm pairs per experiment (mean ± SEM). Significant differences vs the control are indicated (*$p < 0.05$, Wilcoxon rank sum test), Video S1: *Schistosoma mansoni* pair in the control group. The male worm was attached via its suckers to the base of the culture plate and showed normal motility. The female resides within the ventral grove of the male partner. Normal motility involves whole body movements (displayed by the male in the video from 10 sec onwards), Video S2: *Schistosoma mansoni* pair after treatment with 25 μg/mL *Rhynocoris iracundus* venom for 72 h, showing reduced motility (motility score 2). The male worm was detached with its sucker from the base of the culture plate and did not show whole-body movements, Video S3: *Schistosoma mansoni* male treated with 50 μg/mL *Rhynocoris iracundus* venom for 72 h, showing severe loss of motility (little movement detected, confined to the posterior end, motility score 1), Video S4: *Schistosoma mansoni* female treated with 50 μg/mL *Rhynocoris iracundus* venom for 72 h, showing severe loss of motility (little movement detected, confined to the anterior and posterior ends, motility score 1).

Author Contributions: Conceptualization, M.T. and S.H.; Methodology, M.T. and S.H.; Investigation, S.H.; Resources, A.V. and C.G.G.; Writing – Original Draft Preparation, M.T. and S.H.; Writing – Review & Editing, M.T., S.H., A.V. and C.G.G.; Visualization, M.T. and S.H.; Supervision, S.H.; Funding Acquisition, M.T., S.H., A.V. and C.G.G.

Funding: SH and CGG would like to acknowledge funding by the LOEWE Centre for Novel Drug Targets against Poverty-Related and Neglected Tropical Infectious Diseases (DRUID), which is part of the excellence initiative of the Hessen State Ministry of Higher Education, Research and the Arts (HMWK). MT and AV would like to acknowledge generous funding by the HMWK via the LOEWE Centre for Translational Biodiversity Genomics (LOEWE-TBG) and the LOEWE Center for Insect Biotechnology and Bioresources.

Acknowledgments: The authors thank Zeinab Waad Zadiq for experimental support, and Christina Scheld, Bianca Kulik and Georgette Stovall for excellent technical assistance in the maintenance of the *S. mansoni* life cycle. We are grateful to Nicolai Rügen for insect collection and technical support for venom collection, Paul Bauer for maintaining *R. iracundus*, and Dr. Irina Häcker for providing the porcine blood. The authors thank Richard Twyman for editing the manuscript.

Conflicts of Interest: The authors declare no conflict of interest. The funders had no role in the design of the study; in the collection, analysis, or interpretation of data; in the writing of the manuscript, or in the decision to publish the results.

References

1. Hotez, P.J., Bundy, D.A.P., Beegle, K., Brooker, S., Drake, L., de Silva, N., Montresor, A., Engels, D., Jukes, M., Chitsulo, L., Chow, J., Laxminarayan, R., Michaud, C., Bethony, J., Correa-Oliveira, R., Shuhua, X., Fenwick, A., Savioli, L. Helminth infections: soil-transmitted helminth infections and schistosomiasis. In *Disease Control Priorities in Developing Countries*; Jamison, D.T., Breman, J.G., Measham, A.R., Alleyne, G., Claeson, M., Evans, D.B., Jha, P., Mills, A.,Musgrove, P., Eds.; Oxford University Press: Washington (DC), New York, USA, 2006.
2. GBD 2015, C. Global, regional, and national incidence, prevalence, and years lived with disability for 310 diseases and injuries, 1990-2015: a systematic analysis for the Global Burden of Disease Study 2015. *Lancet*, **2016**, *388*, 1545-1602.
3. Newman, D.J., Cragg, G.M. Natural products as sources of new drugs over the 30 years from 1981 to 2010. *J Nat Prod*, **2012**, *75*, 311-335.
4. Neves, B.J., Andrade, C.H., Cravo, P.V. Natural products as leads in schistosome drug discovery. *Molecules*, **2015**, *20*, 1872-1903.
5. Moser, W., Schindler, C., Keiser, J. Drug Combinations Against Soil-Transmitted Helminth Infections. *Adv Parasitol*, **2019**, *103*, 91-115.
6. Colley, D.G., Bustinduy, A.L., Secor, W.E., King, C.H. Human schistosomiasis. *Lancet*, **2014**, *383*, 2253-2264.
7. Hotez, P.J., Alvarado, M., Basanez, M.G., Bolliger, I., Bourne, R., Boussinesq, M., Brooker, S.J., Brown, A.S., Buckle, G., Budke, C.M., Carabin, H., Coffeng, L.E., Fevre, E.M., Furst, T., Halasa, Y.A., Jasrasaria, R., Johns, N.E., Keiser, J., King, C.H., Lozano, R., Murdoch, M.E., O'Hanlon, S., Pion, S.D., Pullan, R.L., Ramaiah, K.D., Roberts, T., Shepard, D.S., Smith, J.L., Stolk, W.A., Undurraga, E.A., Utzinger, J., Wang, M., Murray, C.J., Naghavi, M. The global burden of disease study 2010: interpretation and implications for the neglected tropical diseases. *PLoS Negl Trop Dis*, **2014**, *8*, e2865.
8. Cheever, A.W., Macedonia, J.G., Mosimann, J.E., Cheever, E.A. Kinetics of egg production and egg excretion by *Schistosoma mansoni* and *S. japonicum* in mice infected with a single pair of worms. *Am J Trop Med Hyg*, **1994**, *50*, 281-295.
9. Doenhoff, M.J., Cioli, D., Utzinger, J. Praziquantel: mechanisms of action, resistance and new derivatives for schistosomiasis. *Curr Opin Infect Dis*, **2008**, *21*, 659-667.
10. Fallon, P.G., Doenhoff, M.J. Drug-resistant schistosomiasis: resistance to praziquantel and oxamniquine induced in *Schistosoma mansoni* in mice is drug specific. *Am J Trop Med Hyg*, **1994**, *51*, 83-88.
11. Botros, S.S., Bennett, J.L. Praziquantel resistance. *Expert Opin Drug Discov*, **2007**, *2*, S35-40.
12. Mwangi, I.N., Sanchez, M.C., Mkoji, G.M., Agola, L.E., Runo, S.M., Cupit, P.M., Cunningham, C. Praziquantel sensitivity of Kenyan *Schistosoma mansoni* isolates and the generation of a laboratory strain with reduced susceptibility to the drug. *Int J Parasitol Drugs Drug Resist*, **2014**, *4*, 296-300.
13. Cioli, D., Pica-Mattoccia, L., Basso, A., Guidi, A. Schistosomiasis control: praziquantel forever? *Mol Biochem Parasitol*, **2014**, *195*, 23-29.
14. de Moraes, J. Natural products with antischistosomal activity. *Future Med Chem*, **2015**, *7*, 801-820.
15. Herzig, V., Cristofori-Armstrong, B., Israel, M.R., Nixon, S.A., Vetter, I., King, G.F. Animal toxins - Nature's evolutionary-refined toolkit for basic research and drug discovery. *Biochem Pharmacol*, **2020**, 114096.
16. Mohamed Abd El-Aziz, T., Garcia Soares, A., Stockand, J.D. Snake venoms in drug discovery: valuable therapeutic tools for life saving. *Toxins (Basel)*, **2019**, *11*, 564.

17. El-Asmar, M.F., Swelam, N., Abdel Aal, T.M., Ghoneim, K., Hodhod, S.S. Factor(s) in the venom of scorpions toxic to *Schistosoma mansoni* (intestinal belharzia) cercariae. *Toxicon*, **1980**, *18*, 711-715.
18. Stábeli, R.G., Amui, S.F., Sant'Ana, C.D., Pires, M.G., Nomizo, A., Monteiro, M.C., Romão, P.R., Guerra-Sá, R., Vieira, C.A., Giglio, J.R., Fontes, M.R., Soares, A.M. *Bothrops moojeni* myotoxin-II, a Lys49-phospholipase A2 homologue: an example of function versatility of snake venom proteins. *Comp Biochem Physiol C Toxicol Pharmacol*, **2006**, *142*, 371-381.
19. de Moraes, J., Nascimento, C., Miura, L.M., Leite, J.R., Nakano, E., Kawano, T. Evaluation of the *in vitro* activity of dermaseptin 01, a cationic antimicrobial peptide, against *Schistosoma mansoni*. *Chem Biodivers*, **2011**, *8*, 548-558.
20. Hassan, E.A., Abdel-Rahman, M.A., Ibrahim, M.M., Soliman, M.F. *In vitro* antischistosomal activity of venom from the Egyptian snake *Cerastes cerastes*. *Rev Soc Bras Med Trop*, **2016**, *49*, 752-757.
21. Mohamed, A.H., Hassab El-Nabi, S.E., Bayomi, A.E., Abdelaal, A.A. Effect of bee venom or proplis on molecular and parasitological aspects of *Schistosoma mansoni* infected mice. *J Parasit Dis*, **2016**, *40*, 390-400.
22. Bailey, P.C. The feeding behaviour of a sit-and wait-predator, *Ranatra dispar* (Heteroptera: Nepidae): optimal foraging and feeding dynamics. *Oecologia*, **1986**, *68*, 291-297.
23. Sano-Martins, I.S., González, C., Anjos, I.V., Díaz, J., Gonçalves, L.R.C. Effectiveness of *Lonomia* antivenom in recovery from the coagulopathy induced by *Lonomia orientoandensis* and *Lonomia casanarensis* caterpillars in rats. *PLoS Negl Trop Dis*, **2018**, *12*, e0006721.
24. Arif, F., Williams, M. Hymenoptera Stings (Bee, Vespids and Ants). StatPearls Publishing LLC: Treasure Island, FL, USA, 2020.
25. Walker, A.A., Weirauch, C., Fry, B.G., King, G.F. Venoms of heteropteran insects: a treasure trove of diverse pharmacological toolkits. *Toxins (Basel)*, **2016**, *8*, 43.
26. Hwang, W.S., Weirauch, C. Evolutionary history of assassin bugs (insecta: hemiptera: Reduviidae): insights from divergence dating and ancestral state reconstruction. *PLoS One*, **2012**, *7*, e45523.
27. Edwards, J.S. The action and composition of the saliva of an assassin bug *Platymeris rhadamanthus* Gaerst. (Hemiptera, Reduviidae). *Journal of Experimental Biology*, **1961**, *38*, 61-77.
28. Fischer, G., Conceicao, F.R., Leite, F.P., Dummer, L.A., Vargas, G.D., Hubner Sde, O., Dellagostin, O.A., Paulino, N., Paulino, A.S., Vidor, T. Immunomodulation produced by a green propolis extract on humoral and cellular responses of mice immunized with SuHV-1. *Vaccine*, **2007**, *25*, 1250-1256.
29. Kellershohn, J., Thomas, L., Hahnel, S.R., Grunweller, A., Hartmann, R.K., Hardt, M., Vilcinskas, A., Grevelding, C.G., Haeberlein, S. Insects in anthelminthics research: Lady beetle-derived harmonine affects survival, reproduction and stem cell proliferation of *Schistosoma mansoni*. *PLoS Negl Trop Dis*, **2019**, *13*, e0007240.
30. Wendt, G.R., Collins, J.J., 3rd. Schistosomiasis as a disease of stem cells. *Curr Opin Genet Dev*, **2016**, *40*, 95-102.
31. Collins, J.J., 3rd, Wang, B., Lambrus, B.G., Tharp, M.E., Iyer, H., Newmark, P.A. Adult somatic stem cells in the human parasite *Schistosoma mansoni*. *Nature*, **2013**, *494*, 476-479.
32. Monincová, L., Budesínský, M., Slaninová, J., Hovorka, O., Cvacka, J., Voburka, Z., Fucík, V., Borovicková, L., Bednárová, L., Straka, J., Cerovský, V. Novel antimicrobial peptides from the venom of the eusocial bee *Halictus sexcinctus* (Hymenoptera: Halictidae) and their analogs. *Amino Acids*, **2010**, *39*, 763-775.
33. Mortari, M.R., do Couto, L.L., dos Anjos, L.C., Mourão, C.B., Camargos, T.S., Vargas, J.A., Oliveira, F.N., Gati Cdel, C., Schwartz, C.A., Schwartz, E.F. Pharmacological characterization of *Synoeca cyanea*

venom: an aggressive social wasp widely distributed in the Neotropical region. *Toxicon*, **2012**, *59*, 163-170.

34. Erasmus, D.A. A comparative study of the reproductive system of mature, immature and "unisexual" female *Schistosoma mansoni*. *Parasitology*, **1973**, *67*, 165-183.
35. Cornara, L., Biagi, M., Xiao, J., Burlando, B. Therapeutic properties of bioactive compounds from different honeybee products. *Front Pharmacol*, **2017**, *8*, 412.
36. Vilcinskas, A., Stoecker, K., Schmidtberg, H., Rohrich, C.R., Vogel, H. Invasive harlequin ladybird carries biological weapons against native competitors. *Science*, **2013**, *340*, 862-863.
37. Van Hellemond, J.J., Retra, K., Brouwers, J.F., van Balkom, B.W., Yazdanbakhsh, M., Shoemaker, C.B., Tielens, A.G. Functions of the tegument of schistosomes: clues from the proteome and lipidome. *Int J Parasitol*, **2006**, *36*, 691-699.
38. Tonk, M. (Institute for Insect Biotechnology, Justus Liebig University of Giessen, Giessen, Germany). Personal communication, 2020.
39. Koziol, U., Rauschendorfer, T., Zanon Rodriguez, L., Krohne, G., Brehm, K. The unique stem cell system of the immortal larva of the human parasite *Echinococcus multilocularis*. *Evodevo*, **2014**, *5*, 10.
40. Zhou, H., Li, D., Shi, C., Xin, T., Yang, J., Zhou, Y., Hu, S., Tian, F., Wang, J., Chen, Y. Effects of Exendin-4 on bone marrow mesenchymal stem cell proliferation, migration and apoptosis *in vitro*. *Sci Rep*, **2015**, *5*, 12898.
41. Miao, Z., Lu, Z., Luo, S., Lei, D., He, Y., Wu, H., Zhao, J., Zheng, L. Murine and Chinese cobra venom-derived nerve growth factor stimulate chondrogenic differentiation of BMSCs *in vitro*: A comparative study. *Mol Med Rep*, **2018**, *18*, 3341-3349.
42. Assimakopoulos, S.F., Tsamandas, A.C., Georgiou, C.D., Vagianos, C.E., Scopa, C.D. Bombesin and neurotensin exert antiproliferative effects on oval cells and augment the regenerative response of the cholestatic rat liver. *Peptides*, **2010**, *31*, 2294-2303.
43. Liu, J., Zhang, Y., Sun, S., Zhang, G., Jiang, K., Sun, P., Zhang, Y., Yao, B., Sui, R., Chen, Y., Guo, X., Tang, T., Shi, J., Liang, H., Piao, H. Bufalin induces apoptosis and improves the sensitivity of human glioma stem-like sells to temozolamide. *Oncol Res*, **2019**, *27*, 475-486.
44. White, J. Bites and stings from venomous animals: a global overview. *Ther Drug Monit*, **2000**, *22*, 65-68.
45. Walker, A.A., Madio, B., Jin, J., Undheim, E.A., Fry, B.G., King, G.F. Melt with this kiss: paralyzing and liquefying venom of the assassin bug *Pristhesancus plagipennis* (hemiptera: reduviidae). *Mol Cell Proteomics*, **2017**, *16*, 552-566.
46. Walker, A.A., Robinson, S.D., Undheim, E.A.B., Jin, J., Han, X., Fry, B.G., Vetter, I., King, G.F. Missiles of mass disruption: composition and glandular origin of venom used as a projectile defensive weapon by the assassin bug *Platymeris rhadamanthus*. *Toxins (Basel)*, **2019**, *11*, 673.
47. Gönnert, R. Schistosomiasis-Studien. II. Über die Eibildung bei *Schistosoma mansoni* und das Schicksal der Eier im Wirtsorganismus. *Z Tropenmed Parasitol*, **1955**, *6*, 33-52.
48. Dettman, C.D., Higgins-Opitz, S.B., Saikoolal, A. Enhanced efficacy of the paddling method for schistosome infection of rodents by a four-step pre-soaking procedure. *Parasitol Res*, **1989**, *76*, 183-184.
49. Grevelding, C.G. The female-specific W1 sequence of the Puerto Rican strain of *Schistosoma mansoni* occurs in both genders of a Liberian strain. *Mol Biochem Parasitol*, **1995**, *71*, 269-272.
50. Ramirez, B., Bickle, Q., Yousif, F., Fakorede, F., Mouries, M.A., Nwaka, S. Schistosomes: challenges in compound screening. *Expert Opin Drug Discov*, **2007**, *2*, S53-61.

51. Hahnel, S., Quack, T., Parker-Manuel, S.J., Lu, Z., Vanderstraete, M., Morel, M., Dissous, C., Cailliau, K., Grevelding, C.G. Gonad RNA-specific qRT-PCR analyses identify genes with potential functions in schistosome reproduction such as SmFz1 and SmFGFRs. *Front Genet*, **2014**, *5*, 170.
52. Neves, R.H., de Lamare Biolchini, C., Machado-Silva, J.R., Carvalho, J.J., Branquinho, T.B., Lenzi, H.L., Hulstijn, M., Gomes, D.C. A new description of the reproductive system of *Schistosoma mansoni* (Trematoda: Schistosomatidae) analyzed by confocal laser scanning microscopy. *Parasitol Res*, **2005**, *95*, 43-49.
53. Beckmann, S., Grevelding, C.G. Imatinib has a fatal impact on morphology, pairing stability and survival of adult *Schistosoma mansoni in vitro. Int J Parasitol*, **2010**, *40*, 521-526.
54. Tonk, M., Pierrot, C., Cabezas-Cruz, A., Rahnamaeian, M., Khalife, J., Vilcinskas, A. The *Drosophila melanogaster* antimicrobial peptides Mtk-1 and Mtk-2 are active against the malarial parasite *Plasmodium falciparum. Parasitol Res*, **2019**, *118*, 1993-1998.
55. Marx, A., Backes, C., Meese, E., Lenhof, H.P., Keller, A. EDISON-WMW: exact dynamic programing solution of the Wilcoxon-Mann-Whitney test. *Genomics Proteomics Bioinformatics*, **2016**, *14*, 55-61.

Literaturverzeichnis

Akinsolu FT, Nemieboka PO, Njuguna DW, Ahadji MN, Dezso D, Varga O (2019). Emerging resistance of neglected tropical diseases: a scoping review of the literature. Int J Environ Res Public Health 16(11): 1925.

Aragon AD, Imani RA, Blackburn VR, Cunningham C (2008). Microarray based analysis of temperature and oxidative stress induced messenger RNA in *Schistosoma mansoni*. Mol Biochem Parasitol 162(2): 134-141.

Ashburn TT, Thor KB (2004). Drug repositioning: identifying and developing new uses for existing drugs. Nat Rev Drug Discov 3(8): 673-683.

Atanasov AG, Zotchev SB, Dirsch VM, Supuran CT (2021). Natural products in drug discovery: advances and opportunities. Nat Rev Drug Discov 20(3): 200-216.

Aveic S, Pantile M, Polo P, Sidarovich V, De Mariano M, Quattrone A, Longo L, Tonini GP (2018). Autophagy inhibition improves the cytotoxic effects of receptor tyrosine kinase inhibitors. Cancer Cell Int 18: 63.

Balakrishnan VS (2021). WHO's 2021–30 roadmap for neglected tropical diseases. The Lancet Microbe 2(1): E11.

Bayat Mokhtari R, Homayouni TS, Baluch N, Morgatskaya E, Kumar S, Das B, Yeger H (2017). Combination therapy in combating cancer. Oncotarget 8(23): 38022-38043.

Beckmann S, Grevelding CG (2010). Imatinib has a fatal impact on morphology, pairing stability and survival of adult *Schistosoma mansoni* in vitro. Int J Parasitol 40(5): 521-526.

Beckmann S, Hahnel S, Cailliau K, Vanderstraete M, Browaeys E, Dissous C, Grevelding CG (2011). Characterization of the Src/Abl Hybrid Kinase SmTK6 of *Schistosoma mansoni*. J Biol Chem 286(49): 42325-42336.

Beckmann S, Leutner S, Gouignard N, Dissous C, Grevelding CG (2012). Protein kinases as potential targets for novel anti-schistosomal strategies. Curr Pharm Des 18(24): 3579-3594.

Beckmann S, Long T, Scheld C, Geyer R, Caffrey CR, Grevelding CG (2014). Serum albumin and α-1 acid glycoprotein impede the killing of *Schistosoma mansoni* by the tyrosine kinase inhibitor Imatinib. Int J Parasitol Drugs Drug Resist 4(3): 287-295.

Berry A, Fillaux J, Martin-Blondel G, Boissier J, Iriart X, Marchou B, Magnaval JF, Delobel P (2016). Evidence for a permanent presence of schistosomiasis in Corsica, France, 2015. Euro Surveill 21(1).

Bodimeade C, Marks M, Mabey D (2019). Neglected tropical diseases: elimination and eradication. Clin Med (Lond) 19(2): 157-160.

Boisson S, Engels D, Gordon BA, Medlicott KO, Neira MP, Montresor A, Solomon AW, Velleman Y (2016). Water, sanitation and hygiene for accelerating and sustaining progress on neglected tropical diseases: a new Global Strategy 2015-20. Int Health 8 Suppl 1(Suppl 1): i19-21.

Brumlik MJ, Pandeswara S, Ludwig SM, Murthy K, Curiel TJ (2011). Parasite mitogen-activated protein kinases as drug discovery targets to treat human protozoan pathogens. J Signal Transduct 2011: 971968.

Buck SB, Bradford J, Gee KR, Agnew BJ, Clarke ST, Salic A (2008). Detection of S-phase cell cycle progression using 5-ethynyl-2'-deoxyuridine incorporation with click chemistry, an alternative to using 5-bromo-2'-deoxyuridine antibodies. Biotechniques 44(7): 927-929.

Buro C, Beckmann S, Oliveira KC, Dissous C, Cailliau K, Marhöfer RJ, Selzer PM, Verjovski-Almeida S, Grevelding CG (2014). Imatinib treatment causes substantial transcriptional changes in adult *Schistosoma mansoni in vitro* exhibiting pleiotropic effects. PLoS Negl Trop Dis 8(6): e2923.

Carrasco-Torres G, Baltiérrez-Hoyos R, Andrade-Jorge E, Villa-Treviño S, Trujillo-Ferrara JG, Vásquez-Garzón VR (2017). Cytotoxicity, oxidative stress, cell cycle arrest, and mitochondrial apoptosis after combined treatment of hepatocarcinoma cells with maleic anhydride derivatives and quercetin. Oxid Med Cell Longev 2017: 2734976.

Chapman JR, Waldenström J (2015). With reference to reference genes: a systematic review of endogenous controls in gene expression studies. PLoS One 10(11): e0141853.

Cheng YS, Williamson PR, Zheng W (2019). Improving therapy of severe infections through drug repurposing of synergistic combinations. Curr Opin Pharmacol 48: 92-98.

Collins JJ, 3rd, Wang B, Lambrus BG, Tharp ME, Iyer H, Newmark PA (2013). Adult somatic stem cells in the human parasite *Schistosoma mansoni*. Nature 494(7438): 476-479.

Costa-Silva J, Domingues D, Lopes FM (2017). RNA-Seq differential expression analysis: an extended review and a software tool. PLoS One 12(12): e0190152.

Cwiklinski K, Jewhurst H, McVeigh P, Barbour T, Maule AG, Tort J, O'Neill SM, Robinson MW, Donnelly S, Dalton JP (2018). Infection by the helminth parasite *Fasciola hepatica* requires rapid

regulation of metabolic, virulence, and invasive factors to adjust to its mammalian host. Mol Cell Proteomics 17(4): 792-809.

Daleprane JB, Abdalla DS (2013). Emerging roles of propolis: antioxidant, cardioprotective, and antiangiogenic actions. Evid Based Complement Alternat Med 2013: 175135.

Das KC, Kalita P, Tripathi T (2020). Genome-wide identification and characterization of eukaryotic protein kinases. Front Biosci (Landmark Ed) 25: 1787-1827.

Dawes B, Hughes DL (1970). Fascioliasis: the invasive stages in mammals. Adv Parasitol 8: 259-274.

De Bont J, Vercruysse J (1997). The epidemiology and control of cattle schistosomiasis. Parasitol Today 13(7): 255-262.

de Moraes J (2015). Natural products with antischistosomal activity. Future Med Chem 7(6): 801-820.

de Moraes J, Nascimento C, Miura LM, Leite JR, Nakano E, Kawano T (2011). Evaluation of the *in vitro* activity of dermaseptin 01, a cationic antimicrobial peptide, against *Schistosoma mansoni*. Chem Biodivers 8(3): 548-558.

De Rycker M, Baragaña B, Duce SL, Gilbert IH (2018). Challenges and recent progress in drug discovery for tropical diseases. Nature 559(7715): 498-506.

Di Maggio LS, Tirloni L, Pinto AF, Diedrich JK, Yates Iii JR, Benavides U, Carmona C, da Silva Vaz I, Jr., Berasain P (2016). Across intra-mammalian stages of the liver fluke *Fasciola hepatica*: a proteomic study. Sci Rep 6: 32796.

Ding S, Qiao X, Suryadi J, Marrs GS, Kucera GL, Bierbach U (2013). Using fluorescent post-labeling to probe the subcellular localization of DNA-targeted platinum anticancer agents. Angew Chem Int Ed Engl 52(12): 3350-3354.

Dissous C, Grevelding CG (2011). Piggy-backing the concept of cancer drugs for schistosomiasis treatment: a tangible perspective? Trends Parasitol 27(2): 59-66.

Du X, McManus DP, French JD, Jones MK, You H (2021). CRISPR/Cas9: a new tool for the study and control of helminth parasites. Bioessays 43(1): e2000185.

Eckersall PD, Lawson FP, Bence L, Waterston MM, Lang TL, Donachie W, Fontaine MC (2007). Acute phase protein response in an experimental model of ovine caseous lymphadenitis. BMC Vet Res 3: 35.

Edwards JS (1961). The action and composition of the saliva of an assassin bug *Platymeris rhadamanthus* Gaerst. (Hemiptera, Reduviidae). J Exp Biol 38(1): 61-77.

El-Asmar MF, Swelam N, Abdel Aal TM, Ghoneim K, Hodhod SS (1980). Factor(s) in the venom of scorpions toxic to *Schistosoma mansoni* (intestinal belharzia) cercariae. Toxicon 18(5-6): 711-715.

El-Sayed A, Kamel M (2020). Climatic changes and their role in emergence and re-emergence of diseases. Environ Sci Pollut Res Int 27(18): 22336-22352.

Endrullat C, Glökler J, Franke P, Frohme M (2016). Standardization and quality management in next-generation sequencing. Appl Transl Genom 10: 2-9.

Fairweather I, Boray JC (1999). Fasciolicides: efficacy, actions, resistance and its management. Vet J 158(2): 81-112.

Fairweather I, Holmes SD, Threadgold LT (1984). *Fasciola hepatica*: motility response to fasciolicides in vitro. Exp Parasitol 57(3): 209-224.

Filip Z, Jan K, Vendula S, Jana KZ, Kamil M, Kamil K (2013). Albumin and α1-acid glycoprotein: old acquaintances. Expert Opin Drug Metab Toxicol 9(8): 943-954.

Fürst T, Keiser J, Utzinger J (2012). Global burden of human food-borne trematodiasis: a systematic review and meta-analysis. Lancet Infect Dis 12(3): 210-221.

Gelmedin V, Dissous C, Grevelding CG (2015). Re-positioning protein-kinase inhibitors against schistosomiasis. Future Med Chem 7(6): 737-752.

Giri BR, Du X, Xia T, Chen Y, Li H, Cheng G (2017). Molecular characterization and expression profile of nanos in *Schistosoma japonicum* and its influence on the expression several mammalian stem cell factors. Parasitol Res 116(7): 1947-1954.

Giuliani S, Silva AC, Borba J, Ramos PIP, Paveley RA, Muratov EN, Andrade CH, Furnham N (2018). Computationally-guided drug repurposing enables the discovery of kinase targets and inhibitors as new schistosomicidal agents. PLoS Comput Biol 14(10): e1006515.

Gryseels B (2012). Schistosomiasis. Infect Dis Clin North Am 26(2): 383-397.

Guidi A, Mansour NR, Paveley RA, Carruthers IM, Besnard J, Hopkins AL, Gilbert IH, Bickle QD (2015). Application of RNAi to genomic drug target validation in schistosomes. PLoS Negl Trop Dis 9(5): e0003801.

Haeberlein S, Angrisano A, Quack T, Lu Z, Kellershohn J, Blohm A, Grevelding CG, Hahnel SR (2019). Identification of a new panel of reference genes to study pairing-dependent gene expression in *Schistosoma mansoni*. Int J Parasitol 49(8): 615-624.

Hahnel S, Quack T, Parker-Manuel SJ, Lu Z, Vanderstraete M, Morel M, Dissous C, Cailliau K, Grevelding CG (2014). Gonad RNA-specific qRT-PCR analyses identify genes with potential functions in schistosome reproduction such as SmFz1 and SmFGFRs. Front Genet 5: 170.

Hahnel S, Wheeler N, Lu Z, Wangwiwatsin A, McVeigh P, Maule A, Berriman M, Day T, Ribeiro P, Grevelding CG (2018). Tissue-specific transcriptome analyses provide new insights into GPCR signalling in adult *Schistosoma mansoni*. PLoS Pathog 14(1): e1006718.

Hassan EA, Abdel-Rahman MA, Ibrahim MM, Soliman MF (2016). *In vitro* antischistosomal activity of venom from the Egyptian snake *Cerastes cerastes*. Rev Soc Bras Med Trop 49(6): 752-757.

Hassan I, Khan AA, Aman S, Qamar W, Ebaid H, Al-Tamimi J, Alhazza IM, Rady AM (2018). Restrained management of copper level enhances the antineoplastic activity of imatinib in vitro and in vivo. Sci Rep 8(1): 1682.

Hayes A, Rash BM, Zeef LA (2011). Absolute and relative quantification of mRNA expression (transcript analysis). Methods Mol Biol 759: 73-86.

Hegazi AG, Abd El Hady FK, Abd Allah FA (2000). Chemical composition and antimicrobial activity of European propolis. Z Naturforsch C 55(1-2): 70-75.

Hemer S, Brehm K (2012). *In vitro* efficacy of the anticancer drug imatinib on *Echinococcus multilocularis* larvae. Int J Antimicrob Agents 40(5): 458-462.

Hill MD, Briscoe PR, Abramson FP (1989). Comparison of propranolol-binding plasma proteins in sheep with those in humans, dogs and rats. Biochem Pharmacol 38(23): 4199-4205.

Houhou H, Puckelwaldt O, Strube C, Haeberlein S (2019). Reference gene analysis and its use for kinase expression profiling in *Fasciola hepatica*. Sci Rep 9(1): 15867.

Hwang WS, Weirauch C (2012). Evolutionary history of assassin bugs (insecta: hemiptera: Reduviidae): insights from divergence dating and ancestral state reconstruction. PLoS One 7(9): e45523.

Ismail M, Metwally A, Farghaly A, Bruce J, Tao LF, Bennett JL (1996). Characterization of isolates of *Schistosoma mansoni* from Egyptian villagers that tolerate high doses of praziquantel. Am J Trop Med Hyg 55(2): 214-218.

Jeremias WJ, Araújo FMG, Queiroz FR, Pais FSM, Mattos ACA, Salim ACM, Coelho PMZ, Oliveira GC, Kusel JR, Guerra-Sá R, Coimbra RS, Babá É H (2017). Comparative sequence analysis reveals regulation of genes in developing schistosomula of *Schistosoma mansoni* exposed to host portal serum. PLoS One 12(6): e0178829.

Jonker FAM, Te Poel E, Bates I, Boele van Hensbroek M (2017). Anaemia, iron deficiency and susceptibility to infection in children in sub-Saharan Africa, guideline dilemmas. Br J Haematol 177(6): 878-883.

Kadesch P, Quack T, Gerbig S, Grevelding CG, Spengler B (2019). Lipid topography in *Schistosoma mansoni* cryosections, revealed by microembedding and high-resolution atmospheric-pressure matrix-assisted laser desorption/ionization (MALDI) mass spectrometry imaging. Anal Chem 91(7): 4520-4528.

Karlsson O, Hanrieder J (2017). Imaging mass spectrometry in drug development and toxicology. Arch Toxicol 91(6): 2283-2294.

Keiser J, Rinaldi L, Veneziano V, Mezzino L, Tanner M, Utzinger J, Cringoli G (2008). Efficacy and safety of artemether against a natural *Fasciola hepatica* infection in sheep. Parasitol Res 103(3): 517-522.

Keiser J, Shu-Hua X, Tanner M, Utzinger J (2006). Artesunate and artemether are effective fasciolicides in the rat model and *in vitro*. J Antimicrob Chemother 57(6): 1139-1145.

Keiser J, Utzinger J (2012). Antimalarials in the treatment of schistosomiasis. Curr Pharm Des 18(24): 3531-3538.

Kelley JM, Elliott TP, Beddoe T, Anderson G, Skuce P, Spithill TW (2016). Current threat of triclabendazole resistance in *Fasciola hepatica*. Trends Parasitol 32(6): 458-469.

Kelley JM, Rathinasamy V, Elliott TP, Rawlin G, Beddoe T, Stevenson MA, Spithill TW (2020). Determination of the prevalence and intensity of *Fasciola hepatica* infection in dairy cattle from six irrigation regions of Victoria, South-eastern Australia, further identifying significant triclabendazole resistance on three properties. Vet Parasitol 277: 109019.

Kim D, Hwang HY, Kwon HJ (2020). Targeting autophagy in disease: recent advances in drug discovery. Expert Opin Drug Discov 15(9): 1045-1064.

Klionsky DJ, Emr SD (2000). Autophagy as a regulated pathway of cellular degradation. Science 290(5497): 1717-1721.

Knight GWA, McLellan D (2004). Use and limitations of imatinib mesylate (Glivec), a selective inhibitor of the tyrosine kinase Abl transcript in the treatment of chronic myeloid leukaemia. Br J Biomed Sci 61(2): 103-111.

Koziol U, Rauschendorfer T, Zanon Rodriguez L, Krohne G, Brehm K (2014). The unique stem cell system of the immortal larva of the human parasite *Echinococcus multilocularis*. Evodevo 5(1): 10.

Kuntz AN, Davioud-Charvet E, Sayed AA, Califf LL, Dessolin J, Arnér ES, Williams DL (2007). Thioredoxin glutathione reductase from *Schistosoma mansoni*: an essential parasite enzyme and a key drug target. PLoS Med 4(6): e206.

Laing G, Vigilato MAN, Cleaveland S, Thumbi SM, Blumberg L, Salahuddin N, Abdela-Ridder B, Harrison W (2021). One Health for neglected tropical diseases. Trans R Soc Trop Med Hyg 115(2): 182-184.

Lane HA, Nigg EA (1996). Antibody microinjection reveals an essential role for human polo-like kinase 1 (Plk1) in the functional maturation of mitotic centrosomes. J Cell Biol 135(6 Pt 2): 1701-1713.

Lee WR, Pak SC, Park KK (2015). The protective effect of bee venom on fibrosis causing inflammatory diseases. Toxins (Basel) 7(11): 4758-4772.

Leong RL, Xing H, Braekman JC, Kem WR (2015). Non-competitive inhibition of nicotinic acetylcholine receptors by ladybird beetle alkaloids. Neurochem Res 40(10): 2078-2086.

Lernoux M, Schnekenburger M, Losson H, Vermeulen K, Hahn H, Gérard D, Lee JY, Mazumder A, Ahamed M, Christov C, Kim DW, Dicato M, Bormans G, Han BW, Diederich M (2020). Novel HDAC inhibitor MAKV-8 and imatinib synergistically kill chronic myeloid leukemia cells via inhibition of BCR-ABL/MYC-signaling: effect on imatinib resistance and stem cells. Clin Epigenetics 12(1): 69.

Li XS, Haeberlein S, Zhao L, Mughal MN, Zhu T, Liu L, Fang R, Zhou YQ, Zhao JL, Grevelding CG, Hu M (2019). The ABL kinase inhibitor imatinib causes phenotypic changes and lethality in adult *Schistosoma japonicum*. Parasitol Res 118(3): 881-890.

Long T, Cailliau K, Beckmann S, Browaeys E, Trolet J, Grevelding CG, Dissous C (2010). *Schistosoma mansoni* polo-like kinase 1: A mitotic kinase with key functions in parasite reproduction. Int J Parasitol 40(9): 1075-1086.

Lu C, Li X, Ren Y, Zhang X (2021). Disulfiram: a novel repurposed drug for cancer therapy. Cancer Chemother Pharmacol 87(2): 159-172.

Lu Z, Spänig S, Weth O, Grevelding CG (2019). Males, the wrongly neglected partners of the biologically unprecedented male-female interaction of schistosomes. Front Genet 10: 796.

Mahmoud TY, Rizk SM, Maghraby AS, Shaheen AA (2014). Propolis enhances the effectiveness of praziquantel in experimental schistosomiasis: biochemical and histopathological study. Parasitol Res 113(12): 4513-4523.

Maizels RM, Smits HH, McSorley HJ (2018). Modulation of host immunity by helminths: the expanding repertoire of parasite effector molecules. Immunity 49(5): 801-818.

Manley PW, Cowan-Jacob SW, Buchdunger E, Fabbro D, Fendrich G, Furet P, Meyer T, Zimmermann J (2002). Imatinib: a selective tyrosine kinase inhibitor. European Journal of Cancer 38: S19-S27.

Manning G (2005). Genomic overview of protein kinases. WormBook: 1-19.

Mansour TE, Mansour JM (1962). Effects of serotonin (5-hydroxytryptamine) and adenosine 3',5'-phosphate on phosphofructokinase from the liver fluke *Fasciola hepatica*. J Biol Chem 237: 629-634.

Mas-Coma S, Valero MA, Bargues MD (2009). Chapter 2. *Fasciola*, lymnaeids and human fascioliasis, with a global overview on disease transmission, epidemiology, evolutionary genetics, molecular epidemiology and control. Adv Parasitol 69: 41-146.

May K, Bohlsen E, König S, Strube C (2020). *Fasciola hepatica* seroprevalence in Northern German dairy herds and associations with milk production parameters and milk ketone bodies. Vet Parasitol 277: 109016.

McCusker P, McVeigh P, Rathinasamy V, Toet H, McCammick E, O'Connor A, Marks NJ, Mousley A, Brennan GP, Halton DW, Spithill TW, Maule AG (2016). Stimulating neoblast-like cell proliferation in juvenile *Fasciola hepatica* supports growth and progression towards the adult phenotype *in vitro*. PLoS Negl Trop Dis 10(9): e0004994.

McVeigh P, McCammick EM, McCusker P, Morphew RM, Mousley A, Abidi A, Saifullah KM, Muthusamy R, Gopalakrishnan R, Spithill TW, Dalton JP, Brophy PM, Marks NJ, Maule AG (2014). RNAi dynamics in juvenile *Fasciola* spp. liver flukes reveals the persistence of gene silencing in vitro. PLoS Negl Trop Dis 8(9): e3185.

Mehmood K, Zhang H, Sabir AJ, Abbas RZ, Ijaz M, Durrani AZ, Saleem MH, Ur Rehman M, Iqbal MK, Wang Y, Ahmad HI, Abbas T, Hussain R, Ghori MT, Ali S, Khan AU, Li J (2017). A review on epidemiology, global prevalence and economical losses of fasciolosis in ruminants. Microb Pathog 109: 253-262.

Melek FR, Tadros MM, Yousif F, Selim MA, Hassan MH (2012). Screening of marine extracts for schistosomicidal activity in vitro. Isolation of the triterpene glycosides echinosides A and B with potential activity from the sea cucumbers *Actinopyga echinites* and *Holothuria polii*. Pharm Biol 50(4): 490-496.

Mengarda AC, Mendonça PS, Morais CS, Cogo RM, Mazloum SF, Salvadori MC, Teixeira FS, Morais TR, Antar GM, Lago JHG, Moraes J (2020). Antiparasitic activity of piplartine (piperlongumine) in a mouse model of schistosomiasis. Acta Trop 205: 105350.

Mlejnek P, Dolezel P, Faber E, Kosztyu P (2011). Interactions of N-desmethyl imatinib, an active metabolite of imatinib, with P-glycoprotein in human leukemia cells. Ann Hematol 90(7): 837-842.

Mnkugwe RH, Minzi O, Kinung'hi S, Kamuhabwa A, Aklillu E (2020). Efficacy and safety of praziquantel and dihydroartemisinin piperaquine combination for treatment and control of intestinal schistosomiasis: A randomized, non-inferiority clinical trial. PLoS Negl Trop Dis 14(9): e0008619.

Mohamed AH, Hassab El-Nabi SE, Bayomi AE, Abdelaal AA (2016). Effect of bee venom or proplis on molecular and parasitological aspects of *Schistosoma mansoni* infected mice. J Parasit Dis 40(2): 390-400.

Mokbel KEM, Baiuomy IR, Sabry AEA, Mohammed MM, El-Dardiry MA (2020). In vivo assessment of the antischistosomal activity of curcumin loaded nanoparticles versus praziquantel in the treatment of *Schistosoma mansoni*. Sci Rep 10(1): 15742.

Mokosch AS, Gerbig S, Grevelding CG, Haeberlein S, Spengler B (2021). High-resolution AP-SMALDI MSI as a tool for drug imaging in *Schistosoma mansoni*. Anal Bioanal Chem 413(10): 2755-2766.

Mona MH, Omran NE, Mansoor MA, El-Fakharany ZM (2012). Antischistosomal effect of holothurin extracted from some Egyptian sea cucumbers. Pharm Biol 50(9): 1144-1150.

Morawietz CM, Houhou H, Puckelwaldt O, Hehr L, Dreisbach D, Mokosch A, Roeb E, Roderfeld M, Spengler B, Haeberlein S (2020). Targeting kinases in *Fasciola hepatica*: anthelminthic effects and tissue distribution of selected kinase inhibitors. Front Vet Sci 7: 611270.

Morel M, Vanderstraete M, Cailliau K, Lescuyer A, Lancelot J, Dissous C (2014). Compound library screening identified Akt/PKB kinase pathway inhibitors as potential key molecules for the development of new chemotherapeutics against schistosomiasis. Int J Parasitol Drugs Drug Resist 4(3): 256-266.

Mughal MN, Grevelding CG, Haeberlein S (2021). First insights into the autophagy machinery of adult *Schistosoma mansoni*. Int J Parasitol.

Nawaratna SSK, McManus DP, Gasser RB, Brindley PJ, Boyle GM, Rivera V, Ranasinghe SL, Jones MK, You H, Gobert GN (2020). Use of kinase inhibitors against schistosomes to improve and broaden praziquantel efficacy. Parasitology 147(13): 1488-1498.

Nebot N, Crettol S, d'Esposito F, Tattam B, Hibbs DE, Murray M (2010). Participation of CYP2C8 and CYP3A4 in the N-demethylation of imatinib in human hepatic microsomes. Br J Pharmacol 161(5): 1059-1069.

Neves BJ, Andrade CH, Cravo PV (2015). Natural products as leads in schistosome drug discovery. Molecules 20(2): 1872-1903.

Newman DJ, Cragg GM (2012). Natural products as sources of new drugs over the 30 years from 1981 to 2010. J Nat Prod 75(3): 311-335.

Ng SS, Tsao MS, Nicklee T, Hedley DW (2001). Wortmannin inhibits pkb/akt phosphorylation and promotes gemcitabine antitumor activity in orthotopic human pancreatic cancer xenografts in immunodeficient mice. Clin Cancer Res 7(10): 3269-3275.

O'Connell EM, Bennuru S, Steel C, Dolan MA, Nutman TB (2015). Targeting filarial Abl-like kinases: orally available, food and drug administration-approved tyrosine kinase inhibitors are microfilaricidal and macrofilaricidal. J Infect Dis 212(5): 684-693.

O'Connell EM, Kamenyeva O, Lustigman S, Bell A, Nutman TB (2017). Defining the target and the effect of imatinib on the filarial c-Abl homologue. PloS Negl Trop Dis 11(7): 17.

O'Connell EM, Nutman TB (2017). Reduction of *Loa loa* microfilaremia with imatinib - A case report. N Engl J Med 377(21): 2095-2096.

Oliveira RN, Corrêa SAP, Vieira KM, Mendes T, Allegretti SM, Miguel DC (2019). *In vitro* schistosomicidal activity of tamoxifen and its effectiveness in a murine model of schistosomiasis at a single dose. Parasitol Res 118(5): 1625-1631.

Oršolić N (2012). Bee venom in cancer therapy. Cancer Metastasis Rev 31(1-2): 173-194.

Osakunor DNM, Woolhouse MEJ, Mutapi F (2018). Paediatric schistosomiasis: What we know and what we need to know. PLoS Negl Trop Dis 12(2): e0006144.

Panic G, Duthaler U, Speich B, Keiser J (2014). Repurposing drugs for the treatment and control of helminth infections. Int J Parasitol Drugs Drug Resist 4(3): 185-200.

Panic G, Vargas M, Scandale I, Keiser J (2015). Activity profile of an FDA-approved compound library against *Schistosoma mansoni*. PLoS Negl Trop Dis 9(7): e0003962.

Peng Q, Qin J, Zhang Y, Cheng X, Wang X, Lu W, Xie X, Zhang S (2017). Autophagy maintains the stemness of ovarian cancer stem cells by FOXA2. J Exp Clin Cancer Res 36(1): 171.

Pérez del Villar L, Burguillo FJ, López-Abán J, Muro A (2012). Systematic review and meta-analysis of artemisinin based therapies for the treatment and prevention of schistosomiasis. PLoS One 7(9): e45867.

Phillipson JD (1994). Natural products as drugs. Trans R Soc Trop Med Hyg 88 Suppl 1: S17-19.

Popiel I, Basch PF (1984). Reproductive development of female *Schistosoma mansoni* (Digenea: Schistosomatidae) following bisexual pairing of worms and worm segments. J Exp Zool 232(1): 141-150.

Ressurreicao M, De Saram P, Kirk RS, Rollinson D, Emery AM, Page NM, Davies AJ, Walker AJ (2014). Protein kinase C and extracellular signal-regulated kinase regulate movement, attachment, pairing and egg release in *Schistosoma mansoni*. PLoS Negl Trop Dis 8(6): e2924.

Rinaldi G, Morales ME, Cancela M, Castillo E, Brindley PJ, Tort JF (2008). Development of functional genomic tools in trematodes: RNA interference and luciferase reporter gene activity in *Fasciola hepatica*. PLoS Negl Trop Dis 2(7): e260.

Robinson MW, Menon R, Donnelly SM, Dalton JP, Ranganathan S (2009). An integrated transcriptomics and proteomics analysis of the secretome of the helminth pathogen *Fasciola hepatica*: proteins associated with invasion and infection of the mammalian host. Mol Cell Proteomics 8(8): 1891-1907.

Rodrigues DA, Sagrillo FS, Fraga CAM (2019). Duvelisib: a 2018 novel FDA-approved small molecule inhibiting phosphoinositide 3-kinases. Pharmaceuticals 12(2): 69.

Rompp A, Guenther S, Takats Z, Spengler B (2011). Mass spectrometry imaging with high resolution in mass and space (HR(2) MSI) for reliable investigation of drug compound distributions on the cellular level. Anal Bioanal Chem 401(1): 65-73.

Schmid-Hempel P (2017). Parasites and their social hosts. Trends Parasitol 33(6): 453-462.

Schulman MD, Valentino D, Cifelli S, Ostlind DA (1982). Dose-dependent pharmacokinetics and efficacy of MK-401 against old, and young-mature infections of *Fasciola hepatica* in the rat. J Parasitol 68(4): 603-608.

Shapiro-Ilan DI, Cottrell TE (2005). Susceptibility of lady beetles (Coleoptera: Coccinellidae) to entomopathogenic nematodes. J Invertebr Pathol 89(2): 150-156.

Shenberger JS, Dixon PS (1999). Oxygen induces S-phase growth arrest and increases p53 and p21(WAF1/CIP1) expression in human bronchial smooth-muscle cells. Am J Respir Cell Mol Biol 21(3): 395-402.

Shibata M, Hoque MO (2019). Targeting cancer stem cells: a strategy for effective eradication of cancer. Cancers (Basel) 11(5): 732.

Shoriki T, Ichikawa-Seki M, Suganuma K, Naito I, Hayashi K, Nakao M, Aita J, Mohanta UK, Inoue N, Murakami K, Itagaki T (2016). Novel methods for the molecular discrimination of *Fasciola* spp. on the basis of nuclear protein-coding genes. Parasitol Int 65(3): 180-183.

Slupphaug G, Kavli B, Krokan HE (2003). The interacting pathways for prevention and repair of oxidative DNA damage. Mutat Res 531(1-2): 231-251.

Smith SA, Waters NJ (2018). Pharmacokinetic and pharmacodynamic considerations for drugs binding to alpha-1-acid glycoprotein. Pharm Res 36(2): 30.

Son DS, Osabe M, Shimoda M, Kokue E (1998). Contribution of alpha 1-acid glycoprotein to species difference in lincosamides-plasma protein binding kinetics. J Vet Pharmacol Ther 21(1): 34-40.

Song Q, Liu H, Zhen H, Zhao B (2020). Autophagy and its role in regeneration and remodeling within invertebrate. Cell Biosci 10: 111.

Stábeli RG, Amui SF, Sant'Ana CD, Pires MG, Nomizo A, Monteiro MC, Romão PR, Guerra-Sá R, Vieira CA, Giglio JR, Fontes MR, Soares AM (2006). *Bothrops moojeni* myotoxin-II, a Lys49-phospholipase A2 homologue: an example of function versatility of snake venom proteins. Comp Biochem Physiol C Toxicol Pharmacol 142(3-4): 371-381.

Standley CJ, Mugisha L, Dobson AP, Stothard JR (2012). Zoonotic schistosomiasis in non-human primates: past, present and future activities at the human-wildlife interface in Africa. J Helminthol 86(2): 131-140.

Sukumar S, Krishman A, Khan MKA (2020). Protein kinases as antituberculosis targets: The case of thymidylate kinases. Front Biosci (Landmark Ed) 25: 1636-1654.

Tagboto S, Townson S (2001). Antiparasitic properties of medicinal plants and other naturally occurring products. Adv Parasitol 50: 199-295.

Tonk M, Vilcinskas A (2017). The medical potential of antimicrobial peptides from insects. Curr Top Med Chem 17(5): 554-575.

Vale N, Gouveia MJ, Rinaldi G, Brindley PJ, Gartner F, da Costa JMC (2017). Praziquantel for schistosomiasis: single-drug metabolism revisited, mode of action, and resistance. Antimicrob Agents Chemother 61(5): e02582-02516.

Vandesompele J, De Preter K, Pattyn F, Poppe B, Van Roy N, De Paepe A, Speleman F (2002). Accurate normalization of real-time quantitative RT-PCR data by geometric averaging of multiple internal control genes. Genome Biol 3(7): Research0034.

Vilcinskas A, Stoecker K, Schmidtberg H, Röhrich CR, Vogel H (2013). Invasive harlequin ladybird carries biological weapons against native competitors. Science 340(6134): 862-863.

Vogel H, Schmidtberg H, Vilcinskas A (2017). Comparative transcriptomics in three ladybird species supports a role for immunity in invasion biology. Dev Comp Immunol 67: 452-456.

Walker AA, Weirauch C, Fry BG, King GF (2016). Venoms of heteropteran insects: a treasure trove of diverse pharmacological toolkits. Toxins (Basel) 8(2): 43.

Waller CF (2018). Imatinib mesylate. Small molecules in hematology. U. M. Martens. Cham, Springer International Publishing: 1-27.

Wang J, Paz C, Padalino G, Coghlan A, Lu Z, Gradinaru I, Collins JNR, Berriman M, Hoffmann KF, Collins JJ, 3rd (2020). Large-scale RNAi screening uncovers therapeutic targets in the parasite *Schistosoma mansoni*. Science 369(6511): 1649-1653.

Wang JY (2014). The capable ABL: what is its biological function? Mol Cell Biol 34(7): 1188-1197.

Wang Q, Bu S, Xin D, Li B, Wang L, Lai D (2018). Autophagy is indispensable for the self-renewal and quiescence of ovarian cancer spheroid cells with stem cell-like properties. Oxid Med Cell Longev 2018: 7010472.

Wang Y, Zayas RM, Guo T, Newmark PA (2007). Nanos function is essential for development and regeneration of planarian germ cells. Proc Natl Acad Sci U S A 104(14): 5901-5906.

Wangwiwatsin A, Protasio AV, Wilson S, Owusu C, Holroyd NE, Sanders MJ, Keane J, Doenhoff MJ, Rinaldi G, Berriman M (2020). Transcriptome of the parasitic flatworm *Schistosoma mansoni* during intra-mammalian development. PLoS Negl Trop Dis 14(5): e0007743.

Webster JP, Gower CM, Knowles SCL, Molyneux DH, Fenton A (2016). One health - an ecological and evolutionary framework for tackling neglected zoonotic diseases. Evol Appl 9(2): 313-333.

Wendt G, Zhao L, Chen R, Liu C, O'Donoghue AJ, Caffrey CR, Reese ML, Collins JJ, 3rd (2020). A single-cell RNA-seq atlas of *Schistosoma mansoni* identifies a key regulator of blood feeding. Science 369(6511): 1644-1649.

Wendt GR, Collins JJ, 3rd (2016). Schistosomiasis as a disease of stem cells. Curr Opin Genet Dev 40: 95-102.

Wesolowska A, Zawistowska-Deniziak A, Norbury LJ, Wilkowski P, Januszkiewicz K, Pyziel AM, Zygner W, Wedrychowicz H (2016). Immune responses in rats and sheep induced by a DNA vaccine containing the phosphoglycerate kinase gene of *Fasciola hepatica* and liver fluke infection. Acta Parasitol 61(2): 212-220.

WHO (2020). "Schistosomiasis. Key facts." from https://www.who.int/en/news-room/fact-sheets/detail/schistosomiasis.

WHO (2021). "Latest News ", from http://www.who.int/neglected_diseases/diseases/en/.

You H, Mayer JU, Johnston RL, Sivakumaran H, Ranasinghe S, Rivera V, Kondrashova O, Koufariotis LT, Du X, Driguez P, French JD, Waddell N, Duke MG, Ittiprasert W, Mann VH, Brindley PJ, Jones MK, McManus DP (2021). CRISPR/Cas9-mediated genome editing of *Schistosoma mansoni* acetylcholinesterase. Faseb j 35(1): e21205.

Yuan N, Song L, Zhang S, Lin W, Cao Y, Xu F, Fang Y, Wang Z, Zhang H, Li X, Wang Z, Cai J, Wang J, Zhang Y, Mao X, Zhao W, Hu S, Chen S, Wang J (2015). Bafilomycin A1 targets both autophagy and apoptosis pathways in pediatric B-cell acute lymphoblastic leukemia. Haematologica 100(3): 345-356.

Yuan ZM, Huang Y, Ishiko T, Kharbanda S, Weichselbaum R, Kufe D (1997). Regulation of DNA damage-induced apoptosis by the c-Abl tyrosine kinase. Proc Natl Acad Sci U S A 94(4): 1437-1440.

Zheng S, Shu Y, Lu Y, Sun Y (2020). Chloroquine combined with imatinib overcomes imatinib resistance in gastrointestinal stromal tumors by inhibiting autophagy via the MAPK/ERK pathway. Onco Targets Ther 13: 6433-6441.

Danksagung

Die letzten Seiten meiner Habilitationsschrift möchte ich den Personen widmen, die meinen Werdegang in den letzten fünf Jahren an der Justus-Liebig-Universität maßgeblich unterstützt und positiv beeinflusst haben.

Mein größter Dank gilt meinem Mentor, Prof. Dr. Christoph Grevelding. Sein genialer Weitblick beim Vorschlag, die molekulare Leberegelforschung zu meinem neuen Forschungsgebiet zu machen, war wegweisend für den Erfolg meiner Arbeiten. Sehr dankbar bin ich für die vielen gemeinsamen wissenschaftlichen Diskussionen und für seine unglaublich humorvolle und motivierende Art, die mich durch so manche Stressphase gerettet hat und meine Begeisterung für die Parasitologie immer weiter anfacht. Für sein Vertrauen in mich danke ich ihm von ganzem Herzen.

Ein besonderes Dankeschön an Prof. Dr. Adriaan Dorresteijn für die herzlichen und informativen Gespräche in Vorbereitung zur Habilitation.

Herrn Dekan Prof. Dr. Dr. h.c. Martin Kramer möchte ich für die Unterstützung durch ein Nachwuchsstipendium von Seiten des Fachbereichs 10 und das damit entgegen gebrachte Vertrauen in besonderem Maße danken.

Den Chef-„DRUIDen“ Prof. Dr. Katja Becker und Prof. Dr. Stephan Becker danke ich für die großartige Unterstützung und Förderung im Rahmen unseres LOEWE-Zentrums. Es ist eine fantastische Erfahrung, Projektleiterin in einem solch lebendigen Konsortium zu sein.

Meinen engen Kooperationspartnern an den Universitäten in Gießen und Marburg, dem Uniklinikum Gießen und der TiHo Hannover möchte ich ganz besonders danken: Prof. Dr. Bernhard Spengler, Prof. Dr. Andreas Vilcinskas, Dr. Miray Tonk, Dr. Stefanie Gerbig, Dr. Martin Roderfeld, Dr. Janine Köpke, Prof. Dr. Martin Schlitzer, Prof. Dr. Arnold Grünweller, und Prof. Dr. Christina Strube.

Die erfolgreiche Veröffentlichung zahlreicher Forschungsarbeiten wäre nicht möglich gewesen ohne die herausragende Leistung und das experimentelle Geschick meiner drei Doktoranden: Hicham Houhou, Mudassar Mughal und Oliver Puckelwaldt.

Den Doktoranden und „Ehemaligen“ aus der AG Schlitzer und AG Spengler sage ich Danke für die großartige Zusammenarbeit in den letzten Jahren: Dr. Georg Rennar, Dr. Alejandra Peter-Ventura, Tom Gallinger, Carolin Morawietz und Annika Mokosch.

Allen Kollegen und „Ehemaligen“ in der AG Grevelding möchte ich für die vielen schönen Laborerlebnisse, die Unterstützung und intensive wissenschaftliche Diskussionen danken: Dr. Oliver Weth, Dr. Steffen Hahnel, Mandy Beutler, Max Möscheid, Xuesong Li, Monique Überall, Martin Haimann, Josina Kellershohn und Svenja Gramberg. Insbesondere danke ich meinem Büronachbarn Dr. Thomas Quack, mit dem man ganz wunderbar Forschungsideen lebhaft diskutieren kann.

Dank an unsere fleißigen Assistentinnen Christina Scheld, Georgette Stovall und Bianca Kulik, die den Schistosomen-Zyklus nonstop am Laufen halten und mir meine Untersuchungsobjekte sichern.

Den „Leberegel“-HiWis Marcel Haas, Corinna Wyst und Florian Schalk danke ich für die tatkräftige Unterstützung beim „ploppen lassen“ von Leberegel-Metacercarien und ihre Begeisterung für Parasitologie.

Bei allen Mitgliedern des Instituts möchte ich mich für die überaus angenehme und kollegiale Atmosphäre bedanken.

Ganz besonders danken möchte ich meiner Schwester Sandra für ungezählte Gespräche, die sehr halfen, sich immer wieder auf das Wesentliche zu fokussieren und den Mittelpunkt im Leben beizubehalten.

Meinen Eltern danke ich von ganzem Herzen für die unentwegte Unterstützung. Meiner Mutter, die das Interesse für Biologie mit mir teilt, und meinem Vater, der immer ein passendes motivierendes Zitat parat hat. Ich bin dankbar, dass sie mir stets das Gefühl geben, sie sehr stolz zu machen. Das bedeutet mir sehr viel.